Analyses of atmospheric CHF_2Cl, heavy ozone, HDO and CH_3D from ATMOS spectra

Thesis by
Fredrick W. Irion

In partial fulfillment of the requirements
for the Degree of
Doctor of Philosophy

California Institute of Technology
Pasadena, California

1996

(Submitted January 3, 1996)

For my grandparents, Reinhold and Martha Kautz.

The most important fact about Spaceship Earth:
an instruction book didn't come with it. -Buckminster Fuller

Acknowledgements

There are two people that I owe far more than I can easily articulate. Thank you Mike Gunson and Yuk Yung, for your patience, your guidance, your wisdom, and for believing in me.

It's been a privilege to work with and learn from many people at JPL and the ATMOS project. Thank you Mark Abrams, Mark Allen, Reinhard Beer, Jean-François Blavier, Linda Brown, Margaret Brown, Tyler Brown, Albert Chang, Bill DeMore, Barney Farmer, Julie Foster, John Gieselman, Aaron Goldman, Greg Goodson, Leslie Lowes, Gindi Lynch, Jim Margitan, Jack Margolis, Hope Michelsen, Liz Moyer, Emmanuel Mahieu, the late Bob Norton, Susan Paradise, Dave Petterson, Herb Pickett, Geoff Toon, Odell Raper, Curtis Rinsland, Ross Salawitch, Stan Sander, Bhaswar Sen, Jim Szeto, Bob Toth, Chris Webster, and Rudi Zander.

For guiding me through the bureaucracy with a smile, thank you Irma Betters, Kathy Bubash, Kay Campbell, Cliff Heindl, Maria Klein, Adria McMillan, Marjorie Miller, Darlene Padgett and thanks especially again to Odell Raper.

Thanks to Fred Shair, for his generosity and insight.

Thank you Joel Beane, Chris McColeman and Peter Klassen, for helping me start on this long journey.

For giving me courage when I needed it, thank you Jim O'Donnell, Jon Pederson, the people of CLU, Gil Mason and Lani Kaahumanu. Thank you Kerry Sieh for the Thanksgivings.

Thanks and a hug to Alison Gunson.

Thank you Bill Mitchell and Majid Saghafi for helping me get through my first couple of years at Caltech. Thanks to the Euclidians and the fellow travellers for a lot more than some nice dinners: Achim Ditzen, Suzanne Elsasser, Anita Harper, Daniel Hurley, Mike Kelsey, Thyra Lansdowne, John Marohn, Mike Pahre, Michal Peri, Anthony Perry, Niranjan Sardesai, Joel Schwartz, Patti Sipman, and especially Tyler Holcomb.

None of this would have been possible without the unwavering love and support of my family.

And finally, thank you Robert Southworth, for putting up with it all and still being there.

Abstract

Mixing ratio measurements of tropospheric CHF_2Cl and stratospheric heavy ozone ($^{16}O^{18}O^{16}O$ and $^{16}O^{16}O^{18}O$), HDO and CH_3D were derived from Atmospheric Trace Molecule Spectroscopy Experiment (ATMOS) spectra. The ATMOS instrument is a 0.01 cm^{-1} resolution, solar-absorption Fourier-transform spectrometer with a frequency response of 600-4800 cm^{-1} in the mid-infrared. It has recorded ground-based spectra over Table Mountain Facility (TMF), Wrightwood CA (34.4°N, 117.7°W, 2.2 km altitude) between 1985 to 1990, and space-based measurements during the four shuttle missions Spacelab 3 (April/May 1985), ATLAS-1 (March, 1992), ATLAS-2 (April, 1993) and ATLAS-3 (November, 1994).

The measured column burden of CHF_2Cl over TMF showed an exponential increase rate of (6.7±0.5)% yr^{-1} from October, 1985 to July, 1990. The current uncertainty in historical CHF_2Cl emissions was found to be too large for CHF_2Cl measurements to be used to infer adequately either its lifetime or the OH field.

Enrichments of heavy ozone (with respect to $^{48}O_3$) were measured from both space and ground-based observations. Average enrichments between 26 to 2.6 mb inclusive (≈25 to 41 km) were (15±6)% for $^{16}O^{16}O^{18}O$, (10±7)% for $^{16}O^{18}O^{16}O$, and (13±5)% for $^{50}O_3$ (1σ standard deviation). Enrichments increased slightly with altitude, but with no discernable latitudinal variability. From TMF, an average total column $^{16}O^{16}O^{18}O$ enrichment of (17±4)% (1σ standard deviation) was determined, with no discernable seasonal variation. Possible biases in the spectral intensities that affect the determination of absolute enrichments are discussed, but any corrections to these intensities would not affect the observed lack of latitudinal and seasonal variability.

From space-based measurements, stratospheric mixing ratios of CH_3D from 100 mb to 17mb (≈15 to 28 km) and HDO from 100 mb to 10 mb (≈15 to 32 km) were inferred. The average lifetime of CH_3D was found to be (1.19±0.02) times that of CH_4, with an average of (1.0±0.1) molecules of stratospheric HDO produced for each CH_3D destroyed (1σ combined precision and systematic error), indicating that the rate of stratospheric HDO production is approximately equal to the rate of CH_3D destruction.

Table of Contents

List of Figures

List of Tables

Chapter I

Introduction

This work is concerned with three studies of atmospheric composition using the Atmospheric Trace Molecule Absorption Experiment (ATMOS) spectrometer, and the bulk of this thesis is three independent papers that have been either accepted or submitted to Geophysical Research Letters. The first paper, in chapter II, deals with measurement of the secular increase of CHF_2Cl (HCFC-22). Chapter III investigates the stratospheric abundance of the heavy ozone isotopomers $^{16}O^{16}O^{18}O$ and $^{16}O^{18}O^{16}O$, and their anomalous enrichment (that is, their abundance above that expected statistically from standard isotopic ratios of ^{18}O to ^{16}O). Chapter IV is concerned with stratospheric measurements of the water isotopomer HDO and the methane isotopomer CH_3D.

All three papers have a bearing on the prediction of changes in the terrestrial atmosphere. CHF_2Cl is a so-called replacement gas for the chlorofluorocarbons CF_2Cl_2 (CFC-12) and $CFCl_3$ (CFC-11). The manufacture of CHF_2Cl is controlled by the Montreal Protocol and subsequent amendments, which restricts production of anthropogenic gases whose photolytic products destroy ozone (see, for example, *Ko et al.* [1994]). Heavy ozone has shown anomalously large enrichments in the stratosphere using several observation techniques. Enrichments have also been reproduced in the laboratory, but to date this has had no satisfactory scientific explanation. This problem has been somewhat more than an academic curiosity because its existence suggests regions of ozone chemistry that are not fully understood. Understanding heavy ozone enrichment may help in better understanding ozone chemistry in general. The third paper on HDO and CH_3D relates to chemistry, but as discussed by *Moyer et al.* [1995] and summarized later in this chapter, measurements of the stratospheric HDO/H_2O ratio may help elucidate mechanisms of tropospheric-stratospheric transport of water. As discussed in *WMO* [1995] and *Wennberg et al.* [1995], ozone destruction in the lower stratosphere is caused to a large extent by catalytic cycles involving HO_x ($=OH + HO_2$), which in turn has its origin in the reaction of $O(^1D)$ with H_2O and CH_4. Changes in the amount of stratospheric water

injected by, say, changes in tropospheric humidity due to global warming could affect the concentration of HO_x in the lower stratosphere. Better understanding of the mechanisms of cross-tropopause transport of water would help in model predictions of global change.

As submissions to Geophysical Research Letters are brief by necessity, this introductory chapter attempts to give more detail on the ATMOS spectrometer and data reduction methods used to analyze its output, and then to place the three aforementioned papers in a broader scientific context.

1.1 The ATMOS experiment

1.1.1 Rationale

Concern over possible changes to the earth's stratosphere in the late 1970's, particularly the destruction of ozone by chlorofluorocarbons and nitrogen oxides from emissions of proposed supersonic aircraft, prompted the development of research programs to better understand the roles of chemistry, radiation and dynamics in earth's stratosphere. Distributions of the so-called source, sink, reservoir and active species involved in ozone destruction were not well known at the time. Experimental validation of the stratospheric inventory of gases is required as both input to and tests for models, not only to calculate the current state of the atmosphere, but also to gain confidence in their predictive capabilities using plausible anthropogenic or natural forcings. As a contribution towards this end, the Atmospheric Trace Molecule Spectroscopy Experiment (ATMOS) program was developed, and as stated by *Farmer et al.* [1987], "the primary objective of the ATMOS experiment is to measure simultaneously as many of the minor and trace species as possible and to determine their spatial distribution."

1.1.2 Spectrometer design and operation

The ATMOS instrument (Figure 1.1.1) is a modified Fourier-transform infrared (FTIR) interferomer. It has a spectral response of 600 - 4800 cm^{-1} (2.2 - 16μm), from which spectral intervals are selected using optical bandpass filters (Table 1.1). Most of the minor species in the stratosphere (e.g., those in the part-per-million range) and many of the trace species (e.g., those in the part-per-billion range and less) have observable rotational-vibrational spectral transitions in the mid-infrared. A broad band spectrometer such as the ATMOS instrument is particularly useful as the spectra it obtains provide measurements on many gases of interest. Designed for use in the payload bay of the Space Shuttle, the ATMOS instrument makes measurements in the solar occultation mode. Using the sun as a light source, absorption spectra through the Earth's limb at different tangent altitudes are

obtained during an orbital sunrise or sunset. It has a scan time of 2.2 seconds, which for a 4 minute occultation event, provides about 100 measurements ranging in altitude from over 200 km to cloud top levels. The vertical spacing of these observations correspond to 4 km at the tangent altitude, decreasing to 2 km near 20 km due to refraction effects. With a shuttle distance of about 2000 km to the tangent point, selectable instrument field-of-views, ranging from 1 to 2.8 mrad, limit the vertical resolution from about 2 to 5 km. A simplified illustration of ATMOS measurement geometry is given in Figure 1.1.2.

A full description of the ATMOS instrument is given by *Farmer et al.* [1987]. A block diagram of ATMOS instrument components is given in Figure 1.1.3 and a schematic illustration of the optical components is given in Figure 1.1.4. The suntracker uses visible wavelength photodiode sensors on its outside face such that the sensor's field-of-view is centered on the solar disk. Solar radiation enters the foreoptics to a mirrored field stop with selectable arpertures corresponding to instrument field-of-views of 1, 1.4, 2.0, and 2.8 mrad. Light reflected by the field stop is passed to an on-board camera which records the positioning of the instrument on the sun. Light passing through the field stop is transferred to the interferometer's KBr beamsplitter at an incidence angle of 45°. The transmitted and reflected light from the beamsplitter are passed to one of two moving cat's-eye retroreflectors, each consisting of a paraboloid primary mirror and a slightly convex secondary mirror. In order to minimize the distance travelled by the mirrors, the beams are double-passed down each arm of the interferometer using a retroreflector. An optical path difference of ±50 cm for the two light beams is achieved by continuously moving the retroreflectors in opposite directions at 50 cm s^{-1}. The light rays returning from the retroreflectors are recombined in the beamsplitter and the resulting intensity-modulated radiation is transferred to the exit optics, where the light passes through a selectable spectral filter (see Table 1.1) and is focused on a HgCdTe detector cooled to 77K.

In addition to the solar radiation, a 0.633 μm beam from a HeNe laser is passed parallel to the solar radiation in the interferometer and is independently sampled. The laser is used for two reasons. First, sampling of the laser fringes allows precise velocity control for the retroreflectors using electronic feedback loops. Second, sampling of the analog output by the HgCdTe detector is selectably triggered every second or third laser fringe. The output from the detector is passed to a low gain channel to record the central fringe, and a high gain channel to record the interferogram. These signals are digitized, combined with instrument housekeeping data, and are stored on board the shuttle in a flight recorder or telemetried for recording on earth.

Processing of the interferograms is described by *Norton and Rinsland* [1991]. The interferograms are then corrected for phase and detector non-linearity errors, and fast Fourier transformed to power spectra. For space-based measurements, these power spectra were ratioed against exo-atmospheric solar spectra (obtained with each occultation) to remove solar spectral features and absorptions of residual H_2O and CO_2 within the instrument, producing pure atmospheric transmission spectra. Retrieved spectra from several tangent altitudes from bandpass filter 1 is illustrated in Figure 1.1.5.

1.1.3 ATMOS profile measurements from the space shuttle

The ATMOS instrument first flew aboard the space shuttle as part of the scientific payload of the Spacelab 3 mission of April 29 - May 7, 1985. Nineteen atmospheric observations were completed until operations were terminated on the third day of the mission due to a pressure leak in the reference HeNe laser housing. Despite the early cessation of observations, data were obtained over the ≈32°N and ≈44°S latitude bands. Figure 1.1.6 illustrates the latitude and longitude of the 30 km tangent point locations of the Spacelab 3 and subsequent flights. A full discussion of ATMOS on Spacelab 3 can be found in *Farmer et al.* [1987].

The next flights of the ATMOS instrument were on the Atmospheric Laboratory for Applications and Science (ATLAS) series beginning with ATLAS-1, March 24 - April 3, 1992. During the ATLAS-1 mission, approximately 41 sunset occultations were made between 55°S and 24°S, and 52 sunrise occultations between 31°S and 29°N. The timing of ATLAS-1 is important as it occurred about 9 months after the eruption of Mount Pinatubo, which injected large quantities of SO_2 into the lower stratosphere which subsequently formed a sulfuric acid aerosol layer (e.g., *Winkler and Osborn* [1992]). While the presence of the layer allowed analysis of the mid-infrared extinction by aerosol below about 30 km [*Rinsland et al.,* 1994], operationally it had the deleterious effect of causing the ATMOS suntracker, which uses visible wavelength photodiode sensors, to lose lock on the sun at tangent altitudes below about 25 km in the tropics; the aerosol was too opaque in the visible wavelengths for the limb viewing geometry. Consequently, many sunrise observations from the southern subtropics to northern subtropics at tangent altitudes below about 25 km could not be made, although southern mid-latitude measurements were largely unaffected because of a lower aerosol loading.

The third flight of ATMOS was on the ATLAS-2 mission, April 8 - 16, 1993. The mission timing and shuttle orbit were arranged to allow sunrise observations to be made in high northern latitudes inside and outside the Arctic polar vortex during the boreal spring. About 65 sunrise occultations were obtained around 65°N and about 39 sunset occultations were obtained between 50°S and 9°S. The vortex measurements proved exceptionally useful for measurement of CH_3D because, as discussed in Chapter IV, the descent (and compression) of high altitude air to lower altitudes within the vortex allowed measurement of air of low CH_3D mixing ratio ($\lesssim 0.6 \times 10^{-9}$) that could not be measured directly at mid-latitudes. Much as had happened during ATLAS-1, many observations in the southern mid-latitudes below about 25 km were lost due to increased sulfuric acid aerosol opacity from the Mt. Pinatubo eruption.

The fourth shuttle flight of ATMOS was on the ATLAS-3 mission, November 3-14, 1994. Here, the timing and orbit of the mission was arranged for measurements inside and outside the Antarctic polar vortex in the late austral spring, and from the northern subtropics to northern mid-latitudes. Approximately 83 sunrise occultations were obtained at about 68°N and 96 sunset occultations were obtained from 5°N-48°N. As was the case with ATLAS-2, descent inside the vortex allowed measurement of air with low CH_3D mixing ratios. By time of ATLAS-3, the opacity of the Pinatubo aerosol had sufficiently decayed so as not to affect instrument suntracker performance, and sunset measurements in the northern sub-tropics and mid-latitudes were achieved at altitudes down to 10 km and below.

1.1.4 ATMOS observations at Table Mountain

After the Spacelab 3 mission of April/May 1985, the ATMOS instrument was briefly at Table Mountain Facility (TMF; 34.4°N, 117.7°W, 2.23 km altitude) in October, 1985 to test it for a planned re-flight. The instrument was returned to TMF in December, 1986 because of the interruption of shuttle flights after the Challenger disaster. Data were taken when possible until July, 1990 when the instrument was prepared for the ATLAS-1 flight. The site at TMF has a clear view of the eastern horizon, and its altitude of 2.23 km eliminates much of the interference from tropospheric H_2O, CH_4 and CO_2 infrared absorptions. Unfortunately, the site can be quite humid at times, and its proximity to Los Angeles makes it susceptible to smog spilling over the intervening San Gabriel mountains in the afternoon. Data were gathered at TMF on some 51 days between 1985 and 1990, and have been used in measurement of several stratospheric trace gases [*Gunson and Irion,* 1991], and CHF_2Cl and heavy ozone as described in this thesis.

1.1.5 ATMOS data analysis methods

The ATMOS project data analysis software has been described by *Norton and Rinsland* [1991]. Atmospheric temperature, pressure and molecular density profiles are

derived for the spectra within each occultation. The procedure for this is briefly outlined in Appendix A. These temperature-pressure profiles were mapped onto a 150 layer model atmosphere for each occultation, each layer 1 km thick and homogeneous, along with assumed mixing ratio profiles for some 50 gas species which contribute to infrared absorption in the stratosphere.

To determine the mixing ratio of a target gas at a particular tangent pressure (or altitude), synthetic spectra were calculated for the ray path from the sun to the instrument and fitted to the observed spectra over selected spectral intervals (e.g., those in the lower panels of Figure 1.1.5). The synthetic spectra were calculated line-by-line using the ATMOS spectral linelist for both target and background gases for each model layer, except that for certain gases (e.g., N_2O_5, $CFCl_3$, CF_2Cl_2, CHF_2Cl), laboratory measured cross-sections were used directly [*Brown et al.,* 1995]. (Note that at the time the studies described in Chapter II were made, empirical spectral line parameters were being used for CHF_2Cl, but these had been verified against laboratory cross-sections of *Varanasi* [1992] and *McDaniel et al.* [1991].) Following the description of *Abrams et al.* [1995], the spectrum within a particular layer can be modelled by:

$$T_s(\nu_i,z)=\exp[-\Sigma_j \Sigma_k \kappa_{ijk} n_k \vartheta_{jk} \chi g_k] \qquad \text{(E1.1)}$$

where: T_s = synthetic (i.e., modelled) transmission

ν_i = frequency at spectral grid point i (cm^{-1})

z = altitude (km)

κ_{ijk} = absorption of the jth gas at the kth layer at frequency ν_i

n_k = total molecular density in the kth layer (molecules cm^{-3})

ϑ_{jk} = assumed mixing ratio of the jth gas in the kth layer

χ is a scale factor for ϑ_{jk} and equals unity for a non-target gas

g_k = slant path through the layer (cm).

Least-squares techniques were used to adjust the mixing ratio scale factor, χ, to achieve:

$$\Sigma_i \frac{\partial T_s(\upsilon_i,z)}{\partial \chi} R_i = 0 \qquad \text{(E1.2)}$$

where R_i is the residual, equal to the observed minus the synthetic transmission:

$$R_i = \left(T_o(\upsilon_i,z) - T_s(\upsilon_i,z)\right) \qquad \text{(E1.3)}$$

where T_o is the observed transmission. Note that the partial derivative in (E1.2) acts as a weighting function. The retrieval of a vertical mixing ratio profile was begun by fitting a spectral microwindow at the highest altitude for which there is discernable absorption by the target gas. In an onion-peeling technique, successively lower spectra were fitted in a similar fashion (while keeping mixing ratios above at the just determined values). This was repeated until a pre-determined lower altitude cutoff is reached, usually determined on the basis of the line opacity. Where several microwindows were evaluated for a target gas, a weighted average was made of the resultant individual profiles:

$$\chi_{mn} = \frac{\Sigma_n \left(\chi_n / \varepsilon_n^2\right)}{\Sigma_n \left(1/\varepsilon_n^2\right)} \qquad \text{(E1.4)}$$

where ε_n is the estimated precision error of the retrieved mixing ratio (discussed further in Appendix A). To avoid "staircases" from the atmospheric model's vertical resolution being smaller than the tangent height spacing of the measurements, resultant profiles were then smoothed by a five-point polynomial (corresponding to about 3 km in the vertical), while preserving the total column amount of the gas above the lowest retrieval height. This

smoothed profile was used as the assumed profile for a second retrieval. The entire process was repeated twice more, with the final profile produced on the third iteration interpolated on an atmospheric pressure grid of 12 levels per decade in mb.

For ground-based column spectra, the procedures were somewhat different. As the ATMOS instrument has a very fast scan time (2.2 s), several measurements were taken over a small range of solar zenith angles, and resulting spectra were averaged to increase signal-to-noise ratios. An appropriate atmospheric model was selected (e.g., the *U. S. Standard Atmosphere* [1976]), and the column absorption calculated using the 150 km layer model. Column densities were derived by scaling assumed trace gas mixing ratio profiles to best fit selected spectral microwindows. Error sources and treatment are discussed briefly in Appendix A.

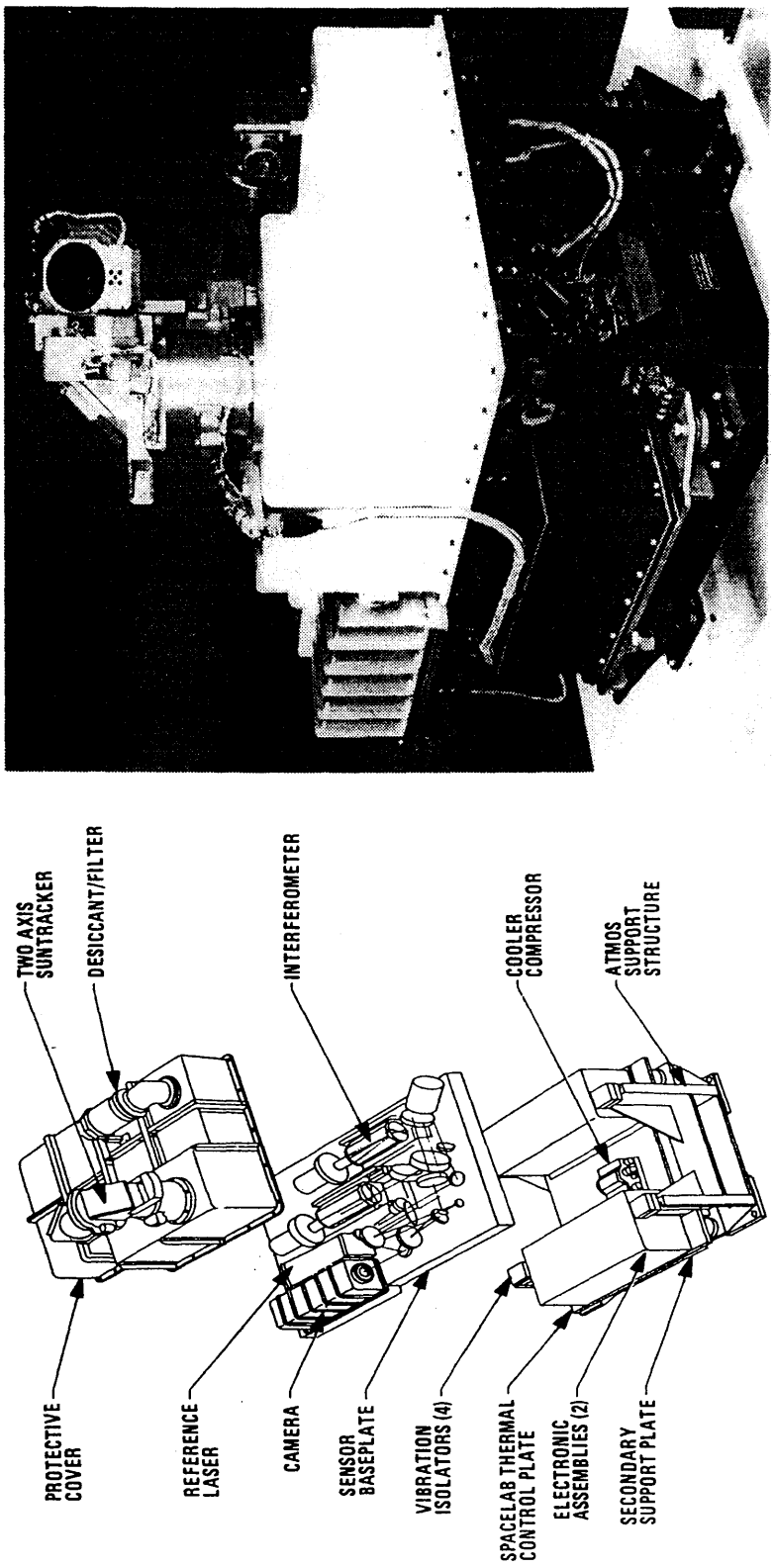

Figure 1.1.1: The ATMOS Fourier Transform Interferometer. The schematic on the left illustrates the optical and electronic subsystems, while a photograph of the assembled instrument is on the right.

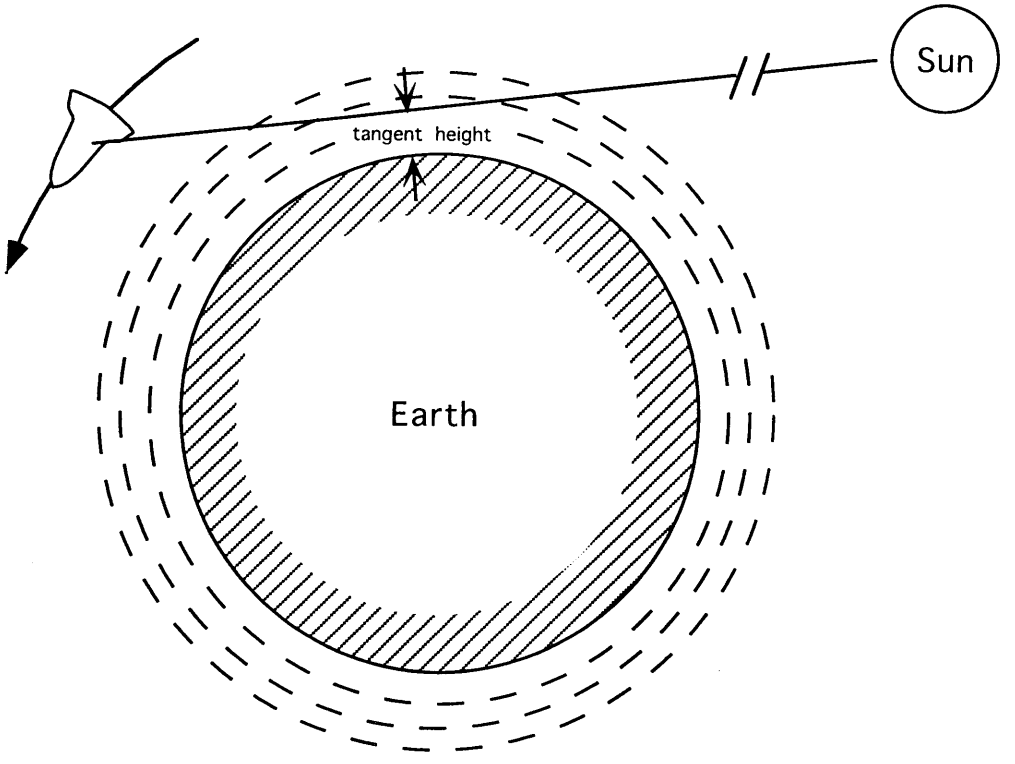

Figure 1.1.2: Simplified viewing geometry by ATMOS during a shuttle occultation.

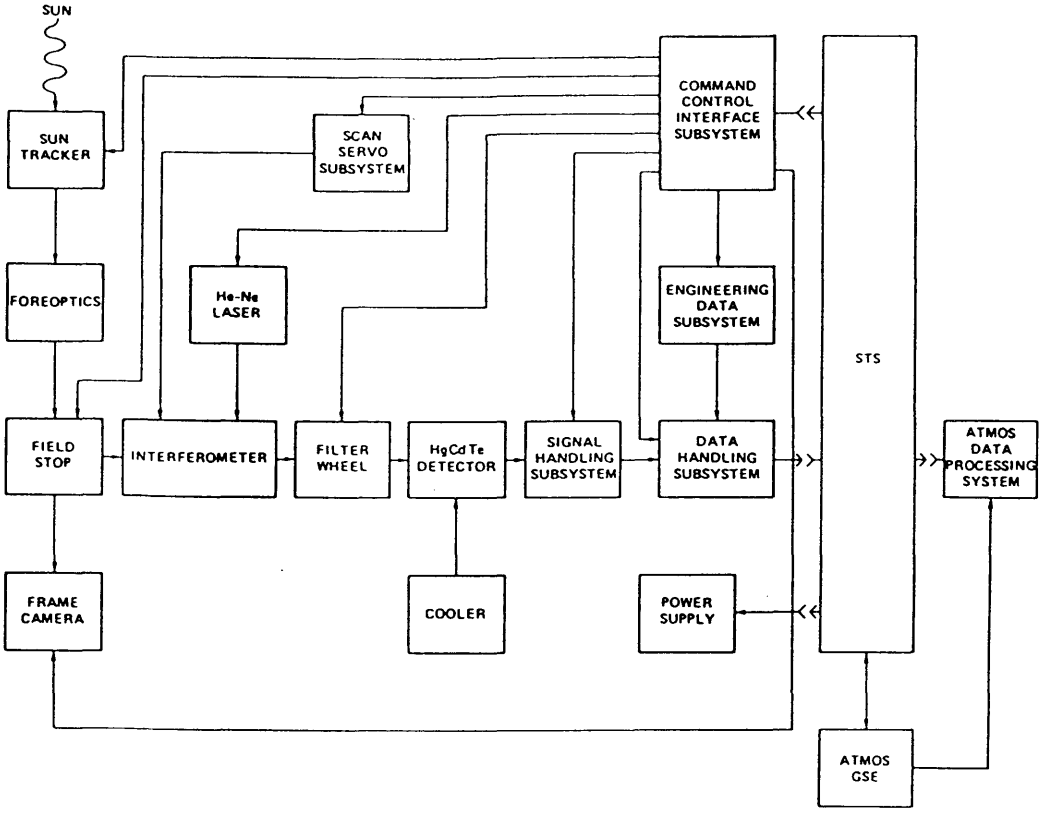

Figure 1.1.3: Block diagram of ATMOS instrument components (from *Farmer et al.* [1987])

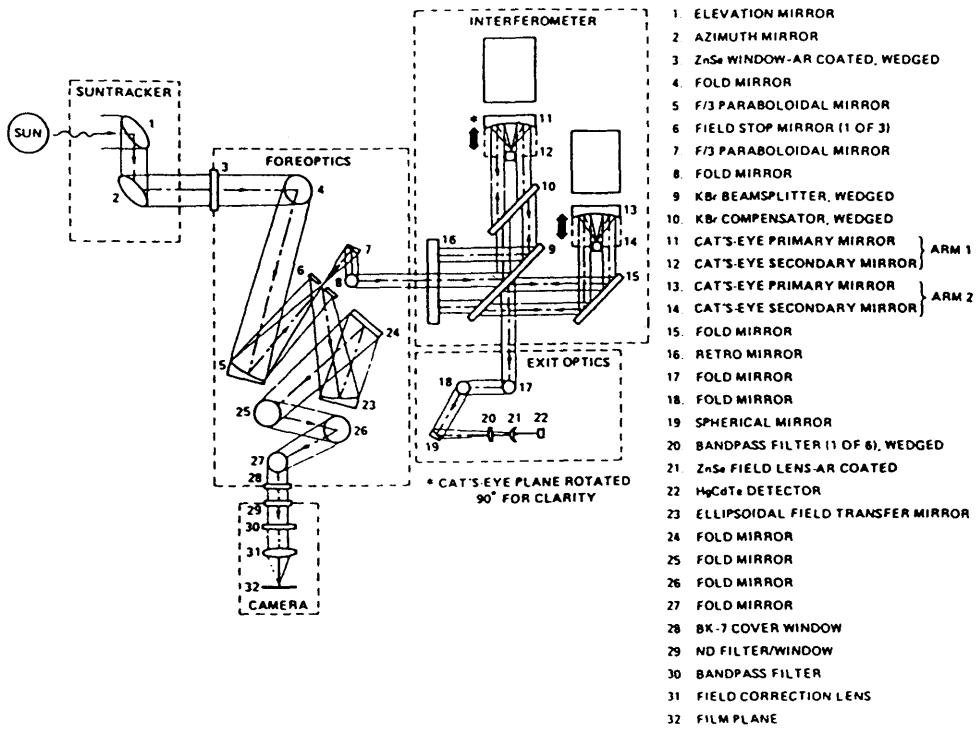

Figure 1.1.4: Schematic diagram of ATMOS optical components (from *Farmer et al.* [1987]).

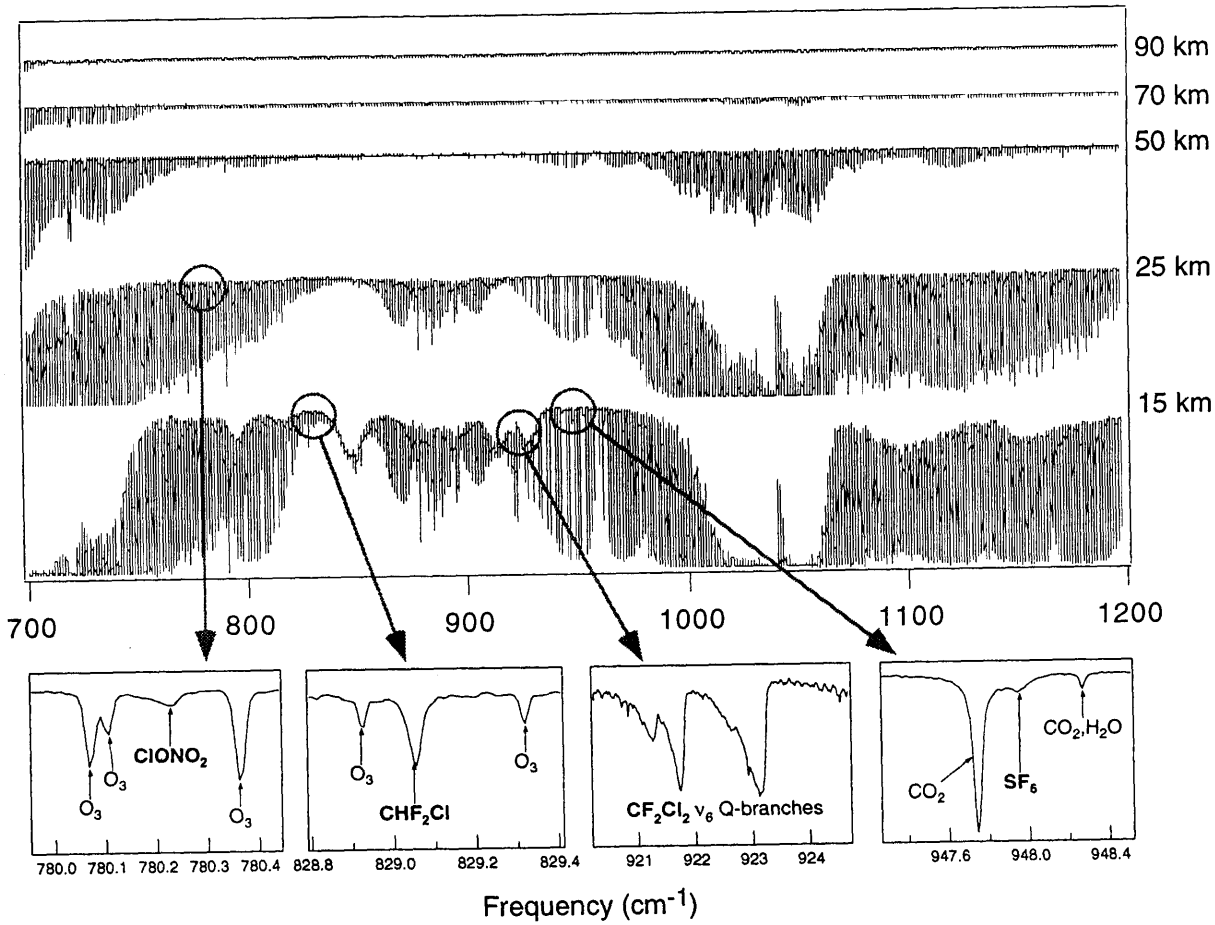

Figure 1.1.5: Typical ATMOS filter 1 spectra. The upper panel shows the same broad spectral region in successively lower tangent altitude observations while the lower panels show small spectral intervals ("microwindows") from which gas mixing ratios are determined. For clarity, vertical scales differ among displayed spectra.

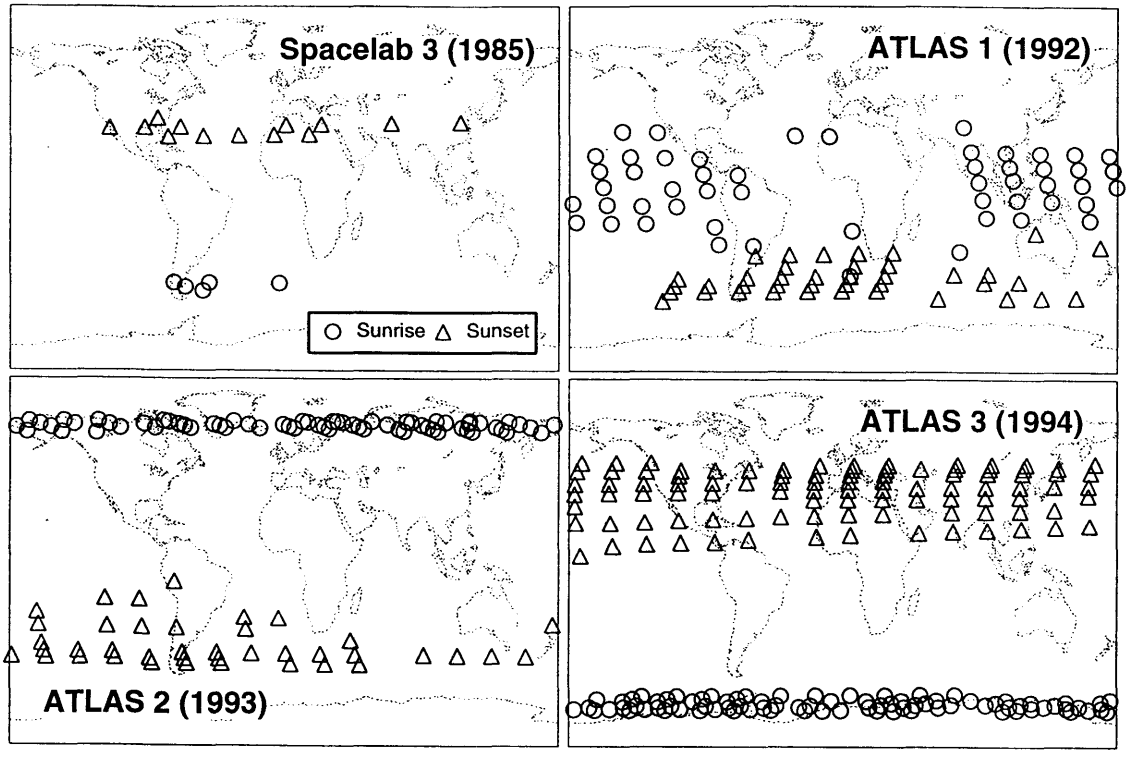

Figure 1.1.6: Distribution of ATMOS observations during each of four Space Shuttle missions. Spacelab 3: April 29-May 7, 1985; ATLAS-1: March 24-April 3, 1992; ATLAS-2: April 8-16, 1993; ATLAS-3: November 3-14, 1994.

1.2 CHF_2Cl and other replacement gases

As replacements for the fully halogenated chlorofluorocarbons (CFCs; e.g., CF_2Cl_2 and CCl_3F) and halons (e.g., CF_3Br and CF_2ClBr), hydrochlorofluorocarbons (HCFCs) such as CHF_2Cl (HCFC-22) and CH_3CClF_2 (HCFC-142b) have been increasingly emitted into the atmosphere. As the CFCs and halons are almost insoluble and chemically inert in the troposphere, their lifetimes are long compared to their tropospheric residence time. Their only effective sink is destruction by ultraviolet radiation in the stratosphere, where their chlorinated and brominated photolysis products can destroy ozone. On the other hand, HCFCs are hydrogenated, and can be destroyed by tropospheric OH. Their tropospheric lifetime is therefore much shorter, and their ability to reach the stratosphere is greatly reduced. (See, for example, *Kaye et al.* [1994].)

CHF_2Cl is the most widely used of the HCFCs finding its major application as a refrigerant [*Midgley and Fisher,* 1993]. It is expected to have only about 5% the ozone destruction capability of $CFCl_3$ when compared on the basis of unit mass emitted in the troposphere [*WMO,* 1995]. However, that HCFC emissions like those of CHF_2Cl are less harmful to stratospheric ozone does not make them benign, and the necessity to not just slow the growth of atmospheric chlorine loading but actually reduce it led to restrictions on the production of HCFCs, including that of CHF_2Cl, being added to the Montreal Protocol [*Rowlands,* 1993]. It therefore is important to monitor the rate of growth of CHF_2Cl to characterize and help predict its contribution to atmospheric chlorine loading.

A second reason to evaluate the trend in CHF_2Cl is that CFCs and HCFCs can have significant greenhouse absorptions. On a molecule-per-molecule basis, these gases can have a greater impact on atmospheric radiative forcing than those of CO_2 or CH_4 as many of their absorption bands (including some of CHF_2Cl) occur in the relatively transparent "atmospheric window" between 8 and 13 μm. The long-term amount of forcing by a gas depends not just on its total spectral absorption in the infrared, but also its

lifetime in the troposphere. For example, in a simplified scenario assuming current CO_2 levels and ignoring feedbacks, the radiative forcing of 1kg of CHF_2Cl released into the atmosphere is about 4300 times that of 1kg of CO_2 integrated over 20 years [*WMO*, 1995]. While their tropospheric concentrations may be much less than CO_2, radiative forcing by cumulative CFC and HCFC absorptions can be significant compared to the extra forcing caused by increasing levels of CO_2 [*Ramanathan*, 1988], and therefore justifies the monitoring of the growth of CHF_2Cl and other halocarbons.

Another reason to study CHF_2Cl growth in particular is to evaluate its utility in determining the global OH field. Historically, emission estimates and field measurements of methyl chloroform (CH_3CCl_3) have been used in models to simultaneously evaluate CH_3CCl_3 lifetime and the OH field; CH_3CCl_3 is a completely anthropogenic gas whose major sink is reaction with OH. (See *Prinn et al.* [1992] and references therein). It was suggested that gases with accurate emission histories and well calibrated measurements other than CH_3CCl_3 could be used for calculation of the OH field [*Prather and Spivakovsky*, 1990]. CHF_2Cl could be evaluated for such a purpose as it is also of completely anthropogenic origin, and its primary sink is reaction with OH.

Prior to 1993, calibration problems between spectroscopic methods and *in situ* techniques had prevented agreement on the atmospheric concentration of CHF_2Cl [*Kaye et al.*, 1994]. Therefore, updated spectroscopic cross-sections for CHF_2Cl in the infrared [*McDaniel et al.*, 1991; *Varanasi*, 1992] and new calibration scales for gas chromatography-mass spectrometry techniques [*Montzka et al.*, 1993] prompted re-analysis of the global increase of CHF_2Cl, and comparison between *in situ* and spectroscopic results. From ATMOS results at Table Mountain (described in Chapter II), the column CHF_2Cl amounts had increased by an exponential growth rate of (6.7±0.5)% from October, 1995 to July, 1990. These results were found to be slightly lower than, but within experimental error of the *in situ* results of *Montzka et al.* [1993] and infrared

column measurements at Kitt Peak, Arizona and the Jungfraujoch, Switzerland [*Zander et al.*, 1994]. However, modelling studies by Margaret Brown, described in Chapter II, indicated that the current uncertainty in CHF_2Cl emission estimates prevented adequate constraint of either the CHF_2Cl lifetime or the OH field, and so the use of CHF_2Cl measurement to infer OH levels offered no advantages over using CH_3CCl_3.

Continued tropospheric and stratospheric measurement of CHF_2Cl is warranted to evaluate any changes in its growth rate from changes in its emission levels or even changes in global OH field. As mentioned previously, many CFCs and HCFCs have significant absorptions in the infrared, and ATMOS spectra have been used to infer stratospheric increases in CF_2Cl_2 and CF_3Cl [*Zander et al.*, 1995] and CHF_2Cl [*Rinsland et al.*, 1995]. It is expected that as the concentration of other replacement HCFCs increase, their infrared absorptions will become significant (and measurable). Figure 1.2.1 illustrates an ATMOS/ATLAS-3 space-based spectral microwindow at a tangent altitude of 6.4 km, superimposed on which are modelled absorptions of CH_3CF_2Cl (HCFC-142b), the tropospheric concentration of which is currently increasing at 30% yr^{-1} [*WMO*, 1995]. Synthetic spectra assume current, and 10 and 30 times current mixing ratios. The increasing absorption expected of CH_3CF_2Cl is clearly apparent, and the illustration shows one of the many roles that infrared spectroscopy can play in monitoring secular changes in the atmosphere.

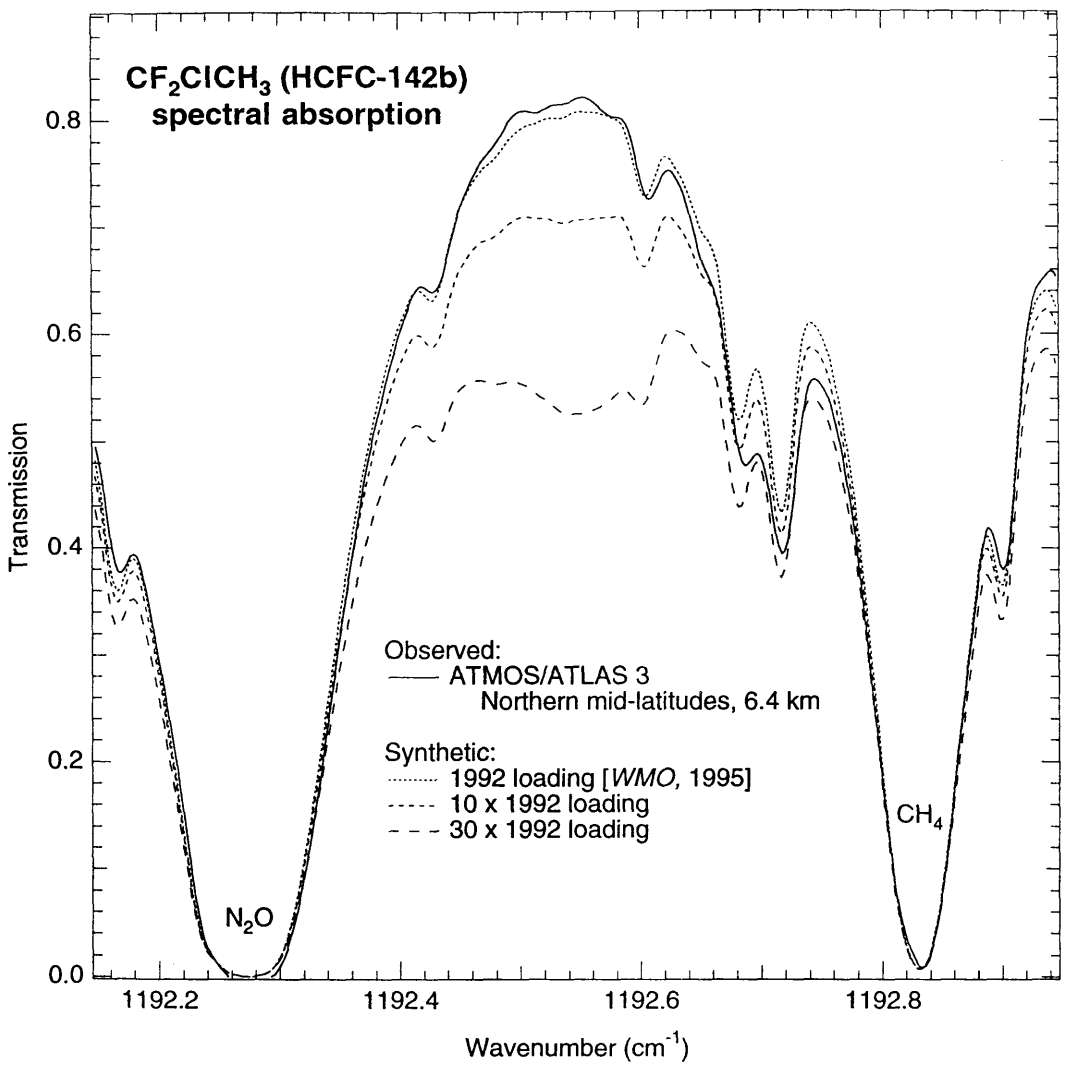

Figure 1.2.1: Modelled absorptions of CF_2ClCH_3 at about 1192 cm^{-1}. Computed absorptions of CF_2ClCH_3 are shown at a 1992 tropospheric mixing ratio of 3.5 pptv [*WMO*, 1995], 35 pptv and 105 pptv. For comparison, a November, 1994 spectrum from ATMOS/ATLAS-3 at tangent altitude of 6.4 km is displayed.

1.3 A note on the measurement of atmospheric isotopomers

It is often the case that the abundance of a trace isotopomer (an isotopically substituted species such as $^{16}O^{16}O^{18}O$ or $^{16}O^{18}O^{16}O$), in and of itself, is not of interest. Rather it is the ratio of such an abundance to that of the "regular" isotopomer, e.g. $[^{16}O^{16}O^{18}O]/[^{48}O_3]$, and how and where that ratio varies from a standard. (The standard used for the D/H and $^{18}O/^{16}O$ ratios is usually that of Standard Mean Ocean Water, SMOW, which reports the standard D/H ratio as 155.76×10^{-6} and the $^{18}O/^{16}O$ ratio as 2.005×10^{-3} [*IUPAC*, 1983].) Investigations of why such ratios vary can reveal subtle processes in geophysics and geochemistry. For example, isotopically labeled water has long been used in better understanding mechanisms of precipitation and its global patterns (e.g., *Dansgaard* [1964]), and validation of global circulation models [*Jouzel et al.*, 1991]. Data of excess carbon-14 (from nuclear weapon tests) have been used in evaluating advection and diffusion coefficients in the stratospheric modelling [*Shia et al.*, 1989]. A review of the mechanisms of isotopic fractionation and their effects on different planetary atmospheres can be found in *Kaye* [1987].

Enrichments (or depletions) of isotopomers from standard ratios are often expressed in percentages:

$$\text{Enrichment}\,(\%) = \frac{R_{sample} - R_{standard}}{R_{standard}} \times 100 \qquad \text{(E1.5)}$$

where R_{sample} is the isotopic abundance ratio in a sample (e.g. D/H in water), and $R_{standard}$ is the isotopic abundance calculated from a standard ratio. A slightly different notation widely used (particularly for water isotopes and used in Chapter IV of this work) is the so-

called delta notation, which expresses isotopic deviations on a per mil basis rather than a percentage:

$$\delta\,(‰) = \frac{R_{\text{sample}} - R_{\text{standard}}}{R_{\text{standard}}} \times 1000 \qquad \text{(E1.6)}$$

Chapter III and Section 1.4 of this introduction involve studies of stratospheric heavy ozone, while Chapter IV and Section 1.5 deal with isotopomers of water and methane. These two issues pose different scientific problems. In the case of heavy ozone, there have been numerous atmospheric, laboratory and theoretical studies done, but there is little apparent agreement on its stratospheric fractionation pattern or the mechanisms by which ozone is isotopically fractionated at all. ATMOS measurements provide the most extensive set of stratospheric heavy ozone observations, and may help to characterize any vertical, latitudinal and seasonal variation of the enrichments. For deuterated water and methane, the fractionation microphysics are thought to be well understood, but stratospheric measurement has been lacking, particularly for CH_3D. The study described in Chapter IV represents the most extensive set of stratospheric observations for these species, which may provide a powerful constraint for model calculations of water transport from the troposphere to the stratosphere.

1.4 Heavy ozone

This section reviews previous experimental and theoretical work done on the phenomenon of heavy ozone enrichment, expanding on the brief introduction on the subject given in Chapter III. Analysis results of ATMOS spectra are discussed.

1.4.1 Previous atmospheric measurements of heavy ozone

Stratospheric heavy ozone enrichment (which, for the purposes of this section, refer to those of $^{16}O^{16}O^{18}O$, $^{16}O^{18}O^{16}O$ and their sum in the form of $^{50}O_3$, except where otherwise noted) was first reported by *Mauersberger* [1981] using a balloon-borne mass spectrometer. (Note that in determining concentrations of heavy ozone, mass spectrometry does not distinguish between symmetric and asymmetric isotopomers.) *Mauersberger* [1981] found stratospheric enrichments of 0-40% in $^{50}O_3$, with a braod maximum between 28 and 38 km and a minimum at 20 km. The error was 15% at 30km, increasing above and below. (Stratospheric measurements are graphically summarized in Figure 3.1 on page 88.) Using mass-spectrometry, significant enrichments were again reported from two later balloon flights by *Mauersberger* [1987].

Using far-infrared thermal infrared emission measurements from a balloon-borne platform, *Abbas et al.* [1987a] were able to measure the individual absorptions of the $^{16}O^{18}O^{16}O$ and $^{16}O^{16}O^{18}O$ isotopomers. The $^{16}O^{16}O^{18}O$ enrichment had a maximum of $(40 \pm 14)\%$ at 37km, decreasing to $(-2 \pm 12)\%$ at 29 km, and increasing to $(20 \pm 15)\%$ at 25km. The $^{16}O^{18}O^{16}O$ enrichment was about $(18 \pm 15)\%$ at 25 km increasing to $(60 \pm 11)\%$ at 33 km. The finding of seemingly higher enrichments for $^{16}O^{18}O^{16}O$ than $^{16}O^{16}O^{18}O$ appears contradictory to laboratory production experiments of heavy ozone (discussed below) that tend to show symmetric isotopomers less enriched than asymmetric isotopomers [*Morton et al.*, 1989, 1990; *Anderson et al.* 1989; *Mauersberger et al.*, 1993].

Carli and Park [1988], also using thermal emission measurements, reported a $^{50}O_3$ enrichment of (10±10)% between 27 and 45km, which did not significantly vary with altitude. While they could measure individual $^{16}O^{18}O^{16}O$ and $^{16}O^{16}O^{18}O$ lines, they combined the measurements and did not report the individual enrichments. From balloon flights, *Schueler et al.* [1990] collected samples cryogenically, which were later analyzed by mass spectrometry.for both $^{50}O_3$ and $^{49}O_3$. In the first flight, $^{50}O_3$ was enriched 12--14%, and $^{49}O_3$ was enriched by 9–11%. In the remaining two flights, the enrichment was nearly mass-independent at 8–9%. The errors ranged from 0.5–1.5% for $^{50}O_3$.

Spectroscopic methods in the mid-infrared have been used to measure the abundance of the two $^{50}O_3$ isotopomers. *Rinsland et al.* [1985], using a ground-based Fourier-transform infrared (FTIR) spectrometer, found the column enrichments of $^{16}O^{16}O^{18}O$ and $^{16}O^{18}O^{16}O$ over Kitt Peak, Arizona to be (11 ± 11)% and (5 ± 7)% respectively, noting that no column enrichment could be shown within the range of the error bars. *Goldman et al.* [1989], from two balloon-based measurements using a Fourier transform infrared spectrometer, reported column averaged enrichments above 37 km of (20 ± 14)% and (16 ± 8)% for $^{16}O^{18}O^{16}O$, and (40 ± 18)% and (25 ± 12)% for $^{16}O^{16}O^{18}O$.

Krankowsky et al. [1995] reported the first seasonal study of heavy ozone enrichment and the first reported study of its behavior in the troposphere. They analyzed urban air samples using a mass spectrometer over a period of 12 months. They found that the $^{50}O_3$ enrichment was about 8 to 10% and did not vary with O_3 concentration. They could not find any seasonal variation or significant correlation with temperature. These results were consistent with laboratory measurements at similar temperatures and pressures.

To summarize, it seems to be well established that stratospheric enrichments of heavy ozone exist. However, the magnitude and vertical structure of this enrichment are a

source of confusion. An obvious question remains: Do the dissimilar obtained by the different techniques, as illustrated in Figure 3.1, reveal a highly variable structure as suggested by *Mauersberger et al.* [1993], or are the profiles dissimilar due to instrumental error and/or calibration bias?

1.4.2 Laboratory studies on heavy ozone

To our knowledge, the first laboratory study of heavy ozone enrichment was reported by *Sander et al.* [1977], using ultraviolet photolysis of oxygen. Results were variable; in one experimental run, they reported an exceedingly high enrichment of 95% for $^{50}O_3$, but all other runs were below 10%. Since that study, no other laboratory enrichments higher than about 20% have been reported.

Heidenreich and Thiemens [1983] synthesized heavy ozone with an electric discharge in a liquid N_2 cooled vessel. They found that both $^{50}O_3$ and $^{49}O_3$ were enriched almost equally (1-4%), while from mass-dependent fractionation chemistry, one would expect $^{49}O_3$ to have only about half the enrichment of $^{50}O_3$. To reduce the effect of isotopic exchange between O and O_2, *Heidenreich and Thiemens* [1986] essentially repeated their previous experiment, but at a temperature of 77K. Again, nearly equal enrichments for $^{49}O_3$ and $^{50}O_3$ were found. They proposed that three-body ozone formation was responsible for the observed enhancements:

$$O + O_2 + M \rightarrow O_3 + M \qquad \text{(R1.1)}$$

and suggested a symmetry effect, with the C_s (i.e., asymmetric) reaction intermediates $^{49}O_3^*$ and $^{50}O_3^*$ having longer lifetimes than the C_{2v} (i.e., symmetric) $^{48}O_3^*$. Since the C_s isotopomer has twice the number of rotational states as the C_{2v} isotopomer, more energy levels are made available for those of the collision partners in an inverse predissociative state, and the collisions may become "stickier." (See *Hertzberg* [1966], pg. 455.) *Yang and Epstein* [1987ab] also suggested a symmetry effect in the predissociation of "vibrationally hot" ozone.

Anderson et al. [1989] investigated symmetry effects by using a tunable diode laser and a mass spectrometer, and separately measured the enrichments of symmetric and asymmetric $^{50}O_3$ produced by electric discharge. It was found that the $^{16}O^{16}O^{18}O$ isotopomer accounted for 4/5ths of the enrichment, not 2/3rds as one would expect on purely statistical grounds. The symmetries of the ozone products were further investigated by *Morton et al.* [1989], who synthesized ozone with an electric discharge, and measured the resultant products from atomic masses 48 (i.e., $^{16}O^{16}O^{16}O$) to 54 (i.e., $^{18}O^{18}O^{18}O$). Results suggested the "more asymmetric" an ozone isotopomer (e.g. $^{16}O^{16}O^{18}O$ more asymmetric than $^{16}O^{18}O^{16}O$ or $^{16}O^{16}O^{17}O$), the greater the enrichment. For example, a maximum enrichment of (20.3 ± 0.2) % was found for $^{51}O_3$ (which would be primarily formed from one each of the ^{16}O, ^{17}O, and ^{18}O isotopes with very little $^{17}O^{17}O^{17}O$), while a slight depletion (0.9 ± 0.2) % was found for the symmetrical $^{18}O^{18}O^{18}O$.

In an attempt to identify the reactions controlling enrichment, *Morton et al.* [1990] dissociated ozone in the Chappuis band (500-700 nm), so that resultant oxygen and oxygen radicals were in their ground electronic states. A small amount of ozone was photodissociated within a bath of O_2 to see if enrichment was produced by the reaction

$$O(^3P) + O_2\,(^3\Sigma_g) + M \rightarrow O_3 + M \qquad \text{(R1.2)}$$

which is dominant at low O_3 and high O_2 concentrations. Pure ozone was photodissociated to measure isotope effects in the reaction:

$$O + O_3 \rightarrow 2O_2 \qquad \text{(R1.3)}$$

which dominates at low pressures and high O_3 concentrations. Enrichments were observed when O_2 was present in significant quantities, but no enrichments were seen when the pure ozone was dissociated. Thus, it was concluded that (R1.2) was a reaction producing enrichment. Morton et al. also investigated the temperature dependence of the $^{50}O_3$ enrichments via (R1.2), and found them linearly increasing from 7.5% at 100K to 17.5% at 400K. They also observed a decreasing enrichment with pressures above about

0.5 atm at a temperature of 321K (behavior later confirmed by *Thiemens and Jackson* [1990]). As discussed by *Morton et al.* [1990] and *Thiemens* [1992], if a longer-lived activated complex for the heavy isotopomers is used to explain the enrichment, that is, the reaction proceeds by the mechanism,

$$O + O_2 \leftrightarrow O_3^* \quad \text{(R1.4)}$$

$$O_3^* + M \rightarrow O_3 + M \quad \text{(R1.5)}$$

with heavier O_3^* longer lived than unsubstituted O_3^*, then enrichment should not be affected by pressure until deviation from third-order to second-order reaction kinetics begins to occur. (This change from third to second-order kinetics at high pressures had been shown for regular ozone formation, and was suggested to occur by the complexing of O or O_2 with M (e.g., N_2):

$$O + M \leftrightarrow OM \quad \text{(R1.6)}$$

$$OM + O_2 \rightarrow O_3 + M \quad \text{(R1.7)}$$

or:

$$O_2 + M \leftrightarrow O_2M \quad \text{(R1.8)}$$

$$O_2M + O \rightarrow O_3 + M \quad \text{(R1.9)}$$

with reactions (R1.7) or (R1.9) rate-limiting [*Croce de Cobos and Troe,* 1984]). Such a change in the reaction kinetics affecting the enrichments would be expected near about 8 atm at the temperature used in the experiment of *Morton et al.* [1990], much higher than where decreasing enrichment was observed to begin. From this, *Thiemens* [1992] concluded that theories explaining enrichments from differential lifetimes of the metastable states were therefore unlikely to be correct. (Although we note that new results reported by *Anderson and Mauersberger* [1995], discussed below, may lead to new insights into such activated complexes, and different interpretations of the results of *Morton et al.* [1990].)

Wen and Thiemens [1991] found a non-mass-dependent *depletion* effect in the thermal decomposition of heavy ozone. At a high temperature (110°C), thermally

decomposing ozone by the reaction

$$O_3 + M \rightarrow O + O_2 + M \qquad (R1.10)$$

produces isotopically heavy product O_2, enriched in ^{18}O and ^{17}O to a maximum of about 2%. The reason for this behavior was not understood.

Mauersberger et al. [1993] reported results from an experiment that was similar to two experiments by *Morton et al.* [1989, 1990] in that it examined enrichments of all possible molecular weights of ozone, and molecular oxygen and oxygen radicals were kept in their electronic ground state. Results indicated that heavy ozone enrichment occurred *only* in the asymmetric isotopomers, with asymmetric $^{51}O_3$ enriched by 18%, other isotopomers enriched between about 8% and 14%, and symmetric $^{18}O^{18}O^{18}O$ and $^{17}O^{17}O^{17}O$ depleted. Comparison of these results with those of *Morton et al.* [1989] showed that the enrichments produced by *Mauersberger et al.* [1993] using the visible light source were slightly less (≈1-4%) that which would be obtained using an electric discharge. This suggested the ground-state three-body reaction (R1.2):

$$O(^3P) + O_2\,(^3\Sigma_g) + M \rightarrow O_3 + M \qquad (R1.2)$$

was the predominant mechanism producing enrichment, but additional processes involving higher energy states could be involved in the enrichment of asymmetric heavy ozone.

It thus appears that the asymmetric isotopomers are enriched through the ground-state three-body ozone formation reaction (R1.2), but what other electronic states participate in the enrichment of symmetric and asymmetric isotopomers remains unclear. As will be seen below, the laboratory measurements have nevertheless played a strong role in disproving, or at least discounting, many of the attempts to explain theoretically the enrichments. Still, with the exception of the single run of *Sander et al.* [1977] previously noted, and which has not since been repeated, none of the laboratory measurements

reproduce the high enrichments seen in the stratosphere (e.g., the $^{50}O_3$ enrichment of 40% seen by *Mauersberger* [1981]).

1.4.3 Theoretical studies on heavy ozone enrichments

In an attempt to explain enrichments produced in an electric discharge, *Thiemens and Heidenreich* [1983] proposed that the cause of the enrichment was due to optical shielding by $^{16}O^{16}O$. The selective removal of lines from the Schumann-Runge bands resulted in preferential dissociation of $^{18}O^{16}O$ and $^{17}O^{16}O$. However, this was discounted on theoretical grounds by *Kaye and Strobel* [1983] and experimentally by *Yang and Epstein* [1987a]. Isotopic effects of O_2 dissociation should be obscured by isotopic exchange between atomic O and molecular O_2. In detailed theoretical calculations, *Kaye and Strobel* [1983] argued that the rapidity of the exchange reaction

$$^{18}O + {}^{32}O_2 \leftrightarrow {}^{16}O + {}^{34}O_2 \qquad \text{(R1.11)}$$

would prevent a heavy ozone enrichment, and predicted a slight depletion of heavy ozone at stratospheric conditions ($\approx$ -3.2% at 241.5K and 35 km altitude). *Kaye* [1986] examined theoretically the effect of isotopic substitutions on the ozone formation reaction:

$$O + O_2 + M \rightarrow O_3 + M \qquad \text{(R1.1)}$$

and the oxygen exchange reaction

$$O + O_2 \rightarrow O_2 + O \qquad \text{(R1.12)}$$

and found the reaction rates affected only slightly. Calculations predicted a small depletion of $^{50}O_3$ ($\approx$ -4.3% at 300K), although model uncertainties and approximations added considerable uncertainty. *Kaye* [1986] suggested that the effect of such model uncertainties and approximations may be important in understanding (then current) laboratory results.

Bates [1986] proposed that by taking account of the symmetry numbers (as they relate to the partition functions) in the three-body formation of ozone (R1.1), the formation reaction producing asymmetric heavy ozone would have twice the rate of regular ozone.

For symmetric heavy ozone, the rate would be one half times that of regular ozone. The net result was that heavy ozone was naturally enriched by 2/3. *Anderson and Kaye* [1987] pointed out that Bates had neglected that in an activated complex of an ozone isotopomer, the complex can decay into molecular and atomic oxygen isotopically distinct from the reactants, e.g.

$$^{16}O + {}^{16}O^{18}O \rightarrow {}^{16}O^{16}O^{18}O^* \qquad \text{(R1.13)}$$

$$^{16}O^{16}O^{18}O^* + M \rightarrow {}^{18}O + {}^{16}O^{16}O + M \qquad \text{(R1.14)}$$

Any enrichment of heavy ozone solely by symmetry effects would thus be eliminated. *Bates* [1987] accepted their conclusion.

A novel mechanism for mass-independent isotopic fractionation of ozone was proposed by *Valentini* [1987], which involved curve-crossing between photo-fragmentary $O_2(^1\Delta_g) + O(^1D)$ and $O_2(^3\Sigma_g) + O(^3P)$. Now, homonuclear $^{16}O^{16}O(^3\Sigma_g)$ can only have odd-J rotational states, but $^{18}O^{16}O(^3\Sigma_g)$ can have odd and even-J rotational states. So only $^{16}O^{16}O(^1\Delta_g)$ in odd-J rotational states can cross to $^{16}O^{16}O(^3\Sigma_g)$, while heteronuclear $^{17}O^{16}O$ and $^{18}O^{16}O$ in both odd and even-J rotational states can cross from the $^1\Delta_g$ to the $^3\Sigma_g$ state. Thus, via the curve crossing channel, the yield of heteronuclear $^{17}O^{16}O(^3\Sigma_g)$ and $^{18}O^{16}O(^3\Sigma_g)$ were both twice that of homonuclear $^{16}O^{16}O(^3\Sigma_g)$. The controlling effect was symmetry, not isotopic mass. The $O_2(^3\Sigma_g)$ reservoir would be enriched in heavy isotopes, the $O_2(^1\Delta_g)$ reservoir depleted, and since there are no bound O_3 states that correlate with $O_2(^1\Delta_g) + O(^1D)$ or $O_2(^1\Delta_g) + O(^3P)$, the product ozone would be enriched in heavy isotopes.

For explaining stratospheric heavy ozone enrichment, the mechanism of *Valentini* [1987] was deficient in some respects. First, as pointed out by Valentini the stratospheric $O(^3P) + O_2(^3\Sigma_g)$ recombination rate, and the production rate of $O_2(^1\Delta_g)$ via O_3 dissociation, are both very slow compared to $O_2(^1\Delta_g)$ quenching. Isotopic fractionation among O and O_2 reactants dissipates faster than a heavy ozone enrichment can be

produced. *Valentini* [1987] estimated that stratospheric enrichment of O_3 and $O_2(^3\Sigma_g)$ would only be about 10^{-5} with this scheme. Second, the curve-crossing mechanism of *Valentini* [1987] would predict that resulting heavy ozone isotopomers would be partitioned two-thirds in $^{16}O^{16}O^{18}O$ and one-third in $^{16}O^{18}O^{16}O$, as would be statistically expected. This turned out to be contrary to the laboratory results of *Anderson et al.* [1989], *Morton et al.* [1990], and *Mauersberger et al.* [1993], who found the asymmetric isotopomers preferentially enriched. Third, *Morton et al.* [1990], had enriched heavy ozone with molecular oxygen in the ground $^3\Sigma_g$ state, not the excited $^1\Delta_g$ state, and no curve-crossing mechanism was required.

Symmetry again played a role in papers by *Bates* [1988, 1990] in which it was suggested that at steady-state conditions, metastable states of asymmetric heavy ozone, $^{16}O^{16}O^{18}O^*$ are preferentially formed. Distinguishing between the states $^{16}O\sim^{16}O^{18}O^*$ and $^{18}O\sim^{16}O^{16}O^*$, where ~ signifies a newly formed bond and the energy is non-randomized, he argued that the rates of formation of these two isotopomers are additive as long as they can be distinguished from one another. He suggested that the rate of formation of $^{16}O^{16}O^{18}O$ is $(1+\delta)$ times that of regular ozone, where δ is the "rate additivity", given by the formula:

$$\delta = \frac{1}{\tau_D}\int_0^{\tau_D} \exp(-t/\tau_R)\,dt$$

$$= \left\{\frac{\tau_R}{\tau_D}\right\}\left\{1-\exp\left(-\frac{\tau_D}{\tau_R}\right)\right\} \qquad \text{(E1.3)}$$

where τ_D and τ_R are the dissociation and energy randomization time constants respectively. *Bates* [1990] presented calculations estimating that δ=0.74. This scheme would lead to enrichments in asymmetric heavy ozone only. The predicted enrichments were consistent with some of the higher enrichments seen in the stratosphere, but could not account for the

lower enrichments seen in the laboratory. *Bates* [1990] suggested that the lower enrichments in the laboratory were due to the reaction:

$$^{50}O_3 + {}^{32}O_2 \rightarrow {}^{48}O_3 + {}^{34}O_2 \qquad \text{(R1.15)}$$

either in the gas phase or on the walls of the surface vessel. This was disputed by *Thiemens* [1992], because (R1.13) would be a mass-dependent reaction while in the laboratory, low (<5%) mass-independent enrichments of $^{50}O_3$ and $^{49}O_3$ have been produced. To account for enrichments in asymmetric heavy ozone, *Bates* [1990] proposed "flips" of a terminal oxygen atom on an activated ozone complex, e.g.

$$^{16}O\text{~}^{16}O^{18}O^* \rightarrow {}^{16}O\text{~}^{18}O^{16}O^* \qquad \text{(R1.16)}$$

$$^{16}O\text{~}^{18}O^{16}O^* \rightarrow {}^{18}O\text{~}^{16}O^{16}O^* \qquad \text{(R1.17)}$$

$$^{18}O\text{~}^{16}O^{16}O^* \rightarrow {}^{16}O\text{~}^{16}O^{18}O^* \qquad \text{(R1.18)}$$

In later Monte Carlo simulations, *Morgan and Bates* [1992], presented calculations indicating that because of such flips, the ratio of enrichment of the symmetric isotopomer to that of the asymmetric isotopomer should be about 0.38, which was in good agreement with the result of *Anderson et al.* [1989] of 0.40 ± 0.17. Experimentally, however, *Larsen et al.* [1992] presented evidence that ozone formation is primarily "end-on," although measurement error could allow for a 15% cyclic intermediate channel.

An explanation for some of the enrichment of heavy ozone may have been provided by *Miller et al.* [1994]. In a series of experiments, Miller et al. found that in the photodissociation of ozone at 226 nm:

$$O_3 + h\nu \rightarrow O_2(^1\Delta_g) + O(^1D) \qquad \text{(R1.19)}$$

$$\rightarrow O_2(^3\Sigma_g) + O(^3P) \qquad \text{(R1.20)}$$

the distribution of vibrational states of $O_2(^3\Sigma_g)$ was remarkably bi-modal, with peaks at

v=14 and v=27. They theorized that such "vibrationally hot" $O_2(^3\Sigma_g)$ can quickly react further with oxygen in a net production sequence for ozone:

$$O_3 + hv \rightarrow O_2(^3\Sigma_g, v > 26) + O \quad \text{(R1.21)}$$

$$O_2(^3\Sigma_g, v > 26) + O_2 \rightarrow O_3 + O \quad \text{(R1.22)}$$

$$2\,(O_2 + O) \rightarrow 2O_3 \quad \text{(R1.23)}$$

$$\text{Net: } 3\,O_2 \rightarrow 2\,O_3$$

As discussed by Miller et al., the new mechanism can have implications for heavy ozone enrichment. Recalling the results of *Valentini* [1987], $^{16}O^{18}O(^1\Delta_g) + O(^1D)$ is twice as likely to "curve-cross" to $^{16}O^{18}O(^3\Sigma_g)+O(^3P)$ than $^{16}O^{16}O(^1\Delta_g)+O(^3P)$ will cross to $^{16}O^{16}O(^3\Sigma_g)+O(^3P)$. Thus the channel (R1.20) is more favorable for a photodissociating heavy ozone molecule than for a regular ozone molecule. Note also that at least one of the oxygen atoms in the photodissociating O_3 on the left hand side of (R1.21) is incorporated into the ozone on the right-hand side of (R1.22). The combined effect gives a heavy O atom greater probability to stay within the pool of O_3 and O_2 and not be "scrambled out" by the O-O_2 exchange reaction (R1.11). Reactions (R1.21) and (R1.22) can thus cycle to enrich heavy ozone until a termination reaction, e.g., $O + O_3 \rightarrow 2O_2$, is reached. Miller et al. presented calculations that accounted for a 5% enrichment at 40 km decreasing to 0.6% at 55 km. It is again noted that the reaction scheme of (R1.21) through (R1.23) has not been verified experimentally.

Theoretical studies have, to date, been unable to fully explain the laboratory or atmospheric studies, although some research of late may prove fruitful. Recently, *Anderson and Mauersberger* [1995] reported evidence for three electronically excited states of ozone at an energies slightly above the dissociation energies of the ground state. They discussed the possibility that these low-lying states may be involved in the three-body

ozone formation reaction, and speculated that these excited states may have a role in heavy ozone enrichment. The impact of this new research into ozone chemistry, and heavy ozone enrichment, remains to be determined, however.

1.4.4 Results of ATMOS analyses

It would appear that little scientifically would be gained by analysis of a single ATMOS occultation, other than to add to the set of disparate measurements already made. However, the sheer number of available occultations from the space-based ATMOS data set, their latitudinal range, and the number of measurement days of the ATMOS instrument from Table Mountain allow two outstanding questions to be answered. First, how variable are the vertical profiles of heavy ozone enrichment? Second, does this enrichment vary by latitude or season?

Recalling the laboratory work of *Morton et al.* [1990], who measured relatively little variation within the range of temperatures and pressures typical of the stratosphere, the finding of a low variability by ATMOS might be evidence for the three-body ozone formation reaction (R1.2) primarily operating to enrich stratospheric heavy ozone. It is also useful to characterize any variation of heavy ozone as the photolysis products of enriched heavy ozone can be used in other atmospheric studies. *Yung et al.* [1991] proposed that the observed ≈0.5% ^{18}O enrichment in CO_2 [*Gamo et al.*, 1989; *Thiemens et al.*, 1991] could be used as an indirect measure of $O(^1D)$ in the stratosphere considering the reaction scheme:

$$^{18}O(^1D) \text{ (from } ^{16}O^{16}O^{18}O \text{ photolysis)} + CO_2 \rightarrow CO_3^* \qquad \text{(R1.22)}$$

$$CO_3^* \rightarrow C^{18}O^{16}O + {}^{16}O \qquad \text{(R1.23)}$$

The "heaviness" of the $^{50}O_3$ photolysis products can also be used as a tracer for other stratospheric reactions. *Yung et al.* [1995] lists reactions possibly producing HNO_3 and H_2SO_4 (via photolysis of COS) enriched in heavy oxygen because their production

pathway involves reaction with O_3. Analyses of such reaction schemes will be greatly aided if the vertical structure of the heavy ozone enrichment is well defined.

Results of analyses of ATMOS space-based spectra, described in Chapter III, show an average (15±6)% enrichment for $^{16}O^{16}O^{18}O$, (10±7)% for $^{16}O^{18}O^{16}O$, and (13±5)% for $^{50}O_3$ (1σ standard deviation). Results also indicate that the vertical and latitudinal variability of the $^{16}O^{16}O^{18}O$ and $^{16}O^{18}O^{16}O$ enrichment is relatively small. This suggests a relatively small sensitivity of the enrichments to temperature and pressure representative of the stratosphere, in qualitative agreement with the laboratory results of *Morton et al.* [1990]. Column measurements of the $^{16}O^{16}O^{18}O$ enrichment over TMF, with an average of (17±4)%, show little seasonal variability within the uncertainty, in qualitative agreement with the tropospheric measurements of *Krankowsky et al.* [1995]. On an absolute basis, however, both the $^{16}O^{16}O^{18}O$ and $^{16}O^{18}O^{16}O$ enrichments found in the ATMOS study are, on average, higher than what is expected if stratospheric heavy ozone enrichment were completely (or even primarily) caused by the three-body ozone formation reaction (R1.2), and no other formation mechanism has been shown to create ozone in appreciable amounts in the 25-40 km altitude range of our measurements.

It is therefore difficult to quantitatively reconcile the results described here with those measured previously in the laboratory. This suggests the possibility that the line intensities used for the spectroscopic analyses of $^{16}O^{16}O^{18}O$ and $^{16}O^{18}O^{16}O$ may be biased too low, resulting in heavy ozone retrievals biased too high. A laboratory double-check of these line intensities is warranted to determine if a scaling of the results given in Chapter III is justified. If the current intensities are found to be reasonably accurate, then the ATMOS results indicate that there are currently unknown processes involved in the creation (or destruction) of stratospheric ozone. Other than this, it appears that research should be directed towards better understanding the unknown, but perhaps fundamental, details in the three-body formation of ozone. If laboratory and stratospheric measurements

have not completely elucidated the reasons for the enrichment, they have at least narrowed the range of the problem. Nevertheless, the anomaly of heavy ozone enrichment remains today as much a challenge to explain as it has been for the past 15 years.

1.5 HDO, CH_3D and implications for tropospheric-stratospheric exchange

The study of atmospheric HDO and CH_3D cannot be separated from that of H_2O and CH_4. Some characteristics of H_2O, CH_4, HDO and CH_3D in the stratosphere are briefly reviewed. Competing theories of troposphere-stratosphere exchange and the implications of the measurement of the D/H ratio in water on the validity of these theories are outlined. Finally, ATMOS results of deuterated water and methane and their implications are presented and further areas for study suggested.

1.5.1 Stratospheric water and methane

The hydrogen loading of the stratosphere is effectively $2(H_2O+2CH_4+H_2)$, as the abundance of other hydrogen-containing gases is very small compared to this sum. In an indirect way, these gases play a role in regulating stratospheric ozone, as reaction with $O(^1D)$ is an important source of the OH radical which attacks ozone (e.g., *Brasseur and Solomon* [1986]). Stratospheric water plays another important indirect role in ozone depletion. It is incorporated into sulfuric acid aerosol, leading to heterogeneous surface reactions producing HOCl and Cl_2 from reaction of $ClONO_2$ with H_2O and HCl, respectively. The diurnally varying odd nitrogen species N_2O_5 is converted to HNO_3 by reaction with H_2O on such aerosols, and this indirectly affects ozone destruction because NO_2 (from N_2O_5 photolysis) sequesters ClO into $ClONO_2$. Many reactions sequestering N_2O_5, and converting chlorine reservoir and sink species to active species, occur readily on frozen ice, HNO_3 hydrates and supercooled and frozen sulfate aerosols in the cold polar night, leading to the Antarctic ozone hole in the austral spring [*WMO,* 1995].

Being long-lived in the mid-to-lower stratosphere, water is controlled by a combination of transport and methane oxidation (e.g., *Brasseur and Solomon* [1986]). However, the stratosphere is exceedingly dry, with H_2O mixing ratios of only a few parts-per-million in the lower stratosphere. Excluding extremely cold and dehydrated regions within the Arctic and Antarctic vortices, the mixing ratio of stratospheric H_2O tends to be a

minimum at the tropical tropopause or in a region up to 2 km above. This water vapor minimum, the hygropause, is believed to be a consequence of a seasonal variation in the mixing ratio of water entering the stratosphere. The static stability of the lower stratosphere coupled with the slow rate of ascent allows this "seasonal signature" minimum to be transported upwards with time, and discernable for as long as a year [*Mote et al.*, 1995; *Boering et al.*, 1995; *Abbas et al.*, 1995a; *Holton et al.*, 1995].

Above the tropical hygropause, and throughout the rest of the stratosphere (excluding the vortices), the H_2O mixing ratio increases with altitude as the air becomes older, and CH_4 and H_2 are oxidized by OH, $O(^1D)$ and, for CH_4, Cl. However, in the mid to lower stratosphere at all latitudes except in the dehydrated regions of the polar vortices, the sum $2CH_4+H_2O$ has been shown on average to be about constant. The increase in H_2O is about equal to twice the decrease in CH_4, with the H_2 mixing ratio ($\approx$0.5 ppmv) varying little. This is not to say that H_2 is unreactive. Rather, its production from CH_4 (via a short-lived CH_2O intermediate) and destruction by oxidation roughly balance each other [*Dessler et al.*, 1994; *Abbas et al.*, 1995b]. In order to use ATMOS stratospheric measurements to estimate the average mixing ratio of H_2O as air enters the stratosphere, the *in situ* contribution of CH_4 oxidation to the water mixing ratio must be subtracted (as had been done by *Abbas et al.* [1995a] with ATMOS/ATLAS-3 data).

Analogously to CH_4 and H_2O, stratospheric HDO is controlled by transport and oxidation of CH_3D. Likewise, the contribution of CH_3D loss must be subtracted to estimate the entering HDO mixing ratio (and the D/H ratio in water), as previous measurements of the deuterium content of stratospheric water have shown that the D/H ratio in water increases with altitude [*Pollock et al.*, 1980; *Rinsland et al.*, 1984, 1991; *Abbas et al.*, 1987b; *Carli and Park*, 1988; *Dinelli et al.*, 1991]. It has not been established, however, that the sum CH_3D+HDO is about constant as is the case for $2CH_4+H_2O$; the destruction of CH_3D may not be one-to-one with the production of HDO.

The reaction pathway from CH_3D to HDO and HD is that the D/H branching may not follow simple statistics and HD production may not be in balance with its oxidation. Indeed, in the only previous report of both stratospheric CH_3D and HDO measurements (ATMOS Spacelab 3 measurements by *Rinsland et al.* [1991]), data were too sparse to quantitatively relate the destruction of CH_3D to the creation of HDO.

1.5.2 Mechanisms of exchange across the tropical tropopause

Theories explaining tropospheric-stratospheric transport must quantitatively account for the dryness of the lower stratosphere, but exactly how air is dehydrated as a parcel rises through the troposphere *and* crosses the tropopause is a matter of debate. As discussed in *Holton et al.* [1995] and *Moyer et al.* [1995], widespread gradual uplift of air in the tropics across the tropopause cannot be the only method of water transport into the stratosphere; a large resultant cirrus cloud cover is not seen, and the average tropical tropopause temperatures are too warm for the low stratospheric mixing ratios observed. Other theories have suggested gradual uplift in more isolated (and colder) regions [*Newell and Gould-Stewart*, 1981] or rapid convection by cumulonimbus towers penetrating the tropopause [*Danielsen,* 1982]. The former scenario represents a slow, quasi-equilibrium process. The latter can be a non-equilibrium process as water can be advected rapidly up from the boundary layer and deposited as ice in the stratosphere (although under certain conditions, stratospheric dehydration can occur if stratospheric water is entrained into ice crystals large enough to fall out). These two scenarios can have very different implications for the deuterium content of stratospheric water.

1.5.3 The use of HDO in evaluating tropical cross-tropopause transport

The substitution of a deuterium atom for a hydrogen atom in water significantly decreases its vapor pressure in a manner that is a strong function of temperature, particularly at temperatures representative of the mid-to-upper troposphere (e.g., *Kaye* [1987]; *Dansguaard* [1964]). In the troposphere, the lower vapor pressure of HDO

compared to H_2O isotopically fractionates water vapor as it ascends to regions of lower temperatures, i.e., the water becomes "lighter," and the HDO/H_2O ratio decreases as HDO is preferentially condensed. As discussed by *Moyer et al.* [1995], the slow uplift of air through the tropopause will tend to strongly deplete water in deuterium. On the other hand, the deuterium content of the water may be higher in rapid convective updrafts because it can be carried in the form of lofted ice particles, or because of kinetic fractionation effects under highly supersaturated conditions prevent equilibrium isotopic partitioning. Measurements of the HDO/H_2O ratio in stratospheric water can help discriminate between competing theories of water transport from the troposphere to the stratosphere; any theory that successfully explains the amount of entering water must simultaneously explain the amount of HDO.

1.5.4 ATMOS HDO and CH_3D results

As discussed in Chapter IV, ATMOS measurements from Spacelab 3, and ATLAS-1, -2, and -3 were used first to characterize the relationship of CH_3D to CH_4, and showed that stratospheric methane becomes progressively enriched in deuterium as the CH_4 mixing ratio decreases. This was expected since the reaction rate constants of CH_3D with OH and Cl are less than those for CH_4. From ATMOS HDO measurements and CH_3D mixing ratios inferred from co-located CH_4, it was found that the stratospheric production of HDO is roughly equal to the destruction of CH_3D; a slope of $-(1.0\pm0.1)$ was found for a plot of HDO vs CH_3D mixing ratio (1σ combined systematic and random error). Stratospheric changes in the HD mixing ratio were therefore constrained to be ±0.1 molecules created per molecule of CH_3D destroyed, assuming negligible amounts of total D in other molecules.

The HDO and inferred CH_3D mixing ratios were combined with ATMOS H_2O and CH_4 mixing ratios [*Abbas et al.*, 1995a] to derive stratospheric D/H ratios in water corrected for the hydrogen and deuterium contributions of methane oxidation [*Moyer et al.*, 1995]. Results showed that water entering the stratosphere was depleted in deuterium

(using the SMOW standard) by an average of 68±8% (1σ combined systematic and random error), and showed no latitudinal or seasonal variation. Modelling results by *Moyer et al.* [1995] indicated that the gradual uplift of water in the troposphere and through the tropopause should result in an 80-90% depletion of deuterium, but ATMOS results were consistent with water vapor experiencing rapid convection to at least upper tropospheric levels.

The isotopic signal in water was shown to provide a powerful constraint on theories of water transport, and ATMOS data can still be further analyzed for this purpose. Due to the limited precision of the measurements and few number of observations made directly in the tropics from ATLAS-3 (and none available near the tropical tropopause from ATLAS-1 due to Pinatubo aerosol), ATMOS results (from filters 2 and 9) were not able to be used to determine a seasonal signal in HDO akin to the behavior of the hygropause, which would have helped in determining the exact mechanism of water transport across the tropopause. With improved spectral line parameters for weak HDO lines in the ν_2 band (in filter 3), it may be possible to combine and average results from filters 2, 3 and 9 within narrow latitude bands and determine the seasonal variation. The use of these weak lines would extend the range of HDO measurement below about 100 mb down to the 300 mb level, near the level of the tropopause in the mid-latitudes. Examination of the D/H ratio in water at this level may give information on the extent and effect of tropospheric incursions of water into the lower mid-latitude stratosphere by Rossby waves (see *Holton et al.* [1995]).

References

Abbas, M. M., J. Guo, B. Carli, F. Mencaraglia, M. Carlotti and I. G. Nolt, Heavy ozone distribution in the stratosphere from far-infrared observations, *J. Geophys. Res.*, *92*, 13231, 1987a.

Abbas, M. M., J. Guo, B. Carli, F. Mencaraglia, A. Bonetti, M. Carlotti and I. G. Nolt, Stratopsheric O_3, H_2O, and HDO distributions from balloon-based far-infrared observations, *J. Geophys. Res., 92,* 8354-8364, 1987b.

Abbas, M. M., H. A. Michelsen, M. R. Gunson, M. C. Abrams, M. J. Newchurch, R. J. Salawitch, A. Y. Chang, A. Goldman, F. W. Irion, G. L. Manney, E. J. Moyer, R. Nagaraju, C. P. Rinsland, G. P. Stiller, and R. Zander, Seasonal cycle of water vapor entry into the stratosphere from ATMOS/ATLAS-3 measurements, submitted to *Geophys. Res. Lett.*, 1995a.

Abbas, M. M., M. R. Gunson, M. J. Newchurch, H. A. Michelsen, R. J. Salawitch, M. Allen, M. C. Abrams, A. Y. Chang, A. Goldman, F. W. Irion, E. J. Moyer, R. Nagaraju, C. P. Rinsland, G. P. Stiller, and R. Zander, The hydrogen budget of the stratosphere inferred from ATMOS measurements of H_2O and CH_4, submitted to *Geophys. Res. Lett.,* 1995b.

Abrams, M. C., M. R. Gunson, M. M. Abbas, A. Y. Chang, A. Goldman, F. W. Irion, H. A. Michelsen, M. J. Newchurch, C. P. Rinsland, R. J. Salawitch, G. P. Stiller, and R. Zander, On the assessment of atmospheric trace gas burdens with high resolution infrared solar occultation measurements from space, *Geophys. Res. Lett.,* in preparation, 1995.

Anderson, S. M. and J. A. Kaye, Comment on "Heavy ozone in the stratosphere," *Geophys. Res. Lett., 14*, 91-93, 1987.

Anderson, S. M., J. Morton and K. Mauersberger, Laboratory measurements of ozone isotopomers by tunable diode absorption spectroscopy, *Chem. Phys. Lett., 156*, 175-180, 1989.

Anderson, S. M. and K. Mauersberger, Ozone absorption spectroscopy in search of low-lying electronic states, *J. Geophys. Res., 100*, 3033-3048, 1995.

Bates, D. R., Heavy ozone in the stratosphere, *Geophys. Res. Lett., 13*, 664-666, 1986.

Bates, D. R., Reply, *Geophys. Res. Lett., 14*, 94, 1987.

Bates, D. R., Suggested explanation of heavy ozone, *Geophys. Res. Lett., 15*, 13-16, 1988.

Bates, D. R., Isotopic fractionation in the formation of ozone and of carbon monoxide, *J. Chem. Phys., 93*, 8739-8744, 1990.

Boering, K. A., E. J. Hintsa, S. C. Wofsy, J. G. Anderson, B. C. Daube Jr., A. E. Dessler, M. Loewenstein, M. P. McCormick, J. R. Podolske, E. M. Weinstock, and G. K. Yue, Measurements of stratospheric carbon dioxide and water vapor at northern midlatitudes: Implications for troposphere-to-stratosphere transport, *Geophys. Res. Lett., 22*, 2737-2740, 1995.

Brasseur, G., and S. Solomon, *Aeronomy of the Middle Atmosphere*, 452 pp., D Reidel, Dordrecht, 1986.

Brown, L. R., M. R. Gunson, R. A. Toth, F. W. Irion, and C. P. Rinsland, The 1995 Atmosphere Trace Molecule Spectroscopy (ATMOS) Linelist, submitted to *Appl. Opt.*, 1995.

Carli, B. and Park, J. H., Simultaneous measurement of minor stratospheric constituents with emission far-infrared spectroscopy, *J. Geophys. Res., 93*, 3851-3865, 1988.

Croce de Cobos, A. E. and J. Troe, High-pressure range of the recombination $O+O_2 \rightarrow O_3$, *Int. J. Chem. Kinet., 16*, 1519-1530, 1984.

Danielsen, E. F., A dehydration mechanism for the stratosphere, *Geophys. Res. Lett., 9,* 605-608, 1982.

Dansgaard, W., Stable isotopes in precipitation, *Tellus, 16*, 436-468, 1964.

Dessler, A. E., E. M. Weinstock, E. J. Hintsa, J. G. Anderson, C. R. Webster, R. D. May, J. W. Elkins and G. S. Dutton, An examination of the total hydrogen budget of the lower stratosphere, *Geophys. Res. Lett., 21,* 2563-2566, 1994.

Dinelli, B. M., B. Carli and M. Carlotti, Measurement of stratospheric distributions of $H_2{}^{16}O$, $H_2{}^{18}O$, $H_2{}^{17}O$, and $HD^{16}O$ from far infrared spectra, *J. Geophys. Res., 96*, 7509-7514, 1991.

Farmer, C. B., O. F. Raper and F. G. O'Callaghan, *Final Report on the First Flight of the ATMOS Instrument During the Spacelab 3 Mission, April 29 Through May 6, 1985*, JPL Publication 87-32, Jet Propulsion Laboratory, California Institute of Technology, Pasadena, CA, 1987.

Gamo, T., M. Tsutsumi, H. Sakai, T. Nakazawa, M. Tanaka, H. Honda, H. Kubo, and T. Itoh, Carbon and oxygen isotope ratios of carbon dioxide of a stratospheric profile over Japan, *Tellus, 41B*, 127-133, 1989.

Goldman, A., F. J. Murcray, D. G. Murcray, J. J. Kosters, C. P. Rinsland, C. Camy-Peyret, J.-M. Flaud and A. Barbe, Isotopic abundances of stratospheric ozone from balloon-borne high resolution infrared solar spectra, *J. Geophys. Res., 94*, 8467-8473, 1989.

Gunson, M. R. and F. W. Irion, "Measurement of atmospheric composition by the ATMOS instrument from Table Mountain Observatory" in *Remote Sensing of*

Atmospheric Chemistry, edited by J. L. McElroy and R. J. McNeal, pp. 335-346, Proc. SPIE vol. 1491, 1991.

Heidenreich, J. E. and M. H. Thiemens, A non-mass-dependent isotope effect in the production of ozone from molecular oxygen, *J. Chem. Phys., 78*, 892-895, 1983.

Heidenreich, J. E. and M. H. Thiemens, A non-mass-dependent isotope effect in the production of ozone from molecular oxygen: the role of molecular symmetry in isotope chemistry, *J. Chem. Phys., 84*, 2129-2136, 1986.

Hertzberg, G. H., *Molecular Spectra and Molecular Structure III. Electronic Spectra and Electronic Structure of Polyatomic Molecules*, 745 pp., Van Nostrand Reinhold, New York, 1966.

Holton, J. R., P. H. Haynes, M. E. McIntyre, A. R. Douglass, R. B. Rood, and L. Pfister, Stratospheric-tropospheric exchange, *Rev. Geophys., 33*, 403-439, 1995.

IUPAC commission on Atomic Weights and Isotopic Abundances, Isotopic composition of the elements 1981, *Pure Appl. Chem., 55,* 1119-1136, 1983.

Jouzel, J., R. D. Koster, R. J. Suozzo, G. L. Russell, J. W. C. White, and W. S. Broecker, Simulations of the HDO and $H_2{}^{18}O$ atmospheric cycles using the NASA GISS general circulation model: Sensitivity experiments for present-day conditions, *J. Geophys. Res., 96,* 7495-7507, 1991.

Kaye, J. A. and D. F. Strobel, Enhancement of heavy ozone in earth's atmosphere?, *J. Geophys. Res., 88*, 8447, 1983.

Kaye, J. A., Theoretical analysis of isotope effects on ozone formation in oxygen photochemistry, *J. Geophys. Res., 97,* 7865-7874, 1986.

Kaye, J. A., Mechanisms and observations for isotope fractionation of molecular species in planetary atmospheres, *Rev. Geophys., 25*, 1609-1658, 1987.

Kaye, J. A., S. A. Penkett and F. M. Ormond (Eds.), *Report on Concentrations, Lifetimes and Trends of CFCs, Halons and Related Species*, NASA Reference Publication 1339, National Aeronautics and Space Administration, Washington, D. C., 1994.

Ko, M. K. W., N.-D. Sze, and M. Prather, Better protection of the ozone layer, *Nature, 367*, 505-508, 1994.

Krankowsky, D., F. Bartecki, G. G. Klees, K. Mauersberger, K. Schellenbach and J. Stehr, Measurement of heavy isotope enrichment in tropospheric ozone, *Geophys. Res. Lett., 22*, 13, 1713-1716, 1995.

Larsen, N. W., T. Pedersen and J. Sehested, Isotopic study of the mechanism of ozone formation, in *Isotope effects in gas-phase chemistry*, edited by Jack Kaye, pp. 167-179, American Chemical Society, 1992.

Mauersberger, K., Measurement of heavy ozone in the stratosphere, *Geophys. Res. Lett., 8*, 935, 1981.

Mauersberger, K., Ozone isotope measurements in the stratosphere, *Geophys. Res. Lett., 14*, 80, 1987.

Mauersberger, K., J. Morton, B. Schueler, J. Stehr and S. M. Anderson, Multi-isotope study of ozone: implications for the heavy ozone anomaly, *Geophys. Res. Lett., 20*, 1031-1034, 1993.

McDaniel, A. H., C. A. Cantrell, J. A. Davidson, R. E. Shetter and J. G. Calvert, The temperature dependent infrared cross-sections for the chlorofluorocarbons: CFC-11, CFC-12, CFC-13, CFC-14, CFC-22, CFC-113, CFC-114, CFC-115, *J. Atmos. Chem., 12*, 211-227, 1991.

Midgley, P. M. and Fisher, D. A., The production and release to the atmosphere of chlorodifluoromethane, *Atmos. Envir., 27*, 2215-2223, 1993

Miller, R. L., A. G. Suits, P. L. Houston, R. Toumi, J. A. Mack, and A. M. Wodtke, The "ozone deficit" problem: $O_2(X, v \geq 26) + O(^3P)$ from 226-nm ozone photodissociation, *Science, 265*, 1831 - 1838, 1994.

Montzka, S. A., R. C. Myers, J. H. Butler, J. W. Elkins, and S. O. Cummings, Global tropospheric distribution and calibration scale of HCFC-22, *Geophys. Res. Lett., 20*, 703-706, 1993.

Morgan, W. L. and D. R. Bates, Stratospheric heavy ozone: the symmetric isomer, *Planet. Space Sci., 40*, 1573-1579, 1992.

Morton, J., B. Schueler and K. Mauersberger, Oxygen fractionation of ozone isotopes $^{48}O_3$ through $^{54}O_3$, *Chem. Phys. Lett., 154*, 143-145, 1989.

Morton, J., J. Barnes, B. Schueler, and K. Mauersberger, Laboratory studies of heavy ozone, *J. Geophys. Res., 95*, 901-907, 1990.

Mote, P.W., K. H. Rosenlof, J. R. Holton, R. S. Harwood, and J. W. Waters, Seasonal variations of water vapor in the tropical lower stratosphere, *Geophys. Res. Lett., 22,* 1093-1096, 1995.

Moyer, E. J., F. W. Irion, Y. L. Yung and M. R. Gunson, Implications of stratospheric deuterated water for troposphere-stratosphere transport, submitted to *Geophys. Res. Lett.,* 1995.

Newell, R. J. and S. Gould-Stewart, A stratospheric fountain?, *J. Atmos. Sci., 38*, 2789-2796, 1981.

Norton, R. H. and C. P. Rinsland, ATMOS data processing and science analysis methods, *Appl. Opt., 30*, 389-400, 1991.

Prather, M., and C. M. Spivakovsky, Tropospheric OH and the lifetime of hydrochlorofluorocarbons, *J. Geophys. Res., 95,* 18723-18729, 1990.

Pollock, W., L. E. Heidt, R. Lueb, and D. H. Ehhalt, Measurement of stratospheric water vapor by cryogenic collection, *J. Geophys. Res., 85,* 5555-5568, 1980.

Prinn, R., D. Cunnold, P. Simmonds, F.Alyea, R. Boldi, A. Crawford, P. Fraser, D. Gutzler, D. Hartley, R. Rosen and R. Rasmussen, Global average concentration and trend for hydroxyl radicals deduced from ALE/GAGE trichloroethane (methyl chloroform) data for 1978-1990, *J. Geophys. Res., 97,* 2445-2461, 1992.

Ramanathan, V., The radiateve and climatic consequences of the changing atmospheric composition of trace gases, in *The Changing Atmosphere*, F. S. Rowland and I. S. A. Isaksen, eds., pp 159-186, John Wiley and Sons, Chichester, 1988.

Rinsland, C. P., A. Goldman, V. Malathy Devi, B. Fridovich, D. G. S. Snyder, G. D. Jones, F. Murcray, D. G. Murcray, M. A. H. Smith, R. K. Seals Jr., M. T. Coffey, and W. G. Mankin, Simultaneous stratospheric measurements of H_2O, HDO, and CH_4 from balloon-borne and aircraft infrared solar absoption spectra and tunable diode laser laboratory spectra of HDO, *J. Geophys. Res., 89,* 7259-7266, 1984.

Rinsland, C.P., V. Malathy Devi, J.-M. Flaud, C. Camy-Peyret, M. A. H. Smith, and G. M. Stokes, Identification of ^{18}O-isotopic lines of ozone in infrared ground-based solar absorption spectra, *J. Geophys. Res., 90,* 10719-10725, 1985.

Rinsland, C. P., M. R. Gunson, J. C. Foster, R. A. Toth, C. B. Farmer and R. Zander, Stratospheric profiles of heavy water isotopes and CH_3D from analysis of the ATMOS Spacelab 3 infrared solar spectra, *J. Geophys. Res., 96,* 1057-1068, 1991.

Rinsland, C. P., G. K. Yue, M. R. Gunson, R. Zander, and M. C. Abrams, Mid-infrared extinction by sulfate aerosols from the Mt Pinatubo eruption, *J. Quant. Spectrosc. Radiat. Transfer, 52,* 241-252, 1994.

Rinsland, C. P., E. Mahieu, R. Zander, M. R. Gunson, R. J. Salawitch, A. Y. Chang, A. Goldman, M. C. Abrams, H. A. Michelsen, M. M. Abbas, M. J. Newchurch, and F. W. Irion, Trends of OCS, HCN, SF_6, $CHClF_2$ in the lower stratosphere from 1985 and 1994 Atmospheric Trace Molecule Spectroscopy Experiment measurements near 30°N latitude, submitted to *Geophys. Res. Lett.*, 1995.

Rowlands, I. H., The fourth meeting of the parties to the Montreal Protocol: Report and reflection, *Environment, 35*, 25-34, 1993.

Sander, R. K., T. R. Loree, S. D. Rockwood and S. M. Freund, ArF laser enrichment of oxygen isotopes, *Appl. Phys. Lett., 30,* 150-152, 1977.

Shia, R.-L., Y. L. Yung, M. Allen, R. W. Zurek, and D. Crisp, Sensitivity study of advection and diffusion coefficients in a two-dimensional stratospheric model using excess carbon 14 data, *J. Geophys. Res., 94*, 18467-18484, 1989.

Schueler, B., J. Morton, and K. Mauersberger, Measurement of isotopic abundances in collected stratospheric ozone samples, *Geophys. Res. Lett., 17,* 1295-1298, 1990.

Thiemens, M. H. and Heidenreich, J. E., The mass-independent fractionation of oxygen: a novel isotope effect and its possible cosmochemical implications, *Science, 219*, 1073-1075, 1983.

Thiemens, M. H. and Jackson, T., Pressure dependence for heavy isotope enhancement in ozone formation, *Geophys. Res. Lett., 17,* 717-719, 1990.

Thiemens, M. H., T. Jackson, K. Mauersberger, B. Schueler, and J. Morton, Oxygen isotope fractionation in stratospheric CO_2, *Geophys. Res. Lett., 18,* 669-672, 1991.

Thiemens, M. H., Mass-independent isotopic fractionations and their applications, in *Isotope effects in gas-phase chemistry*, Jack Kaye, ed., pp 138-154, American Chemical Society, 1992.

U. S. Standard Atmosphere, 1976, National Oceanic and Atmospheric Administration, National Aeronautics and Space Administration, and United States Air Force, Washington, D. C., 1976.

Varanasi, P., Absorption spectra of HCFC-22 around 829 cm^{-1} at atmospheric conditions, *J. Quant. Spectrosc. Radiat. Transfer, 47*, 251-255, 1992.

Valentini, J. J., Mass-independent isotopic fractionation in nonadiabatic molecular collisions, *J. Chem. Phys., 86*, 6755-6765, 1987.

Wen, J. and M. H. Thiemens, Experimental and theoretical study of isotope effects on ozone decomposition, *J. Geophys. Res., 96*, 10911-10921, 1991.

Wennberg, P. O., R. C. Cohen, R. M. Stimpfle, J. P. Koplow, J. G. Anderson, R. J. Salawitch, D. W. Fahey, E. L. Woodbridge, E. R. Keim, R. S. Gao, C. R. Webster, R. D. May, D. W. Toohey, L. M. Avallone, M. H. Proffitt, M. Loewenstein, J. R. Podolske, K. R. Chan, and S. C. Wofsy, Removal of stratospheric O_3 by radicals: In situ measurements of OH, HO_2, NO, NO_2, ClO, and BrO, *Science, 266*, 398-404, 1994.

Winkler, D. M., and M. T. Osborn, Airborne Lidar Observations of the Pinatubo Volcanic Plume, *Geophys. Res. Lett., 19*, 167-170, 1992.

WMO, *Atmospheric Ozone 1985: Assessment of our understanding of the processes controlling its present distribution and change,* World Meteorological Organization Global Ozone Research and Monitoring Project - Report No. 16, Geneva, 1986.

WMO, *Scientific Assessment of Ozone Depletion: 1994,* World Meteorological Organization Global Ozone Research and Monitoring Project - Report No. 37, Geneva, 1995.

Yang, J., and S. Epstein, The effect of the isotopic composition of oxygen on the non-mass-dependent isotopic fractionation in the formation of ozone by discharge of O_2*, *Geochim. Acta, 51,* 2011-2017, 1987a.

Yang, J., and S. Epstein, The effect of pressure and excitation energy on the isotopic fractionation in the formation of ozone by discharge of O_2*, *Geochim. Acta, 51,* 2019-2024, 1987b.

Yung, Y. L., W. B. DeMore, and J. P. Pinto, Isotopic exchange between carbon dioxide and ozone via O(^{1}D) in the stratosphere, *Geophys. Res. Lett, 18*, 13-16, 1991.

Yung, Y. L., F. W. Irion, and W. B. DeMore, Heavy ozone in the atmosphere: a useful tracer of chemical species and reaction pathways, submitted to *Geophys. Res. Lett.,* 1995.

Zander, R., E. Mahieu, Ph. Demoulin, C. P. Rinsland, D. K. Weisenstein, M. K. W. Ko, N.-D. Sze, and M. R. Gunson, Secular evolution of the vertical column abundances of $CHClF_2$ (HCFC-22) in the earth's atmosphere inferred from ground-based IR solar observations at the Jungfraujoch and at Kitt Peak, and comparison with model calculations, *J. Atmos. Chem., 18,* 129-148, 1994.

Zander, R., E. Mahieu, M. R. Gunson, M. C. Abrams, A. Y. Chang, M. Abbas, C. Aellig, A. Engel, A. Goldman, F. W. Irion, N. Kämpfer, H. A. Michelsen, M. J. Newchurch, C. P. Rinsland, R. J. Salawitch, G. P. Stiller and G. C. Toon, The 1994 northern midlatitude budget of stratospheric chlorine derived from ATMOS/ATLAS-3 observations, submitted to *Geophys. Res. Lett.,* 1995.

Table 1.1: ATMOS data summary

Filter	Number of Occultations				Spectral Bandpass (cm^{-1})	Molecules
	SL3	AT1	AT2	AT3		
1	1 SR 4 SS	6 SR 7 SS	11 SR 6 SS		600-1180	$^{48}O_3$, $^{16}O^{16}O^{18}O$, $^{16}O^{18}O^{16}O$, N_2O, HNO_3, CCl_3F, CCl_2F2, CHF_2Cl, $ClONO_2$,SF_6, HNO_4, CCl_4, C_2H_2
2	1SR 3SS	1 SR 1 SS	9 SR 7SS		1100-2000	$^{48}O_3$, N_2O, CH_4, HNO_3, H_2O, NO, NO_2, N_2O_5, HDO, $H_2{}^{17}O$, $H_2{}^{18}O$, CF_4
3	1 SR 4SS	15 SR 14 SS	22 SR 9 SS	29 SR 34 SS	1580-3340	$^{48}O_3$, N_2O, CH_4, HNO_3, H_2O, HCl, NO, NO_2, OCS, HCN, $H_2{}^{17}O$, $H_2{}^{18}O$, CH_3D, CO, C_2H_6, CH_3Cl
4	1 SR 2 SS	8 SR 5 SS	10 SR 7 SS	13 SR 15 SS	3150-4800	N_2O, CH_4, H_2O, HF
9		17 SR 14 SS	1 SS	14 SR 17SS	600-2450	$^{48}O_3$, $^{16}O^{16}O^{18}O$, $^{16}O^{18}O^{16}O$, N_2O, CH_4, HNO_3,H_2O, NO, NO_2, CCl_3F,CCl_2F_2, $CHClF_2$, $ClONO_2$, N_2O_5, SF_6, OCS, HDO, $H_2{}^{17}O$, $H_2{}^{18}O$, CO, HNO_4, CCl_4, C_2H_2, CF_4
12			11 SR 9 SS	27 SR 30 SS	600-1400	$^{48}O_3$, $^{16}O^{16}O^{18}O$, $^{16}O^{18}O^{16}O$, N_2O, HNO_3, CCl_3F, CCl_2F2, CHF_2Cl, $ClONO_2$,SF_6, HNO_4, CCl_4, C_2H_2, CF_4

Note: SR=sunrise, SS=sunset, SL3=Spacelab 3, AT1=ATLAS-1, AT2=ATLAS-2, AT2=ATLAS-2

Chapter II

Increase in atmospheric CHF_2Cl (HCFC-22) over southern California from 1985 to 1990

Fredrick W. Irion[1], Margaret Brown[2,3], Geoffrey C. Toon[4] and Michael R. Gunson[4]

[1]Department of Chemical Engineering, California Institute of Technology, Pasadena, California 91125
[2]Department of Applied Mathematics, University of Washington, Seattle, Washington 98195
[3]now at Battelle, Pacific Northwest Laboratories, Richland, Washington 99352
[4]Jet Propulsion Laboratory, California Institute of Technology Pasadena, California 91109

Published in Geophysical Research Letters, Volume 21, No. 16, 1723-1726
August 1, 1994

Abstract.

Column densities of CHF_2Cl (HCFC-22) have been measured over Table Mountain Facility (TMF), Wrightwood, California (34.4°N) using the Atmospheric Trace Molecule Spectroscopy (ATMOS) Fourier-transform infrared (FTIR) spectrometer. Between October 1985 and July 1990, the exponential column increase rate was (6.7±0.5)% yr^{-1}. Additionally, column measurements of CHF_2Cl over McMurdo Sound, Antarctica (78°S) in September and October 1986 by the MarkIV FTIR spectrometer were used to derive a south-north interhemispheric ratio of (0.86±0.08). Model calculations investigated the feasibility of using CHF_2Cl column measurements with a predicted global OH field to determine a globally averaged chemical lifetime for CHF_2Cl, or equivalently, an estimate of the OH field using a predicted lifetime. The current uncertainty in historical CHF_2Cl emissions is too large for CHF_2Cl to be used to infer adequately either the lifetime or the OH field.

2.1 Introduction

Concern over the ozone layer has required the increasing use of hydrochlorofluorocarbons (HCFCs) as an alternative to chloroflurocarbons (CFCs). Unlike CFCs, HCFCs react with OH radicals, shortening their tropospheric lifetimes (e.g., 15.8 years calculated for CHF_2Cl vs. 55 years for $CFCl_3$ and 116 years for CF_2Cl_2 [*WMO*, 1991, pg. 6.7]). With its shorter tropospheric lifetime, the contribution of CHF_2Cl to inorganic chlorine in the stratosphere has been estimated to be quite small (1%) [*Weisenstein et al.*, 1992]. Nevertheless, with the increasing use of CHF_2Cl, accurate prediction of changes in stratospheric ozone and global climate warrants its continued monitoring.

Among recent reports, *Montzka et al.* [1993], using in-situ measurements, determined a compounded rate of increase of (7.3±0.3)% yr^{-1} in the global mean ground-level concentration of CHF_2Cl between mid-1987 through 1992. Total column measurements reported by *Zander et al.* [1994] showed an exponential increase of (7.0±0.35)% yr^{-1} over the Jungfraujoch, Switzerland (46.5°N) from 1986 to 1992, and (7.0±0.23) % yr^{-1} over Kitt Peak, Arizona (31.9°N) from 1980 to 1992. In this study we report measurements taken by the ATMOS spectrometer over Table Mountain and calculate the column accumulation rate between October, 1985 and July, 1990.

Column measurements by the MkIV FTIR spectrometer over McMurdo Sound in 1986 were used to evaluate the interhemispheric ratio of CHF_2Cl, but these columns were not directly comparable to those in northern mid-latitudes because of the lower Antarctic tropopause. Instead, a simple and self-contained comparison was made by ratioing the CHF_2Cl column to that of N_2O, a long-lived tropospheric source gas whose vertical mixing ratio profile is similar in shape to that of CHF_2Cl. As some 90% of the atmospheric N_2O resides in the troposphere, the N_2O column can act as a surrogate for the tropospheric air

burden, and we use such CHF_2Cl/N_2O ratios to estimate the CHF_2Cl interhemispheric ratio.

We discuss the use of CHF_2Cl measurement for inference of the global OH field. Current estimates of OH are based on scaling the OH field produced by chemical transport models to reproduce observed surface concentrations of methyl chloroform, CH_3CCl_3 (e.g. *Spivakovsky et al.* [1990]; *Prinn et al.* [1992]). Differences in the inferred OH fields are discussed in terms of the error in historical emissions of CHF_2Cl.

2.2 Measurements and data analysis

The ATMOS instrument was designed for stratospheric observations from the Space Shuttle [see *Farmer et al.*, 1987], but is also suitable for ground-based column density measurements of various gases [see *Gunson and Irion*, 1991]. It has an unapodized resolution is 0.01 cm^{-1} and its fast response time allows several interferograms to be taken within a narrow range of solar zenith angles. For this study, 8 to 41 successive, double-sided interferograms were transformed with the resulting spectra averaged, giving a signal-to-noise ratio in the resulting spectrum of at least 280. For analyses described here, the Mark IV FTIR spectrometer returned data with an unapodized spectral resolution of 0.008 cm^{-1} and signal-to-noise ratios varying between 100 and 1200. Further details of this instrument, as well as experimental conditions at McMurdo Sound, may be found in *Toon et al.* [1989] and *Toon* [1991].

Analysis software used for column retrievals from both instruments was described by *Norton and Rinsland* [1991]. Constituent and physical parameters were mapped into a 150 layer model atmosphere, each layer homogeneous and 1 km thick. For the ATMOS/-TMF retrievals, the *U. S. Standard Atmosphere* [1976] was used for the temperature and pressure profile while a combination of daily radiosonde and satellite data were used for McMurdo Sound retrievals [see *Toon et al.*, 1989]. Synthetic spectra were calculated for

small frequency intervals containing the target gas, and an assumed mixing ratio profile was scaled until the square of the residual (observed - calculated absorptions) was minimized. Spectral parameters were from the ATMOS main and supplemental linelists, described by *Brown et al.* [1987]. The $2\nu_6$ Q-branch at 829.05 cm^{-1} was used for CHF_2Cl analyses (Figure 2.1), while N_2O lines were the same as in *Toon et al.* [1989]. Initial mixing ratio profiles are shown in Figure 2.2. The TMF CHF_2Cl profile was based on ATMOS Spacelab3 northern hemisphere retrievals in the stratosphere [*Zander et al.*, 1987], with an assumed gradient in the troposphere. The tropospheric gradient used for the TMF profile resulted in better spectral fits to the data compared to a constant mixing ratio profile, however, no statistically significant bias in the derived columns was detected. We found that using a constant CHF_2Cl tropospheric mixing ratio profile for McMurdo Sound, and a constant tropospheric N_2O profile for both TMF and McMurdo, produced satisfactory fits for their respective spectra. Column N_2O for McMurdo Sound is from *Toon et al.* [1989]. Where two or more averaged spectra were available for a particular day, each spectrum was analyzed individually, and the resulting columns averaged. Estimated errors are described in Table 2.1.

2.3 Instrumental results and discussion

CHF_2Cl column results for Table Mountain, McMurdo Sound and, for comparison, Kitt Peak results (*Zander et al.* [1994]) are shown in Figure 2.3. To facilitate comparison of Kitt Peak and TMF columns, retrieved values were divided by the U.S. Standard Atmosphere [1976] pressure (in atmospheres) appropriate to the observation altitude. (Same day measurements of N_2O were not available from Kitt Peak.) An exponential fit to the TMF column data indicates an increase of (6.7±0.5)% yr^{-1}, slightly lower than the figure of (7.0±0.23)% yr^{-1} for Kitt Peak. No significant systematic difference can

be seen between TMF and Kitt Peak results during the time period in which they overlap. Surface mixing ratios were determined directly from the scaled a priori profiles. Calculations for Table Mountain show an increase in the ground-level mixing ratio from (70±6) pptv in October, 1985 to (99±8) pptv in August, 1990, the linear increase being (5.9±0.4) pptv yr^{-1} (1σ error). This agrees within error with the figure of (6.3±0.3) pptv yr^{-1} reported by *Montzka et al.* [1993] for the period between 1987 and December, 1992.

Before using the TMF data to infer the interhemispheric ratio of CHF_2Cl, we first evaluated its suitability for determining an average northern hemispheric CHF_2Cl column by comparison to latitudinally weighted in situ data previously published by *Montzka et al.* [1993]. Rather than using ground-level concentrations estimated from the columns, a more robust comparison may be with ratios of CHF_2Cl to N_2O. Figure 2.4 shows the CHF_2Cl/N_2O column ratios from this work. Also shown are the in situ measurements of CHF_2Cl, reported by Montzka et al., ratioed to estimated N_2O concentrations, obtained either from monthly averaged measurements of N_2O (prior to July, 1988) or extrapolations of equations fitted to those measurements (on or after July, 1988; see *Prinn et al.*, [1990]). These N_2O measurements were from Cape Meares, Oregon (45°N) in the northern hemisphere and Cape Grim, Tasmania (41°S) in the south. Good consistency is seen among latitudinally averaged northern hemispheric in situ measurements, in situ measurements from Niwot Ridge (40°N), and the ATMOS/TMF results. Using the average of the McMurdo Sound observations and the fitted line for the ATMOS data, we calculate a south-north hemispheric ratio of (0.86±0.08). This is in good agreement with the figure of (0.88±0.04) derived from *Montzka et al.* [1993], who reported an interhemispheric CHF_2Cl difference of (13±1) pptv and a 1992 mean southern hemisphere mixing ratio of (95.2±2) pptv.

2.4 Model methodology and results

Model results were obtained using the 2-D chemical transport model developed by *Tung* [1982; 1986], *Yang et al.* [1991] and *Olaguer et al.* [1991]. The model domain extends from 90°S to 90°N with eighteen latitudinal bands and from 0 to 56 km with 24 vertical levels. The model has been validated for tracers which are sensitive to stratospheric and tropospheric chemical and transport parameters [*Yang et al.*, 1991; *Olaguer et al.*, 1992; *Brown*, 1993]. Destruction of CHF_2Cl by photodissociation and by chemical reaction with OH and $O(^1D)$ were modeled. Concentrations of CHF_2Cl were set to zero at the beginning of 1949, when the atmosphere is expected to have none. The model was run forward to the end of 1992 using emission estimates of *Jesson* [1980] prior to 1970, and *Midgley and Fisher* [1993] from 1970 to 1991. For 1992, an emission of 213 x 10^6 kg is used (obtained by linear extrapolation of prior emission estimates). The uncertainty in emissions subsequent to 1970 were estimated to be +12.5% and –8.5% [Don Fisher, private communication, 1993]. The model has been shown to produce modeled atmospheric concentrations of methyl chloroform consistent with observations [*Brown*, 1993]. The globally averaged lifetime of methyl chloroform was calculated to be 7.3 years, longer than previous estimates of 5.7 years [*Prinn et al.*, 1992] and 6.2 years [*Spivakovsky et al.*, 1990]. The model calculated CHF_2Cl lifetime here, 19 years, is expected to be longer than that derived using the OH fields of Prinn et al. and Spivakovsky et al. Here, for CHF_2Cl, we demonstrate the relationship between the lifetime and the OH field as well as the sensitivity of the column density to the emissions.

Six experiments (E1-E6) were performed and modeled column densities of CHF_2Cl were compared with observed column densities. The results are summarized in Figure 2.3. Experiment E1, using emission estimates described above, overestimates column densities at both observation sites. These results reflect uncertainty in emission estimates and the

model OH field. Experiments E2-E5 test the sensitivity of the model results to these uncertainties. Modifications to the OH field and the CHF_2Cl emission, as well as average concentrations for all model experiments are summarized in Table 2.2. The model calculated globally averaged CHF_2Cl lifetime in experiments E1 and E2 is 19 years. The scaling of the OH field in experiments E3 and E4 yields a model calculated globally averaged CHF_2Cl lifetime of 15.5 years, consistent with the estimate in *WMO* [1991], while that for E5 yields a CHF_2Cl lifetime of 13.5 years, consistent with the estimate of *Montzka et al.* [1993]. Experiments E2, E4 and E5 all yield results in agreement with observed column densities in the northern hemisphere.

2.5 Conclusions

CHF_2Cl column retrievals from TMF indicate an exponential increase rate of (6.7±0.5)% yr^{-1} from October, 1985 until July, 1990. Using McMurdo Sound measurements, we calculate a south-north interhemispheric ratio of (0.86±0.08). The method of ratioing the CHF_2Cl and N_2O columns has been shown to be useful for comparing columns of tropospheric gases at different locations. Model results demonstrate that the difference between the modeled and observed CHF_2Cl column densities can be attributed to uncertainty either in the emissions or in the OH concentration. Reduction of the uncertainty in the CHF_2Cl emissions may allow the use of CHF_2Cl observations in adequately constraining the OH field.

Acknowledgments

We thank C. B. Farmer, D. Fisher, D. Gershon, E. Mahieu, C. Montzka, O. F. Raper, C. P. Rinsland, P. Varanasi, C. Webster and R. Zander for their assistance. Research at the Jet Propulsion Laboratory, California Institute of Technology was done under contract to the National Aeronautics and Space Administration. Research by M. Brown was supported by NASA grants NGAW-1605 and NGT-3005.

References

Brown, L. R., C. B. Farmer, C. P. Rinsland, and R. A. Toth, Molecular line parameters for the atmospheric trace molecule spectroscopy experiment, *Appl. Opt., 26*, 5154-5182, 1987.

Brown, M., Deduction of emissions of source gases using an objective inversion algorithm and a chemical transport model, *J. Geophys. Res., 98*, 12639-12660, 1993.

Farmer, C. B., O. F. Raper and F. G. O'Callaghan, *Final Report on the First Flight of the ATMOS Instrument During the Spacelab 3 Mission, April 29 Through May 6, 1985*, JPL Publication 87-32, Jet Propulsion Laboratory, California Institute of Technology, Pasadena, CA, 1987.

Gunson, M. R. and F. W. Irion, Measurement of atmospheric composition by the ATMOS instrument from Table Mountain Observatory, in *Remote Sensing of Atmospheric Chemistry*, edited by J. L. McElroy and R. J. McNeal, Proc. SPIE 1491, pp 335-346, 1991.

Jesson, J. P., Release of industrial halocarbons and tropospheric budget, in *Proceedings of the NATO Advanced Study Institute on Atmospheric Ozone: Its variation and human influences,* U. S. Federal Aviation Administration, Washington D. C., 373-396, 1980.

Midgley, P. M. and Fisher, D. A., The production and release to the atmosphere of chlorodifluoromethane, *Atmos. Envir., 27*, 2215-2223, 1993

Montzka, S. A., R. C. Myers, J. H. Butler, J. W. Elkins, and S. O. Cummings, Global tropospheric distribution and calibration scale of HCFC-22, *Geophys. Res. Lett., 20*, 703-706, 1993.

Norton, R. H. and C. P. Rinsland, ATMOS data processing and science analysis methods, *Appl. Opt., 30*, 389-400, 1991.

Olaguer, E. P., H. Yang and K. K. Tung, A re-examination of the radiative balance of the stratosphere, *J. Atmos. Sci., 49,* 1242 - 1263, 1992.

Prinn, R., D. Cunnold, R. Rasmussen, P. Simmonds, F. Alyea, A. Crawford, P. Fraser, and R. Rosen, Atmospheric emissions and trends of nitrous oxide deduced from 10 years of ALE-GAGE data, *J. Geophys. Res., 95*, 18369 - 18385, 1990.

Prinn, R., D. Cunnold, P. Simmonds, F. Alyea, R. Boldi, A. Crawford, P. Fraser, D. Gutzler, D. Hartley, R. Rosen, and R. Rasmussen, Global average concentration and trend for hydroxyl radicals deduced from ALE/GAGE trichloroethane (methyl chloroform) data for 1978-1990, *J. Geophys. Res., 97*, 2445-2461, 1992.

Spivakovsky, C. M., R. Yevich, J. A. Logan, S. C. Wofsy, M. B. McElroy, and M. J. Prather, Tropospheric OH in a three dimensional chemical tracer model: an assessment based on observations of CH_3CCl_3, *J. Geophys. Res., 95*, 18441-18729, 1990.

Toon G. C., C. B. Farmer, P. W. Schaper, J.-F. Blavier and L. L. Lowes, Ground-based infrared measurements of tropospheric source gases over Antarctica during the 1986 austral spring, *J. Geophys. Res., 94*, 11613-11624, 1989.

Toon, G. C., The MkIV interferometer, *Optics and Photonics News, 2*, 19-21, 1991.

Tung, K. K., On the two dimensional transport of stratospheric gases in isentropic coordinates, *J. Atmos. Sci., 39*, 2330-2355, 1982.

Tung, K. K., Nongeostropic theory of zonally averaged circulation. Averaged circulation., Part I., Formulation, *J. Atmos. Sci., 43*, 2600-2618, 1986.

U. S. Standard Atmosphere, 1976, National Oceanic and Atmospheric Administration, National Aeronautics and Space Administration, and United States Air Force, Washington, D. C., 1976.

Weisenstein, D. K., M. K. W. Ko, and N.-D. Sze, The Chlorine Budget of the Present-Day Atmosphere: A Modeling Study, *J. Geophys. Res., 97*, 2547-2559, 1992.

World Meteorological Organization (WMO), *Scientific Assessment of Ozone Depletion:1991*, WMO Report No. 25., Geneva, 1991.

Yang, H., E. Olaguer and K. K. Tung, Simulation of the present-day atmospheric ozone, odd nitrogen, chlorine and other species using a couple 2-D model in isentropic coordinates, *J. Atmos. Sci., 48*, 442-471, 1991.

Zander, R., C. P. Rinsland, C. B. Farmer and R. H. Norton, Infrared spectroscopic measurements of halogenated source gases in the stratosphere with the ATMOS instrument, *J. Geophys. Res., 92*, 9836-9850, 1987.

Zander, R., E. Mahieu, Ph. Demoulin, C. P. Rinsland, D. K. Weisenstein, M. K. W. Ko, N.-D. Sze, and M. R. Gunson, Secular evolution of the vertical column abundances of $CHClF_2$ (HCFC-22) in the earth's atmosphere inferred from ground-based IR solar observations at the Jungfraujoch and at Kitt Peak, and comparison with model calculations, *J. Atmos. Chem., 18,* 129-148, 1994.

Table 2.1: Error sources for a single spectrum

	CHF_2Cl		N_2O
	ATMOS Table Mtn	MarkIV McMurdo	ATMOS Table Mtn
Random Errors (%)			
Temperature/Pressure	3	3	2
Signal-to-noise	1	1	1
Assumed VMR profile	4	5	2
Zero transmission offset	1	1	1
Interfering absorptions	6	2	2
Total Random Error	8	6	4
Systematic Errors (%)			
Line strengths	10	10	5
Spectral fitting	3.5	3.5	3.5
Total Systematic Error	13.5	13.5	8.5

Table 2.2: Model calculated CHF_2Cl average concentrations at the end of 1992

Experiment	E1	E2	E3	E4	E5
Change in Global OH	--	--	+20%	+20%	+40%
Change in CHF_2Cl	--	-10%	--	-5%	--
Global (pptv)	115	104	107	102	101
S. hemisphere (pptv)	105	98	100	95	94
N. hemisphere (pptv)	123	111	115	109	108
Global troposphere	120	108	111	106	105
Global stratosphere	98	88	90	86	85
Rate of increase (b)	6.6	5.9	6.0	5.7	5.6
CHF_2Cl lifetime	19	19	15.5	15.5	13.5

(a) As compared to experiment E1. Reduction in CHF_2Cl emissions is after 1970.

(b) Average global rate of increase is calculated from 1982 to 1992.

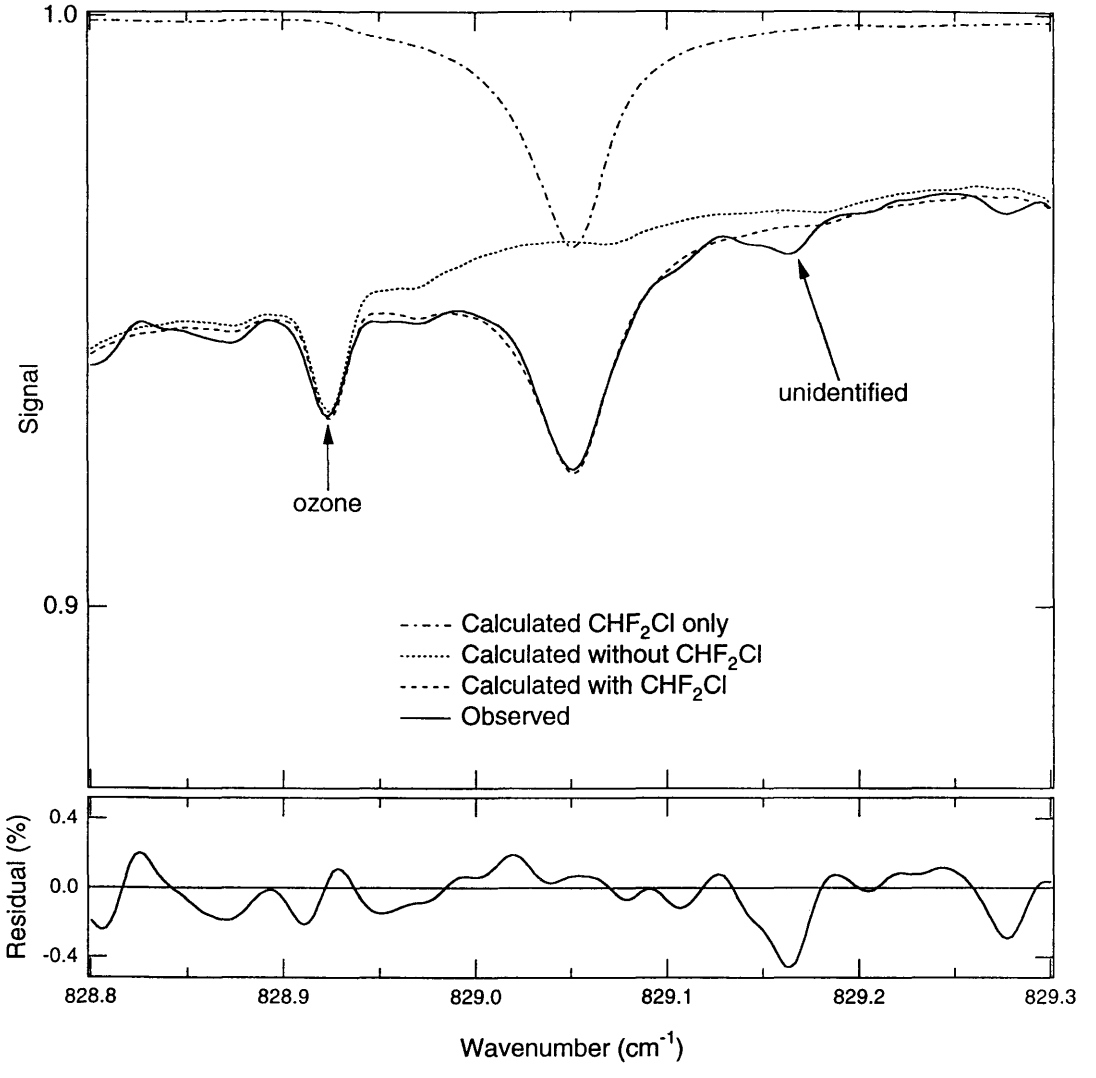

Figure 2.1: Typical ATMOS observed and calculated CHF_2Cl spectra.

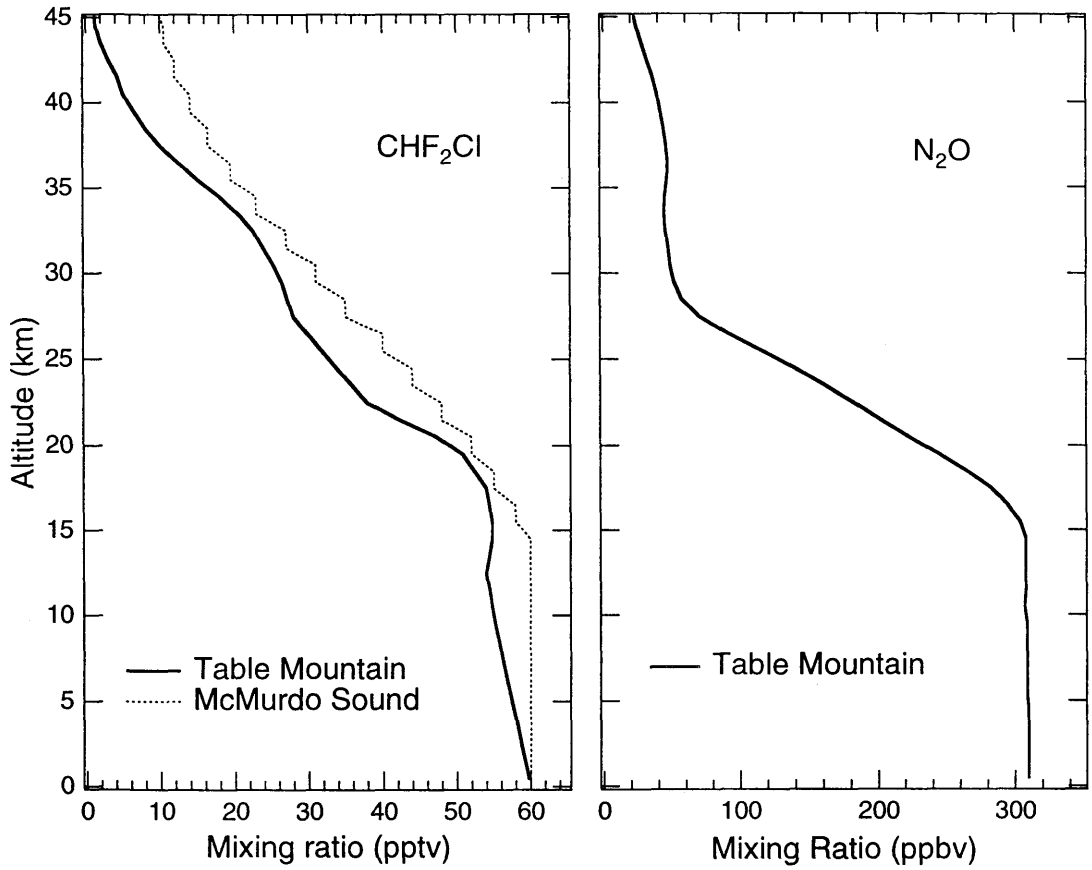

Figure 2.2: Assumed CHF_2Cl and N_2O mixing ratio profiles.

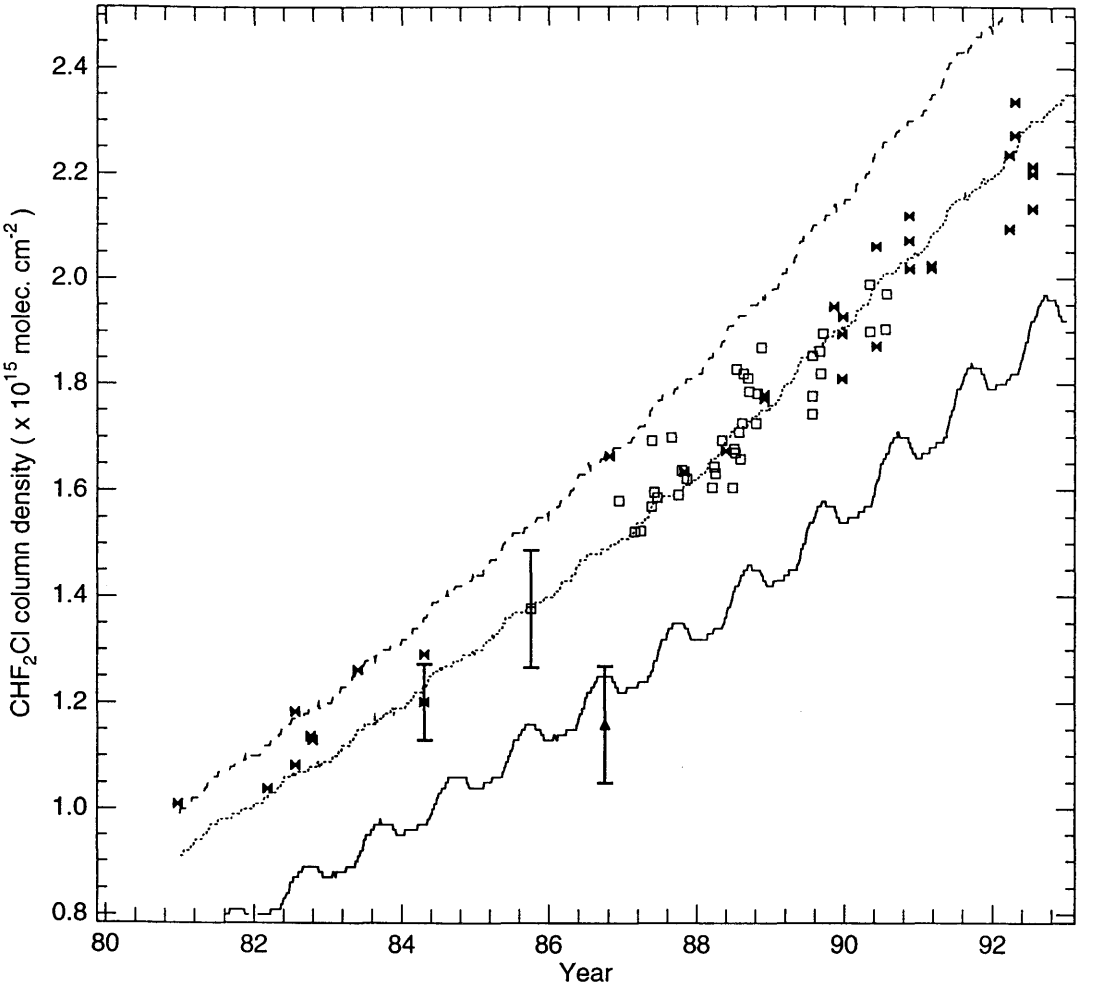

Figure 2.3: CHF_2Cl column retrievals (scaled to sea-level) **and results of model simulations.** Observations: □ Table Mountain (this work), ▲ McMurdo Sound (this work), ⋈ Kitt Peak (*Zander et al.*, 1993). Modelling experiments: - - -E1 North, ····· E5 North, ——E5 South. See Table 1 for random and systematic errors for Table Mountain and McMurdo measurements. The datum for MarkIV-McMurdo Sound is the average of 42 measurements taken in September and October, 1986; the error bar represents their 9% standard deviation. Error bars for other data sets indicate the average fractional random error. For clarity, only modelling experiments E1 (north) and E5 (north) are superimposed on the northern hemisphere results. These two experiments represent the range of results, however, experiments E2 and E4 gave results similar to E5. For the southern hemisphere, only experiment E5 is shown, although E2 and E4 gave similar results.

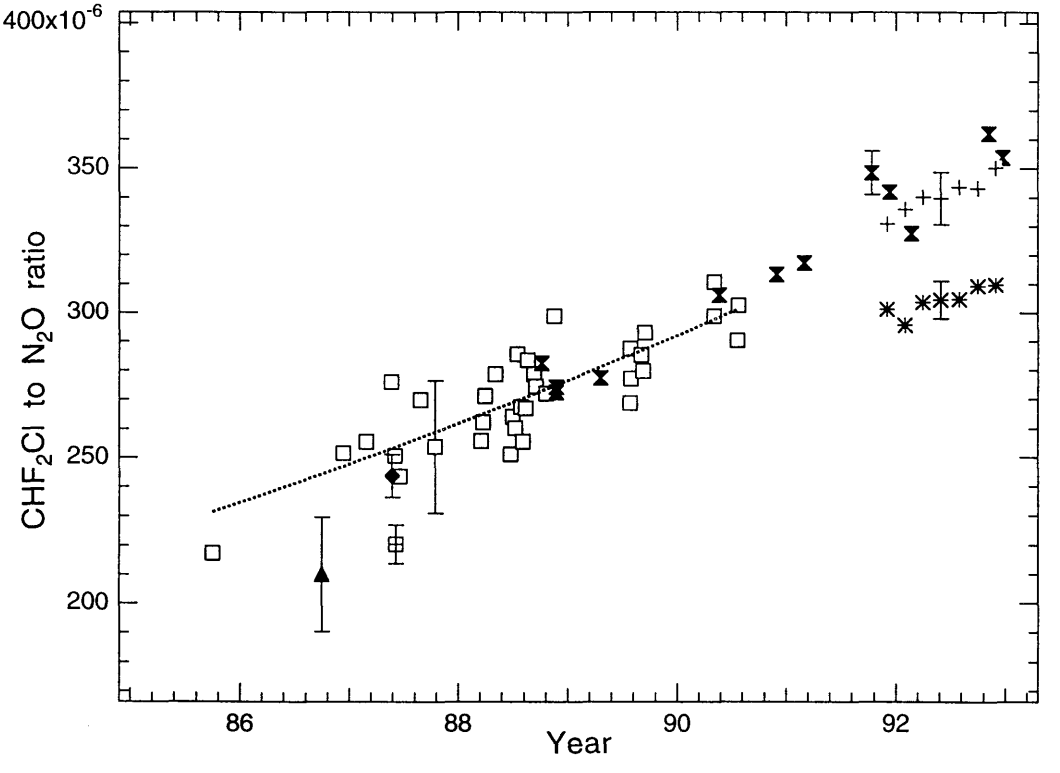

Figure 2.4: CHF_2Cl/N_2O column and in-situ ratios. Column measurements (this work): □ ATMOS, Table Mountain, CA, ▲ Mark IV, McMurdo Sound, Antarctica. Ground-level in-situ measurements (*Montzka et al.*[1993]): ⧗ Niwot Ridge, CO. SAGA cruises: ◆ N. hemisphere, ⊞ S. hemisphere. Weighted averages: + N. hemisphere, ✳ S. hemisphere. Error bars indicate the average fractional random error for their respective data sets. The error for the in situ data of Montzka et al. includes an assumed 2% random error for the N_2O concentration. Line fitted for ATMOS/TMF measurements only.

Chapter III

Heavy ozone enrichments from ATMOS infrared solar spectra

Fredrick W. Irion[1], Michael R. Gunson[2], Curtis P. Rinsland[3], Yuk L. Yung[4], Mark C. Abrams[5], Albert Y. Chang[2], and Aaron Goldman[6]

[1]Department of Chemical Engineering, California Institute of Technology, Pasadena, California 91125
[2]Jet Propulsion Laboratory, California Institute of Technology, Pasadena, California 91109
[3]Atmospheric Sciences Division, NASA Langley Research Center, Hampton, Virginia 23681
[4]Department of Planetary Science, California Institute of Technology, Pasadena, California 91125
[5]SAIC - NASA Langley Research Center, Hampton, Virginia 23681
[6]Department of Physics, University of Denver, Denver, Colorado 80210

(submitted to Geophysical Research Letters, September 26, 1995)

Abstract

Vertical enrichment profiles of stratospheric $^{16}O^{16}O^{18}O$ and $^{16}O^{18}O^{16}O$ have been derived from space-based solar occultation spectra recorded at 0.01 cm^{-1} resolution with the ATMOS (**A**tmospheric **T**race **MO**lecule **S**pectroscopy) Fourier-transform infrared (FTIR) spectrometer. The observations, made during the Spacelab 3 and ATLAS-1, -2, and -3 shuttle missions, cover polar, mid-latitude and tropical regions. Between 26 to 2.6 mb inclusive (≈25 to 41 km), average enrichments, weighted by molecular $^{48}O_3$ density, of (15±6)% were found for $^{16}O^{16}O^{18}O$, (10±7)% for $^{16}O^{18}O^{16}O$, and (13±5)% for $^{50}O_3$ (1σ standard deviation). Enrichments increased slightly with altitude, however no latitudinal variability was apparent. From a series of ground-based measurements by the ATMOS instrument at Table Mountain, California (34.4°N), an average total column $^{16}O^{16}O^{18}O$ enrichment of (17±4)% (1σ standard deviation) was determined, with no significant seasonal variation discerned. Possible biases in the spectral intensities that affect the determination of absolute enrichments are discussed. However, any corrections to the these intensities would probably involve a scaling of the enrichments, and would not affect the observed lack of latitudinal and seasonal variability.

3.1 Introduction

Stratospheric enrichment of $^{50}O_3$ was first reported by *Mauersberger* [1981], who found enrichments ranging from 0% to 40% using a balloon-borne mass spectrometer. (For the purposes of this paper, % enrichment = $[R_{obs}/R_{std} - 1] \times 100$, where R_{obs} is the observed abundance ratio of the heavy isotopomer to the regular isotopomer, and R_{std} is the standard ratio. For $^{50}O_3$ enrichment, $R_{std} = 5.97 \times 10^{-3}$, or three times the natural abundance ratio of ^{18}O to ^{16}O, ignoring a very small abundance of $^{16}O^{17}O^{17}O$. See *IUPAC,* [1983]). Further stratospheric enrichment of $^{50}O_3$ have been reported based on mass spectrometry [*Mauersberger*, 1987], far-infrared emission spectroscopy [*Abbas et al.*, 1987; *Carli and Park*, 1988], and cryogenic grab-sampling followed by mass-spectrometry [*Schueler et al.,* 1990]. These measurements have sometimes shown little consistency with each other. Figure 3.1 summarizes previous measurements of $^{50}O_3$ enrichment profiles as well as averaged results of the analyses presented here. Column enrichments have also been determined using mid-infrared solar-absorption Fourier-transform spectrometry. *Rinsland et al.* [1985] determined a column enrichment of (11±11)% and (5±7)% for $^{16}O^{16}O^{18}O$ and $^{16}O^{18}O^{16}O$, respectively. *Goldman et al.* [1989], from two balloon-based observations, found column enrichments above 37 km of (20±14)% and (40±18)% for $^{16}O^{16}O^{18}O$, and (16±8)% and (25±12)% for $^{16}O^{18}O^{16}O$. Enrichment of $^{50}O_3$ from about 8 to 10% in tropospheric urban air was reported by *Krankowsky et al.* [1995] who found no apparent variation in the enrichment with tropospheric O_3 mixing ratios

Heavy ozone enrichment has also been observed in laboratory measurements. *Anderson et al.* [1989] found ozone created using an electric discharge (which can produce excited states of O and O_2) enriched primarily in the asymmetric isotopomers, such as

$^{16}O^{16}O^{18}O$. *Morton et al.* [1990] found that enrichment can occur via the reaction of ground-state atomic and molecular oxygen, $O(^3P) + O_2(^3\Sigma_g) + M \rightarrow O_3 + M$, the so-called Chapman formation reaction, and under these conditions, *Mauersberger et al.* [1993] found enrichment *totally* in the asymmetric isotopomers. *Miller et al.* [1994] proposed that the reaction of vibrationally hot O_2 ($v \geq 26$) with another O_2 molecule can lead to heavy ozone enrichment via preferential potential energy curve-crossing of heteronuclear O_2 from the $O_2(^1\Delta_g)$ to the $O_2(^3\Sigma_g)$ state (see *Valentini* [1987]). However, appreciable production of such vibrationally hot O_2 was predicted to occur only above about 35 km, and the enrichment produced about 5% at 40 km.

While Miller et al. may have provided an explanation for some of the enrichment in the mid-stratosphere, the bulk of the enrichment lacks a generally accepted theoretical explanation. Indeed, detailed statistical mechanical analyses by *Kaye and Strobel* [1983] and *Kaye* [1986] predicted a slight *depletion* of $^{50}O_3$ under stratospheric conditions. This discrepancy between observation and theory indicates that current understanding of ozone formation is incomplete (see, for example, *Anderson et al.* [1992]). However, a promising advance in finding an enrichment mechanism is the recent discovery of several electronically excited states of ozone near the dissociation threshold [*Anderson and Mauersberger,* 1995]. It may be possible that the formation of ozone via the Chapman mechanism goes through one or more of these states whose quantum properties (such as lifetime) are dependent on the isotopic composition of the reactants.

From Figure 3.1, it is difficult to discern any consistent vertical gradients in previously published measurements, and data are lacking on either seasonal or latitudinal effects in the stratosphere. In this study, we take advantage of the high vertical and latitudinal range of the ATMOS data set from the Spacelab3 and ATLAS series missions to

determine if there are substantial vertical or latitudinal gradients. We also evaluate the $^{16}O^{16}O^{18}O$ column enrichments from ground-based spectra from Table Mountain Facility (TMF), Wrightwood, CA, (34.4°N, 117.7°W, 2.2 km altitude) to determine if there is a seasonal variation.

3.2 Data acquisition

Information about the ATMOS instrument and its use on the shuttle can be found in *Gunson et al.* [1995]. The spectral filters used for analyses described here, filters 1, 9 and 12, had ranges of 650-1100 cm^{-1}, 650-2450 cm^{-1}, and 625-1400 cm^{-1} respectively. The number of vertical profiles used for this study were 4 from Spacelab 3, 39 from ATLAS-1, 29 from ATLAS-2 and 87 from ATLAS-3. Using the ATMOS instrument from Table Mountain Facility, ground-based total column measurements were made on 48 separate days from October, 1985 through July, 1990, usually at solar zenith angles corresponding to about 1, 5 and 10 airmasses. As the ATMOS instrument has a very fast response time (2.2 seconds per scan), between 8 and 41 successive, double-sided interferograms were able to be taken within a narrow range of solar zenith angles, which, after transformation and averaging, produced spectra with a signal-to-noise ratio of at least 280 to 1. Only data taken in the morning from TMF were analyzed, as tropospheric smog from nearby Los Angeles could be advected over the intervening mountains and over the site in the afternoon [see *McDermid and Walsh*, 1991].

3.3 Data analysis

ATMOS analysis techniques for space-based observations have been described by *Norton and Rinsland* [1991]. (See also *Gunson et al.* [1995] on the analyses of $^{48}O_3$ from ATMOS space-based observations.) The narrow, unresolved ν_1 band Q-branch centered at 1090.35 cm^{-1} was analyzed for $^{16}O^{16}O^{18}O$, as were several lines of the ν_3 band P-branch for $^{16}O^{18}O^{16}O$ (see Figure 2.2 and Table 2.1). Interfering $^{48}O_3$ lines were fitted

before final fitting of $^{16}O^{18}O^{16}O$ or $^{16}O^{16}O^{18}O$ was attempted. It was not possible to use all of the $^{16}O^{16}O^{18}O$ and $^{16}O^{18}O^{16}O$ features used by *Rinsland et al.* [1985] and *Goldman et al.* [1989] because, at the spectral resolution of the ATMOS instrument, there was too much interference by other molecules to successfully fit some of the heavy ozone lines. Analyses of enrichments were made in between tangent pressures of 2.6 and 26 mb because only in this region could suitable lines be found that simultaneously had reasonable signal above the noise, were unsaturated and reasonably free from interference by other molecules. Spectral parameters for all lines were from the ATMOS linelist [*Brown et al.*, 1995], which currently incorporates the ozone parameters given by *Flaud et al.* [1990]. Error sources for stratospheric measurements are discussed by *Gunson et al.* [1995], although we note here that the systematic error caused by uncertainties in the line intensities are 4% for $^{48}O_3$, 20% for $^{16}O^{16}O^{18}O$ and 10% for $^{16}O^{18}O^{16}O$.

The analysis procedure for the TMF ground-based retrievals differed in that an assumed vertical ozone mixing ratio profile was scaled by a single multiplicative factor until a best fit was obtained between observed and calculated spectra. Table 3.2 describes the lines used for TMF retrievals. Assumed vertical ozone profiles were created using monthly-averaged profiles from the JPL Lidar on TMF [*McDermid*, 1993]. Vertical temperature and pressure profiles were adapted from daily National Meteorological Center data and merged with the U.S. Standard Atmosphere [1976] for higher altitudes. These profiles were then adjusted so that the atmosphere was in hydrostatic equilibrium. To achieve better consistency in the retrievals among the different airmasses sampled within a day, the height registration of the assumed ozone profiles was shifted up or down 0-3 km. In a similar fashion to the spaced-based measurements, neighboring lines of $^{48}O_3$, CO_2 and H_2O were fitted before final fitting of the $^{16}O^{16}O^{18}O$ absorption was attempted. Measurement of column $^{48}O_3$ by the ATMOS instrument at TMF was previously reported

by *Gunson and Irion* [1991], however, as some of the $^{48}O_3$ lines used in that study may have been saturated at high airmasses, the $^{48}O_3$ columns have been re-analyzed for this study. The $^{16}O^{18}O^{16}O$ column from TMF was not retrieved because interference by neighboring $^{48}O_3$, H_2O and CO_2 lines was too large to achieve acceptable fits. Error sources for the TMF retrievals are listed in Table 3.3.

It should be noted that in the determination of the $^{16}O^{16}O^{18}O$ line intensities by *Camy-Peyret et al.* [1986], and incorporated into the ATMOS spectral linelist [*Brown et al.*, 1995], the concentration of $^{16}O^{16}O^{18}O$ in the sample cell was not directly measured. Rather, the line intensities of $^{16}O^{18}O^{16}O$ were derived from theory, and the $^{16}O^{18}O^{16}O$ concentration in the sample cell calculated from measurement of the spectral lines. The $^{16}O^{16}O^{18}O$ concentration was then assumed to be twice that of $^{16}O^{18}O^{16}O$ (see *Flaud et al.*, [1986]). This makes an implicit assumption that any enrichment of $^{16}O^{16}O^{18}O$ and $^{16}O^{18}O^{16}O$ would be equal. Camy-Peyret et al. produced their ozone sample using an electric discharge in a liquid-N_2 cooled vessel. However, in subsequent production of heavy ozone by *Anderson et al.* [1989], also using an electric discharge, but at room temperature, the $^{16}O^{16}O^{18}O$ produced carried about twice the enrichment of $^{16}O^{18}O^{16}O$. It is thus possible that the heavy ozone sample used by Camy-Peyret et al. had a $^{16}O^{16}O^{18}O$ to $^{16}O^{18}O^{16}O$ abundance ratio greater than 2:1, so the line intensities derived for $^{16}O^{16}O^{18}O$ may have been systematically over-estimated, resulting in an under-estimated $^{16}O^{16}O^{18}O$ abundance when these parameters are used for stratospheric spectra. (We note, however, that the effect of the different reaction temperatures of the Anderson et al. and Camy-Peyret et al. experiments on the enrichment partitioning between $^{16}O^{16}O^{18}O$ and $^{16}O^{18}O^{16}O$ is not known.) If we assume that the $^{50}O_3$ enrichment in the Camy-Peyret et al. experiment was 4% (in the upper range of the enrichments found by *Heidenreich and Thiemens* [1983] under similar conditions) and the enriched $^{16}O^{16}O^{18}O$-$^{16}O^{18}O^{16}O$

partitioning of the was 4:1 (as in *Anderson et al.* [1989]), then the error in the $^{16}O^{16}O^{18}O$ line intensities caused by assuming a 2:1 partitioning is a relatively small 2%.

3.4 Results

Figure 3.3 illustrates vertical enrichment profiles for $^{16}O^{16}O^{18}O$ and $^{16}O^{18}O^{16}O$, averaged within latitude bands covered by ATMOS over four shuttle missions. At least three measurements were used to calculate each datum point. The enrichment profiles tend to increase slightly with altitude, and while the standard deviations can be quite high, there does not appear to be any systematic latitudinal variations. Figure 3.1 illustrates previously published $^{50}O_3$ enrichment measurements and the average ATMOS $^{50}O_3$ enrichment profile (assumed the sum of one-third the $^{16}O^{18}O^{16}O$ enrichment and two-thirds the $^{16}O^{16}O^{18}O$ enrichment). The ATMOS average profile was determined by averaging results across constant pressure surfaces and assigning an approximate altitude. Weighted by the $^{48}O_3$ density, the globally averaged $^{50}O_3$ between 2.6 and 26 mb inclusive is (13±5) %, while that for $^{16}O^{16}O^{18}O$ and $^{16}O^{18}O^{16}O$ are (15±6)% and (10±7)%, respectively (1σ standard deviation).

Figure 3.4 shows the $^{16}O^{16}O^{16}O$ columns measured above TMF The random error for the $^{16}O^{16}O^{18}O$ enrichment data points (lower panel) is, on average, 9%. While the ozone column varies substantially, no seasonal variation in the enrichment can be discerned. This is in qualitative agreement with a lack of variability in tropospheric $^{50}O_3$ enrichments found by *Krankowsky et al.* [1995]. Ignoring systematic error, the average column enrichment is (17±4)% (1σ standard deviation), in good agreement with the $^{16}O^{16}O^{18}O$ enrichment derived from the ATMOS stratospheric profiles.

3.5 Conclusions

We have analyzed ATMOS stratospheric spectra for the enrichments of $^{16}O^{16}O^{18}O$ and $^{16}O^{18}O^{16}O$, and ground-based spectra for the column enrichment of $^{16}O^{16}O^{18}O$. We

can find no discernable seasonal variability in the $^{16}O^{16}O^{18}O$ column enrichment, nor can any latitudinal variation be detected in the vertical enrichment profiles. There appears to be a slight increase with altitude, possibly an effect of increasing temperatures and/or decreasing pressure. These observations suggest the enrichment of heavy ozone in the stratosphere is relatively constant, and only weakly regulated by temperature and pressure.

Although previous studies have not ruled out other enrichment processes, laboratory measurements have shown the most significant enrichment in the Chapman reaction, with O and O_2 in the electronic ground state. Noting that the Chapman mechanism has been shown to produce no enrichment for the $^{16}O^{18}O^{16}O$ isotopomer, our determination of a $^{16}O^{18}O^{16}O$ enrichment of (10±7)% (1σ standard deviation) suggests that the $^{16}O^{18}O^{16}O$ line intensities may be biased too low by 10% with respect to the line intensities of $^{48}O_3$. This is within the expected systematic error, although we note it may be possible that other unknown processes are operating to enrich stratospheric $^{16}O^{18}O^{16}O$, much as ozone produced in an electric discharge becomes enriched in $^{16}O^{18}O^{16}O$. Furthermore, since the $^{16}O^{16}O^{18}O$ line intensities derived by *Camy-Peyret et al.* [1986] were determined making use of the $^{16}O^{18}O^{16}O$ line intensities, the $^{16}O^{16}O^{18}O$ line intensities may also be too low. Laboratory measurement of the $^{16}O^{16}O^{18}O$ and $^{16}O^{18}O^{18}O$ spectral line intensities are necessary for verification of the absolute stratospheric enrichments described here. Since *Flaud et al.* [1986] and *Camy-Peyret et al.*[1986] reported good model fittings to their laboratory spectra, such laboratory measurements would probably produce a constant, corrective scaling of the line intensities (and thus the enrichments), but would not affect the precision of the results described here.

Acknowledgements

We thank L. R. Brown, W. B. DeMore, J. Closs, C. B. Farmer, J. C. Foster, P. L. Houston, H. Pickett, I. S. McDermid and G. C. Toon for their assistance. The research

reported herein was performed at the Jet Propulsion Laboratory, California Institute of Technology under contract to National Aeronautics and Space Administration.

References

Abbas, M. M., J. Guo, B. Carli, F. Mencaraglia, M. Carlotti and I. G. Nolt, Heavy ozone distribution in the stratosphere from far-infrared observations, *J. Geophys. Res., 92*, 13231-13239, 1987.

Anderson, S. M., K. Mauersberger, J. Morton, and B. Schueler, "Heavy ozone anomaly: Evidence for a mysterious mechanism" in *Isotope Effects in Gas-Phase Chemistry,* Jack Kaye, ed., American Chemical Society, 1992.

Anderson, S. M., J. Morton and K. Mauersberger, Laboratory measurements of ozone isotopomers by tunable diode absorption spectroscopy, *Chem. Phys. Lett., 156*, 175-180, 1989.

Anderson, S. M. and K. Mauersberger, Ozone absorption spectroscopy in search of low-lying electronic states, *J. Geophys. Res., 100*, 3033-3048, 1995.

Brown, L. R., M. R. Gunson, R. A. Toth, F. W. Irion, C. P. Rinsland and A. Goldman, The 1995 Atmospheric Trace Molecule Spectroscopy (ATMOS) Linelist, submitted to Applied Optics, 1995.

Camy-Peyret, C., J.-M. Flaud, A. Perrin, V. Malathy Devi, C. P. Rinsland and M. A. H. Smith, The hybrid-type bands ν_1 and ν_3 of $^{16}O^{16}O^{18}O$: line positions and intensities, *J. Mol. Spectrosc., 118*, 345-354, 1986.

Carli, B. and Park, J. H., Simultaneous measurement of minor stratospheric constituents with emission far-infrared spectroscopy, *J. Geophys. Res., 93*, 3851-3865, 1988.

Farmer, C. B., O. F. Raper, and F. G. O'Callaghan, Final report on the first flight of the ATMOS instrument during the Spacelab 3 mission, April 29 through May 6, 1985, *Publ. 87-32*, 45 pp., Jet Propulsion Laboratory., Pasadena, Calif., Oct. 1, 1987.

Flaud, J.-M., C. Camy-Peyret, V. Malathy Devi, C. P. Rinsland and M. A. H. Smith, The ν_1 and ν_3 bands of $^{16}O^{18}O^{16}O$: line positions and intensities, *J. Mol. Spectrosc., 118*, 334-344, 1986.

Flaud, J.-M., C. Camy-Peyret, C. P. Rinsland, M. A. H. Smith and V. M. Devi, *Atlas of Ozone Spectral Parameters from Microwave to Medium Infrared*, Academic Press, San Diego CA, 1990.

Goldman, A., F. J. Murcray, D. G. Murcray, J. J. Kosters, C. P. Rinsland, C. Camy-Peyret, J.-M. Flaud and A. Barbe, Isotopic abundances of stratospheric ozone from balloon-borne high resolution infrared solar spectra, *J. Geophys. Res., 94*, 8467-8473, 1989.

Gunson, M. R. and F. W. Irion, "Measurement of atmospheric composition by the ATMOS instrument from Table Mountain Observatory" in *Remote Sensing of Atmospheric Chemistry,* edited by J. L. McElroy and R. J. McNeal, pg.335-346, Proc. SPIE vol. 1491, 1991.

Gunson, M. R., C. B. Farmer, R. H. Norton, R. Zander, C. P. Rinsland, J. H. Shaw, and B.-C. Gao, Measurements of CH_4, N_2O, CO, H_2O, and O_3 in the middle atmosphere by the Atmospheric Trace Molecule Spectroscopy experiment on Spacelab 3, *J. Geophys. Res., 95*, 13867 - 13882, 1992.

Gunson, M. R. et al., The Atmospheric Trace Molecule Spectroscopy (ATMOS) experiment deployment on the ATLAS-3 Space Shuttle Mission, submitted to *Geophys. Res. Lett.,* 1995.

Heidenreich, J. E. and M. H. Thiemens, A non-mass-dependent isotope effect in the production of ozone from molecular oxygen, *J. Chem. Phys., 78*, 892-895, 1983.

I.U.P.A.C., Isotopic composition of the elements, *Pure. Appl. Chem., 55*, 1119-1136, 1983.

Kaye, J. A. and D. F. Strobel, Enhancement of heavy ozone in earth's atmosphere?, *J. Geophys. Res., 88*, 8447-8452, 1983.

Kaye, J. A., Theoretical analysis of isotope effects on ozone formation in oxygen photochemistry, *J. Geophys. Res., 97*, 7865-7874, 1986.

Krankowsky, D., F. Bartecki, G. G. Klees, K. Mauersberger, K. Schellenbach and J. Stehr, Measurement of heavy isotope enrichment in tropospheric ozone, *Geophys. Res. Lett., 22*, 13, 1713-1716, 1995.

Mauersberger, K., Measurement of heavy ozone in the stratosphere, *Geophys. Res. Lett., 8*, 935-939, 1981.

Mauersberger, K., Ozone isotope measurements in the stratosphere, *Geophys. Res. Lett., 14,* 80-83, 1987.

Mauersberger, K., J. Morton, B. Schueler, J. Stehr and S. M. Anderson, Multi-isotope study of ozone: implications for the heavy ozone anomaly, *Geophys. Res. Lett., 20*, 1031-1034, 1993.

McDermid, I. S. and T. D. Walsh, *Surface Ozone Concentrations at Table Mountain Facility (34.4°N, 117.7°W) During 1989 and 1990*, JPL Document D-8354, March,1991.

McDermid, I. S., A 4-year climatology of stratospheric ozone from lidar measurements at Table Mountain, 34.4°N, *J. Geophys. Res., 98*, 10509-10515, 1993.

Miller, R. L., A. G. Suits, P. L. Houston, R. Toumi, J. A. Mack, and A. M. Wodtke, The "ozone deficit" problem: $O_2(X, v \geq 26) + O(^3P)$ from 226-nm ozone photodissociation, *Science, 265*, 1831 - 1838, 1994.

Morton, J., B. Schueler and K. Mauersberger, Oxygen fractionation of ozone isotopes $^{48}O_3$ through $^{54}O_3$, *Chem. Phys. Lett., 154*, 143-145, 1989.

Morton, J., J. Barnes, B. Schueler, and K. Mauersberger, Laboratory studies of heavy ozone, *J. Geophys. Res., 95*, 901-907, 1990.

Norton, R. H. and C. P. Rinsland, ATMOS data processing and science analysis methods, *Appl. Opt., 30*, 389-400, 1991.

Rinsland, C. P., V. Malathy Devi, J.-M. Flaud, C. Camy-Peyret, M. A. H. Smith, and G. M. Stokes, Identification of ^{18}O-isotopic lines of ozone in infrared ground-based solar absorption spectra, *J. Geophys. Res., 90*, 10719-10725, 1985.

Schueler, B., J. Morton, and K. Mauersberger, Measurement of isotopic abundances in collected stratospheric ozone samples, *Geophys. Res. Lett., 17*, 1295-1298, 1990.

U.S. Standard Atmosphere, 1976, National Oceanic and Atmospheric Administration, National Aeronautics and Space Administration, and United States Air Force, Washington, D. C., 1976.

Valentini, J. J., Mass-independent isotopic fractionation in nonadiabatic molecular collisions, *J. Chem. Phys., 86*, 6755-6765, 1987.

Table 3.1: Spectral intervals used for heavy ozone profile analyses from space

Molecule	Window center frequency (cm^{-1})	Window width (cm^{-1})	Line center(s) (cm^{-1})	Line intensity (cm $molecule^{-1}$) at 296 K	Ground state energy (cm^{-1})	Temperature sensitivity of intensity (%/K at 220K)
$^{16}O^{16}O^{18}O$	1090.445	0.55	unresolved	2.14×10^{-23} (a)	203 (b)	-0.1
	975.27	0.12	975.2503	1.69×10^{-24}	546	1.0
			975.2838	2.30×10^{-24}	495	0.7
	981.715	0.14	981.6756	3.54×10^{-24}	363	0.4
			981.7107	4.46×10^{-24}	328	0.3
$^{16}O^{18}O^{16}O$	985.09	0.44	984.9062	4.32×10^{-23}	298	0.2
			984.9790	5.48×10^{-23}	264	0.1
			985.0321	2.20×10^{-23}	395	0.5
			985.1031	4.78×10^{-23}	279	0.1
			985.1578	3.32×10^{-23}	334	0.3
			985.2171	5.10×10^{-23}	268	0.1
	990.422	0.14	990.3889	1.55×10^{-23}	593	1.3
			990.3895	1.74×10^{-23}	567	1.3
			990.3918	1.74×10^{-23}	567	1.1

Notes:

(a) Sum of intensities between 1090.1 and 1090.6 cm^{-1}.

(b) Average weighted by the intensity of the individual lines.

Table 3.2: Spectral intervals used for column density analyses from Table Mountain

Molecule	Line Center (a) (cm-1)	Line Intensity (x 10^{22} cm molec.$^{-1}$)	Ground State Energy (cm^{-1})	Temperature Sensitivity of Intensity %/K at 220K	Airmass Range
	1095.1008	5.19	310.3	0.2	< 1.5
	1114.8233	1.03	77.1	-0.5	3-10
	1123.4234	6.85	120.3	-0.4	<3
$^{16}O^{16}O^{16}O$	1126.2511	2.49	42.9	-0.5	<5
	1140.9448	1.02	190.2	-0.1	3-10
	1163.4222	2.57	253.9	0.04	<5
	1176.1047	1.41	353.3	0.3	3-10
$^{16}O^{16}O^{18}O$	(b)	2.14(c)	203 (d)	-0.1(d)	all

Notes:
(a) Interval width for all $^{16}O^{16}O^{16}O$ windows was 0.16 cm^{-1}. The window for $^{16}O^{16}O^{18}O$ was 1090.35 cm^{-1} with a width of 0.5 cm^{-1}.
(b) Several unresolved lines between 1090.1 and 1090.6 cm^{-1}
(c) Sum of intensities between 1090.1 and 1090.6 cm^{-1}
(d) Average weighted by the intensities of the individual lines.

Table 3.3: Error sources and resulting percentage uncertainties in retrieved column abundances from Table Mountain for a single spectrum

Random Error Source	$^{16}O_3$	$^{16}O^{16}O^{18}O$
Finite signal-to-noise	0.1 -1	0.1 - 2.6
Error in 100% transmission level	2	2
Error in pressure-temperature profile	3	5
Error in fitting interfering lines	1	3
Error in assumed O_3 vertical distribution	5	5
Random error root sum of squares	6.2 - 6.3	7.9 - 8.4
Systematic Error Source		
Uncertainties in line intensity parameters	4	20
Retrieval algorithm[1]	<5	<5
Total systematic error	<7	<21

1. This error tends to cancel out when retrieved mixing ratios are used to determine the enrichment.

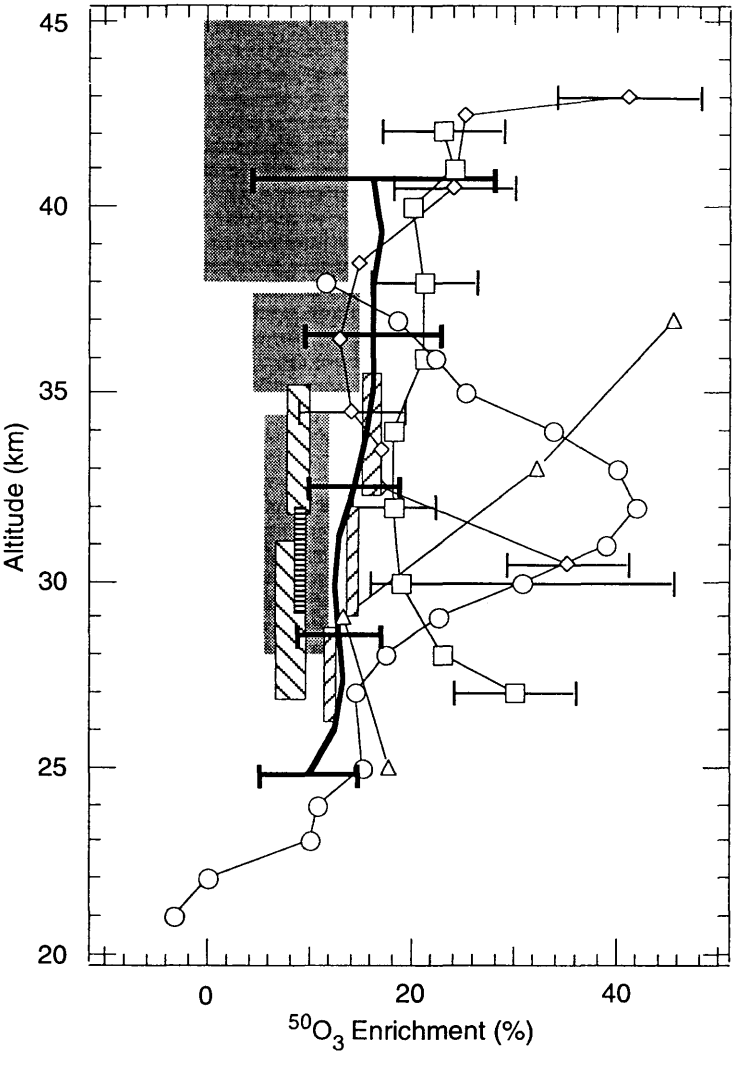

Figure 3.1: Previously reported and globally averaged ATMOS space-borne measurements of $^{50}O_3$ enrichment profiles. The error bars on the ATMOS measurements are the 1σ standard deviations, and do not include systematic error. ATMOS altitudes are approximate and ATMOS $^{50}O_3$ enrichments are assumed to be the sum of two-thirds the $^{16}O^{16}O^{18}O$ enrichment and one-third the $^{16}O^{18}O^{16}O$ enrichment. For clarity, error bars for many of the data points have been omitted, and altitudes for *Mauersberger* [1987], flight a, have been shifted upwards by 0.5 km. Data from *Carli and Park* [1988] are the range of their measurements. *Mauersberger* [1981]: ○; *Mauersberger* [1987], flight a: ◇ , flight b: □; *Abbas et al.* [1987]: △ ; *Carli and Park* [1988]: ▬; *Scheueler et al.* [1990] flight I: ▨, flight II: ▨, flight III: ▤; ATMOS Spacelab 3 and ATLAS-1, -2 and -3 average: ——— .

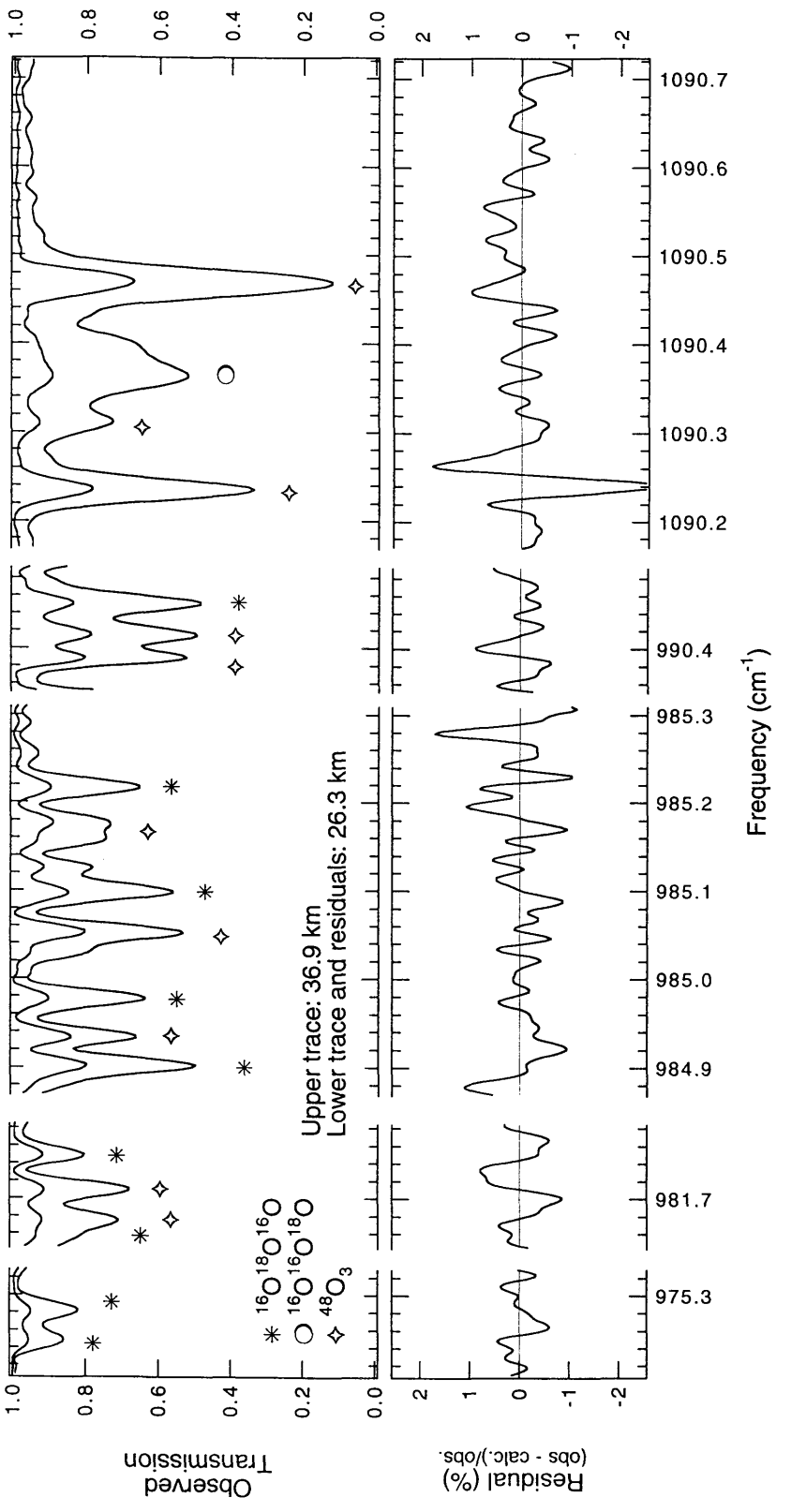

Figure 3.2: Spectral intervals used for space-based profile retrievals of $^{16}O^{16}O^{18}O$ and $^{16}O^{18}O^{16}O$. The residual in the bottom panel was calculated as the fractional difference between the observed and the (not shown) calculated spectrum at 26.3 km.

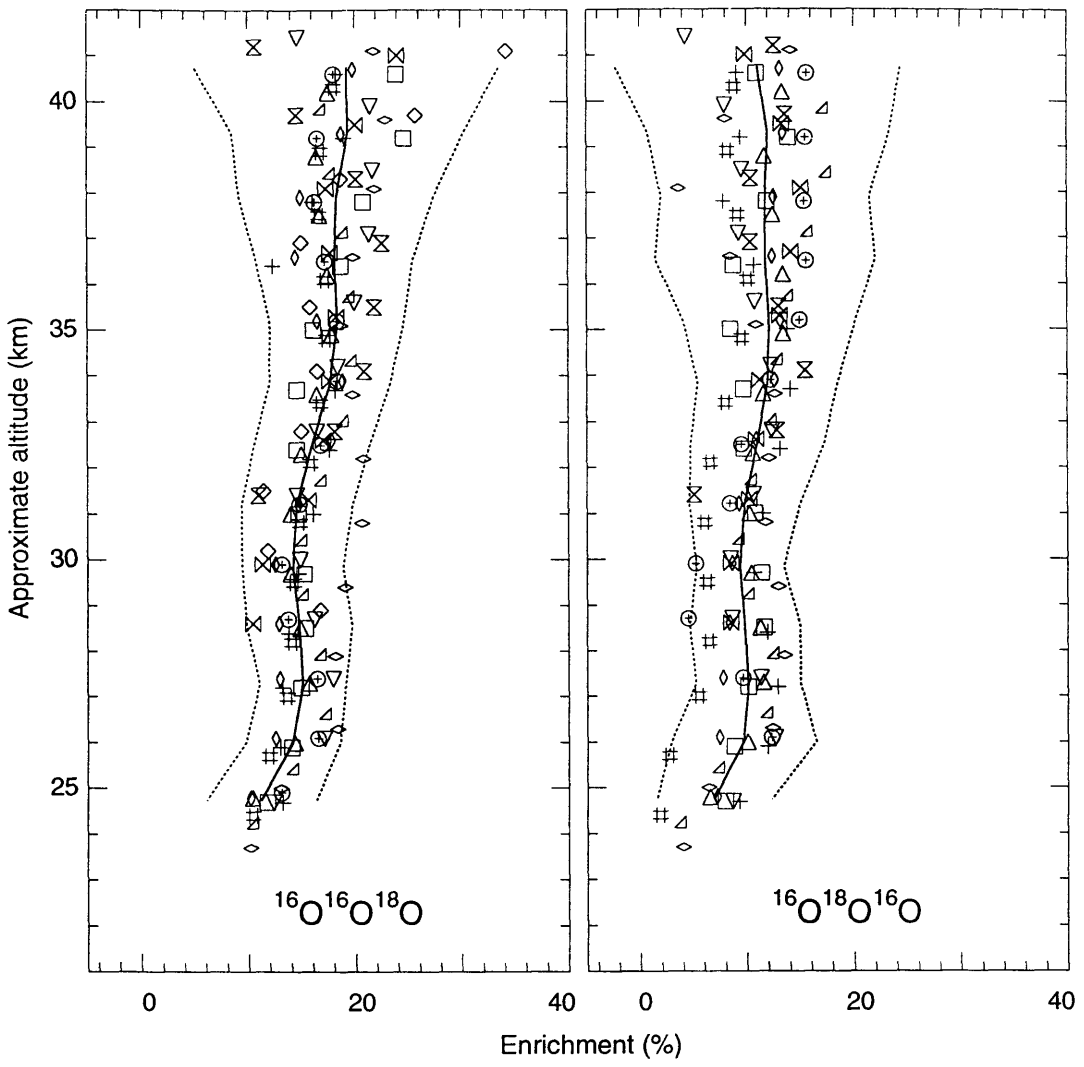

Figure 3.3: $^{16}O^{16}O^{18}O$ and $^{16}O^{18}O^{16}O$ global and latitudinally averaged enrichments from ATMOS space observations. All averages were done on a fixed pressure scale, and for clarity, the altitude shown is the average altitude at each pressure level in its particular latitude bin. All latitudinal averages were weighted by the inverse random square error of the measurement and at least three observations were averaged for each point. The error ranges for the globally averaged profiles are the 1σ standard deviations. See text and *Gunson et al.* [1995] for discussion of systematic errors. ATLAS-3 (Nov. 1994): ▽ 75°S-65°S, inside vortex; ◇ 75°S-65°S inside vortex; + 0°-15°N; □ 15°N-30°N; △ 30°N-50°N. ATLAS-2 (May 1993): ⊕ 50°S-25°S; # 60°N-70°N, outside vortex; ◿ 60°N-70°N, inside vortex. ATLAS-1 (Apr. 1992): ◊ 55°S-30°S; ◇ 30°S-10°S; ⋈ 5°S-10°N; ⧖ 10°N-30°N. ——Global average; ····· 1σ standard deviation.

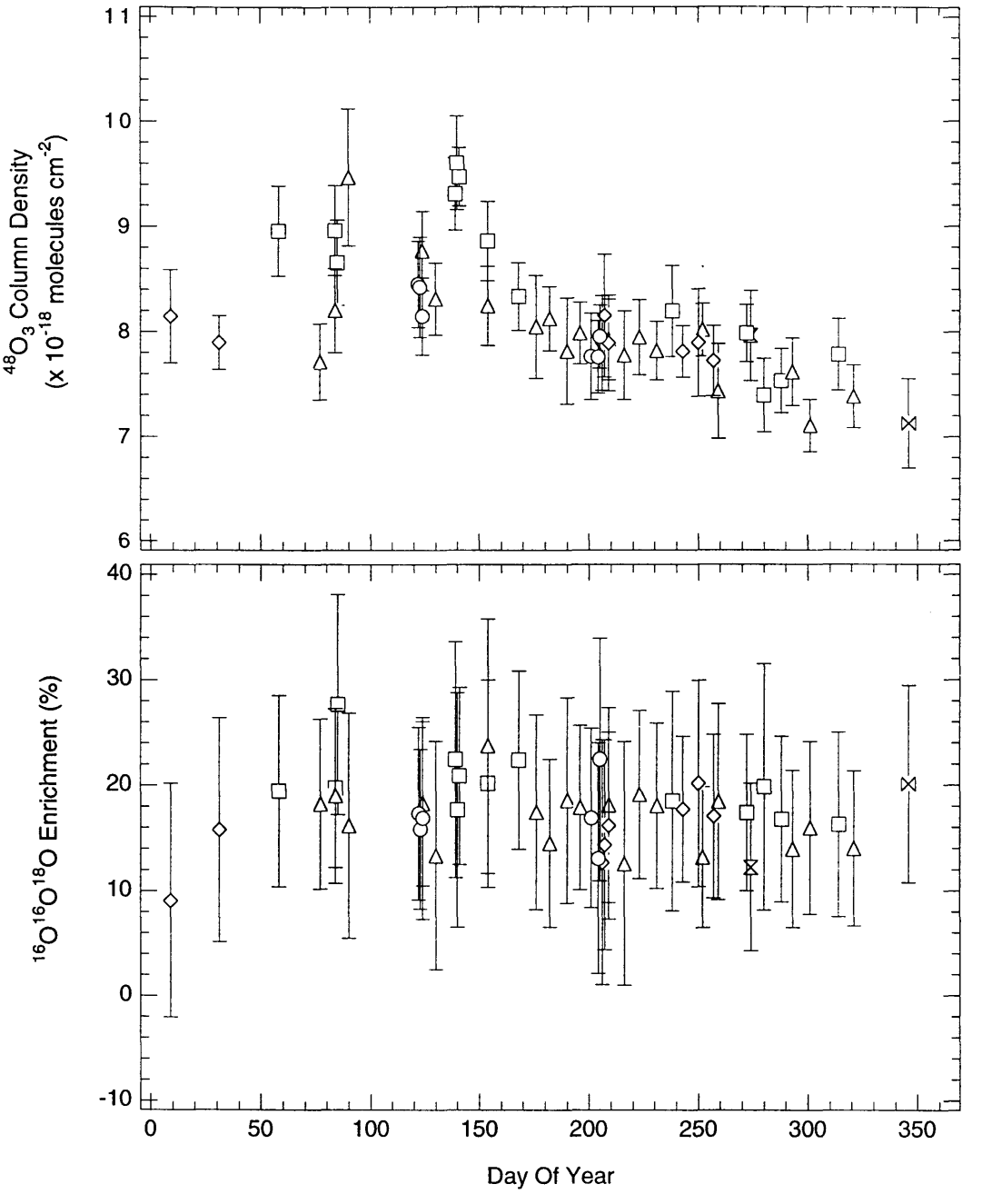

Figure 3.4: $^{48}O_3$ columns and column $^{16}O^{16}O^{18}O$ enrichments from Table Mountain. The error bars do not include systematic error (see text and Table 3.3). ⧖ 1985; ⋈ 1986; □ 1987; △ 1988; ◇ 1989; ○ 1990.

Chapter IV

Stratospheric observations of CH_3D and HDO from ATMOS infrared solar spectra: Enrichments of deuterium in methane and implications for HD

Fredrick W. Irion[1], Elisabeth J. Moyer[2], Michael R. Gunson[3], Curtis P. Rinsland[4], Hope A. Michelsen[5], Ross J. Salawitch[3], Yuk L. Yung[2], Albert Y. Chang[3], Michael J. Newchurch[6], Mian M.Abbas[7], Mark C. Abrams[8], and Rudolphe Zander[9].

[1]Department of Chemical Engineering, California Institute of Technology, Pasadena CA 91125
[2]Division of Geological and Planetary Sciences, California Institute of Technology, Pasadena CA 91125
[3]Jet Propulsion Laboratory, California Institute of Technology, Pasadena CA 91109
[4]NASA Langley Research Center, Hampton VA 23681
[5]Department of Earth and Planetary Sciences, Harvard University, Cambridge, MA 02138
[6]University of Alabama in Huntsville, Huntsville AL 35899
[7]NASA Marshall Space Flight Center, Huntsville AL 35812
[8]SAIC - NASA Langley Research Center, Hampton VA 23681
[9]Institute of Astrophysics, University of Liège, 4000 Liège-Cointe, Belgium

Submitted to Geophysical Research Letters, October 20, 1995

Abstract

Stratospheric mixing ratios of CH_3D from 100 mb to 17mb (≈15 to 28 km) and HDO from 100 mb to 10 mb (≈15 to 32 km) have been inferred from high resolution solar occultation infrared spectra from the Atmospheric Trace MOlecule Spectroscopy (ATMOS) Fourier-transform interferometer. The spectra, taken on board the Space Shuttle during the Spacelab 3 and ATLAS-1, -2, and -3 missions, extend in latitude from 70°S to 65°N. We find CH_3D entering the stratosphere at an average mixing ratio of $(9.9\pm0.8)\times10^{-10}$ with a D/H ratio in methane (7.1±7.4)% less than that in Standard Mean Ocean Water (SMOW) (1σ combined precision and systematic error). In the mid to lower stratosphere, the average lifetime of CH_3D is found to be (1.19±0.02) times that of CH_4, resulting in an increasing D/H ratio in methane as air "ages" and the methane mixing ratio decreases. We find an average of (1.0±0.1) molecules of stratospheric HDO are produced for each CH_3D destroyed (1σ combined precision and systematic error), indicating that the rate of HDO production is approximately equal to the rate of CH_3D destruction. Assuming negligible amounts of deuterium in species other than HDO, CH_3D and HD, this limits the possible change in the stratospheric HD mixing ratio below about 10mb to be ±0.1 molecules HD created per molecule CH_3D destroyed.

4.1 Introduction

In the stratosphere, H_2O is created primarily by oxidation of CH_4 and H_2 by OH, Cl and $O(^1D)$. Likewise, oxidation of CH_3D and HD creates HDO, but these deuterated species show a sufficiently different reactivity with surrounding chemical species so that their measurement can provide additional insight into the stratospheric hydrogen budget. In understanding the deuterium budget of the stratosphere, and relating it to the hydrogen budget, two questions arise. First, what is the lifetime of CH_3D compared to that of CH_4, or put another way, how does the D/H ratio in methane vary with the CH_4 mixing ratio? Second, is the rate of stratospheric HDO production balanced by that of CH_3D oxidation? If not, could there be a net production or destruction of HD, and possibly a change in the D/H ratio of molecular hydrogen, due to a difference in the rates between CH_3D oxidation to HD and HD oxidation to HDO? (Discussion of the D/H ratio in stratospheric water is in an accompanying paper by *Moyer et al.* [1995].)

We address these questions using spectroscopic measurements of stratospheric CH_3D and HDO mixing ratios using data from the ATMOS instrument. The ATMOS instrument, described in detail by *Farmer et al.* [1987], is a Fourier-transform infrared (FTIR) interferometer that gathered spectral absorption measurements at a resolution of 0.01 cm^{-1} from solar occultations on board four Space Shuttle missions (see *Gunson et al.* [1995]). A previous report of HDO and CH_3D results from ATMOS was made by *Rinsland et al.* [1991] with data from the Spacelab 3 mission; however, their report did not relate changes in the CH_3D mixing ratio to those in HDO. With the combined Spacelab 3 and ATLAS-1, -2, and -3 missions, a much broader latitudinal coverage and many more vertical mixing ratio profiles were obtained, allowing characterization of the CH_3D and HDO budget on a more global basis. An important addition to previous reports is measurement of CH_3D inside the Arctic and Antarctic vortices. Above 28 km, the

molecular density of CH_3D is normally too low to gain an adequate spectral absorption signal with the ATMOS instrument. However, the descent of upper stratospheric air to altitudes below 28 km inside the vortices [*Abrams et al.*, 1995a,b] allows measurement of CH_3D in "old" air that would be otherwise impossible to measure. As stratospheric dehydration is not the focus of this letter, we do not report measurements of HDO inside the polar vortices. Analyses are continuing on these vortex HDO measurements, and they will be the focus of an upcoming paper.

In this paper, the delta notation is used to describe isotopic fractionation as the difference in parts per thousand of an isotopically labelled species with respect to a standard, e. g.,

$$\delta D_{sample}\,(‰) = 1000 \times \frac{(D/H)_{sample} - (D/H)_{standard}}{(D/H)_{standard}} \qquad (4.1)$$

Standard Mean Ocean Water (SMOW) is used for the standard D/H ratio (see IUPAC [1983]) and we use the recommended value of $(155.76 \pm 0.05) \times 10^{-6}$ [*Hagemann et al.*, 1970].

4.2 Observations and data analysis

Information about ATMOS on the shuttle missions, and discussion of the mixing ratio retrieval process, can be found in *Gunson et al.* [1995]. For the results described here, spectral lines of the ν_2 band of HDO and the ν_1 band of CH_3D were analyzed, and spectral intervals used for these analyses are described in Table 4.1. HDO is best observed in filters 2 (1100-2000 cm^{-1}) and 9 (600-2450 cm^{-1}), while CH_3D could only be observed in filter 3 (1580 - 3400 cm^{-1}). However, CH_4 can be analyzed in all of these filters and, with a correlation of CH_3D to CH_4 in filter 3, we are able infer the mixing ratio of CH_3D in filters 2 and 9 from CH_4 mixing ratios. At polar latitudes, determination as to whether a

CH_3D measurement was inside or outside the vortex was based on visual inspection of co-located mixing ratio profiles of CH_4 and N_2O, as these gases show markedly smaller mixing ratios inside the vortex than outside at similar altitudes (see *Abrams et al.* [1995a,b]). "Vortex edge" observations were not used. CH_3D results are presented from tangent pressures of 100mb to 17mb, and HDO results are from 100mb to 10mb. Before final analyses, data were filtered by rejecting any observations with an estimated random error greater than 30% for CH_3D and HDO, or 10 % for CH_4. This step eliminated about 16% of the filter 3 CH_3D data and about 19% of the filter 2 and 9 HDO data. Systematic biases, mostly from errors in line intensities, are estimated to be 7% for CH_3D, 6% for HDO, and 5% for CH_4 (see *Gunson et al.* [1995]).

4.3 CH_3D measurement and the D/H ratio in methane

Rate constants for reactions of OH or Cl with CH_3D are lower than those for CH_4 [*DeMore et al.*, 1994; *Wallington and Hurley*, 1992], but any isotope effect between the rate constants of the excited $O(^1D)$ + CH_3D and that of $O(^1D)$ + CH_4 is expected to be relatively minor [*Kaye*, 1987]. To estimate these combined effects on the D/H ratio of methane, we begin by assuming that in the mid to lower stratosphere CH_4 and CH_3D are only destroyed by OH, Cl, and $O(^1D)$ oxidation, and photolysis is negligible. The oxidation of CH_3D and CH_4 can then be described by:

$$\frac{1}{[CH_3D]}\frac{d[CH_3D]}{dt} = -k^*_{OH}[OH] - k^*_{Cl}[Cl] - k^*_{O(^1D)}[O(^1D)] \qquad (4.2)$$

$$\frac{1}{[CH_4]}\frac{d[CH_4]}{dt} = -k_{OH}[OH] - k_{Cl}[Cl] - k_{O(^1D)}[O(^1D)] \qquad (4.3)$$

Let $\gamma_i(T)$ equal the ratios of the rate constants. That is, $\gamma_{OH}(T)=k^*_{OH}/k_{OH}$, $\gamma_{Cl}(T)=k^*_{Cl}/k_{Cl}$, and $\gamma_{O(^1D)}(T)=k^*_{O(^1D)}/k_{O(^1D)}$, where T is temperature. Subtraction of Equation (4.3) from (4.2) gives:

$$\frac{1}{[CH_3D]}\frac{d[CH_3D]}{dt} - \frac{1}{[CH_4]}\frac{d[CH_4]}{dt} = -(\gamma_{OH}-1)k_{OH}[OH] - (\gamma_{Cl}-1)k_{Cl}[Cl] - (\gamma_{O(^1D)}-1)k_{O(^1D)}[O(^1D)] \quad (4.4)$$

But we note that

$$k_{OH}[OH] = \frac{-1}{[CH_4]}\frac{d[CH_4]}{dt} f_{OH}(z) \quad (4.5)$$

where $f_{OH}(z)$ is the fraction of all CH_4 destroyed at altitude z that is destroyed by OH. Similar definitions for $f_{Cl}(z)$ and $f_{O(^1D)}(z)$, substitution in (4.4) for k_{OH}, k_{Cl}, and $k_{O(^1D)}$ (noting that they sum to unity), and rearrangement yield:

$$\frac{1}{[CH_3D]}\frac{d[CH_3D]}{dt} = \left(\gamma_{OH} f_{OH} + \gamma_{Cl} f_{Cl} + \gamma_{O(^1D)} f_{O(^1D)}\right)\frac{1}{[CH_4]}\frac{d[CH_4]}{dt} \quad (4.6)$$

or:

$$\frac{1}{[CH_3D]}\frac{d[CH_3D]}{dt} = \kappa(T,z)\frac{1}{[CH_4]}\frac{d[CH_4]}{dt} \quad (4.7)$$

where $\kappa(T,z)$ is the term inside the parentheses of (4.6). Note that the left-hand side of Equation (4.7) is the time constant for destruction of CH_3D, or equivalently, its inverse lifetime. Thus, for a $\kappa(T,z) < 1$, the lifetime of CH_3D is longer than that of CH_4. We estimate an "average" κ in the mid to lower stratosphere by assuming average fractions for destruction (i.e., f_{OH}, f_{Cl}, and $f_{O(^1D)}$), and assuming that the ratios of the rate constants, γ,

are constant with the temperature range in the mid to lower stratosphere and that mixing effects are minor. Integrating (4.6), assigning boundary conditions, and dividing by total molecular concentration to get mixing ratios (χ) yield:

$$\ln \chi(CH_3D) = \ln \chi_0(CH_3D) + \kappa_{av} \ln\left[\frac{\chi(CH_4)}{\chi_0(CH_4)}\right] \tag{4.8}$$

or equivalently,

$$\frac{\chi(CH_3D)}{\chi_0(CH_3D)} = \left(\frac{\chi(CH_4)}{\chi_0(CH_4)}\right)^{\kappa_{av}} \tag{4.9}$$

where $\chi_0(CH_3D)$ and $\chi_0(CH_4)$ are the initial mixing ratios of these gases as they enter the stratosphere. A rough estimate of κ_{av} can be made if we set γ_{OH}=0.67 (averaged from 190K to 250K using the rate constants reported by *DeMore et al.* [1994]), γ_{Cl}= 0.735 (from the evaluation by *Wallington and Hurley* [1992] at 295K), and $\gamma_{O(^1D)} \approx 1$ (see *Kaye* [1987]). Model calculations by one of us (RJS) indicate that between about 16 km and 30 km, about 50% of the destruction of CH_4 is by OH, 29% by Cl and 21% by $O(^1D)$. Substituting these laboratory data and model results, $\kappa_{av} \approx 0.78$, suggesting that the lifetime of CH_3D is significantly longer than that of CH_4, and enrichment of deuterium in methane can occur as the CH_4 mixing ratio decreases. We emphasize that this is only a rough estimation as none of the experiments measuring the kinetic rate constants of OH or Cl with CH_3D were made at the cold temperatures typical of the lower stratosphere, and we are unaware of any laboratory measurements of the $O(^1D)$+ CH_3D rate constant.

ATMOS measurements of the mixing ratios of CH_3D are plotted against co-located measurements of CH_4 in the upper panel of Figure 4.1. We assume that $\chi_0(CH_4)$ =

$(1.71\pm0.03)\times10^{-6}$ (from global 1992 tropospheric measurements reported in *WMO* [1995], and where we have assumed a 2% error). From a best fit line of ln $\chi(CH_3D)$ vs ln $\chi(CH_4)$, we observe $\kappa_{av} = (0.84 \pm 0.02)$ (1σ precision), higher than our initial estimate of 0.78. Note that the error in κ_{av} is not affected by systematic errors in the measured stratospheric mixing ratios of CH_3D and CH_4 (which instead affect the error in the intercept). On average, the stratospheric lifetime of CH_3D should be κ_{av}^{-1} (=1.19±0.02) times that of CH_4, or about 190 years based on a stratospheric CH_4 lifetime of 160 years [*Prather and Spivakovsky*, 1990]. From the fitted line at a tropospheric CH_4 mixing ratio of $(1.71\pm0.03)\times10^{-6}$, we find the mixing ratio of CH_3D entering the stratosphere to be $(9.9\pm0.8)\times10^{-10}$ (1σ combined precision and systematic error).

The lower panel of Figure 4.1 shows the enrichment of CH_3D with CH_4 mixing ratio, as well as the average enrichment calculated using the fitted line from the upper panel. Although there is considerable scatter in the data, it is seen that methane becomes progressively enriched in deuterium as the mixing ratio of CH_3D decreases. With a tropospheric CH_4 mixing ratio of $(1.71\pm0.03)\times10^{-6}$, the average δD in methane entering the stratosphere is –(71±74)‰ (1σ combined precision and systematic error). This is within error of the ATMOS Spacelab 3 measurements of *Rinsland et al.* [1991], who found δD in stratospheric methane near latitudes of 30°N and 49°S to be –(49±44)‰ and +(24±125)‰ respectively. This is also within error of free tropospheric measurements by *Ehhalt* [1973], who reported values of -86‰ and -94‰, and *Wahlen et al.* [1987], who reported –(80±8)‰.

4.4 Measurement of HDO vs CH_3D and implications for HD

In the mid to lower stratosphere, atomic H is distributed primarily among CH_4, H_2O and H_2, with negligible amounts among other species. It appears that oxidation of H_2 is roughly balanced by its production via oxidation of CH_4 through a short-lived CH_2O intermediate [*Dessler et al,* 1994; *Abbas et al.*, 1995]. Similarly, deuterium is most likely distributed mainly among CH_3D, HDO, and HD (with HD produced by oxidation of CH_3D and destroyed by oxidation to HDO). However, in the mid to lower stratosphere, it may not necessarily be the case that the mixing ratio of HD is as weakly varying as that of H_2. As suggested by *Ehhalt et al.* [1989], the lower reaction rate constant of OH and HD compared to that of OH and H_2 may serve to enrich tropospheric hydrogen gas in deuterium. However, stratospheric destruction of HD is regulated not only by rates of OH attack, but also to a large extent by those of $O(^1D)$, and the rate constant of the $O(^1D)$ reaction is not expected to be significantly affected by deuterium substitution [*Kaye*, 1987]. (Reaction with Cl is a much more minor sink for hydrogen than for methane using the rate constants given by *DeMore et al.* [1994].) For production of HD, account must be taken of not only the oxidation rates of CH_3D, but also the partitioning of D in the short-lived species in the reaction pathway from CH_3D to HD (e.g. the yield of CH_2D vs CH_3, or that of CHDO vs CH_2O). In the absence of direct measurement of HD, a test for changes in the HD mixing ratio is examination of those for HDO and CH_3D. Assuming the sum of the mixing ratios of HDO, CH_3D, and HD constant, then:

$$\frac{d\chi(HDO)}{d\chi(CH_3D)} + \frac{d\chi(HD)}{d\chi(CH_3D)} = -1 \qquad (4.10)$$

and any deviation of $d\chi(HDO)/d\chi(CH_3D)$ from -1 through the mid and lower stratosphere implies a changing mixing ratio of HD.

In order to compare HDO and CH_3D mixing ratios, we use the relationship in Equation 4.8 (with $\kappa = 0.84\pm0.02$, $\chi_0(CH_4) = (1.71\pm0.03)\times10^{-6}$, and $\chi_0(CH_3D) = (9.9\pm0.8)\times10^{-10}$) to estimate the CH_3D mixing ratio in filters 2 and 9 from measurements of CH_4. Figure 4.2 is a scatter plot of the HDO mixing ratio versus this derived CH_3D mixing ratio. We calculate $d\chi(HDO)/d\chi(CH_3D)$ by a least-squares straight line fit, but fitted only where CH_4 mixing ratios were less than 1.4×10^{-6} to avoid seasonal effects in HDO in the lower stratosphere. The calculated slope, $-(1.0\pm0.1)$ (1σ combined precision and systematic error), indicates that HDO production is in near balance with CH_3D destruction. Large effects are still possible for HD within the error, however. As about 10% of stratospheric deuterium is in HD, small deviations in $d\chi(HDO)/d\chi(CH_3D)$ from –1 can have significant effects in the HD mixing ratio, similar to the case for H_2 (e.g., *Dessler et al.* [1994]). Large effects may also occur in the D/H ratio of stratospheric hydrogen, particularly if the H_2 mixing ratio does not change in the mid to lower stratosphere. While we cannot find statistically significant evidence for changes in HD, the results in this report can provide some constraints below about 10 mb. To illustrate this, we assume a constant H_2 mixing ratio of 0.5×10^{-6} and a δD in hydrogen entering the stratosphere of +(70±30)‰ [*Friedman and Scholz*, 1974], giving an initial HD mixing ratio of $(1.67\pm0.05)\times10^{-10}$. Results here indicate that if CH_3D enters the stratosphere at a mixing ratio of 9.9×10^{-10}, then when half of the CH_3D is destroyed, the change in the HD mixing ratio is constrained to be $\pm5\times10^{-11}$ and the change in δD in hydrogen can be constrained to ±320‰.

4.5 Conclusions

We have analyzed ATMOS spectra for mid to lower stratospheric HDO and CH_3D mixing ratios. The average D/H ratio in methane entering the stratosphere was found to be -(71±74)‰, but as the lifetime for CH_3D is greater than that of CH_4 by a factor of (1.19±0.02), this D/H ratio increases as methane becomes oxidized. Stratospheric production of HDO is (1.0±0.1) times that of CH_3D loss, and assuming deuterated species other than HDO, CH_3D and HD are in negligible abundance, changes in HD abundance are thus constrained to be ±0.1 molecules HD per molecule CH_3D destroyed (1σ combined precision and systematic error). To better understand these phenomena, research is warranted into the partitioning of deuterium in CH_3D destruction products (including a comparison of the photolysis rates of CHDO vs that of CH_2O), and direct stratospheric measurements of the HD mixing ratio.

Acknowledgements

We thank L. R. Brown, T. L. Brown, J. C. Foster, C. B. Farmer, G. D. Lynch, O. F. Raper, and G. C. Toon for their assistance. Research was performed at the Jet Propulsion Laboratory, California Institute of Technology, under contract to the National Aeronautics and Space Administration.

References

Abbas, M. M., H. A. Michelsen, M. R. Gunson, M. C. Abrams, M. J. Newchurch, R. J. Salawitch, A. Y. Chang, A. Goldman, F. W. Irion, G. L. Manney, E. J. Moyer, R. Nagaraju, C. P. Rinsland, G. P. Stiller, and R. Zander, Seasonal cycle of water vapor entry into the stratosphere from ATMOS/ATLAS-3 measurements, submitted to *Geophys. Res. Lett.*, 1995.

Abrams, M. C., G. L. Manney, M. R. Gunson, M. M. Abbas, A. Y. Chang, A. Goldman, F. W. Irion, H. A. Michelsen, M. J. Newchurch, C. P. Rinsland, R. J. Salawitch, G. P. Stiller and R. Zander, ATMOS/ATLAS-3 observations of trace gas transport in the Antarctic vortex in November 1994, submitted to *Geophys. Res. Lett.,* 1995a.

Abrams, M. C., G. L. Manney, M. R. Gunson, M. M. Abbas, A. Y. Chang, A. Goldman, F. W. Irion, H. A. Michelsen, M. J. Newchurch, C. P. Rinsland, R. J. Salawitch, G. P. Stiller and R. Zander, Trace gas transport in the Arctic vortex inferred from ATMOS ATLAS-2 observations during April 1993, submitted to *Geophys. Res. Lett.,* 1995b.

Brown, L. R., M. R. Gunson, R. A. Toth, F. W. Irion, C. P. Rinsland, and A. Goldman, The 1995 Atmospheric Trace Molecule Spectroscopy (ATMOS) Linelist, submitted to *Appl. Opt.*, 1995.

DeMore, W. B., S. P. Sander, D. M. Golden, R. F. Hampson, M. J. Kurylo, C. J. Howard, A. R. Ravishankara, C. E. Kolb and M. J. Molina, Chemical Kinetics and Photochemical Data for Use in Stratospheric Modelling - Evaluation Number 11, *JPL Publication 94-26*, 273 pp., Jet Propulsion Laboratory, California Institute of Technology, Pasadena CA, 1994.

Dessler, A. E., E. M. Weinstock, E. J. Hintsa, J. G. Anderson, C. R. Webster, R. D. May, J. W. Elkins and G. S. Dutton, An examination of the total hydrogen budget of the lower stratosphere, *Geophys. Res. Lett., 21,* 2563-2566, 1994.

Ehhalt, D. H., Methane in the atmosphere, in *Carbon and the Biosphere*, edited by G. M. Woodwell and E. V. Pecan, pp. 144-157, U. S. Atomic Energy Commission, Washington, D. C., 1973

Ehhalt, D. H., J. A. Davidson, C. A. Cantrell, I. Friedman, and S. Tyler, The kinetic isotope effect in the reaction of H_2 with OH, *J. Geophys. Res., 94*, 9831-9836, 1989.

Farmer, C. B., O. F. Raper, and F. G. O'Callaghan, Final report on the first flight of the ATMOS instrument during the Spacelab 3 mission, April 29 through May 6, 1985, *JPL Publication 87-32*, 45 pp., Jet Propulsion Laboratory, California Institute of Technology, Pasadena CA, 1987

Friedman, I. and T. G. Scholz, Isotopic composition of atmospheric hydrogen 1967-1969, *J. Geophys. Res., 79*, 783-786, 1974.

Gunson, M. R., M. C. Abrams, L. R. Brown, T. R. Brown, A. Y. Chang, L. L. Lowes, R. J. Salawitch, F. W. Irion, R. Zander, E. Mahieu, C. P. Rinsland, M. J. Newchurch, H. A. Michelsen, A. Goldman, M. M. Abbas, and G. P. Stiller, The Atmospheric Trace Molecule Spectroscopy (ATMOS) experiment deployment on the ATLAS-3 Space Shuttle Mission, submitted to *Geophys. Res. Lett.*, 1995.

Hagemann, R., G. Nief, and E. Roth, Absolute isotopic scale for deuterium analysis in natural waters. Absolute D/H ratio of SMOW, *Tellus, 22*, 712-715, 1970.

IUPAC commission on Atomic Weights and Isotopic Abundances, Isotopic composition of the elements 1981, *Pure Appl. Chem., 55,* 1119-1136, 1983.

Kaye, J. A., Mechanisms and observations for isotope fractionation of molecular species in planetary atmospheres, *Rev. Geophys., 25*, 1609-1658, 1987.

Moyer, E. J., F. W. Irion, Y. L. Yung and M. R. Gunson, Implications of stratospheric deuterated water for troposphere-stratosphere transport, submitted to *Geophys. Res. Lett.,* 1995.

Prather, M. and C. M. Spivakovsky, Tropospheric OH and the lifetimes of hydrochlorofluorocarbons, *J. Geophys. Res., 95*, 18723-18729.

Rinsland, C. P., M. R. Gunson, J. C. Foster, R. A. Toth, C. B. Farmer and R. Zander, Stratospheric profiles of heavy water isotopes and CH_3D from analysis of the ATMOS Spacelab 3 infrared solar spectra, *J. Geophys. Res., 96,* 1057-1068, 1991.

Wahlen, M., N. Tanaka, R. Henry and T. Yoshinari, ^{13}C, D, and ^{14}C in methane (abstract), *Eos. Trans. AGU, 68*, 1220, 1987.

Wallington, T. J. and M. D. Hurley, A kinetic study of the reaction of chlorine atmos with CF_3CHCl_2, CF_3CH_2F, $CFCl_2CH_3$, CF_2ClCH_3, CHF_2CH_3, CH_3D, CH_2D_2, CHD_3, CD_4, and CD_3Cl at 295±2 K, *Chem. Phys. Lett., 189*, 437-442, 1992.

WMO, *Scientific Assessment of Ozone Depletion: 1994,* World Meteorological Organization Global Ozone Research and Monitoring Project - Report No. 37, Geneva, 1995.

Table 4.1: Spectral intervals and lines used for HDO and CH_3D analyses

Spectral Interval Center (cm^{-1})	Interval Width (cm^{-1})	Altitude Range (km)	Line Center (cm^{-1})	Line Intensity at 296 K (cm $molecule^{-1}$)	Air-broadened half-width (cm^{-1}/atm at 296K)	Ground-state energy (cm^{-1})	Temperature Sensitivity of Line Intensity at 230K (% K^{-1})
CH_3D							
2950.84	0.24	10-28	2950.8514	2.81×10^{-23}	0.072	266.3	0.07
3061.56	0.20	15-36	3061.4148	5.21×10^{-23}	0.077	89.9	-0.4
3078.34	0.17	15-28	3078.3125	1.61×10^{-23}	0.070	217.1	-0.07
			3078.3551	2.09×10^{-23}	0.072	184.7	-0.2
3098.91	0.15	10-24	3098.8832	1.58×10^{-23}	0.068	346.0	0.3
HDO							
1408.35	0.25	10-34	1408.3914	9.62×10^{-24}	0.102	29.8	-0.6
1421.62	0.40	13-42	1421.6073	1.26×10^{-23}	0.077	233.1	0.02
1439.93	0.32	15-40	1439.8887	1.54×10^{-23}	0.095	150.1	-0.2
1451.40	0.34	10-29	1451.4597	1.21×10^{-23}	0.093	265.2	0.07
1469.43	0.23	17-40	1469.3658	2.53×10^{-23}	0.095	156.4	-0.2
1474.09	0.31	19-40	1474.1110	1.30×10^{-23}	0.094	156.4	-0.2
1475.62	0.31	20-33	1475.5917	1.37×10^{-23}	0.096	150.2	-0.2
1479.96	0.42	10-26	1480.0941	5.81×10^{-24}	0.093	225.9	-0.04
1484.11	0.25	15-40	1484.1065	2.44×10^{-23}	0.092	225.9	-0.04
1488.16	0.48	20-40	1488.0252	1.09×10^{-23}	0.093	221.9	-0.04
			1488.1937	1.33×10^{-23}	0.100	32.5	-0.6
1494.86	0.29	15-29	1494.8598	8.34×10^{-24}	0.095	221.8	-0.05
1497.85	0.34	15-40	1497.8807	2.08×10^{-23}	0.085	308.6	0.02

Note: The temperature dependence for air-broadened half-widths is $T^{-0.75}$ for CH_3D and $T^{-0.64}$ for HDO. Line parameters for CH_3D are from *Rinsland et al.* [1991]. HDO line parameters are discussed in *Brown et al.* [1995].

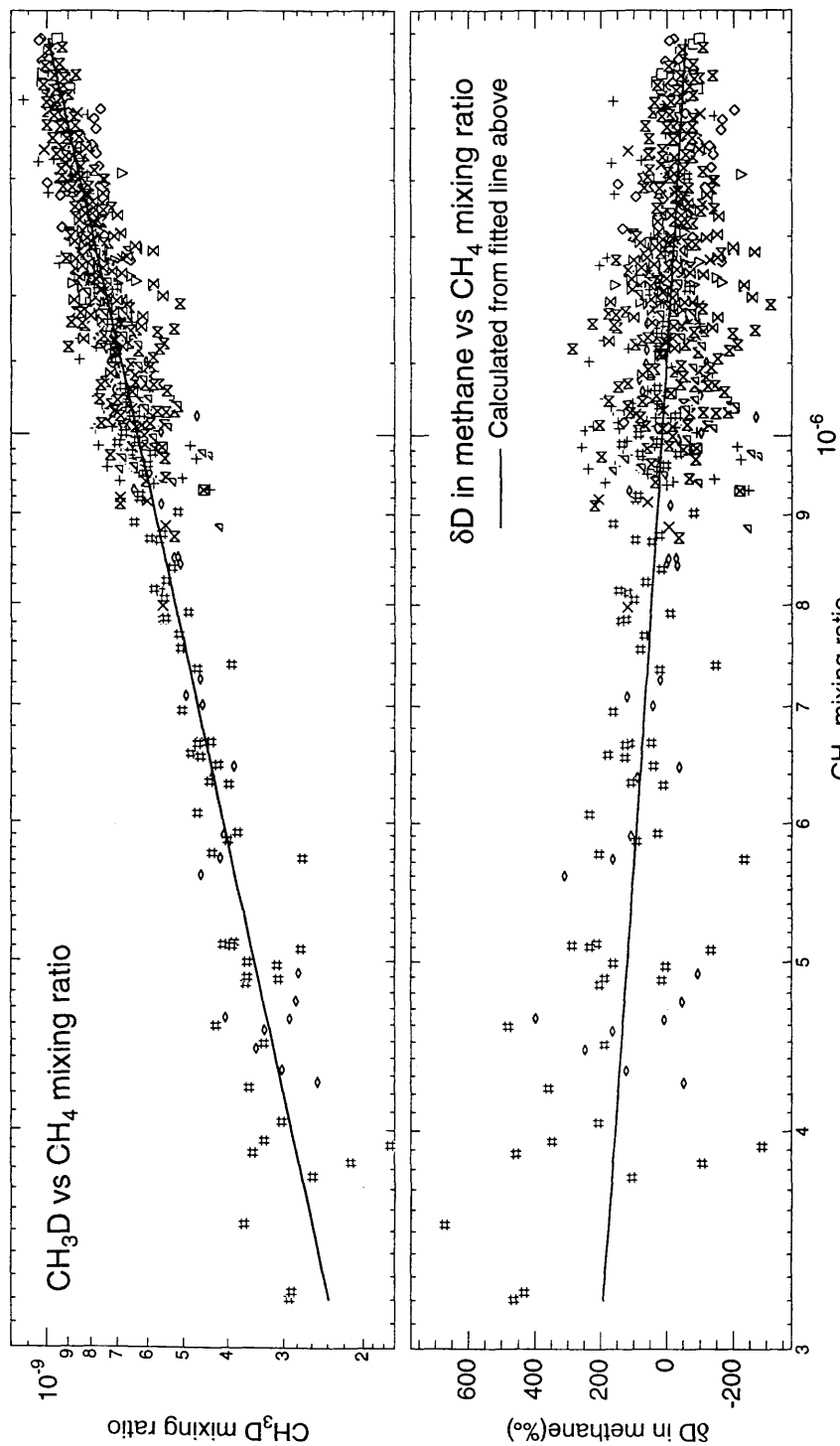

Figure 4.1: CH_3D mixing ratio vs CH_4 mixing ratio (upper panel) **and δD in methane vs CH_4 mixing ratio** (lower panel). Numbers in parentheses indicate the number of observations used: Spacelab 3: ⊠ 48°S (9), × 26°N-31°N (30); ATLAS-1: + 50°S-20°S (94); ATLAS-2: ▽ 50°S-25°S (28), ◁ 65°N-70°N outside vortex, ◇ 65°N-70°N inside vortex(63); ATLAS-3: ⧓ 75°S-65°S outside vortex (86), ⌗ 75°S-65°S inside vortex (86), □ 0°-15°N (22), ◇ 15°N-30°N (58), ⋈ 30°N-50°N (216). Note: Some polar profiles had regions inside and outside the vortex.

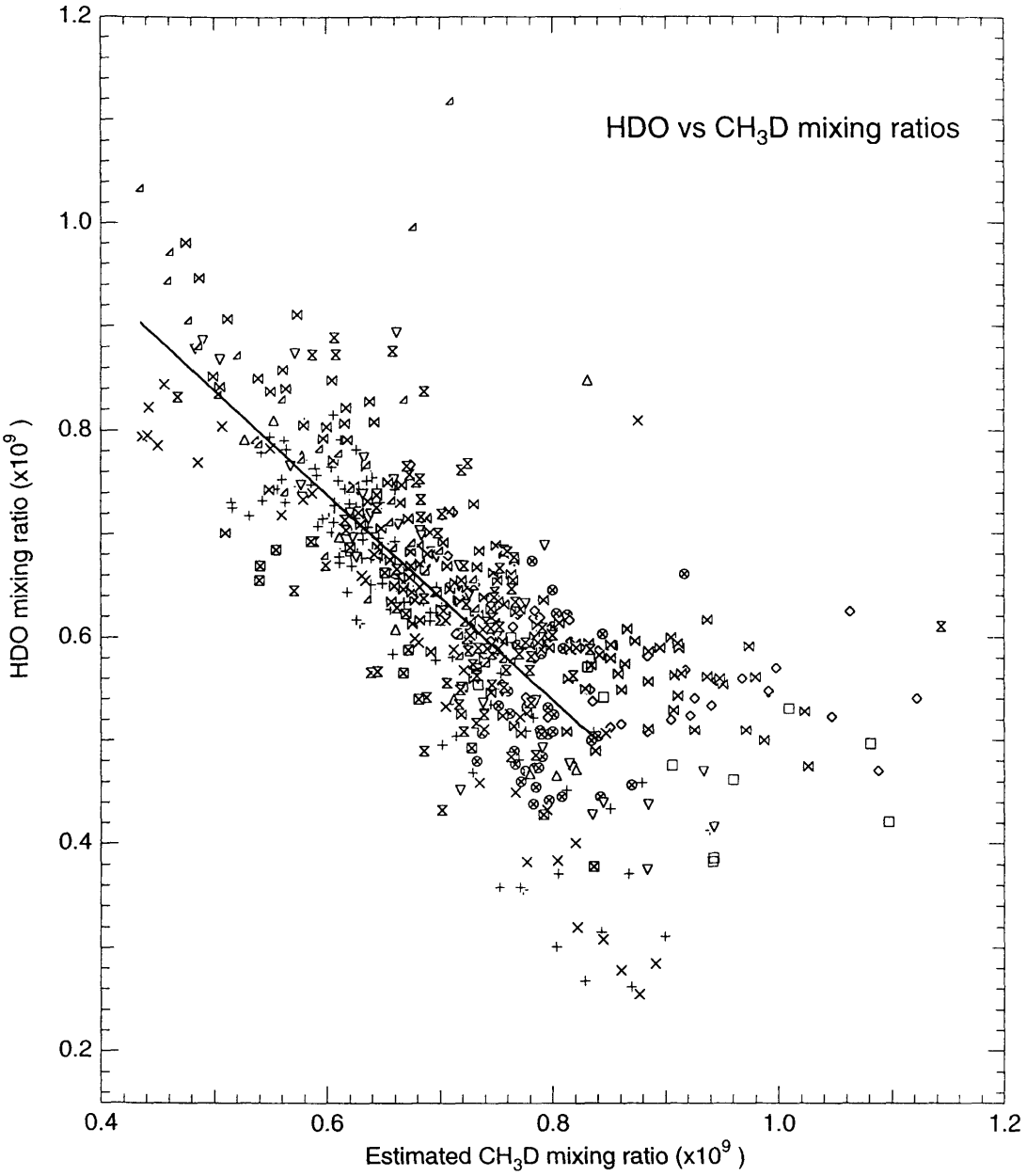

Figure 4.2: HDO mixing ratio vs CH_3D mixing ratio. The line is fitted only where the CH_4 is less than 1.4×10^{-6}. Number in parentheses indicate the number of observations used: Spacelab 3: ⊠ 49°S (13), × 26°N-31°N (33); ATLAS-1: + 55°S-30°S (118), ⊗ 10°S-15°N (36), △ 15°N-30°N (10); ATLAS-2: ▽ 50°S-30°S (40), ◿ 65°N-70°N, outside vortex (35); ATLAS-3: ⧖ 75°S-65°S, outside vortex (82), □ 12°N (4), ◇ 15°N-30°N (25), ⋈ 30°N-50°N (122).

Appendix A

A brief note on error sources and their treatment

This appendix briefly reviews some error sources and their treatment in analyses of ATMOS spectra. Discussion of the instrumental errors of Fourier-transform interferometers is given by *Chamberlain* [1979] and *Beer* [1992]. A full description of the equations used in analyzing ATMOS spectra can be found in *Norton and Rinsland* [1991]. *Shaffer et al.* [1984] discuss systematic sources of error in solar occultation-type measurements in general, while discussions about ATMOS error determinations in particular can be found in *Abrams et al.* [1995] and *Gunson et al.* [1995].

A1.1 Spectral intensities and ground state energies

A full spectra and spectral lineshapes can be found elsewhere (e.g., *Webster et al.* [1988]), but a quick look at spectral line intensities may be helpful in understanding retrieval errors. The spectral intensity of a rotational-vibrational transition at frequency ν is given by

$$S = S_0 \frac{Q_r(T_0)}{Q_r(T)} \frac{Q_v(T_0)}{Q_v(T)} \exp\left(\frac{hcE''}{k}\left[\frac{1}{T_0} - \frac{1}{T}\right]\right) \frac{1-\exp(-hc\nu/kT)}{1-\exp(-hc\nu/kT_0)} \qquad \text{(A1.1)}$$

where S, S_0 = line intensity at temperature T and T_0, respectively (T_0 is usually 296 K)

Q_v, Q_R = vibrational and rotational partition functions, respectively

E" = ground state energy (cm^{-1})

ν = frequency of the line

c = speed of light

h = Planck's constant

k = Boltzmann's constant

Absorption coefficients across a spectrum for an individual line are calculated by multiplying the line intensity by an appropriate lineshape function (e.g., a Voigt or Lorentz profile), followed by convolution with the instrumental function. See *Norton and*

Rinsland [1991]). Spectral databases, such as the ATMOS linelist [*Brown et al.*, 1995], contain information on S_0, E" and ν for over 250,000 lines of some 50 atmospheric gases. Most of the systematic error in a mixing ratio retrieval will be caused by errors in S_0. For example, a line intensity that is 10% too high will result in a retrieved mixing ratio that is 10% too low. Spectral intensity uncertainties for gases studies by ATMOS can range from 2-4% for minor gases such as CO_2, H_2O or N_2O to as high as 15% for HNO_3 and 20 % for CCl_4. *Brown et al.* [1995] lists estimates of line intensity uncertainties for gases retrieved by ATMOS.

Errors in the temperature profile affect the calculated intensity through the partition functions and the ground-state energy, E", but at stratospheric temperatures, it is only the E" term that can lead to significant error in the line intensity. As mentioned in Section 1.1.5, ATMOS trace gas profile retrieval methods utilize a 150 km/150 layer pressure temperature model developed individually for each occultation. The temperature error in such a model profile can range to ±4K. Therefore, wherever possible, lines are chosen with ground-state energies between 100 cm^{-1} and 400 cm^{-1} to keep the temperature sensitivity of the intensities on the order of 1% K^{-1}.

A1.2 Pressure-temperature profiles

The precision and accuracy of ATMOS retrievals from space is greatly aided by CO_2 absorption features within spectra that can be analyzed for determining precise tangent pressures and temperatures, the CO_2 mixing ratio being nearly constant through most of the atmosphere. This makes ATMOS a "self-contained" instrument that does not need external instrumentation to gather temperature and pressure information. ATMOS determination of these profiles is described by *Rinsland et al.* [1992], *Stiller et al.* [1995] and *Abrams et al.* [1995b]. A near-constant CO_2 mixing ratio profile is assumed (e.g., for 1992, 360 ppmv in the troposphere decreasing to a constant 347 ppmv from 21 km to the turbopause

[*Gunson et al.*, 1995]). The software used to determine tangent pressures for individual spectra is the same used to determine mixing ratios, except here the mixing ratio of the target gas, CO_2, is fixed but the pressure is allowed to vary. Temperature sensitive CO_2 are used lines to determine temperatures, while maintaining hydrostatic equilibrium. (An iterative pressure-temperature determination using temperature-sensitive CO_2 lines is used for filters 1 and 3 because they lack adequate temperature-insensitive CO_2 lines. See *Stiller et al.* [1995].)

However, like any other gas that ATMOS measures, errors from noise and spectral parameter inaccuracies affect retrievals of CO_2. As they affect the molecular density within a pressure-temperature model, random errors from pressure soundings become systematic errors in the determination of gas mixing ratios for the occultation from which they were derived. For ATMOS profiles, the random error in a pressure sounding retrieval is determined as

$$\varepsilon_{\text{Pressure}}(z) = \frac{P(z)}{\vartheta_{co_2}(z)} \left[\Sigma_i \frac{\left(\partial T_{i,c}(\nu_i, z) / \partial \vartheta_{co_2} \right)^2}{\left(\frac{1}{SNR} \right)^2 + R_i^2} \right]^{-1/2} \qquad \text{(A1.2)}$$

where: ν_i = frequency at spectral grid point i (cm^{-1})

z = altitude (km)

$T_{i,c}(\nu_i,z)$ = calculated transmission at spectral grid point i

P(z) = pressure at altitude z

ϑ_{CO_2} = assumed mixing ratio for CO_2

SNR = signal-to-noise ratio

Note that the addition of the signal-to-noise error assures that (A1.2) can never be zero, even in the case of a perfect fit. Systematic errors in the CO_2 line intensities add a 4%

error, while an estimated 2% error is from the assumed CO_2 profile. Systematic and precision errors are combined in quadrature to produce a total error varying from about 10% for all filters decreasing to about 5% near 25 km. Tangent pressure errors tend to increase substantially below 100 mb due to CO_2 line saturation; at 10 km, the tangent pressure error is about 30% in filter 9, 10% in filter 3, and about 5-6% in filters 1, 2, 9 and 12.

A1.3 Signal-to-noise and residual errors

The signal-to-noise ratio (SNR) varies for the spectral filters used by ATMOS by the amount of incident radiation on the detector; the broader the spectral bandpass, the lower the SNR. The trade-off is that limiting the spectral bandpass limits the number of co-located gases measurable. While a precise signal-to-noise ratio (SNR) can (and is) calculated by examining out-of-bandpass regions of the spectrum, Filter 1 (600-1200) generally has been shown to have a high SNR of ≈300:1, while with its broad bandpass, Filter 9 has an SNR of ≈100:1. From Table Mountain, however, the ability to take measurements within a narrow range of solar zenith angles allows averaging, and an increased SNR:

$$\mathrm{SNR}_{\mathrm{average}} = \mathrm{SNR}_{\mathrm{individual}} \sqrt{\text{number of individual spectra}} \qquad \text{(A1.3)}$$

Such averaging must be done judiciously, however, because as the solar zenith angle changes, so does the number of molecules in the instrument's line of sight.

The signal-to-noise error will be manifested in fitted spectra's residual of the fitted and observed transmission. The residual error in a mixing ratio retrieval is calculated by:

$$\varepsilon = \sqrt{\frac{\Sigma_i \left[T_o(\upsilon_i,z) - T_s(\upsilon_i,z) \right]^2}{N \, \Sigma_i \left[\partial T_s(\nu_i,z) / \partial \vartheta \right]^2}} \qquad \text{(A1.4)}$$

where: T_o, T_s = observed and synthetic transmission, respectively, at frequency ν_i of spectral grid point i and altitude z.

ϑ = the target gas mixing ratio

N = the number of inflection points in $(\partial T_s/\partial \vartheta)$, usually about the number of target lines in a microwindow.

The residual error is combined into a total root-sum-of-squares error with estimated errors from pressure sounding, zero transmission uncertainty, and propagated error from uncertainties in mixing ratio retrievals from higher altitudes. These latter two errors tend to be small. Note that SNR ratio is implicitly counted twice: once from its contribution to the tangent pressure error and once from its contribution to the residual. This tends to produce a conservative error, even with an excellent spectral fit.

A1.4 Averaging and combined errors

As mentioned in Section 1.1.5, when several microwindows are available for a mixing ratio retrieval, an averaged result is determined weighted by the inverse error of precision:

$$\vartheta_{mn} = \frac{\Sigma_n \left(\vartheta_n / \varepsilon_n^2 \right)}{\Sigma_n \left(1 / \varepsilon_n^2 \right)} \tag{A1.5}$$

The precision of this weighted average is calculated two ways. The first is the reduced standard error of the mean:

$$\varepsilon_{rsa} = \frac{1}{\Sigma_n 1 / \varepsilon_n^2} \tag{A1.6}$$

The second method is the error on the estimation of the mean,

$$\varepsilon_{std}^2 = \frac{\Sigma_n(\vartheta_n^2/\varepsilon_n^2) - \dfrac{\Sigma_n(\vartheta_n/\varepsilon_n^2)^2}{\Sigma_n(1/\varepsilon_n^2)}}{(M-1)\,\Sigma_n(1/\varepsilon_n^2)} \qquad \text{(A1.7)}$$

where M is the number of "effective" microwindows:

$$M = \frac{\left[\Sigma_m(1/\varepsilon_n)\right]^2}{\Sigma_m(1/\varepsilon_n^2)} \qquad \text{(A1.8)}$$

M is less than the actual number of microwindows except where all the precision errors are the same. The final precision quoted is the greater of (A1.6) or (A1.7).

References

Abrams, M. C., M. R. Gunson, M. M. Abbas, A. Y. Chang, A. Goldman, F. W. Irion, H. A. Michelsen, M. J. Newchurch, C. P. Rinsland, R. J. Salawitch, G. P. Stiller, and R. Zander, On the assessment of atmospheric trace gas burdens with high resolution infrared solar occultation measurements from space, *Geophys. Res. Lett.,* in preparation, 1995

Beer, R., *Remote Sensing by Fourier Transform Spectrometry,* John Wiley and Sons, New York, 1992.

Brown, L. R., M. R. Gunson, R. A. Toth, F. W. Irion, C. P. Rinsland, and A. Goldman, The 1995 Atmospheric Trace Molecule Spectroscopy (ATMOS) Linelist, submitted to *Appl. Opt.*, 1995.

Chamberlain, J. E., *The principles of interferometric spectroscopy*, 346 pp., John Wiley & Sons, Chichester, 1979.

Norton, R. H. and C. P. Rinsland, ATMOS data processing and science analysis methods, *Appl. Opt., 30*, 389-400, 1991.

Rinsland, C. P., J. M. Russell III, J. H. Park, and J. Namkung, Retrieval of upper atmosphere pressure-temperature profiles from high resolution solar occultation spectra, *NASA Technical Memorandum 89160,* 33 pp., NASA Langley Research Center, Hampton, VA, 1987.

Shaffer, W. A., J. J. Shaw, and C. B. Farmer, Effects of systematic errors on the mixing ratios of trace gases obtained from occultation spectra, *Appl. Opt.*, *23*, 2818-2826, 1984.

Stiller, G. P., M. R. Gunson, L. L. Lowes, M. C. Abrams, O. F. Raper, C. B. Farmer, R. Zander and C. P. Rinsland, Stratospheric and mesospheric pressure-temperature

profiles from the rotational analysis of CO_2 lines of ATMOS/ATLAS-1 solar occultation spectra, *J. Geophys. Res., 100*, 3107-3117, 1995.

Webster, C. R., R. T. Menzies and E. D. Hinckley, Infrared laser absorption: Theory and observations, in *Laser Remote Chemical Analysis*, edited by R. M. Measures, pp. 163-142, John Wiley and Sons, New York, 1988.

Appendix B

Additional research

This section briefly describes contributions by the author to works in addition to those in Chapters 2, 3, and 4.

B.1 Stratospheric trace gas column burdens from Table Mountain Observatory.

Perturbations to stratospheric chemistry can be long-term, such as the effects of atmospheric loading of the photolysis products of chlorofluorocarbons, and shorter-term such as increased aerosol loading by events such as volcanic eruptions. Such effects may be detected in the mixing ratios of several "active" species, such as O_3, and "sink" species, such as HCl, HF, and HNO_3, all of which primarily reside in the stratosphere and can be measured from ground-based infrared solar absorption techniques. During the delay of shuttle missions due the Challenger accident, the ATMOS instrument was at Table Mountain Facility, Wrightwood, CA (TMF; 34.4°N, 117.7°W), where it took a series of solar absorption spectra spanning from 1985 to 1990. The use of the TMF site has been described in Chapters II and III of this thesis. Measurements of O_3, HCl, HF, and HNO_3 column burdens from TMF were made in order to evaluate the precision attainable by solar absorption Fourier-transform spectrometry for this purpose and evaluate the suitability of TMF as a site for detection of stratospheric change. This research is described in *Gunson and Irion* [1991]. While the time interval in which measurements were taken did not allow a good evaluation of long-term trends in the stratosphere for these gases, the TMF site was shown to be adequate for this purpose, and the spectra and measurements provide a baseline from which future measurements can be compared and trends determined.

B.2 Collation and analyses of previously measured chloroflurocarbon, hydrochlorofluorocarbon and halon mixing ratio profiles in the stratosphere

The loading and location of active chlorine and bromine in the stratosphere depends not only on the stratospheric loading of their source gases, such as the chlorofluorocarbons and halons, but also the stratospheric lifetimes of these source gases; longer-lived gases can reach and be destroyed at higher altitudes. Stratospheric lifetimes of halogenated source gases, with lifetimes larger than transport time scales, are usually not measured directly. They are instead measured relative to that of N_2O by determining the slope of the stratospheric mixing ratio of the source gas plotted against co-located N_2O mixing ratios. In regions where the slope is linear, their lifetimes are related by:

$$\frac{\tau_{\text{source gas}}}{\tau_{N_2O}} = \frac{d\vartheta_{N_2O}}{d\vartheta_{\text{source gas}}} \frac{\vartheta^*_{\text{source gas}}}{\vartheta^*_{N_2O}} \qquad \text{(B1)}$$

where τ is the lifetime, ϑ is mixing ratio, and ϑ^* is a mixing ratio representative of that in the troposphere. (See Plumb, R. A. and M. K. W. Ko, Interrelationships between mixing ratios of long-lived stratospheric constituents, *J. Geophys. Res., 97,* 10145-10156, 1992.) In an effort to quantify stratospheric mixing ratios and lifetimes for several source halocarbons, and intercompare results by different techniques, previously measured results from in-situ and remote sensing techniques for some 20 gases were compiled and compared and, where possible, their mixing ratios plotted against those of N_2O and the slope determined. From these, stratospheric lifetimes with respect to N_2O could be calculated. An example of these plots, for CCl_2F_2, are shown in Figures B.1 and B.2. Full results are given in *Fraser et al.* [1994].

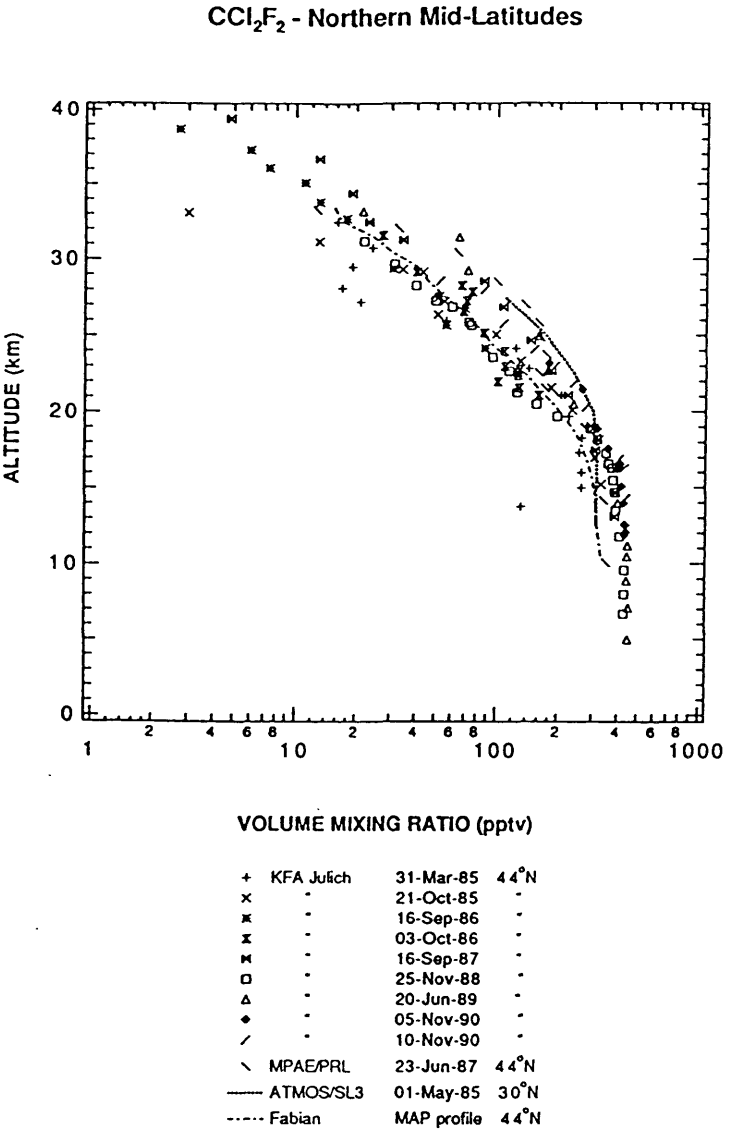

Figure B.1: CCl_2F_2 measurements from northern mid-latitudes (from *Fraser et al.* [1994]).

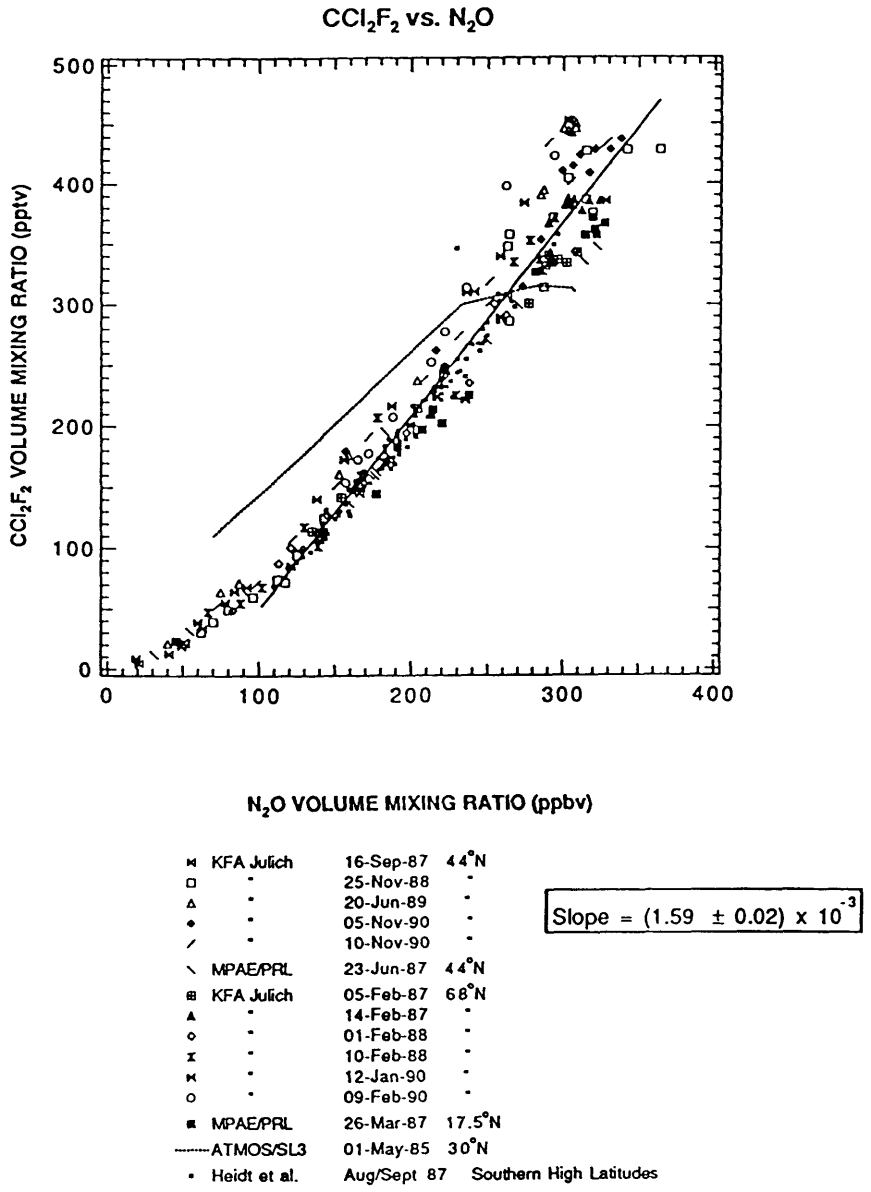

Figure B.2: Simultaneous measurements of CCl_2F_2 and N_2O. The slope is calculated from the data over the range indicated, but excludes measurements by ATMOS. The error is given as 1σ precision. From *Fraser et al.* [1994].

B.3 The use of laboratory spectral cross-sections to infer chlorofluorocarbon and hydrochlorofluorocarbon trace gas mixing ratios

Usually, the modelling of solar absorption spectra requires the calculation of spectral cross-sections based on knowledge of precise spectral line frequencies, line intensities and ground-state energies for the molecules of interest. These spectral line parameters can be difficult to obtain for chlorofluorocarbons, hydrochlorofluorocarbons and N_2O_5 as these molecules show broad, unresolved features in their infrared absorptions even at the best available resolutions. Calculation of their line intensities and frequencies from theory are difficult. Determination of their stratospheric mixing ratios using ATMOS softwate previously relied on empirical pseudo-line parameters, but these were prone to systematic errors in the band intensities and measurement uncertainties from poorly modelled temperature and pressure-broadening effects.

Rather than calculating cross-sections for these gases from pseudo-line parameters, a more efficient, if less flexible approach was to use laboratory-derived cross-sections directly in modelling atmospheric absorptions. This required the integration of new code into existing ATMOS software so that it can simultaneously use both linelists and tables of cross-section data to model absorptions of several gases simultaneously within a spectral window. For a spectral band of a particular molecule, a series of laboratory-derived empirical cross-section data, taken at temperatures and pressures exemplary of the vertical structure of the stratosphere, were first evaluated for suitability and consistency and then converted to a standard binary format. When these cross-sections were used in ATMOS retrievals for a particular model temperature and pressure, the methodology was to interpolate the cross-sections by temperature (or log pressure) to match model parameters, and then to interpolate across wavenumber to match the spectral grid. Absorptions by other molecules (calculated from spectral linelists) were then added into the window to model the total atmospheric absorption. The benefit of this technique was that it was computationally

very fast and avoided the need for psuedo-line parameters. The drawback was that uncertainties increased if an occultation's termperature/pressure profile was highly different from the conditions under which the cross-sections were originally measured, and could give poor results if the cross-section data were of poorer resolution than that of the ATMOS instrument. Overall, however, the approach has been successful for retrievals of various species, and its use is continually extended and modified as new laboratory data become available. (See, for example, the absorption of HCFC-142b in Figure 1.2.1.) The ATMOS linelist and cross-section data currently used are described in *Brown et al.* [1995], and representative ATMOS retrievals using the cross-section algorithm can be found in *Rinsland et al.* [1995a,b], and *Zander et al.* [1995].

B.4 Analyses of stratospheric H_2O and CH_4

There were several motivations to investigate the stratospheric abundances of H_2O and CH_4 from ATMOS measurements. First, as discussed in Section 1.5, the study of the deuterated isotopomers HDO and CH_3D in the stratosphere cannot be done outside the context of the more abundant H_2O and CH_4; it is the variations of deuterium in total water or methane, and the reasons for such variations, that are of interest,. Second, the partitioning of hydrogen among H_2O, CH_4 and H_2 in the upper stratosphere and lower mesosphere was not well measured. Assuming that the total amount of hydrogen residing in species other than H_2O, CH_4 and H_2 is inconsequential, then co-located measurements of H_2O and CH_4 can be used to deduce variations in the vertical H_2 mixing ratio profile. Third, and again as discussed in Section 1.5, the exact mechanisms for transport of water from the troposphere to the stratosphere are not well understood. Much as any proposed mechanism must account for the abundance of HDO in the stratosphere, so must any mechanism account for any seasonal variation of H_2O in the lower stratosphere. As ATMOS can simultaneously determine CH_4 and H_2O, increases in the H_2O mixing ratio

from methane oxidation can be subtracted, and the seasonal variation of water entering the stratosphere through the tropics deduced.

As a contribution in the study of these issues, spectral features of H_2O, HDO, and CH_3D absorptions in ATMOS spectra were selected and tested for their precision in mixing ratio determination and to evaluate their optimal vertical range. (Spectral intervals for CH_4 analyses were not selected by the author.) For the work described by *Moyer et al.* [1995], briefly summarized in Section 1.5, results of ATMOS mixing ratio retrievals were used to determine deuterium depletions in water, both corrected and uncorrected for methane oxidation. When modelled depletions of deuterium in water were compared to ATMOS results, the amounts of deuterium in stratospheric water suggested transport through the troposphere in fast convective updrafts, and not solely by gradual uplift through the troposphere and across the tropopause.

In connection with studies of the stratospheric hydrogen budget, co-located retrievals of H_2O and CH_4 for each mission were plotted against each other over the range of ATMOS measurements. Examples of these are shown in Figure B.3. In order to determine the amount of H_2O produced by the stratospheric oxidation of CH_4, lines were fitted within the 20-35 km range. Again, assuming that the total amount of hydrogen residing in species other than H_2O, CH_4 and H_2 is minor, deviations of the slopes of H_2O vs. CH_4 correlations from -2 indicate net production or destruction of H_2. However, the proximity of the slopes of the solid fitted lines in Figure B.3 to -2 indicate that H_2 oxidation does not consitute a significant net source of H_2O within the 20-35 km range, and that H_2O production is effectively balanced by CH_4 oxidation. In regions where the CH_4 mixing ratio is $\approx$ 250 pptv (about 50 km), the mixing ratios of water are generally higher than that expected by CH_4 oxidation (shown by the dashed curves in Figure B.3), indicating additional net production of H_2O from H_2 oxidation. At even lower CH_4 mixing ratios, the

amount of H_2O decreases because of H_2O photolysis. This study was described in detail by *Abbas et al.* [1995a].

The seasonal variation of water injected into the stratosphere was investigated by analyses of ATMOS retrievals of CH_4 and H_2O in the lower tropical stratosphere. Averaged retrieval results are shown in Figure B.4. As airmasses enter the stratosphere across the tropical tropopause throughout the year and slowly move upwards, a significant seasonal variation is imprinted on the mixing ratio of H_2O, but not on CH_4. Assuming that the minimum at 40 mb (about 22.5 km) in the water vapor mixing ratio corresponds to entry across the tropopause at 100 mb during January and February, and the maximum at 55 mb (about 19 km) corresponds to entry during June and July, an average upward velocity of $\approx$7-8 km year^{-1} was inferred for the region near 22 km. Full details of the study are given in *Abbas et al.* [1995b].

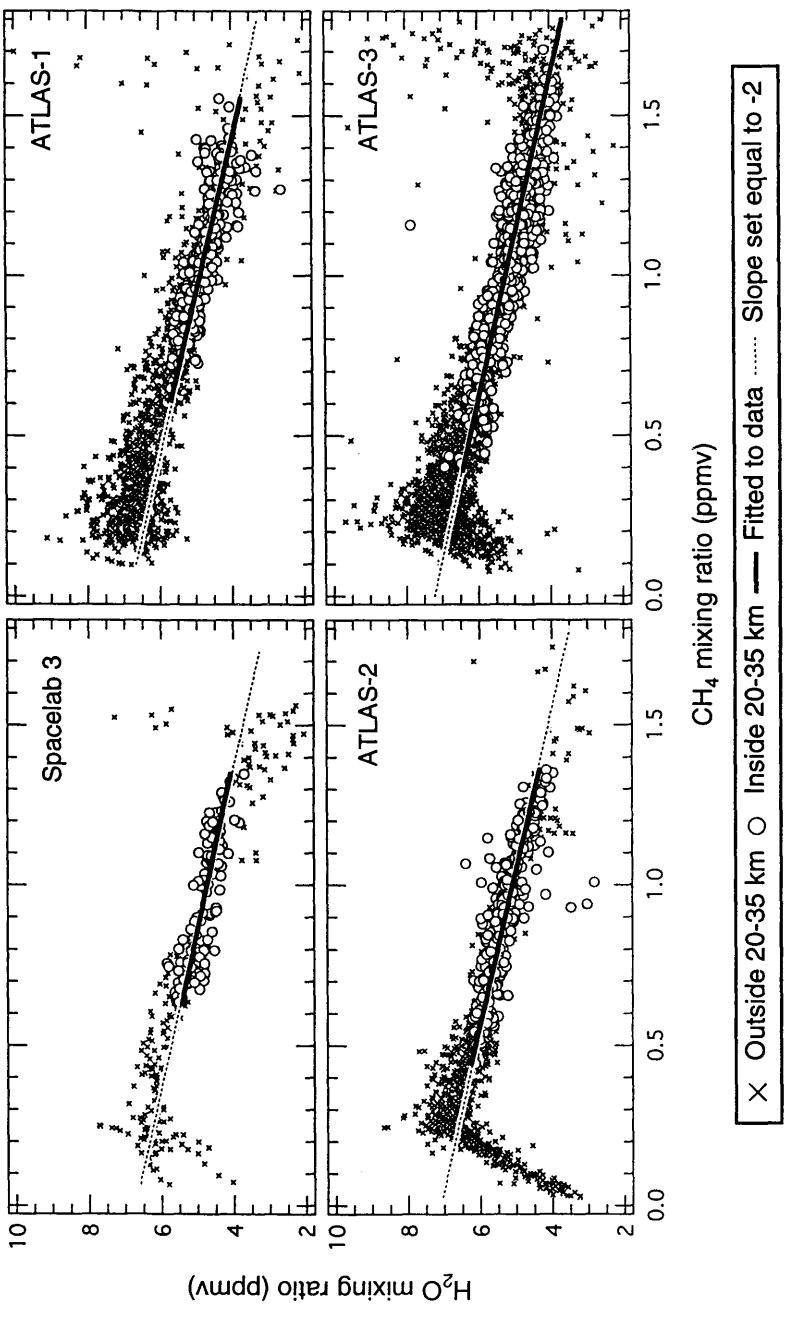

Figure B.3: Stratospheric H_2O vs. CH_4 mixing ratios from ATMOS. Only measurements outside the polar vortices are shown. The solid lines in the above plots are fitted to data between 20 and 35 km, while the dashed lines are fitted to the same region, except that the slope is forced to equal -2 and the line is extrapolated to lower and higher altitudes. Slopes of the solid lines are -(1.89±0.12) for Spacelab 3, -(2.08±0.08) for ATLAS-1, -(2.08±0.09) for ATLAS-2, and -(1.98±0.07) for ATLAS-3 (1σ precision).

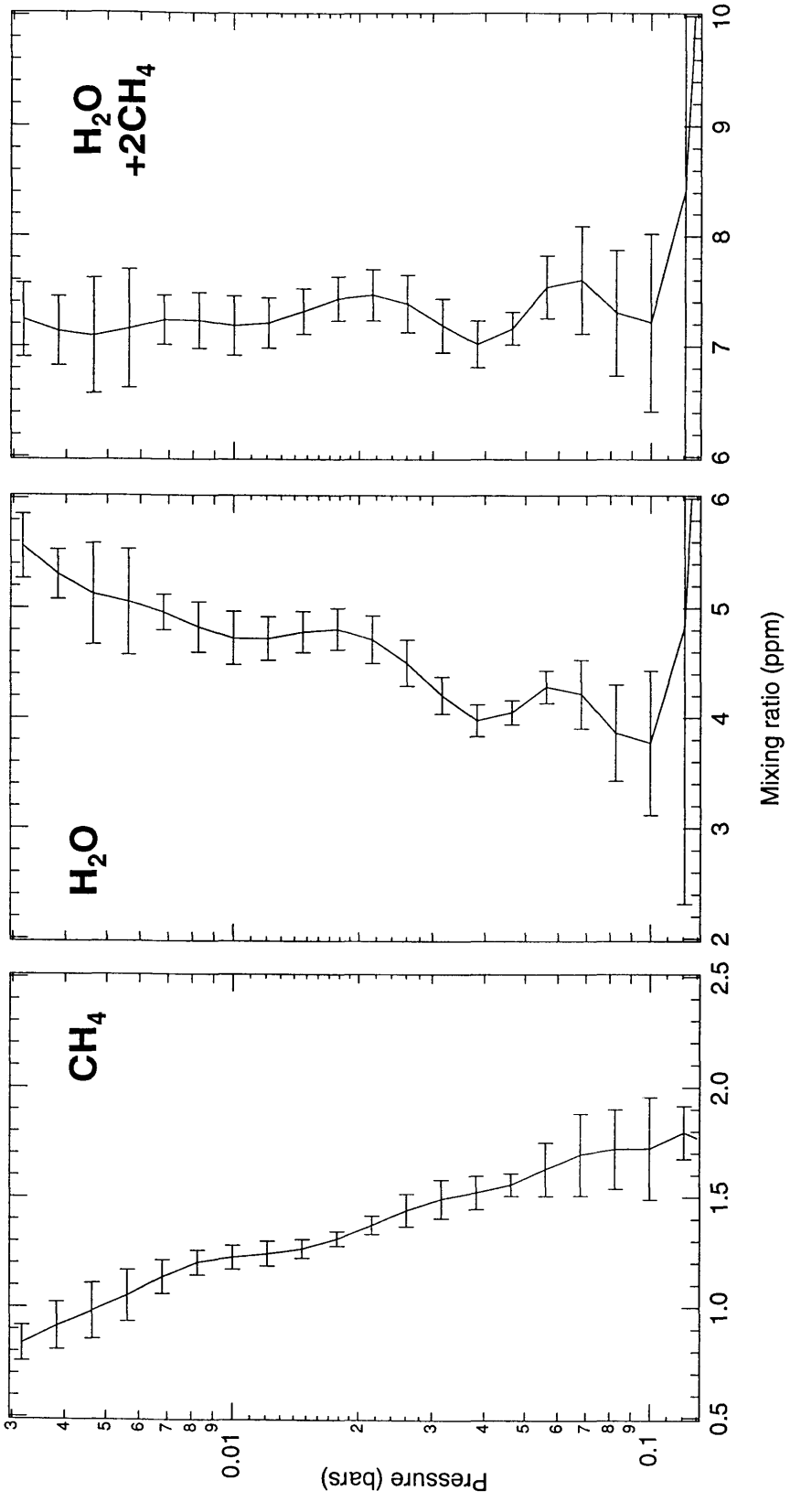

Figure B.4: ATMOS/ATLAS-3 measurements of tropical (8°N-20°N) CH_4, H_2O and H_2O+2CH_4. The structure in the H_2O and H_2O+2CH_4 profiles is indicative of the seasonal variation in water injection into the lower stratosphere and its propagation upwards with time. The vertical velocity of tropical upwelling in the lower stratosphere (≈7 km yr^{-1} near 22 km) can be estimated from the wavelength of this structure.

Publications
(in chronological order)

Gunson, M. R. and F. W. Irion, Measurement of atmospheric composition by the ATMOS instrument from Table Mountain Observatory, in *Remote Sensing of Atmospheric Chemistry*, edited by J. L. McElroy and R. J. McNeal, Proc. SPIE 1491, pp. 335-346, 1991.

Zander, R., M. R. Gunson, C. B. Farmer, C. P. Rinsland, F. W. Irion, and E. Mahieu, The 1985 chlorine and fluorine inventories in the stratosphere based on ATMOS observations at 30° north latitude, *J. Atmos. Chem., 15*, 171-186, 1992.

Fraser, P., M. Gunson, S. Penkett, F. S. Rowland, U. Schmidt, R. Weiss, F. Alyea, D. Blake, E. Brunke, J. Butler, D. Cunnold, J. Elkins, M. Hirota, F. Irion, Y. Makide, R. Prinn, R. Rasmussen, T. Sasaki, H. Scheel, W. Seiler, P. Simmons, and H. Singh, "Measurements" in *Report on Concentrations, Lifetimes, and Trends of CFCs, Halons, and Related Species*, edited by J. A. Kaye, S. A. Penkett, and F. M. Ormond, NASA reference publication 1339, National Aeronautics and Space Administration, Washington, D. C., 1994.

Irion, F. W., M. Brown, G. C. Toon, and M. R. Gunson, Increase in atmospheric CHF_2Cl (HCFC-22) over southern California from 1985 to 1990, *Geophys. Res. Lett., 21,* 1723-1726, 1994.

Rinsland, C. P., M. R. Gunson, M. C. Abrams, L. L. Lowes, R. Zander, E. Mahieu, A. Goldman, and F. W. Irion, April 1993 Arctic profiles of stratospheric HCl, $ClONO_2$, and CCl_2F_2 from atmospheric trace molecule spectroscopy/ATLAS 2 infrared solar spectra, *J. Geophys. Res., 100*, 14019-14027, 1995.

Abbas, M. M., M. R. Gunson, M. J. Newchurch, H. A. Michelsen, R. J. Salawitch, M. Allen, M. C. Abrams, A. Y. Chang, A. Goldman, F. W. Irion, E. J. Moyer, R. Nagaraju, C. P. Rinsland, G. P. Stiller, and R. Zander, The hydrogen budget of

the stratosphere inferred from ATMOS measurements of H_2O and CH_4, submitted to *Geophys. Res. Lett.,* 1995a.

Abbas, M. M., H. A. Michelsen, M. R. Gunson, M. C. Abrams, M. J. Newchurch, R. J. Salawitch, A. Y. Chang, A. Goldman, F. W. Irion, G. L. Manney, E. J. Moyer, R. Nagaraju, C. P. Rinsland, G. P. Stiller, and R. Zander, Seasonal cycle of water vapor entry into the stratosphere from ATMOS/ATLAS-3 measurements, submitted to *Geophys. Res. Lett.*, 1995b.

Abrams, M. C., G. L. Manney, M. R. Gunson, M. M. Abbas, A. Y. Chang, A. Goldman, F. W. Irion, H. A. Michelsen, M. J. Newchurch, C. P. Rinsland, R. J. Salawitch, G. P. Stiller and R. Zander, ATMOS/ATLAS-3 observations of trace gas transport in the Antarctic vortex in November 1994, submitted to *Geophys. Res. Lett.,* 1995a.

Abrams, M. C., G. L. Manney, M. R. Gunson, M. M. Abbas, A. Y. Chang, A. Goldman, F. W. Irion, H. A. Michelsen, M. J. Newchurch, C. P. Rinsland, R. J. Salawitch, G. P. Stiller and R. Zander, Trace gas transport in the Arctic vortex inferred from ATMOS ATLAS-2 observations during April 1993, submitted to *Geophys. Res. Lett.,* 1995b.

Brown, L. R., M. R. Gunson, R. A. Toth, F. W. Irion, and C. P. Rinsland, The 1995 Atmosphere Trace Molecule Spectroscopy (ATMOS) Linelist, submitted to *Appl. Opt.*, 1995.

Gunson, M. R., M. C. Abrams, L. R. Brown, T. R. Brown, A. Y. Chang, L. L. Lowes, R. J. Salawitch, F. W. Irion, R. Zander, E. Mahieu, C. P. Rinsland, M. J. Newchurch, H. A. Michelsen, A. Goldman, M. M. Abbas, and G. P. Stiller, The Atmospheric Trace Molecule Spectroscopy (ATMOS) experiment deployment on the ATLAS-3 Space Shuttle Mission, submitted to *Geophys. Res. Lett.*, 1995.

Irion, F. W., M. R. Gunson, C. P. Rinsland, Y. L. Yung, M. C. Abrams, A Y. Chang, and A. Goldman, Heavy ozone enrichments from ATMOS infrared solar spectra, submitted to *Geophys. Res. Lett.,* 1995a.

Irion, F. W., E. J. Moyer, M. R. Gunson, C. P. Rinsland, H. A. Michelsen, R. J. Salawitch, Y. L. Yung, A. Y. Chang, M. J. Newchurch, M. M.Abbas, M. C. Abrams, and R. Zander, Stratospheric observations of CH_3D and HDO from ATMOS infrared solar spectra: Enrichments of deuterium in methane and implications for HD, submitted to *Geophys. Res. Lett.,* 1995b.

Moyer, E. J., F. W. Irion, Y. L. Yung and M. R. Gunson, Implications of stratospheric deuterated water for troposphere-stratosphere transport, submitted to *Geophys. Res. Lett.,* 1995.

Rinsland, C. P., E. Mahieu, R. Zander, M. R. Gunson, R. J. Salawitch, A. Y. Chang, A. Goldman, M. C. Abrams, H. A. Michelsen, M. M. Abbas, M. J. Newchurch, and F. W. Irion, Trends of OCS, HCN, SF_6, $CHClF_2$ in the lower stratosphere from 1985 and 1994 Atmospheric Trace Molecule Spectroscopy Experiment measurements near 30°N latitude, submitted to *Geophys. Res. Lett.,* 1995.

Yung, Y. L., F. W. Irion, and W. B. DeMore, Heavy ozone in the atmosphere: a useful tracer of chemical species and reaction pathways, submitted to *Geophys. Res. Lett.,* 1995.

Zander, R., E. Mahieu, M. R. Gunson, M. C. Abrams, A. Y. Chang, M. Abbas, C. Aellig, A. Engel, A. Goldman, F. W. Irion, N. Kämpfer, H. A. Michelsen, M. J. Newchurch, C. P. Rinsland, R. J. Salawitch, G. P. Stiller and G. C. Toon, The 1994 northern midlatitude budget of stratospheric chlorine derived from ATMOS/ATLAS-3 observations, submitted to *Geophys. Res. Lett.,* 1995.

Appendix C

Column and profile data from ATMOS on the Space Shuttle and at Table Mountain

Note: ATMOS space-based retrieval data for CH_4, H_2O, HDO, CH_3D and most other gases are publicly available through the internet:

ftp:	remus.jpl.nasa.gov; login anonymous
WWW:	ftp://remus.jpl.nasa.gov/pub/results/vers2/

Table C.1: Average column burdens over Table Mountain Facility

Columns have not been scaled to sea level. Read col. error=random error in column; $^{668}O_3$ enrich=$^{16}O^{16}O^{18}O$ enrichment; $^{668}O_3$ enr. err=random error in $^{16}O^{16}O^{18}O$ enrichment.

Year	Day of Year	$^{48}O_3$ column ($\times 10^{18}$ molec. cm^{-2})	$^{48}O_3$ col. error ($\times 10^{18}$ molec. cm^{-2})	$^{668}O_3$ column ($\times 10^{15}$ molec. cm^{-2})	$^{668}O_3$ col. error ($\times 10^{15}$ molec. cm^{-2})	$^{668}O_3$ enrich (%)	$^{668}O_3$ enr. err (%)	CHF_2Cl column ($\times 10^{15}$ molec. cm^{-2})	CHF_2Cl col. error ($\times 10^{15}$ molec. cm^{-2})
1985	274	7.96	0.43	3.58	0.16	12.2	7.9	1.05	0.08
1986	345							1.21	0.10
	346	7.13	0.43	3.42	0.17	20.1	9.3		
1987	58	8.96	0.40	4.28	0.26	19.5	9.0	1.16	0.09
	84	8.96	0.34	4.29	0.21	19.8	7.5		
	85	8.65	0.45	4.42	0.28	27.7	10.4	1.16	0.09
	139	9.31	0.28	4.56	0.39	22.5	11.1		
	140	9.60	0.38	4.52	0.39	17.7	11.1	1.29	0.10
	141	9.47	0.32	4.58	0.28	20.9	8.4	1.20	0.10
	154	8.86	0.43	4.26	0.28	20.2	9.8	1.22	0.10
	168	8.34	0.27	4.08	0.25	22.4	8.5	1.21	0.10
	238	8.19	0.35	3.88	0.30	18.5	10.4	1.30	0.10
	272	7.98	0.31	3.75	0.19	17.4	7.4	1.21	0.10
	280	7.39	0.34	3.54	0.30	19.9	11.7		
	288	7.53	0.34	3.52	0.17	16.8	7.8	1.25	0.10
	314	7.78	0.34	3.62	0.22	16.3	8.7	1.24	0.10
1988	77	7.71	0.36	3.65	0.18	18.2	8.1	1.22	0.10
	84	8.20	0.40	3.90	0.19	19.0	8.3	1.25	0.10
	90	9.47	0.65	4.40	0.27	16.9	10.7	1.24	0.10
	124	8.76	0.38	4.15	0.21	18.8	7.8	1.29	0.10
	130	8.31	0.34	3.77	0.32	13.4	10.8		
	154	8.25	0.38	4.08	0.35	23.7	12.1		
	176	8.05	0.49	3.78	0.19	17.4	9.2	1.22	0.10
	182	8.12	0.30	3.72	0.22	14.5	7.9	1.28	0.10
	190	7.81	0.51	3.70	0.18	18.6	9.7	1.27	0.10
	196	7.98	0.30	3.77	0.21	17.9	7.8	1.39	0.11
	209	7.92	0.39	3.74	0.23	18.1	9.2	1.30	0.10
	216	7.77	0.42	3.50	0.31	12.6	11.6	1.26	0.10
	223	7.94	0.35	3.79	0.19	19.1	8.0	1.32	0.11
	231	7.82	0.28	3.69	0.21	18.1	7.8	1.39	0.11
	252	8.02	0.25	3.63	0.18	13.2	6.6	1.38	0.11
	259	7.43	0.45	3.52	0.17	18.4	9.3	1.36	0.11
	293	7.62	0.32	3.47	0.17	13.9	7.5	1.32	0.11
	301	7.11	0.25	3.30	0.20	16.0	8.2	1.36	0.11
	321	7.38	0.30	3.37	0.17	14.0	7.3	1.43	0.11

Table C.1 continued

Year	Day of Year	$^{48}O_3$ column ($x10^{18}$ molec. cm^{-2})	$^{48}O_3$ col. error ($x10^{18}$ molec. cm^{-2})	$^{668}O_3$ column ($x10^{15}$ molec. cm^{-2})	$^{668}O_3$ col. error ($x10^{15}$ molec. cm^{-2})	$^{668}O_3$ enrich (%)	$^{668}O_3$ enrich. (%)	CHF_2Cl column ($x10^{15}$ molec. cm^{-2})	CHF_2Cl col. error ($x10^{15}$ molec. cm^{-2})
1989	9	8.14	0.45	3.55	0.31	9.1	11.1		
	31	7.89	0.25	3.66	0.31	15.8	10.6		
	206	7.89	0.45	3.56	0.31	12.7	11.6		
	207	8.15	0.58	3.73	0.19	14.3	9.9	1.41	0.11
	208							1.33	0.11
	209	7.89	0.46	3.67	0.18	16.2	8.9	1.36	0.11
	243	7.81	0.25	3.68	0.18	17.0	6.9	1.42	0.11
	250	7.90	0.51	3.80	0.19	20.2	9.8	1.39	0.11
	257	7.72	0.33	3.61	0.18	17.0	7.7	1.45	0.12
1990	122	8.45	0.41	3.97	0.20	17.3	8.2		
	123	8.42	0.48	3.90	0.13	15.8	7.6	1.45	0.12
	124	8.15	0.37	3.81	0.26	16.9	9.6	1.52	0.12
	201	7.76	0.41	3.63	0.18	16.9	8.5	1.45	0.12
	204	7.76	0.34	3.51	0.30	13.1	10.9		
	205	7.95	0.30	3.89	0.33	22.4	11.5		
	206							1.50	0.12

Table C.2: ATMOS ozone volume mixing ratios and heavy ozone enrichments.

This table contains data only from 26 to 2.6 mb retrievals only where $^{16}O^{16}O^{18}O$ and/or $^{16}O^{18}O^{16}O$ were simultaneously measurable with $^{16}O^{16}O^{16}O$.

Mixing ratios and random errors are in units of 10^{-6} for $^{16}O^{16}O^{16}O$. Latitude and longitude are given for the 30 km tangent height. Random errors for the enrichments were calculated as:

$$\text{Enrichment error (\%)} = 100 \times \left(\frac{\delta_s (\%)}{100} + 1 \right) \sqrt{\left(\frac{RE_s}{MR_s} \right)^2 + \left(\frac{RE_u}{MR_u} \right)^2}$$

where: RE_s and RE_u are the mixing ratio random errors of the substituted ozone molecule ($^{16}O^{16}O^{18}O$ or $^{16}O^{18}O^{16}O$) and $^{48}O_3$, respectively,

MR_s and MR_u are the mixing ratios of the substituted ozone molecule and $^{48}O_3$, respectively,

δ_s is the enrichment of the substituted ozone molecule in %.

Read: sl3=Spacelab 3, at1=ATLAS-1, at2=ATLAS-2, at3=ATLAS-3

Alt=altitude, Press=pressure, vmr=volume mixing ratio, err=random error

sr=sunrise occultation, ss=sunset occultation

$^{48}O_3$ vmr = $^{16}O^{16}O^{16}O$ volume mixing ratio x 10^6

$^{48}O_3$ err = $^{16}O^{16}O^{16}O$ volume mixing ratio random error x 10^6

$^{668}O_3$ enr=$^{16}O^{16}O^{18}O$ enrichment (%)

$^{668}O_3$ enr err =$^{16}O^{16}O^{18}O$ enrichment random error (%)

$^{686}O_3$ enr=$^{16}O^{18}O^{16}O$ enrichment (%)

$^{686}O_3$ enr err =$^{16}O^{18}O^{16}O$ enrichment random error (%)

Table B.2: ATMOS ozone volume mixing ratios and heavy ozone enrichments. (See notes on page 135.)

Alt (km)	Temp (K)	Press (mb)	$^{48}O_3$ vmr	$^{48}O_3$ err	$^{668}O_3$ enr	$^{668}O_3$ enr err	$^{686}O_3$ enr	$^{686}O_3$ enr err
sl3 sr06		*Latitude:-46.9*		*Longitude:309.9*			*Filter: 1*	
40.0	233.3	2.6	6.80	0.98	16.8	26.3	21.5	22.3
38.7	231.8	3.2	6.68	0.97	15.9	26.5	24.0	23.0
37.4	230.3	3.8	6.56	0.94	16.6	26.2	23.1	22.7
36.1	228.6	4.6	6.44	0.91	17.5	25.8	20.3	22.8
34.8	226.7	5.6	6.31	0.90	17.1	26.0	16.5	22.3
33.5	224.9	6.8	6.08	0.85	16.1	25.3	12.4	21.3
32.2	223.2	8.3	5.75	0.76	16.5	24.2	9.7	20.8
30.9	221.7	10.0	5.48	0.68	17.3	23.1	9.0	20.0
29.7	220.1	12.1	5.36	0.61	16.7	21.6	9.5	19.5
28.4	218.8	14.7	5.35	0.56	14.5	20.3	10.3	19.4
27.2	217.6	17.8	5.26	0.50	13.6	18.8	11.8	18.9
26.0	216.6	21.5	5.00	0.43	14.8	18.0	14.1	18.9
24.8	215.6	26.1	4.57	0.35	15.3	17.3	14.6	18.9
sl3 ss02		*Latitude: 32.8*		*Longitude:115.5*			*Filter: 1*	
41.0	258.6	2.6	4.57	0.65	17.7	29.5	22.9	26.9
39.5	254.8	3.2	5.71	0.83	18.7	27.2	21.6	25.3
38.1	250.7	3.8	6.75	0.97	19.0	26.7	19.4	24.5
36.7	246.6	4.6	7.44	1.06	20.0	26.6	17.0	23.8
35.3	242.4	5.6	7.91	1.13	21.1	26.3	14.8	23.0
33.9	238.1	6.8	8.43	1.17	19.8	25.5	12.3	22.3
32.6	234.2	8.3	9.04	1.20	15.5	23.6	9.3	21.2
31.3	233.2	10.0	9.47	1.18	12.0	21.8	7.7	20.8
30.0	232.5	12.1	9.40	1.08	13.0	20.5	9.7	20.3
28.6	230.6	14.7	8.83	0.92	16.6	20.3	13.0	20.3
27.3	226.6	17.8	7.88	0.75	15.0	18.7	10.7	19.2
26.1	222.8	21.5	6.77	0.58	5.1	16.2	0.2	16.9
24.8	220.1	26.1	5.61	0.43	-4.8	14.3	-9.8	15.2

Alt (km)	Temp (K)	Press (mb)	$^{48}O_3$ vmr	$^{48}O_3$ err	$^{668}O_3$ enr	$^{668}O_3$ enr err	$^{686}O_3$ enr	$^{686}O_3$ enr err
sl3 ss05		*Latitude: 31.4*		*Longitude: 0.4*			*Filter: 1*	
41.1	257.2	2.6	5.00	0.72	18.3	28.9	26.3	25.9
39.6	252.8	3.2	5.61	0.82	20.0	27.8	17.2	24.7
38.2	248.3	3.8	6.18	0.89	21.4	27.6	12.7	23.7
36.8	244.4	4.6	6.56	0.93	21.5	27.4	14.1	23.8
35.4	243.0	5.6	6.81	0.97	20.8	26.6	18.1	24.4
34.0	242.0	6.8	7.24	1.01	18.9	25.6	19.5	24.3
32.6	240.4	8.3	7.96	1.06	16.6	24.1	16.9	23.1
31.3	237.6	10.0	8.60	1.07	14.7	22.5	13.4	22.5
30.0	234.7	12.1	8.62	0.99	13.9	20.9	12.1	21.4
28.6	231.3	14.7	8.01	0.84	14.3	19.6	13.1	20.4
27.3	227.3	17.8	7.11	0.67	14.2	18.3	12.7	19.8
26.1	223.4	21.5	6.23	0.53	9.6	16.9	5.9	18.8
24.8	220.0	26.1	5.33	0.41	1.7	15.4	-4.6	17.2
sl3 ss08		*Latitude: 29.9*		*Longitude:245.4*			*Filter: 1*	
41.0	257.5	2.6	4.61	0.66	24.1	30.4	27.2	28.0
39.5	254.3	3.2	4.89	0.72	22.8	28.3	26.7	26.6
38.1	250.9	3.8	5.35	0.77	22.0	27.8	25.1	26.0
36.7	247.3	4.6	6.05	0.86	21.8	27.4	21.3	25.0
35.3	243.0	5.6	6.92	0.99	21.0	26.3	16.7	23.7
33.9	238.6	6.8	7.77	1.08	19.2	25.3	13.2	22.6
32.6	235.3	8.3	8.56	1.14	17.3	23.9	11.6	21.6
31.3	233.6	10.0	9.07	1.13	16.0	22.5	11.2	21.4
29.9	232.1	12.1	9.04	1.04	15.4	20.9	11.1	20.6
28.6	229.4	14.7	8.47	0.89	15.6	19.7	11.4	19.5
27.3	225.8	17.8	7.63	0.72	14.8	18.2	10.6	18.8
26.1	222.2	21.5	6.72	0.57	8.9	16.7	5.4	18.0
24.8	220.0	26.1	5.75	0.44	-1.3	15.0	-3.7	16.6

Table B.2 continued. (See notes on page 135.)

Alt (km)	Temp (K)	Press (mb)	$^{48}O_3$ vmr	$^{48}O_3$ err	$^{668}O_3$ enr	$^{668}O_3$ enr err	$^{686}O_3$ enr	$^{686}O_3$ enr err
at1 sr03		*Latitude:-28.2*		*Longitude:300.7*		*Filter: 1*		
41.0	250.1	2.6	5.84	0.15	19.6	23.9		
39.5	248.7	3.2	6.25	0.15	16.1	23.4		
38.1	246.3	3.8	6.84	0.23	15.4	24.2		
36.8	243.5	4.6	7.36	0.21	15.2	22.7		
35.4	240.1	5.6	7.85	0.21	15.5	22.5		
34.0	236.0	6.8	8.33	0.20	15.2	22.2		
32.7	234.0	8.3	8.75	0.18	14.0	22.9		
31.4	231.1	10.0	9.14	0.20	12.8	19.3		
30.1	229.2	12.1	9.38	0.21	12.4	17.7		
28.8	228.7	14.7	9.12	0.20	12.0	19.5		
27.5	226.9	17.8	8.12	0.16	10.3	17.2		
26.2	224.3	21.5	6.56	0.13	3.8	15.8		
24.9	220.8	26.1	5.02	0.12	-0.9	15.2		
at1 sr09		*Latitude:-16.7*		*Longitude:184.8*		*Filter: 1*		
41.2	252.7	2.6	6.12	0.14	15.2	22.2	11.5	17.1
39.8	250.4	3.2	6.60	0.19	18.4	23.2	9.6	19.1
38.4	248.0	3.8	7.40	0.22	18.0	23.2	9.3	19.8
37.0	243.2	4.6	8.32	0.26	14.8	22.0	10.2	21.5
35.6	238.3	5.6	8.99	0.26	13.2	20.4	11.0	19.3
34.3	235.2	6.8	9.31	0.23	13.7	21.3	10.8	22.9
32.9	233.6	8.3	9.69	0.23	11.8	22.7	8.1	28.1
31.6	231.9	10.0	10.3	0.21	7.5	19.7	4.2	24.2
30.3	229.8	12.1	10.2	0.21	11.5	17.5	11.3	20.0
29.0	227.5	14.7	8.32	0.20	37.1	20.6	42.0	25.5
at1 sr20		*Latitude: -5.8*		*Longitude:114.2*		*Filter: 9*		
41.0	259.1	2.6	6.61	0.21	11.9	21.9	15.0	24.2
39.5	255.9	3.2	7.16	0.22	10.3	23.4	19.1	25.9
38.1	249.8	3.8	7.73	0.21	16.5	17.7	11.3	19.9
36.7	243.3	4.6	8.86	0.22	22.5	15.4	8.1	19.5
35.3	237.8	5.6	9.72	0.23	22.9	14.8	11.4	20.5
34.0	235.4	6.8	9.96	0.23	20.5	15.0	13.9	22.6
32.6	234.4	8.3	10.2	0.30	17.5	15.1	13.2	23.0
31.3	233.7	10.0	10.5	0.32	13.0	16.4	11.6	26.1
at1 sr21		*Latitude: -5.4*		*Longitude: 91.5*		*Filter: 9*		
41.0	256.8	2.6	6.70	0.19	45.1	13.1	32.8	17.3
39.5	252.2	3.2	7.52	0.21	37.3	12.0	21.8	15.6
38.1	247.5	3.8	8.20	0.21	23.1	10.6	10.3	13.9
36.7	242.9	4.6	8.87	0.21	14.8	9.8	7.8	13.4
35.4	239.7	5.6	9.44	0.21	13.8	11.2	13.7	16.6
34.0	239.8	6.8	9.63	0.24	18.3	15.3	19.8	24.5
32.6	238.2	8.3	9.53	0.22	23.5	10.6	20.6	17.8
31.3	236.1	10.0	9.51	0.21	22.7	11.1	15.5	18.3
at1 sr22		*Latitude: -1.6*		*Longitude:292.9*		*Filter: 9*		
40.9	256.0	2.6	6.48	0.21	16.1	25.9	1.2	22.9
39.5	251.2	3.2	6.47	0.19	19.8	23.2	9.6	23.6
38.0	246.9	3.8	6.73	0.34	28.7	17.3	17.1	20.3
36.7	242.8	4.6	7.96	0.40	26.0	16.9	16.4	20.0
35.3	238.9	5.6	9.46	0.37	17.8	17.0	12.5	24.0
33.9	236.4	6.8	10.2	0.32	15.9	12.0	10.4	18.6
32.6	235.0	8.3	10.3	0.25	17.0	13.3	9.5	20.9
31.3	234.0	10.0	10.3	0.26	15.7	13.4	9.2	21.3

Table B.2 continued. (See notes on page 135.)

Alt (km)	Temp (K)	Press (mb)	$^{48}O_3$ vmr	$^{48}O_3$ err	$^{668}O_3$ enr	$^{668}O_3$ enr err	$^{686}O_3$ enr	$^{686}O_3$ enr err
at1 sr23	*Latitude: -1.0*	*Longitude:270.2*	*Filter: 9*					
41.0	258.8	2.6	6.85	0.24	36.8	18.9	11.5	17.7
39.6	253.8	3.2	7.28	0.20	23.1	13.4	14.9	17.2
38.1	249.9	3.8	7.77	0.20	11.6	11.9	15.4	17.0
36.7	246.1	4.6	8.32	0.20	8.7	11.4	12.9	16.4
35.3	242.5	5.6	8.92	0.20	15.4	12.4	11.7	17.3
34.0	240.2	6.8	9.60	0.24	21.0	15.3	11.5	22.8
32.6	236.0	8.3	10.3	0.24	17.8	16.8	8.8	26.5
31.3	232.5	10.0	10.7	0.31	10.9	12.4	5.6	20.8
at1 sr26	*Latitude: 0.6*	*Longitude:202.2*	*Filter: 1*					
40.9	255.1	2.6	6.36	0.17	19.5	25.2	15.6	22.0
39.4	252.1	3.2	7.65	0.21	14.4	24.3	14.1	22.3
38.0	247.7	3.8	7.83	0.23	15.8	21.5	17.4	19.6
36.6	243.4	4.6	8.02	0.22	18.7	20.9	17.5	19.6
35.3	240.5	5.6	8.69	0.24	18.5	20.9	14.3	19.1
33.9	238.6	6.8	9.50	0.24	16.3	21.8	13.1	23.7
32.5	237.0	8.3	10.3	0.26	14.1	19.6	12.8	21.8
31.2	234.5	10.0	10.7	0.25	12.0	19.1	11.1	23.0
29.9	232.1	12.1	10.2	0.20	10.6	17.9	9.6	22.5
28.6	229.4	14.7	9.28	0.18	12.4	16.2	11.3	19.8
at1 sr27	*Latitude: 1.1*	*Longitude:179.5*	*Filter: 9*					
41.0	258.6	2.6	7.28	0.21	23.6	14.8	-3.5	17.1
39.6	253.0	3.2	7.30	0.20	22.3	14.6	5.3	18.6
38.1	248.4	3.8	7.02	0.19	24.8	14.8	22.3	18.3
36.7	245.2	4.6	7.31	0.18	24.1	14.7	28.6	19.0
35.4	242.1	5.6	8.44	0.19	19.0	13.2	19.0	17.3
34.0	239.4	6.8	9.72	0.21	14.8	9.3	9.2	14.7
32.6	236.8	8.3	10.4	0.22	13.4	9.1	7.9	14.4
31.3	234.4	10.0	10.3	0.21	12.9	9.6	13.2	16.0
at1 sr31	*Latitude: 3.2*	*Longitude: 88.9*	*Filter: 1*					
40.8	251.5	2.6	6.16	0.19	19.6	23.5	18.8	19.2
39.4	248.8	3.2	7.62	0.22	18.2	22.3	14.8	17.5
38.0	245.7	3.8	8.33	0.25	16.1	21.9	10.9	18.5
36.6	241.8	4.6	8.33	0.25	14.9	21.7	12.2	20.3
35.2	239.1	5.6	8.49	0.24	14.7	20.6	15.4	19.7
33.9	237.6	6.8	9.37	0.24	13.8	20.2	13.7	20.9
32.5	236.6	8.3	10.5	0.24	12.8	19.5	10.0	20.8
31.2	234.6	10.0	10.9	0.26	12.1	19.4	8.8	23.3
29.8	233.0	12.1	10.6	0.24	11.7	17.1	9.2	20.0
28.5	230.2	14.7	9.68	0.19	12.3	17.0	10.5	21.0
at1 sr32	*Latitude: 6.7*	*Longitude:290.3*	*Filter: 9*					
40.9	258.5	2.6	6.22	0.19	1.1	21.6	3.7	23.2
39.5	250.5	3.2	7.09	0.21	3.4	20.0	18.0	22.8
38.0	245.3	3.8	7.39	0.19	14.0	12.7	15.2	17.9
36.7	242.2	4.6	8.00	0.19	22.0	13.3	9.4	16.9
35.3	239.9	5.6	8.78	0.21	22.0	14.8	6.5	20.7
33.9	238.1	6.8	8.99	0.20	18.4	13.0	6.3	19.1
32.6	235.8	8.3	9.07	0.19	15.5	11.9	9.2	18.4
31.3	233.4	10.0	9.61	0.22	16.9	15.8	12.1	25.3
at1 sr33	*Latitude: 7.2*	*Longitude:267.6*	*Filter: 9*					
41.1	257.3	2.6	6.40	0.21	22.9	24.5	-4.7	23.2
39.6	253.5	3.2	7.09	0.20	18.1	13.8	11.7	16.7
38.2	250.2	3.8	7.71	0.20	16.1	12.1	24.0	16.9
36.8	246.8	4.6	8.30	0.20	14.5	11.6	23.4	16.4
35.4	243.6	5.6	8.92	0.20	16.4	11.9	14.8	16.0
34.0	241.7	6.8	9.56	0.22	19.3	14.4	4.6	21.1
32.7	239.0	8.3	10.0	0.26	19.0	14.5	-1.7	21.5
31.3	236.0	10.0	10.1	0.25	15.6	14.5	-0.6	22.6

Table B.2 continued. (See notes on page 135.)

Alt (km)	Temp (K)	Press (mb)	$^{48}O_3$ vmr	$^{48}O_3$ err	$^{668}O_3$ enr	$^{668}O_3$ enr err	$^{686}O_3$ enr	$^{686}O_3$ enr err
atl sr35		*Latitude: 8.2*		*Longitude:222.3*			*Filter: 1*	
40.9	257.6	2.6	5.87	0.16	14.8	23.3	14.7	19.4
39.5	252.4	3.2	6.66	0.21	19.7	23.5	14.2	19.2
38.0	247.4	3.8	7.60	0.23	17.8	22.7	12.2	19.3
36.6	242.6	4.6	8.48	0.25	11.3	21.1	10.6	19.7
35.3	239.1	5.6	9.13	0.23	7.5	20.2	11.1	20.4
33.9	237.1	6.8	9.68	0.25	10.7	19.9	12.9	20.6
32.6	236.6	8.3	10.3	0.26	15.0	19.6	12.5	20.4
31.2	234.7	10.0	10.8	0.26	14.2	19.3	8.9	22.5
29.9	232.8	12.1	10.7	0.23	10.8	16.6	6.3	18.5
28.6	230.8	14.7	9.95	0.19	8.6	16.3	6.8	19.8
atl sr37		*Latitude: 9.2*		*Longitude:177.0*			*Filter: 1*	
40.8	259.9	2.6	4.71	0.12	18.3	23.6	11.7	19.5
39.4	253.3	3.2	5.74	0.17	18.2	22.7	9.4	18.5
37.9	246.7	3.8	7.13	0.21	18.8	22.0	14.1	19.0
36.5	240.6	4.6	8.32	0.25	18.7	21.5	17.3	19.5
35.2	237.3	5.6	8.98	0.24	17.3	20.5	15.4	18.8
33.8	236.0	6.8	9.45	0.23	15.7	19.7	12.0	18.8
32.5	235.4	8.3	10.0	0.23	14.9	18.9	10.7	18.8
31.2	233.8	10.0	10.5	0.25	14.2	19.0	11.3	21.9
29.9	231.9	12.1	10.3	0.22	12.2	18.9	10.0	24.2
28.5	229.2	14.7	9.40	0.18	8.5	16.1	5.9	19.0
27.3	226.0	17.8	8.46	0.17	10.9	15.7	7.4	19.0

Alt (km)	Temp (K)	Press (mb)	$^{48}O_3$ vmr	$^{48}O_3$ err	$^{668}O_3$ enr	$^{668}O_3$ enr err	$^{686}O_3$ enr	$^{686}O_3$ enr err
atl sr39		*Latitude: 10.2*		*Longitude:131.7*			*Filter: 9*	
41.2	258.7	2.6	5.94	0.18	8.7	23.7	-4.8	26.9
39.7	253.4	3.2	6.90	0.20	30.4	18.2	11.0	20.0
38.3	248.9	3.8	7.89	0.21	37.9	18.7	19.5	21.8
36.9	249.3	4.6	8.48	0.22	32.6	17.4	17.1	24.0
35.5	246.9	5.6	8.66	0.21	22.9	14.6	11.5	20.9
34.1	241.2	6.8	8.96	0.20	17.1	14.1	13.0	22.0
32.7	238.5	8.3	9.57	0.20	13.9	13.8	14.1	23.3
31.4	236.1	10.0	10.2	0.28	11.8	12.8	8.4	21.8
atl sr41		*Latitude: 11.1*		*Longitude: 86.3*			*Filter: 9*	
41.0	258.6	2.6	5.79	0.20	37.8	22.8	6.4	22.5
39.6	259.4	3.2	6.52	0.22	27.4	21.4	18.2	24.3
38.1	254.3	3.8	7.63	0.20	20.2	15.3	14.0	20.4
36.7	248.7	4.6	8.36	0.21	22.2	15.2	7.9	19.4
35.3	244.1	5.6	8.79	0.23	24.8	15.5	5.8	21.2
33.9	240.3	6.8	9.44	0.26	21.0	14.1	8.5	20.8
32.5	237.1	8.3	10.2	0.29	17.3	13.1	12.8	20.9
31.2	232.8	10.0	10.5	0.27	18.0	14.7	15.7	23.9
atl sr42		*Latitude: 14.8*		*Longitude:265.1*			*Filter: 9*	
41.0	256.1	2.6	5.99	0.17	15.8	17.4	4.0	18.6
39.5	253.1	3.2	5.98	0.17	-0.1	13.8	6.6	17.1
38.1	250.0	3.8	6.35	0.17	-3.4	13.2	10.3	18.0
36.7	246.9	4.6	7.39	0.18	10.7	14.5	14.3	18.2
35.3	241.5	5.6	8.76	0.21	22.5	16.8	16.4	23.9
33.9	237.5	6.8	9.76	0.24	22.7	16.0	15.1	24.2
32.6	235.6	8.3	10.3	0.25	21.2	12.1	12.1	19.9
31.2	234.4	10.0	10.4	0.24	22.6	12.2	9.7	19.5

Table B.2 continued. (See notes on page 135.)

Alt (km)	Temp (K)	Press (mb)	$^{48}O_3$ vmr	$^{48}O_3$ err	$^{668}O_3$ enr	$^{668}O_3$ enr err	$^{686}O_3$ enr	$^{686}O_3$ enr err
at1 sr43		*Latitude: 15.3*		*Longitude:242.4*			*Filter: 9*	
41.1	260.3	2.6	5.92	0.18	45.6	22.1	16.3	21.1
39.6	254.6	3.2	6.78	0.19	41.8	21.5	11.8	20.3
38.2	249.3	3.8	7.64	0.20	26.6	16.5	2.9	18.4
36.8	244.3	4.6	8.37	0.21	17.6	15.4	1.4	18.3
35.4	241.6	5.6	8.96	0.20	16.1	10.3	6.1	15.6
34.0	239.6	6.8	9.52	0.20	16.8	10.2	10.2	16.0
32.7	237.0	8.3	10.0	0.20	17.1	10.1	11.3	15.9
31.3	233.8	10.0	10.2	0.21	17.1	14.0	11.0	23.1
at1 sr44		*Latitude: 15.7*		*Longitude:219.8*			*Filter: 1*	
40.9	256.8	2.6	4.61	0.14	15.6	24.3	16.0	20.7
39.5	253.5	3.2	5.99	0.17	17.0	24.4	14.4	20.3
38.0	250.2	3.8	7.57	0.21	20.9	23.4	13.0	20.7
36.6	245.7	4.6	8.45	0.24	22.8	21.9	13.4	19.0
35.2	239.5	5.6	8.79	0.24	20.3	21.2	14.3	18.8
33.9	235.3	6.8	9.40	0.23	15.9	19.6	14.0	18.4
32.6	233.6	8.3	10.4	0.27	13.2	18.7	12.4	19.2
31.2	232.9	10.0	11.1	0.26	12.2	17.8	10.1	19.2
29.9	231.4	12.1	10.9	0.21	11.0	17.2	7.8	20.0
28.6	229.4	14.7	9.78	0.20	10.2	16.6	6.8	19.8
at1 sr49		*Latitude: 17.8*		*Longitude:106.5*			*Filter: 9*	
41.8	260.0	2.6	6.21	0.24	26.8	20.8	29.3	26.6
40.3	259.2	3.2	6.64	0.19	17.8	19.1	20.7	24.6
38.8	257.7	3.8	7.33	0.20	14.2	18.5	11.3	22.7
37.4	253.1	4.6	8.09	0.22	27.5	15.7	9.0	20.8
36.0	246.4	5.6	8.57	0.20	31.5	13.1	13.2	21.5
34.6	241.6	6.8	8.73	0.18	28.4	10.2	19.2	17.4
33.2	237.7	8.3	8.84	0.17	22.4	9.7	19.6	16.9
31.9	234.1	10.0	9.24	0.17	13.4	9.0	10.5	15.6

Alt (km)	Temp (K)	Press (mb)	$^{48}O_3$ vmr	$^{48}O_3$ err	$^{668}O_3$ enr	$^{668}O_3$ enr err	$^{686}O_3$ enr	$^{686}O_3$ enr err
at1 sr50		*Latitude: 18.2*		*Longitude: 83.9*			*Filter: 9*	
41.3	261.5	2.6	5.40	0.18	-19.9	15.4	-0.3	21.6
39.8	256.6	3.2	5.59	0.16	-16.3	16.0	7.7	22.6
38.4	251.7	3.8	6.51	0.17	3.9	17.9	3.8	21.3
37.0	245.7	4.6	7.83	0.19	22.1	14.8	3.7	19.3
35.6	240.0	5.6	8.98	0.21	28.0	12.1	11.8	17.7
34.2	237.1	6.8	9.90	0.22	23.8	11.3	17.8	18.2
32.9	234.1	8.3	10.8	0.28	14.1	13.6	11.7	22.1
31.6	231.0	10.0	11.3	0.27	2.3	8.2	-2.5	12.9
at1 sr56		*Latitude: 27.8*		*Longitude:237.7*			*Filter: 9*	
40.9	262.4	2.6	5.95	0.18	16.0	21.7	0.1	31.5
39.5	258.2	3.2	5.70	0.16	25.1	14.6	14.4	19.1
38.0	252.2	3.8	5.71	0.15	30.1	15.1	22.3	20.3
36.6	246.2	4.6	6.78	0.17	23.0	14.1	26.6	20.4
35.2	243.2	5.6	8.37	0.21	15.1	12.6	25.4	20.9
33.8	242.6	6.8	9.30	0.23	14.3	12.3	17.7	19.5
32.5	237.5	8.3	9.30	0.23	18.0	11.6	7.6	19.1
31.1	231.5	10.0	8.85	0.21	19.6	11.8	4.4	18.8

Table B.2 continued. (See notes on page 135.)

Alt (km)	Temp (K)	Press (mb)	$^{48}O_3$ vmr	$^{48}O_3$ err	$^{668}O_3$ enr	$^{668}O_3$ enr err	$^{686}O_3$ enr	$^{686}O_3$ enr err
atl ss05		*Latitude:-28.7*		*Longitude:169.0*		*Filter: 9*		
41.2	260.7	2.6	6.69	0.20	46.0	13.5		
39.7	256.0	3.2	7.49	0.21	30.2	12.0		
38.3	251.4	3.8	8.17	0.22	19.5	10.9		
36.9	246.8	4.6	8.52	0.21	15.0	10.3		
35.5	242.2	5.6	8.45	0.20	16.6	10.5		
34.1	239.6	6.8	8.39	0.19	18.7	15.9		
32.8	237.1	8.3	8.75	0.25	15.9	10.9		
31.4	234.2	10.0	9.20	0.27	12.0	9.1		
30.1	231.3	12.1	9.13	0.27	11.8	9.0		
28.8	228.3	14.7	8.51	0.25	13.8	9.1		
27.5	224.9	17.8	7.48	0.19	13.7	14.4		
26.3	221.6	21.5	6.18	0.15	7.6	14.0		
25.0	219.4	26.1	4.91	0.11	2.7	14.8		
atl ss08		*Latitude:-31.8*		*Longitude: 10.2*		*Filter: 9*		
41.1	259.3	2.6	5.76	0.19	22.8	24.0		
39.6	252.4	3.2	6.20	0.21	12.1	22.0		
38.2	246.1	3.8	7.33	0.21	8.7	15.9		
36.8	242.1	4.6	7.71	0.21	10.6	16.0		
35.5	240.3	5.6	7.30	0.22	16.7	16.4		
34.1	238.6	6.8	7.44	0.22	22.3	16.6		
32.8	235.4	8.3	8.27	0.23	18.9	15.1		
31.4	232.5	10.0	8.82	0.24	10.7	10.6		
30.1	229.8	12.1	8.29	0.22	7.5	10.3		
28.8	227.4	14.7	7.30	0.17	11.4	13.5		
27.5	225.6	17.8	6.57	0.14	14.9	15.2		
26.3	224.2	21.5	6.07	0.20	8.2	18.1		
25.0	221.8	26.1	5.22	0.14	-2.3	11.0		
atl ss18		*Latitude:-42.0*		*Longitude: 95.2*		*Filter: 9*		
39.5	249.9	3.2	6.72	0.21	40.6	23.1	-3.8	22.0
38.1	246.0	3.8	7.17	0.19	22.9	15.3	5.8	17.6
36.8	242.1	4.6	7.39	0.18	14.1	14.2	15.2	18.9
35.4	239.6	5.6	7.52	0.18	14.3	13.8	14.7	19.9
34.0	237.8	6.8	7.53	0.18	18.8	14.3	9.6	19.2
32.7	235.2	8.3	7.49	0.18	21.2	14.4	7.7	20.2
31.4	232.3	10.0	7.52	0.18	17.8	13.9	10.0	20.8
30.0	230.1	12.1	7.45	0.21	12.8	13.5	10.7	21.0
28.7	228.2	14.7	7.00	0.17	12.2	13.7	7.9	20.3
27.5	226.2	17.8	6.21	0.14	15.2	14.4	5.7	20.2
26.2	224.3	21.5	5.45	0.12	15.2	18.5	6.5	25.5
24.9	222.4	26.1	4.81	0.13	9.6	16.3	5.3	22.1
atl ss25		*Latitude:-44.5*		*Longitude:251.2*		*Filter: 1*		
40.8	250.2	2.6	5.57	0.16	18.1	24.8	18.5	21.0
39.4	248.5	3.2	6.13	0.18	19.2	24.3	16.4	20.6
38.0	244.6	3.8	6.63	0.21	18.7	21.5	11.8	17.3
36.6	239.9	4.6	6.98	0.21	17.1	21.0	12.7	17.3
35.3	237.3	5.6	7.09	0.25	16.0	21.3	16.5	20.1
33.9	234.8	6.8	7.02	0.19	16.4	20.3	15.7	18.9
32.6	232.0	8.3	6.94	0.15	17.3	19.3	11.8	17.5
31.3	229.5	10.0	6.92	0.15	16.7	18.7	10.6	18.1
30.0	227.6	12.1	6.80	0.16	14.3	19.0	11.7	21.3
28.7	225.3	14.7	6.41	0.14	11.7	18.6	11.7	22.3
27.4	222.9	17.8	5.83	0.13	10.9	18.1	10.3	22.7
26.2	221.0	21.5	5.23	0.12	11.5	19.7	8.4	25.6
24.9	219.9	26.1	4.60	0.11	11.0	18.0	5.5	22.5

Table B.2 continued. (See notes on page 135.)

Alt (km)	Temp (K)	Press (mb)	$^{48}O_3$ vmr	$^{48}O_3$ err	$^{668}O_3$ enr	$^{668}O_3$ enr err	$^{686}O_3$ enr	$^{686}O_3$ enr err
atl ss26		*Latitude:-46.2*		*Longitude: 92.5*			*Filter: 1*	
41.0	246.5	2.6	5.77	0.16	17.4	23.9	17.1	19.1
39.7	243.7	3.2	5.94	0.20	20.6	23.8	17.8	19.2
38.3	241.9	3.8	6.14	0.20	17.8	23.1	15.5	19.3
36.9	240.9	4.6	6.41	0.21	14.1	22.2	15.1	20.7
35.5	239.0	5.6	6.75	0.18	13.8	20.3	17.0	19.0
34.2	235.7	6.8	7.14	0.19	15.5	20.2	16.4	18.7
32.9	234.0	8.3	7.54	0.17	15.9	20.0	12.2	19.6
31.5	232.9	10.0	7.86	0.16	14.0	19.1	7.9	19.8
30.2	231.6	12.1	7.82	0.16	11.2	17.5	6.7	18.8
28.9	229.8	14.7	7.33	0.16	10.3	16.7	7.8	19.0
27.6	227.5	17.8	6.55	0.15	11.8	16.3	9.3	19.4
26.3	225.5	21.5	5.74	0.12	13.0	17.8	9.2	22.2
25.1	224.0	26.1	4.96	0.11	10.6	19.0	7.0	24.9
atl ss27		*Latitude:-46.8*		*Longitude: 24.5*			*Filter: 9*	
40.9	248.8	2.6	6.61	0.19	30.9	21.8	9.9	19.6
39.5	246.3	3.2	7.42	0.21	36.0	19.7	8.9	19.6
38.1	244.0	3.8	7.71	0.21	27.0	17.9	6.8	19.0
36.8	240.8	4.6	7.45	0.19	14.9	15.9	6.6	18.9
35.4	237.8	5.6	6.87	0.16	7.3	15.1	10.3	19.7
34.1	235.5	6.8	6.53	0.17	8.4	14.9	15.6	21.4
32.7	233.3	8.3	6.67	0.16	13.8	13.2	17.6	20.0
31.4	231.4	10.0	7.05	0.15	16.6	12.7	15.5	19.2
30.1	229.6	12.1	7.23	0.17	13.9	14.2	11.8	18.9
28.8	228.1	14.7	7.22	0.19	10.3	13.4	9.1	18.1
27.5	226.4	17.8	7.02	0.18	10.4	12.0	8.4	17.8
26.2	224.9	21.5	6.34	0.19	13.7	15.5	9.1	22.6
25.0	223.6	26.1	5.17	0.14	15.3	14.8	8.7	20.2
atl ss29		*Latitude:-47.3*		*Longitude:339.1*			*Filter: 9*	
40.9	254.2	2.6	6.29	0.19	6.0	19.1	15.9	20.5
39.5	249.4	3.2	6.94	0.20	13.4	20.3	15.7	20.8
38.0	247.6	3.8	7.45	0.21	21.3	18.9	17.9	24.5
36.6	244.7	4.6	7.70	0.25	24.9	15.0	16.5	20.7
35.3	240.5	5.6	7.46	0.24	27.4	14.6	14.6	19.9
33.9	236.9	6.8	7.06	0.18	29.5	14.7	14.8	20.5
32.6	234.4	8.3	7.18	0.15	24.2	14.1	13.7	20.7
31.3	232.7	10.0	7.98	0.24	12.9	11.2	9.6	16.9
29.9	231.5	12.1	8.59	0.25	6.8	10.5	6.7	16.3
28.6	230.2	14.7	8.47	0.25	7.3	12.7	6.6	19.7
27.3	229.0	17.8	7.57	0.21	11.0	13.7	8.7	21.0
26.0	228.4	21.5	6.27	0.15	13.4	15.5	9.6	23.0
24.7	225.9	26.1	4.99	0.11	12.4	19.5	6.7	27.7
atl ss31		*Latitude:-47.7*		*Longitude:293.8*			*Filter: 1*	
40.5	248.5	2.6	4.76	0.13	19.1	23.5	25.2	20.0
39.1	244.4	3.2	5.37	0.16	17.0	22.8	23.1	19.6
37.8	240.6	3.8	6.05	0.18	17.4	21.7	16.7	18.7
36.4	237.8	4.6	6.61	0.19	17.8	21.6	11.9	18.0
35.1	236.4	5.6	6.86	0.20	17.4	21.8	11.1	19.3
33.7	234.0	6.8	6.84	0.18	16.2	20.2	12.8	17.8
32.4	230.3	8.3	6.78	0.16	14.5	19.1	13.5	17.4
31.1	227.5	10.0	6.80	0.14	12.9	18.6	11.0	18.5
29.8	225.7	12.1	6.67	0.12	11.9	18.5	7.9	20.1
28.5	223.6	14.7	6.22	0.12	11.7	18.2	6.3	20.4
27.3	221.2	17.8	5.55	0.12	11.7	18.0	6.3	21.0
26.0	218.7	21.5	4.88	0.10	11.0	18.1	6.1	21.4
24.8	217.1	26.1	4.25	0.10	9.5	16.2	4.9	18.9

Table B.2 continued. (See notes on page 135.)

Alt (km)	Temp (K)	Press (mb)	$^{48}O_3$ vmr	$^{48}O_3$ err	$^{668}O_3$ enr	$^{668}O_3$ enr err	$^{686}O_3$ enr	$^{686}O_3$ enr err
atl ss32		*Latitude:-47.9*		*Longitude:271.2*			*Filter: 9*	
40.5	252.3	2.6	6.15	0.20	16.2	25.1	31.9	26.5
39.1	249.5	3.2	6.76	0.21	10.1	19.9	22.8	22.7
37.7	243.6	3.8	7.19	0.20	8.7	13.8	8.6	17.3
36.3	236.9	4.6	7.26	0.19	11.0	13.8	0.2	16.3
35.0	233.4	5.6	7.05	0.20	13.0	13.0	0.6	17.3
33.7	232.5	6.8	6.70	0.19	12.0	12.9	7.1	18.4
32.4	230.1	8.3	6.31	0.16	10.7	13.1	14.6	19.6
31.1	226.7	10.0	6.05	0.15	14.6	13.5	14.7	19.6
29.8	224.7	12.1	6.00	0.17	20.4	15.4	9.0	21.7
28.5	223.5	14.7	6.05	0.19	20.9	16.0	6.6	22.5
27.3	222.4	17.8	5.93	0.14	16.1	15.5	9.7	22.3
26.0	220.8	21.5	5.52	0.13	11.8	16.9	10.6	24.3
24.8	219.1	26.1	4.88	0.14	8.4	16.2	7.6	21.6
atl ss36		*Latitude:-50.3*		*Longitude:359.2*			*Filter: 9*	
40.9	249.9	2.6	6.73	0.20	18.3	17.1	30.6	20.0
39.5	246.5	3.2	6.62	0.19	14.9	16.8	27.8	19.7
38.1	243.5	3.8	6.91	0.18	14.2	16.0	14.8	19.2
36.7	242.4	4.6	7.34	0.18	15.7	15.0	4.3	19.4
35.4	241.8	5.6	7.74	0.18	18.5	14.9	3.1	18.9
34.0	239.2	6.8	7.81	0.20	20.2	13.7	8.8	18.2
32.7	236.5	8.3	7.41	0.18	18.8	13.6	15.2	19.2
31.3	235.3	10.0	6.80	0.15	15.4	15.6	18.5	24.4
30.0	233.9	12.1	6.53	0.14	14.4	14.1	15.7	22.5
28.7	230.6	14.7	6.71	0.14	17.0	13.1	9.2	20.0
27.4	228.7	17.8	6.97	0.17	18.8	13.4	5.5	19.0
26.1	228.5	21.5	6.78	0.16	16.5	13.9	7.0	19.7
24.8	227.9	26.1	5.94	0.15	9.9	14.4	7.7	20.4

Alt (km)	Temp (K)	Press (mb)	$^{48}O_3$ vmr	$^{48}O_3$ err	$^{668}O_3$ enr	$^{668}O_3$ enr err	$^{686}O_3$ enr	$^{686}O_3$ enr err
atl ss37		*Latitude:-50.6*		*Longitude:336.5*			*Filter: 1*	
40.9	250.9	2.6	5.51	0.13	14.3	23.0	14.5	18.3
39.5	247.7	3.2	6.40	0.19	14.3	21.7	13.5	18.0
38.1	244.7	3.8	6.99	0.21	16.5	21.8	16.0	18.1
36.7	242.4	4.6	7.21	0.20	17.4	21.1	18.4	19.0
35.4	240.9	5.6	7.24	0.20	16.8	21.0	18.3	19.1
34.0	239.5	6.8	7.26	0.19	15.7	20.5	14.5	19.5
32.7	238.1	8.3	7.29	0.17	14.3	19.7	9.6	19.5
31.3	236.1	10.0	7.18	0.13	12.9	17.8	6.5	17.2
30.0	233.4	12.1	6.69	0.11	11.9	16.9	6.7	17.3
28.7	230.1	14.7	5.94	0.12	11.5	17.8	8.4	21.0
27.4	226.4	17.8	5.22	0.11	11.5	17.7	8.6	22.1
26.1	224.0	21.5	4.69	0.10	10.9	18.8	6.3	24.1
24.8	221.8	26.1	4.22	0.11	8.7	20.6	3.2	26.8
atl ss38		*Latitude:-50.7*		*Longitude:313.8*			*Filter: 9*	
40.8	255.9	2.6	6.43	0.20	25.2	19.2	4.0	18.7
39.3	251.5	3.2	7.23	0.22	20.6	18.4	7.7	19.7
37.9	247.9	3.8	7.23	0.20	14.6	16.3	12.2	19.5
36.5	245.4	4.6	6.74	0.17	12.6	15.0	17.8	19.8
35.1	242.8	5.6	6.23	0.15	20.0	15.4	23.0	20.8
33.8	239.2	6.8	5.95	0.15	26.0	15.0	22.7	20.9
32.4	235.1	8.3	5.90	0.14	20.7	14.3	14.6	19.5
31.1	230.7	10.0	5.83	0.15	11.2	12.9	5.8	18.3
29.8	226.3	12.1	5.51	0.14	9.8	12.8	3.6	18.0
28.5	223.1	14.7	4.94	0.10	16.5	16.5	6.2	23.9
27.3	220.7	17.8	4.34	0.09	21.1	17.4	5.6	23.8
26.0	219.4	21.5	3.87	0.09	17.8	17.4	0.8	22.6
24.8	218.3	26.1	3.59	0.08	12.1	20.9	2.8	26.9

Table B.2 continued. (See notes on page 135.)

Alt (km)	Temp (K)	Press (mb)	$^{48}O_3$ vmr	$^{48}O_3$ err	$^{668}O_3$ enr	$^{668}O_3$ enr err	$^{686}O_3$ enr	$^{686}O_3$ enr err
atl ss40		*Latitude:-50.8*		*Longitude:268.6*			*Filter: 9*	
40.4	244.1	2.6	5.87	0.17	18.7	19.2	-15.6	22.5
39.1	240.7	3.2	6.68	0.19	6.9	16.4	-7.0	24.6
37.7	238.7	3.8	7.29	0.19	1.4	14.4	5.6	21.6
36.3	237.3	4.6	7.14	0.18	5.2	13.9	15.5	20.1
35.0	234.7	5.6	6.59	0.15	14.0	9.6	19.1	13.6
33.7	231.7	6.8	6.23	0.13	20.3	10.1	19.3	13.8
32.4	228.7	8.3	6.16	0.12	21.0	10.1	18.4	13.8
31.1	225.7	10.0	6.13	0.11	19.0	9.9	16.0	13.5
29.8	223.8	12.1	6.04	0.14	16.3	12.5	11.5	17.6
28.6	222.6	14.7	5.95	0.15	13.5	13.5	6.2	18.8
27.3	221.6	17.8	5.82	0.15	11.7	14.0	4.4	18.4
26.0	220.7	21.5	5.46	0.13	11.3	14.6	6.1	19.3
24.8	219.8	26.1	4.82	0.11	11.4	15.6	6.6	20.3
atl ss41		*Latitude:-51.0*		*Longitude:245.9*			*Filter: 1*	
40.4	239.4	2.6	6.91	0.17	15.4	22.5	15.4	15.9
39.1	236.5	3.2	7.21	0.21	17.9	21.7	16.9	16.2
37.7	233.7	3.8	7.26	0.20	19.1	21.7	16.4	16.1
36.4	231.4	4.6	7.18	0.22	17.9	20.9	14.3	16.6
35.1	229.6	5.6	7.04	0.22	16.3	20.7	12.2	16.4
33.8	228.3	6.8	6.90	0.17	15.4	20.2	11.0	17.0
32.5	227.4	8.3	6.86	0.14	14.5	19.5	9.4	17.0
31.2	226.3	10.0	6.88	0.13	12.7	17.4	7.3	15.0
29.9	225.0	12.1	6.74	0.13	11.2	16.3	6.0	14.7
28.7	223.6	14.7	6.36	0.14	10.5	16.6	6.2	17.2
27.4	222.1	17.8	5.81	0.14	10.6	16.3	7.2	17.9
26.1	221.0	21.5	5.20	0.11	11.5	16.6	8.3	19.0
24.9	220.1	26.1	4.55	0.11	12.0	18.0	8.5	21.5

Alt (km)	Temp (K)	Press (mb)	$^{48}O_3$ vmr	$^{48}O_3$ err	$^{668}O_3$ enr	$^{668}O_3$ enr err	$^{686}O_3$ enr	$^{686}O_3$ enr err
atl ss43		*Latitude:-53.6*		*Longitude:130.3*			*Filter: 1*	
40.6	243.7	2.6	6.58	0.15	20.8	22.6	5.7	14.6
39.2	241.0	3.2	6.75	0.18	18.0	22.1	12.6	16.4
37.8	238.6	3.8	6.63	0.17	16.1	21.6	18.6	17.3
36.5	236.5	4.6	6.41	0.18	14.5	20.0	20.6	17.2
35.1	234.6	5.6	6.41	0.17	14.4	20.1	17.2	16.8
33.8	233.2	6.8	6.68	0.16	16.0	19.5	11.8	16.0
32.5	232.9	8.3	7.08	0.15	17.0	18.7	7.7	15.4
31.2	232.4	10.0	7.40	0.15	15.2	17.6	6.5	15.3
29.9	230.8	12.1	7.36	0.14	12.6	16.6	6.8	15.7
28.5	228.6	14.7	6.82	0.13	9.9	15.4	6.8	15.8
27.3	226.0	17.8	6.08	0.14	6.9	15.8	5.3	18.0
26.0	223.3	21.5	5.58	0.13	11.7	15.9	10.2	18.9
24.7	222.0	26.1	5.23	0.12	21.6	16.6	19.9	20.5
atl ss44		*Latitude:-53.8*		*Longitude:107.6*			*Filter: 9*	
40.6	248.2	2.6	5.68	0.19	24.5	22.4	22.1	23.4
39.2	245.8	3.2	5.89	0.19	26.8	22.7	27.3	24.2
37.8	243.8	3.8	6.29	0.19	23.0	17.9	17.6	21.1
36.4	242.0	4.6	6.50	0.18	19.8	15.5	7.1	19.0
35.1	240.2	5.6	6.27	0.18	19.9	14.5	3.8	17.8
33.7	238.3	6.8	6.04	0.19	19.8	13.2	6.1	17.0
32.4	236.4	8.3	6.14	0.18	17.2	12.7	11.4	17.5
31.0	234.2	10.0	6.33	0.16	14.3	11.5	15.6	17.0
29.7	231.7	12.1	6.22	0.16	13.6	11.4	16.5	17.1
28.4	229.8	14.7	5.80	0.11	15.0	11.9	13.9	18.2
27.1	229.0	17.8	5.37	0.10	16.7	12.1	10.2	17.7
25.8	227.6	21.5	4.94	0.11	17.4	14.2	7.7	19.9
24.5	225.5	26.1	4.37	0.11	16.1	15.0	5.8	20.7

Table B.2 continued. (See notes on page 135.)

Alt (km)	Temp (K)	Press (mb)	$^{48}O_3$ vmr	$^{48}O_3$ err	$^{668}O_3$ enr	$^{668}O_3$ enr err	$^{686}O_3$ enr	$^{686}O_3$ enr err
at1 ss47		*Latitude:-54.2*		*Longitude: 39.6*		*Filter: 9*		
40.9	249.7	2.6	6.28	0.19	37.6	21.7	10.4	19.0
39.5	246.2	3.2	6.80	0.19	21.2	15.4	8.5	17.3
38.1	243.0	3.8	7.02	0.18	8.2	13.8	8.0	17.1
36.7	239.7	4.6	6.74	0.16	9.7	14.2	12.6	17.7
35.4	236.9	5.6	6.23	0.14	21.0	13.0	19.5	19.6
34.1	234.8	6.8	6.14	0.14	26.9	13.5	16.6	19.3
32.7	233.1	8.3	6.48	0.17	23.9	12.0	6.1	16.3
31.4	231.9	10.0	6.78	0.19	20.2	11.3	2.2	15.4
30.1	230.8	12.1	6.75	0.16	19.0	12.0	9.1	17.1
28.8	229.0	14.7	6.70	0.13	15.2	12.8	13.5	18.5
27.5	227.2	17.8	6.78	0.19	9.3	10.0	9.4	13.8
26.2	226.0	21.5	6.58	0.18	8.6	9.8	5.6	13.2
24.9	224.8	26.1	5.87	0.16	11.6	10.3	6.4	13.8
at1 ss48		*Latitude:-55.5*		*Longitude:241.0*		*Filter: 1*		
40.2	238.8	2.6	6.06	0.14	14.5	20.4	8.7	12.9
38.9	235.9	3.2	6.80	0.18	19.2	21.6	7.7	15.2
37.6	233.1	3.8	7.29	0.19	21.1	21.7	10.2	15.4
36.2	230.5	4.6	7.46	0.17	18.6	20.3	12.6	15.0
34.9	228.2	5.6	7.43	0.16	13.7	19.6	11.2	14.7
33.6	226.3	6.8	7.29	0.15	9.0	17.2	6.8	11.8
32.4	225.3	8.3	7.10	0.13	6.9	16.0	3.4	11.0
31.1	224.3	10.0	6.90	0.12	8.1	15.4	3.8	11.1
29.8	223.4	12.1	6.66	0.11	11.0	14.9	6.1	11.4
28.6	222.4	14.7	6.33	0.11	13.3	14.3	7.9	11.7
27.3	221.4	17.8	5.88	0.12	13.9	16.8	8.9	18.2
26.0	220.6	21.5	5.35	0.10	12.5	16.5	9.0	18.6
24.8	220.0	26.1	4.75	0.09	8.0	16.0	5.6	18.7

Alt (km)	Temp (K)	Press (mb)	$^{48}O_3$ vmr	$^{48}O_3$ err	$^{668}O_3$ enr	$^{668}O_3$ enr err	$^{686}O_3$ enr	$^{686}O_3$ enr err
at2 sr02		*Latitude: 63.5*		*Longitude:213.8*		*Filter: 1*		
40.1	238.3	2.6	6.24	0.17	17.2	20.4	9.6	13.3
38.8	234.4	3.2	6.48	0.19	16.9	20.6	9.8	13.3
37.4	230.5	3.8	6.72	0.19	17.0	20.3	11.4	13.4
36.1	228.3	4.6	6.94	0.15	16.5	19.3	12.7	13.9
34.8	227.5	5.6	7.10	0.15	14.8	19.2	11.6	13.7
33.6	226.5	6.8	7.12	0.14	12.8	18.5	8.5	13.2
32.3	225.0	8.3	6.92	0.13	12.2	17.7	6.0	13.9
31.0	223.4	10.0	6.56	0.12	13.8	17.2	5.9	14.0
29.7	221.9	12.1	6.12	0.11	16.5	16.7	7.4	14.2
28.5	221.3	14.7	5.68	0.11	17.7	16.9	8.1	15.9
27.2	221.0	17.8	5.33	0.11	15.1	15.7	6.4	15.7
26.0	221.0	21.5	4.99	0.13	11.5	14.9	4.9	15.4
24.7	221.3	26.1	4.64	0.13	10.6	14.5	6.3	15.6
at2 sr05		*Latitude: 63.8*		*Longitude:145.7*		*Filter:12*		
40.4	243.6	2.6	5.25	0.13	16.2	13.8	15.4	15.2
39.0	240.4	3.2	5.84	0.13	14.6	13.5	16.5	15.1
37.6	237.5	3.8	6.29	0.18	15.5	11.4	18.4	15.4
36.3	234.6	4.6	6.76	0.20	16.0	11.2	18.6	15.4
35.0	232.1	5.6	7.32	0.21	15.6	11.0	16.5	15.0
33.6	230.7	6.8	7.83	0.17	15.5	10.2	13.7	15.1
32.3	229.8	8.3	8.04	0.16	15.5	10.0	11.4	14.9
31.0	229.0	10.0	7.88	0.16	14.9	9.6	9.2	14.4
29.7	228.1	12.1	7.50	0.16	14.2	9.3	7.8	14.0
28.5	227.3	14.7	7.02	0.15	14.6	9.4	8.2	14.2
27.2	226.4	17.8	6.48	0.14	15.7	10.3	9.9	15.3
25.9	225.8	21.5	5.90	0.13	14.7	11.9	10.3	17.2
24.6	225.2	26.1	5.31	0.12	10.1	11.5	7.4	16.9

Table B.2 continued. (See notes on page 135.)

Alt (km)	Temp (K)	Press (mb)	$^{48}O_3$ vmr	$^{48}O_3$ err	$^{668}O_3$ enr	$^{668}O_3$ enr err	$^{686}O_3$ enr	$^{686}O_3$ enr err
at2 sr07		*Latitude: 63.9*		*Longitude:100.2*			*Filter: 1*	
40.2	259.7	2.6	5.26	0.13	20.4	23.2	15.0	18.3
38.7	255.8	3.2	6.02	0.16	24.0	22.1	13.5	17.3
37.3	251.9	3.8	6.81	0.18	23.4	21.6	11.1	16.6
35.9	248.1	4.6	7.65	0.20	20.4	20.5	8.3	16.4
34.5	244.4	5.6	8.18	0.21	17.2	20.0	5.8	16.3
33.1	240.7	6.8	7.77	0.19	14.7	19.2	4.3	16.1
31.7	236.5	8.3	6.69	0.15	12.8	18.5	3.9	16.5
30.4	232.1	10.0	5.61	0.11	12.4	17.7	5.1	16.9
29.1	227.8	12.1	5.04	0.11	13.3	17.2	7.1	17.6
27.8	224.9	14.7	4.86	0.10	14.3	17.0	8.3	18.2
26.5	222.9	17.8	4.92	0.10	14.4	16.3	7.9	18.1
25.3	221.1	21.5	5.07	0.13	12.5	15.7	4.8	18.0
24.0	220.1	26.1	5.02	0.15	7.3	16.0	-1.2	18.7
at2 sr12		*Latitude: 64.9*		*Longitude:142.2*			*Filter: 1*	
40.4	248.5	2.6	6.44	0.15	21.7	22.5	6.4	15.3
39.0	244.7	3.2	7.21	0.18	18.0	20.8	2.3	14.5
37.6	240.9	3.8	7.72	0.19	15.5	20.1	1.3	14.3
36.2	237.3	4.6	7.87	0.19	14.4	19.6	4.0	14.5
34.9	234.4	5.6	7.87	0.20	13.7	19.2	7.4	15.0
33.6	231.7	6.8	7.84	0.19	13.7	18.8	9.5	15.3
32.3	229.5	8.3	7.73	0.18	14.8	18.3	10.1	15.4
31.0	228.7	10.0	7.50	0.15	15.7	17.6	9.8	15.8
29.7	227.8	12.1	7.20	0.15	14.5	16.6	8.0	15.6
28.4	227.2	14.7	6.85	0.15	12.1	15.5	5.8	15.5
27.1	227.0	17.8	6.43	0.15	12.0	14.7	5.9	15.6
25.8	226.8	21.5	5.91	0.16	14.3	14.4	7.8	16.0
24.5	225.8	26.1	5.34	0.16	14.8	17.6	7.8	21.9

Alt (km)	Temp (K)	Press (mb)	$^{48}O_3$ vmr	$^{48}O_3$ err	$^{668}O_3$ enr	$^{668}O_3$ enr err	$^{686}O_3$ enr	$^{686}O_3$ enr err
at2 sr15		*Latitude: 65.2*		*Longitude: 74.0*			*Filter:12*	
39.8	254.2	2.6	4.56	0.11	5.4	17.1	21.8	20.0
38.4	251.2	3.2	5.55	0.13	14.8	12.8	20.6	17.7
37.0	248.7	3.8	6.26	0.14	19.7	13.1	18.5	17.2
35.6	245.3	4.6	6.48	0.14	20.6	12.9	15.2	16.6
34.2	240.2	5.6	6.32	0.15	20.5	11.7	12.3	17.2
32.8	235.0	6.8	6.09	0.14	20.1	11.7	11.2	17.2
31.5	231.1	8.3	5.86	0.13	17.8	11.5	11.4	17.3
30.2	229.7	10.0	5.57	0.11	15.1	11.8	12.5	18.0
28.9	228.4	12.1	5.22	0.10	16.0	11.8	14.8	18.2
27.6	226.4	14.7	4.89	0.10	19.7	11.8	16.9	17.3
26.4	223.3	17.8	4.66	0.10	18.6	11.7	13.7	16.8
25.1	220.3	21.5	4.48	0.10	9.9	11.2	5.2	15.6
23.9	217.8	26.1	4.21	0.09	4.0	11.1	0.6	15.0
at2 sr21		*Latitude: 65.5*		*Longitude:297.8*			*Filter:12*	
40.2	240.2	2.6	5.92	0.15	21.9	13.6		
38.9	235.1	3.2	6.27	0.14	18.3	13.0		
37.5	232.5	3.8	6.45	0.15	16.8	12.6		
36.2	230.8	4.6	6.33	0.14	18.8	12.7		
34.9	229.0	5.6	6.02	0.13	21.3	11.9		
33.6	227.1	6.8	5.75	0.12	21.9	11.2		
32.3	225.3	8.3	5.64	0.12	19.4	11.0		
31.1	223.6	10.0	5.61	0.11	15.6	10.6		
29.8	221.9	12.1	5.57	0.10	12.7	10.4		
28.5	220.2	14.7	5.48	0.10	11.6	10.3		
27.3	219.3	17.8	5.33	0.10	12.9	10.6		
26.1	219.0	21.5	5.08	0.10	15.6	10.8		
24.8	219.0	26.1	4.76	0.10	16.1	12.8		

Table B.2 continued. (See notes on page 135.)

Alt (km)	Temp (K)	Press (mb)	$^{48}O_3$ vmr	$^{48}O_3$ err	$^{668}O_3$ enr	$^{668}O_3$ enr err	$^{686}O_3$ enr	$^{686}O_3$ enr err
at2 sr24	*Latitude: 65.7*	*Longitude:252.3*	*Filter: 1*					
40.1	244.4	2.6	8.11	0.22	16.1	21.5	2.6	14.2
38.7	240.3	3.2	7.38	0.20	17.2	20.5	6.9	13.7
37.3	235.8	3.8	6.56	0.17	18.6	20.2	10.3	13.8
36.0	231.0	4.6	6.43	0.17	16.2	19.7	8.9	13.7
34.7	226.3	5.6	6.68	0.17	13.1	19.3	6.6	13.4
33.4	224.9	6.8	6.86	0.16	12.1	19.0	6.4	14.9
32.2	224.1	8.3	6.77	0.15	12.1	18.3	7.0	14.9
30.9	223.2	10.0	6.53	0.13	11.6	17.1	6.6	14.1
29.6	221.6	12.1	6.25	0.12	11.1	15.9	5.9	13.5
28.4	219.8	14.7	6.00	0.11	11.1	15.0	5.7	13.5
27.1	218.8	17.8	5.73	0.12	11.5	14.8	6.3	14.6
25.9	219.5	21.5	5.40	0.15	12.4	15.5	6.9	16.7
24.7	220.0	26.1	4.97	0.16	13.3	15.1	7.0	16.8
at2 sr27	*Latitude: 66.0*	*Longitude:161.3*	*Filter:12*					
40.3	244.1	2.6	6.03	0.16	20.2	15.4		
38.9	240.3	3.2	6.10	0.15	15.5	12.8		
37.6	236.3	3.8	6.22	0.15	13.8	12.6		
36.3	233.0	4.6	6.43	0.14	15.5	12.2		
34.9	231.0	5.6	6.61	0.15	17.6	11.1		
33.6	229.3	6.8	6.60	0.14	18.5	11.2		
32.3	227.7	8.3	6.31	0.13	18.7	11.2		
31.0	226.5	10.0	5.87	0.10	19.1	11.3		
29.8	225.3	12.1	5.50	0.09	19.6	11.4		
28.5	224.4	14.7	5.30	0.09	18.9	11.1		
27.2	223.9	17.8	5.22	0.09	16.4	10.9		
26.0	223.4	21.5	5.10	0.10	13.7	11.6		
24.7	222.9	26.1	4.87	0.09	11.9	12.2		

Alt (km)	Temp (K)	Press (mb)	$^{48}O_3$ vmr	$^{48}O_3$ err	$^{668}O_3$ enr	$^{668}O_3$ enr err	$^{686}O_3$ enr	$^{686}O_3$ enr err
at2 sr30	*Latitude: 66.1*	*Longitude: 93.3*	*Filter: 1*					
40.1	258.5	2.6	5.52	0.14	24.9	22.7	6.6	16.6
38.7	255.1	3.2	6.26	0.15	19.9	21.9	4.4	16.0
37.2	251.4	3.8	6.55	0.15	20.3	21.5	6.9	16.3
35.8	246.4	4.6	6.68	0.16	22.1	21.0	10.7	16.9
34.4	241.3	5.6	6.89	0.16	20.6	20.8	10.7	16.9
33.1	238.1	6.8	7.08	0.15	16.7	19.9	7.5	17.0
31.7	237.1	8.3	6.99	0.13	13.4	18.9	4.9	17.5
30.4	235.7	10.0	6.53	0.12	11.9	17.8	4.3	17.2
29.0	231.6	12.1	5.90	0.14	12.0	16.7	5.4	16.4
27.7	227.5	14.7	5.25	0.13	13.4	16.2	7.1	16.8
26.5	223.9	17.8	4.60	0.12	15.4	15.8	8.6	17.4
25.2	221.8	21.5	4.06	0.12	16.3	17.1	8.4	20.0
24.0	219.7	26.1	3.78	0.13	14.4	16.3	5.9	19.6
at2 sr36	*Latitude: 66.3*	*Longitude: 25.1*	*Filter:12*					
39.6	251.3	2.6	4.79	0.12	15.8	15.3	16.4	17.8
38.2	247.1	3.2	5.13	0.12	17.6	15.4	16.6	17.6
36.8	244.2	3.8	5.39	0.12	21.6	14.2	18.3	17.9
35.4	241.8	4.6	5.61	0.12	23.5	13.7	18.1	17.9
34.1	239.2	5.6	5.81	0.11	21.0	12.6	14.0	16.8
32.7	236.4	6.8	5.91	0.11	17.6	11.4	9.7	15.8
31.4	233.5	8.3	5.79	0.10	15.9	11.2	8.1	15.6
30.1	230.6	10.0	5.48	0.10	15.9	11.6	8.7	16.2
28.8	227.8	12.1	5.09	0.09	16.3	12.0	9.7	17.0
27.5	225.0	14.7	4.70	0.08	16.7	12.0	10.1	17.0
26.2	221.9	17.8	4.36	0.08	15.7	12.6	8.9	17.1
25.0	218.8	21.5	4.05	0.08	12.2	12.3	5.6	16.7
23.7	214.8	26.1	3.74	0.09	8.1	13.2	2.2	17.2

Table B.2 continued. (See notes on page 135.)

Alt (km)	Temp (K)	Press (mb)	$^{48}O_3$ vmr	$^{48}O_3$ err	$^{668}O_3$ enr	$^{668}O_3$ enr err	$^{686}O_3$ enr	$^{686}O_3$ enr err
at2 sr40		*Latitude: 67.1*		*Longitude: 89.4*			*Filter: 1*	
40.2	259.3	2.6	4.96	0.12	10.4	22.6	10.8	18.8
38.7	254.0	3.2	5.43	0.16	20.1	22.4	9.0	17.8
37.3	249.0	3.8	5.90	0.17	22.1	22.4	9.0	17.6
35.9	245.8	4.6	6.37	0.18	19.2	21.4	10.0	18.3
34.5	243.3	5.6	6.80	0.19	16.4	20.9	9.5	18.6
33.1	241.1	6.8	7.02	0.18	15.7	20.2	6.0	18.0
31.7	239.4	8.3	6.87	0.15	15.6	19.3	3.2	17.6
30.4	237.6	10.0	6.27	0.13	14.8	18.4	4.0	17.8
29.1	233.9	12.1	5.52	0.11	13.3	17.6	6.9	18.3
27.7	230.1	14.7	4.96	0.10	13.0	16.7	7.8	18.5
26.4	227.0	17.8	4.65	0.10	13.5	16.6	5.0	18.4
25.2	224.6	21.5	4.41	0.12	10.8	15.7	0.0	17.7
23.9	221.3	26.1	4.10	0.13	5.8	15.1	-3.5	17.3
at2 sr43		*Latitude: 67.2*		*Longitude: 21.3*			*Filter:12*	
39.5	248.5	2.6	4.62	0.12	19.5	17.3		
38.1	245.2	3.2	4.81	0.12	17.2	15.9		
36.8	242.5	3.8	5.03	0.13	16.8	14.1		
35.4	239.9	4.6	5.39	0.13	19.0	14.0		
34.0	237.8	5.6	5.70	0.11	20.2	12.4		
32.7	235.7	6.8	5.71	0.11	18.4	12.1		
31.4	231.7	8.3	5.40	0.10	15.0	10.5		
30.1	227.0	10.0	5.05	0.09	13.9	10.5		
28.8	222.8	12.1	4.78	0.08	16.2	10.7		
27.5	220.0	14.7	4.56	0.08	19.9	12.4		
26.3	217.7	17.8	4.30	0.08	21.7	12.6		
25.1	215.7	21.5	4.04	0.08	19.8	13.8		
23.8	214.0	26.1	3.80	0.08	15.4	15.1		

Alt (km)	Temp (K)	Press (mb)	$^{48}O_3$ vmr	$^{48}O_3$ err	$^{668}O_3$ enr	$^{668}O_3$ enr err	$^{686}O_3$ enr	$^{686}O_3$ enr err
at2 sr46		*Latitude: 67.5*		*Longitude:312.9*			*Filter: 1*	
40.5	238.5	2.6	5.92	0.17	12.3	21.7	3.7	16.3
39.1	236.6	3.2	6.23	0.17	10.8	21.7	-0.2	15.8
37.8	234.5	3.8	6.50	0.18	12.8	20.6	2.1	15.0
36.4	232.3	4.6	6.82	0.19	14.8	20.3	5.9	15.1
35.1	230.2	5.6	7.20	0.19	14.4	20.0	7.1	15.0
33.8	228.5	6.8	7.45	0.18	13.1	19.0	6.4	14.6
32.5	227.0	8.3	7.39	0.17	12.1	18.2	5.4	14.4
31.2	226.0	10.0	7.05	0.15	12.1	17.1	4.8	14.3
30.0	225.3	12.1	6.70	0.14	12.3	16.3	4.7	14.4
28.7	224.9	14.7	6.41	0.14	12.5	15.7	4.9	14.9
27.4	224.8	17.8	6.12	0.14	13.2	15.1	5.8	15.2
26.1	224.6	21.5	5.73	0.15	13.6	15.2	6.4	16.5
24.9	224.2	26.1	5.26	0.16	11.2	15.9	4.2	18.4
at2 sr49		*Latitude: 67.4*		*Longitude:245.1*			*Filter:12*	
40.0	239.9	2.6	5.67	0.15	25.4	15.7		
38.7	236.5	3.2	6.44	0.16	25.3	14.1		
37.3	233.3	3.8	6.81	0.16	23.1	13.6		
36.0	231.1	4.6	6.76	0.14	19.7	12.5		
34.7	228.9	5.6	6.48	0.13	17.3	12.2		
33.4	226.8	6.8	6.10	0.11	16.6	11.3		
32.2	224.6	8.3	5.81	0.10	16.1	11.2		
30.9	222.6	10.0	5.63	0.10	14.9	10.7		
29.6	220.9	12.1	5.49	0.09	13.7	10.3		
28.4	219.2	14.7	5.31	0.09	13.4	10.3		
27.1	218.6	17.8	5.08	0.09	14.1	11.0		
25.9	218.8	21.5	4.80	0.09	14.8	11.1		
24.7	219.0	26.1	4.50	0.09	14.3	13.4		

Table B.2 continued. (See notes on page 135.)

Alt (km)	Temp (K)	Press (mb)	$^{48}O_3$ vmr	$^{48}O_3$ err	$^{668}O_3$ enr	$^{668}O_3$ enr err	$^{686}O_3$ enr	$^{686}O_3$ enr err
at2 sr52		*Latitude: 67.6*		*Longitude:176.9*			*Filter: 1*	
40.3	242.9	2.6	5.83	0.15	10.8	21.5	9.6	16.4
38.9	238.7	3.2	5.87	0.19	10.6	20.5	12.5	15.7
37.6	234.6	3.8	5.94	0.19	12.1	20.5	13.4	15.8
36.2	231.6	4.6	6.06	0.19	15.7	20.9	13.4	16.2
34.9	229.8	5.6	6.22	0.17	19.0	21.3	12.6	17.3
33.6	228.2	6.8	6.41	0.17	19.0	21.0	10.4	16.9
32.3	227.2	8.3	6.56	0.14	16.1	19.3	7.5	16.4
31.0	226.2	10.0	6.53	0.14	13.3	18.0	5.7	16.0
29.8	225.4	12.1	6.30	0.13	12.1	17.3	5.2	16.6
28.5	224.6	14.7	5.95	0.12	12.0	16.5	5.0	16.8
27.2	224.0	17.8	5.58	0.13	12.3	15.3	4.5	15.4
25.9	223.7	21.5	5.26	0.15	12.4	14.6	3.8	15.3
24.7	223.4	26.1	4.95	0.15	11.5	16.3	3.0	18.6
at2 sr64		*Latitude: 68.4*		*Longitude: 82.5*			*Filter: 1*	
40.3	261.6	2.6	4.81	0.12	17.0	24.7	15.0	21.2
38.8	257.2	3.2	5.10	0.14	18.9	22.9	10.7	20.0
37.4	252.6	3.8	5.54	0.14	21.9	23.1	8.3	19.6
35.9	248.1	4.6	6.14	0.14	22.9	22.0	7.5	18.7
34.5	244.3	5.6	6.69	0.15	20.8	21.7	6.9	18.5
33.2	243.6	6.8	6.85	0.16	17.9	21.5	6.6	20.4
31.8	241.9	8.3	6.56	0.13	16.2	19.8	6.5	19.0
30.4	237.6	10.0	5.97	0.11	15.6	18.6	6.5	18.5
29.1	233.1	12.1	5.36	0.10	15.1	18.1	7.0	19.2
27.8	228.8	14.7	4.86	0.11	14.8	17.9	7.9	20.3
26.5	225.2	17.8	4.52	0.11	14.7	17.2	8.1	20.4
25.2	222.9	21.5	4.33	0.11	13.3	18.6	5.0	23.6
24.0	220.7	26.1	4.02	0.13	14.0	18.7	3.2	23.1

Alt (km)	Temp (K)	Press (mb)	$^{48}O_3$ vmr	$^{48}O_3$ err	$^{668}O_3$ enr	$^{668}O_3$ enr err	$^{686}O_3$ enr	$^{686}O_3$ enr err
at2 sr72		*Latitude: 68.8*		*Longitude:238.0*			*Filter:12*	
40.1	242.5	2.6	5.92	0.15	16.9	16.7	14.5	17.7
38.7	238.2	3.2	5.99	0.15	14.4	15.0	15.5	17.4
37.4	234.8	3.8	6.42	0.15	12.8	14.6	11.0	16.9
36.1	232.7	4.6	6.96	0.15	15.1	13.5	8.7	17.2
34.8	229.5	5.6	7.12	0.14	19.7	12.2	12.8	16.3
33.5	224.8	6.8	6.95	0.13	22.7	11.9	16.5	16.4
32.2	222.9	8.3	6.69	0.12	20.7	12.4	12.5	16.8
30.9	222.7	10.0	6.37	0.12	16.6	13.6	7.0	18.7
29.7	221.9	12.1	5.95	0.11	14.3	12.8	6.7	17.5
28.4	220.9	14.7	5.51	0.10	15.4	12.8	10.7	17.9
27.2	220.2	17.8	5.10	0.10	17.3	13.1	13.3	18.0
25.9	219.9	21.5	4.70	0.10	17.0	13.6	12.9	18.2
24.7	219.6	26.1	4.30	0.10	15.5	13.8	10.6	18.2
at2 sr81		*Latitude: 68.9*		*Longitude: 11.2*			*Filter: 1*	
40.3	249.5	2.6	4.73	0.11	16.6	24.3	8.7	19.3
38.9	245.2	3.2	5.06	0.13	14.2	23.2	7.1	19.0
37.5	240.8	3.8	5.46	0.13	15.4	23.2	8.9	19.2
36.1	236.8	4.6	5.98	0.16	17.5	22.7	10.7	20.1
34.8	233.9	5.6	6.54	0.16	18.0	21.9	9.0	18.8
33.5	232.0	6.8	7.04	0.16	16.6	20.9	5.8	17.9
32.2	229.5	8.3	7.48	0.16	13.7	19.2	3.3	16.9
30.9	227.6	10.0	7.80	0.15	12.9	18.1	2.5	16.9
29.6	226.3	12.1	7.76	0.14	15.7	17.6	4.4	17.2
28.3	224.7	14.7	7.29	0.13	15.6	17.2	4.2	17.3
27.0	223.3	17.8	6.72	0.13	6.4	14.5	-3.3	14.5
25.8	222.5	21.5	6.12	0.15	-4.1	12.0	-11.7	11.7
24.5	221.8	26.1	5.32	0.15	-1.7	12.0	-8.7	12.4

Table B.2 continued. (See notes on page 135.)

Alt (km)	Temp (K)	Press (mb)	$^{48}O_3$ vmr	$^{48}O_3$ err	$^{668}O_3$ enr	$^{668}O_3$ enr err	$^{686}O_3$ enr	$^{686}O_3$ enr err
at2 sr87	*Latitude: 69.1*	*Longitude: 98.8*	*Filter: 1*					
40.6	257.7	2.6	5.21	0.12	22.4	25.9	7.6	20.9
39.2	254.7	3.2	5.62	0.14	21.1	24.7	7.0	20.0
37.7	247.6	3.8	5.91	0.17	17.6	22.4	9.5	19.0
36.3	242.3	4.6	6.22	0.17	16.3	22.0	11.0	19.6
35.0	241.4	5.6	6.60	0.18	17.4	22.6	11.0	21.8
33.6	239.6	6.8	6.97	0.16	18.7	21.8	10.4	21.7
32.2	237.8	8.3	7.08	0.15	18.4	21.1	8.4	21.6
30.9	236.3	10.0	6.80	0.13	16.5	20.3	6.2	22.1
29.6	234.2	12.1	6.27	0.13	14.4	19.3	5.1	22.0
28.2	232.1	14.7	5.71	0.12	13.8	18.6	4.5	22.3
26.9	230.4	17.8	5.19	0.11	14.6	18.7	3.5	23.1
25.6	227.8	21.5	4.59	0.12	15.5	19.6	3.1	24.5
24.4	225.0	26.1	4.01	0.12	15.5	19.6	3.4	24.9
at2 ss02	*Latitude:-50.0*	*Longitude: 26.2*	*Filter: 1*					
40.9	244.3	2.6	5.66	0.14	22.3	22.0	19.1	15.3
39.5	241.6	3.2	5.71	0.16	19.4	21.1	20.8	15.4
38.1	238.7	3.8	5.98	0.16	16.1	20.3	17.7	14.9
36.8	236.5	4.6	6.37	0.17	15.6	20.0	13.4	14.3
35.4	235.8	5.6	6.77	0.16	17.4	20.1	10.1	16.0
34.1	235.4	6.8	7.08	0.16	18.2	19.8	9.0	15.8
32.8	234.6	8.3	7.26	0.15	17.1	18.4	9.7	14.8
31.5	232.8	10.0	7.26	0.14	15.3	17.0	10.4	14.4
30.1	230.7	12.1	7.14	0.14	13.3	15.8	9.2	14.2
28.8	228.9	14.7	6.94	0.13	11.9	15.1	6.8	14.7
27.5	227.2	17.8	6.61	0.13	11.4	14.5	5.2	14.9
26.3	225.6	21.5	6.04	0.15	12.1	13.9	5.7	15.2
25.0	224.1	26.1	5.26	0.15	12.8	15.2	7.2	18.0
at2 ss05	*Latitude:-49.5*	*Longitude:295.8*	*Filter:12*					
40.3	240.6	2.6	5.49	0.15	11.2	15.4		
38.9	237.0	3.2	6.32	0.16	15.8	11.7		
37.6	233.6	3.8	6.82	0.16	18.7	11.8		
36.2	230.7	4.6	6.94	0.15	19.4	11.5		
34.9	228.2	5.6	6.94	0.13	19.0	10.8		
33.7	225.9	6.8	6.94	0.13	17.4	10.7		
32.4	224.3	8.3	6.94	0.13	15.5	9.3		
31.1	223.4	10.0	6.82	0.12	15.7	9.3		
29.8	222.6	12.1	6.55	0.11	19.0	9.5		
28.6	221.8	14.7	6.26	0.29	22.7	12.7		
27.3	220.9	17.8	6.24	0.31	22.4	13.0		
26.1	220.0	21.5	6.39	0.52	20.0	15.0		
at2 ss11	*Latitude:-47.3*	*Longitude:316.9*	*Filter: 1*					
40.6	247.1	2.6	6.65	0.15	17.7	21.8	7.8	15.2
39.3	243.7	3.2	6.86	0.18	17.6	20.8	9.9	15.0
37.9	240.0	3.8	6.99	0.18	17.8	20.6	11.5	15.2
36.5	236.3	4.6	7.07	0.18	18.9	20.6	12.3	15.3
35.2	232.5	5.6	7.14	0.17	19.4	20.4	11.8	15.8
33.9	228.7	6.8	7.29	0.17	17.5	19.7	9.7	15.6
32.6	226.1	8.3	7.49	0.15	14.0	17.9	7.0	14.5
31.3	225.8	10.0	7.62	0.15	11.4	16.7	5.2	14.1
30.0	225.4	12.1	7.60	0.15	10.3	15.7	4.7	14.0
28.8	224.2	14.7	7.36	0.14	9.9	14.8	5.1	15.6
27.5	222.7	17.8	6.81	0.14	10.5	14.0	5.6	16.1
26.2	221.3	21.5	5.94	0.15	12.4	14.3	6.0	16.9
25.0	220.4	26.1	5.03	0.15	13.0	16.3	5.2	18.8

Table B.2 continued. (See notes on page 135.)

Alt (km)	Temp (K)	Press (mb)	$^{48}O_3$ vmr	$^{48}O_3$ err	$^{668}O_3$ enr	$^{668}O_3$ enr err	$^{686}O_3$ enr	$^{686}O_3$ enr err
at2 ss14		*Latitude:-46.7*		*Longitude:249.1*			*Filter:12*	
40.5	248.8	2.6	6.23	0.16	25.3	14.7	17.4	16.0
39.1	245.0	3.2	6.73	0.17	19.3	13.1	14.6	15.4
37.7	240.6	3.8	6.99	0.16	15.6	11.7	13.0	15.2
36.3	236.1	4.6	6.94	0.16	15.1	11.6	13.7	15.3
35.0	232.5	5.6	6.61	0.14	17.4	11.4	16.8	16.1
33.7	230.2	6.8	6.21	0.12	20.7	11.3	20.1	17.1
32.4	228.0	8.3	5.92	0.11	21.5	11.4	18.6	16.9
31.1	226.1	10.0	5.73	0.10	19.1	11.7	12.1	16.7
29.8	224.3	12.1	5.43	0.09	16.2	12.3	8.9	17.2
28.6	222.7	14.7	4.93	0.09	15.2	12.2	16.6	18.4
27.3	221.4	17.8	4.31	0.40	18.9	21.3	37.6	26.2
26.0	220.3	21.5	3.81	0.35	30.4	23.4	58.1	30.1
at2 ss17		*Latitude:-46.2*		*Longitude:181.3*			*Filter: 1*	
40.4	241.6	2.6	6.62	0.20	15.8	20.7	8.6	14.4
39.0	237.7	3.2	6.78	0.20	14.4	20.7	9.3	14.6
37.7	233.9	3.8	6.65	0.19	14.8	20.6	12.6	15.0
36.4	230.9	4.6	6.36	0.15	16.6	20.1	17.3	16.1
35.1	228.3	5.6	6.29	0.14	18.1	20.5	18.4	16.2
33.8	225.8	6.8	6.50	0.14	18.1	19.6	15.1	15.5
32.5	224.3	8.3	6.78	0.12	16.5	18.4	9.7	14.7
31.2	223.0	10.0	6.89	0.12	13.0	17.0	4.2	13.8
30.0	222.2	12.1	6.81	0.13	9.4	15.5	-0.3	13.0
28.7	221.8	14.7	6.55	0.13	9.2	14.6	-1.2	12.9

Alt (km)	Temp (K)	Press (mb)	$^{48}O_3$ vmr	$^{48}O_3$ err	$^{668}O_3$ enr	$^{668}O_3$ enr err	$^{686}O_3$ enr	$^{686}O_3$ enr err
at2 ss20		*Latitude:-45.8*		*Longitude:113.5*			*Filter:12*	
40.8	240.6	2.6	5.68	0.15	12.0	15.1	25.6	16.3
39.4	238.0	3.2	6.09	0.16	16.3	12.6	24.4	16.2
38.0	235.3	3.8	6.38	0.16	19.0	12.8	22.6	15.9
36.7	233.1	4.6	6.51	0.15	19.7	12.7	20.1	15.6
35.4	231.7	5.6	6.52	0.16	19.3	12.4	17.5	17.4
34.1	230.4	6.8	6.51	0.15	18.7	12.4	16.1	17.1
32.8	229.4	8.3	6.53	0.12	17.5	11.4	15.4	16.8
31.5	228.6	10.0	6.59	0.11	14.8	10.8	12.6	16.3
30.2	227.4	12.1	6.63	0.13	10.7	10.4	5.9	15.2
28.9	225.9	14.7	6.54	0.19	9.2	10.3	1.3	14.5
27.6	224.8	17.8	6.12	0.18	16.9	11.1	8.4	15.5
at2 ss23		*Latitude:-45.3*		*Longitude: 45.8*			*Filter: 1*	
41.2	246.9	2.6	6.07	0.15	18.5	22.3	18.1	16.3
39.8	243.6	3.2	6.25	0.16	14.8	21.1	15.9	16.3
38.4	240.3	3.8	6.34	0.16	13.7	20.7	15.4	16.2
37.1	238.2	4.6	6.29	0.16	16.7	20.8	18.0	17.4
35.7	237.6	5.6	6.50	0.16	17.8	20.6	15.9	18.0
34.4	236.9	6.8	7.30	0.16	12.4	19.2	4.6	16.2
33.0	235.4	8.3	7.71	0.14	12.5	18.0	-0.1	15.2
at2 ss32		*Latitude:-43.6*		*Longitude:202.5*			*Filter:12*	
40.3	246.1	2.6	6.37	0.16	19.2	14.0		
38.9	241.6	3.2	6.67	0.15	12.5	13.3		
37.5	238.6	3.8	6.61	0.15	11.9	12.2		
36.2	236.3	4.6	6.63	0.14	17.2	12.6		
34.8	234.0	5.6	6.83	0.15	23.2	12.5		
33.5	231.5	6.8	6.90	0.15	24.3	12.2		
32.2	228.8	8.3	6.48	0.16	17.1	12.0		
30.9	225.7	10.0	5.84	0.19	7.5	12.5		
29.6	223.3	12.1	5.30	0.17	3.3	12.3		

Table B.2 continued. (See notes on page 135.)

Alt (km)	Temp (K)	Press (mb)	$^{48}O_3$ vmr	$^{48}O_3$ err	$^{668}O_3$ enr	$^{668}O_3$ enr err	$^{686}O_3$ enr	$^{686}O_3$ enr err
at2 ss42		*Latitude:-38.3*		*Longitude: 42.9*			*Filter:12*	
40.5	248.0	2.6	5.84	0.15	22.4	18.3		
39.1	244.6	3.2	6.17	0.14	20.2	16.5		
37.7	241.8	3.8	6.35	0.14	17.3	13.8		
36.4	239.2	4.6	6.64	0.14	14.7	13.3		
35.0	237.4	5.6	6.98	0.14	13.4	11.8		
33.7	235.7	6.8	7.14	0.13	13.6	11.8		
32.3	234.6	8.3	7.05	0.13	15.6	11.8		
31.0	233.1	10.0	6.88	0.12	17.6	12.0		
29.7	229.9	12.1	6.61	0.12	18.7	14.0		
28.4	226.3	14.7	6.08	0.11	18.7	14.4		
27.1	222.9	17.8	5.41	0.10	18.1	13.6		
25.9	219.6	21.5	4.81	0.14	16.8	14.0		
24.6	216.9	26.1	4.24	0.16	13.4	14.3		
at2 ss59		*Latitude:-27.4*		*Longitude:355.8*			*Filter:12*	
40.9	248.4	2.6	6.37	0.16	15.8	16.5	18.2	18.5
39.5	245.4	3.2	6.84	0.19	17.6	14.5	11.2	18.0
38.1	243.0	3.8	7.21	0.19	17.0	14.4	11.5	17.9
36.7	240.0	4.6	7.50	0.19	14.9	13.5	17.1	19.2
35.4	236.9	5.6	7.72	0.19	14.4	12.9	19.5	19.4
34.0	234.7	6.8	7.91	0.17	16.4	10.8	16.0	17.3
32.7	233.0	8.3	8.16	0.17	18.3	10.9	12.9	16.9
31.4	231.6	10.0	8.50	0.18	18.4	11.9	12.5	18.9
30.1	229.8	12.1	8.73	0.17	16.3	11.9	11.7	19.0
28.8	227.6	14.7	8.52	0.16	13.5	11.9	9.7	19.0
27.5	225.4	17.8	7.70	0.15	11.4	13.6	8.4	20.7
26.2	223.4	21.5	6.45	0.13	11.7	14.4	10.2	21.9
25.0	220.8	26.1	5.15	0.11	13.6	17.2	13.1	25.5

Alt (km)	Temp (K)	Press (mb)	$^{48}O_3$ vmr	$^{48}O_3$ err	$^{668}O_3$ enr	$^{668}O_3$ enr err	$^{686}O_3$ enr	$^{686}O_3$ enr err
at3 sr02		*Latitude:-64.6*		*Longitude: 50.9*			*Filter:12*	
41.5	253.0	2.6	6.19	0.19	27.0	16.6	12.2	16.9
40.0	250.2	3.2	6.43	0.17	24.2	14.9	12.3	16.8
38.6	248.6	3.8	6.55	0.15	20.8	13.2	11.6	16.7
37.2	247.5	4.6	6.62	0.15	19.1	13.0	11.7	16.8
35.8	246.3	5.6	6.65	0.14	18.6	12.0	12.5	17.3
34.4	245.3	6.8	6.69	0.14	17.6	11.5	12.4	17.6
33.0	244.3	8.3	6.80	0.14	15.4	11.3	10.4	17.2
31.6	242.8	10.0	6.89	0.14	13.5	10.4	8.3	16.8
30.3	241.0	12.1	6.82	0.13	13.9	10.3	8.9	16.9
28.9	239.3	14.7	6.57	0.12	16.8	10.5	13.4	17.6
27.6	237.8	17.8	6.30	0.12	19.1	12.0	18.1	19.9
26.2	236.6	21.5	6.18	0.11	14.4	11.6	14.6	19.4
24.9	235.5	26.1	6.04	0.10	6.7	11.5	6.1	18.5
at3 sr03		*Latitude:-64.8*		*Longitude: 27.9*			*Filter: 9*	
41.6	259.3	2.6	6.38	0.27	77.6	38.0	50.9	32.9
40.1	256.0	3.2	6.95	0.28	59.1	30.3	18.5	26.7
38.7	254.3	3.8	7.41	0.27	36.3	21.2	-15.3	21.2
37.3	253.1	4.6	7.56	0.25	20.6	19.0	-24.7	19.4
35.8	251.8	5.6	7.42	0.27	9.2	16.1	-15.1	18.8
34.4	250.1	6.8	7.34	0.28	0.6	14.2	-3.8	19.4
33.0	248.2	8.3	7.57	0.27	-1.8	13.9	-1.4	19.6
31.6	246.8	10.0	7.91	0.19	0.7	10.9	-3.4	17.9
30.2	245.7	12.1	8.10	0.18	6.4	11.1	-3.3	17.7
28.8	244.7	14.7	8.14	0.18	15.2	11.7	1.0	18.2
27.4	243.6	17.8	8.08	0.19	22.7	12.8	5.9	19.4
26.0	242.5	21.5	7.76	0.17	19.6	12.5	5.2	19.2
24.7	241.1	26.1	7.06	0.14	8.5	13.2	1.2	19.0

Table B.2 continued. (See notes on page 135.)

Alt (km)	Temp (K)	Press (mb)	$^{48}O_3$ vmr	$^{48}O_3$ err	$^{668}O_3$ enr	$^{668}O_3$ enr err	$^{686}O_3$ enr	$^{686}O_3$ enr err
at3 sr05		*Latitude:-64.9*		*Longitude:342.3*			*Filter:12*	
41.0	274.6	2.6	4.35	0.13	16.9	20.7	7.7	21.7
39.4	271.1	3.2	4.60	0.12	33.4	17.6	10.9	20.3
37.9	267.5	3.8	5.00	0.12	33.9	17.4	14.5	20.7
36.4	265.4	4.6	5.46	0.12	27.0	14.1	18.3	21.3
34.9	265.5	5.6	5.85	0.12	20.3	13.3	18.2	21.0
33.4	265.6	6.8	6.12	0.12	16.8	12.7	14.9	20.2
31.9	263.7	8.3	6.09	0.12	16.7	12.6	12.6	21.7
24.8	232.3	21.5	3.12	0.06	8.9	13.9	5.4	22.4
23.5	226.6	26.1	2.84	0.06	6.0	13.8	5.6	22.1
at3 sr08		*Latitude:-65.2*		*Longitude:273.6*			*Filter:12*	
27.2	236.5	14.7	3.74	0.07	22.8	13.3	13.7	19.2
25.9	230.2	17.8	3.27	0.07	18.0	12.8	11.7	18.3
24.6	223.1	21.5	2.83	0.06	12.9	12.6	8.9	18.3
23.4	216.6	26.1	2.42	0.05	4.6	12.6	0.6	18.1
at3 sr09		*Latitude:-65.3*		*Longitude:250.7*			*Filter: 9*	
26.3	233.2	17.8	3.28	0.09	35.5	18.1	16.9	23.3
25.0	231.3	21.5	2.96	0.08	30.7	17.5	9.0	22.0
23.7	228.1	26.1	2.61	0.10	1.7	16.3	-6.8	19.0

Alt (km)	Temp (K)	Press (mb)	$^{48}O_3$ vmr	$^{48}O_3$ err	$^{668}O_3$ enr	$^{668}O_3$ enr err	$^{686}O_3$ enr	$^{686}O_3$ enr err
at3 sr11		*Latitude:-66.4*		*Longitude:290.5*			*Filter:12*	
40.4	278.9	2.6	3.23	0.09	24.0	26.9	30.2	29.3
38.8	277.9	3.2	3.75	0.10	30.7	22.2	17.2	26.8
37.3	277.6	3.8	4.32	0.10	33.8	19.7	7.4	24.8
35.7	275.1	4.6	4.86	0.11	29.5	18.7	6.0	24.2
34.1	269.0	5.6	5.22	0.11	23.3	16.4	8.6	23.5
32.6	262.2	6.8	5.23	0.11	19.3	15.8	10.5	23.7
31.2	254.0	8.3	4.90	0.10	18.2	13.0	11.2	20.2
29.8	245.3	10.0	4.42	0.08	19.9	13.3	12.6	20.6
28.4	237.9	12.1	3.86	0.07	23.7	13.9	15.2	21.5
27.1	232.9	14.7	3.37	0.07	23.5	15.7	14.4	23.9
25.8	228.2	17.8	3.05	0.06	14.6	14.6	7.4	22.6
24.5	223.0	21.5	2.82	0.06	3.0	13.1	0.1	19.1
23.2	217.4	26.1	2.46	0.05	10.0	14.0	9.2	20.8
at3 sr12		*Latitude:-66.5*		*Longitude:267.6*			*Filter:12*	
26.0	229.7	17.8	3.00	0.06	23.9	13.7	15.9	20.5
24.7	225.9	21.5	2.95	0.06	5.8	12.0	1.0	17.3
23.4	221.2	26.1	2.69	0.05	0.6	11.6	-0.7	16.9

Table B.2 continued. (See notes on page 135.)

Alt (km)	Temp (K)	Press (mb)	$^{48}O_3$ vmr	$^{48}O_3$ err	$^{668}O_3$ enr	$^{668}O_3$ enr err	$^{686}O_3$ enr	$^{686}O_3$ enr err
at3 sr15		*Latitude:-66.9*		*Longitude:198.6*			*Filter:12*	
41.3	260.4	2.6	4.02	0.11	26.8	21.6	5.1	20.4
39.8	257.6	3.2	4.39	0.11	25.4	16.8	4.3	18.3
38.3	254.6	3.8	4.65	0.11	24.8	16.6	6.8	18.6
36.9	251.3	4.6	4.80	0.11	26.1	15.1	13.4	18.8
35.5	247.7	5.6	5.08	0.11	25.6	13.9	17.7	19.0
34.1	244.6	6.8	5.66	0.11	20.9	12.4	14.3	17.8
32.7	243.9	8.3	6.25	0.12	16.2	10.7	9.4	16.1
31.3	244.0	10.0	6.51	0.12	14.5	10.5	7.4	15.9
29.9	243.2	12.1	6.48	0.11	15.3	10.5	8.3	16.6
28.6	241.3	14.7	6.55	0.11	17.4	10.5	11.5	17.1
27.2	239.5	17.8	6.86	0.12	20.2	11.0	16.4	18.0
25.9	238.2	21.5	6.90	0.13	19.8	11.9	18.0	19.0
24.5	237.3	26.1	6.26	0.11	13.1	11.2	12.8	18.1
at3 sr16		*Latitude:-66.9*		*Longitude:175.9*			*Filter: 9*	
41.8	260.4	2.6	4.89	0.19	-37.1	15.5	6.5	39.1
40.3	256.2	3.2	5.11	0.20	10.4	25.8	33.4	30.4
38.8	251.1	3.8	5.29	0.19	28.4	29.0	38.0	30.9
37.4	247.5	4.6	5.46	0.21	31.3	20.7	25.1	22.2
36.0	246.7	5.6	5.64	0.25	32.0	21.1	14.5	20.7
34.6	246.0	6.8	5.79	0.26	35.8	21.5	15.8	21.0
33.2	243.9	8.3	5.99	0.24	38.4	16.0	20.7	20.6
31.9	241.4	10.0	6.42	0.25	32.4	15.3	16.2	19.9
30.5	239.4	12.1	6.98	0.19	21.3	11.9	4.9	16.4
29.1	240.5	14.7	7.31	0.19	14.9	11.3	-0.8	15.5
27.8	241.6	17.8	7.29	0.18	15.8	11.2	3.4	15.9
26.4	242.2	21.5	7.04	0.16	18.7	14.0	11.4	20.6
25.0	242.5	26.1	6.63	0.14	13.9	13.5	9.9	20.5
at3 sr17		*Latitude:-67.2*		*Longitude:107.2*			*Filter: 9*	
41.7	253.6	2.6	5.85	0.25	10.9	31.0	-4.0	26.2
40.3	249.7	3.2	5.92	0.23	36.6	28.4	9.3	27.0
38.9	246.1	3.8	5.84	0.21	50.2	24.1	1.9	21.6
37.5	244.2	4.6	5.79	0.20	49.1	20.2	-11.4	16.9
36.1	242.9	5.6	5.93	0.19	32.6	18.2	-6.2	17.8
34.7	241.8	6.8	6.14	0.24	11.3	16.6	13.0	19.1
33.3	240.5	8.3	6.30	0.25	-2.4	14.9	27.1	20.8
32.0	239.3	10.0	6.36	0.24	-0.5	15.2	21.1	19.8
30.6	238.6	12.1	6.37	0.16	11.0	13.6	3.8	20.7
29.3	238.3	14.7	6.46	0.15	20.0	14.0	-3.0	19.8
27.9	238.0	17.8	6.58	0.14	20.5	13.6	7.0	19.4
26.6	237.6	21.5	6.50	0.14	15.6	12.8	17.3	19.7
25.2	237.3	26.1	5.96	0.13	9.5	12.9	11.3	19.5
at3 sr19		*Latitude:-67.2*		*Longitude: 61.6*			*Filter:12*	
41.5	256.4	2.6	5.81	0.17	28.5	16.7	5.7	17.0
40.0	252.0	3.2	6.18	0.16	23.1	14.9	7.1	16.7
38.6	248.3	3.8	6.42	0.15	17.8	13.4	9.1	16.8
37.2	244.9	4.6	6.46	0.14	15.3	13.1	10.3	17.0
35.8	243.2	5.6	6.33	0.13	14.8	12.7	11.3	17.9
34.4	242.8	6.8	6.23	0.12	16.1	12.6	12.9	18.6
33.0	242.1	8.3	6.29	0.12	18.3	12.0	14.6	18.4
31.7	240.5	10.0	6.48	0.12	18.9	11.0	14.4	17.7
30.3	238.8	12.1	6.69	0.12	16.7	10.7	11.9	17.2
29.0	237.7	14.7	6.76	0.12	14.8	10.2	10.1	16.7
27.6	237.1	17.8	6.60	0.12	16.0	10.3	11.4	16.9
26.3	236.6	21.5	6.27	0.11	17.7	11.3	13.3	18.3
24.9	236.4	26.1	5.93	0.09	13.8	14.0	9.7	21.8

Table B.2 continued. (See notes on page 135.)

Alt (km)	Temp (K)	Press (mb)	$^{48}O_3$ vmr	$^{48}O_3$ err	$^{668}O_3$ enr	$^{668}O_3$ enr err	$^{686}O_3$ enr	$^{686}O_3$ enr err
at3 sr22		*Latitude:-67.5*		*Longitude:352.7*			*Filter:12*	
41.1	265.6	2.6	4.27	0.12	20.6	20.4	0.7	20.4
39.6	263.5	3.2	4.59	0.12	25.6	17.0	8.6	20.1
38.1	262.0	3.8	4.95	0.13	26.0	16.6	14.4	20.8
36.6	261.1	4.6	5.39	0.13	19.6	15.8	17.0	21.1
35.1	261.9	5.6	5.95	0.13	14.1	14.2	17.5	23.0
33.7	262.5	6.8	6.51	0.13	18.2	14.6	16.8	22.8
32.2	260.5	8.3	6.86	0.13	26.4	13.0	14.9	21.8
30.7	258.2	10.0	6.92	0.13	26.8	12.8	12.1	21.1
29.3	253.1	12.1	6.70	0.14	19.6	12.0	10.1	20.1
27.8	246.2	14.7	6.07	0.12	14.3	11.6	11.0	20.6
23.8	234.4	26.1	3.38	0.07	10.9	16.3	10.3	27.9
at3 sr24		*Latitude:-67.8*		*Longitude:284.0*			*Filter:12*	
40.7	281.9	2.6	3.24	0.09	-4.0	22.7	13.9	27.7
39.1	277.9	3.2	3.53	0.09	8.2	23.3	29.3	29.4
37.5	274.6	3.8	3.92	0.10	25.5	17.6	28.4	25.3
36.0	271.8	4.6	4.38	0.10	30.8	17.7	19.9	23.3
34.5	268.7	5.6	4.81	0.11	24.3	16.6	13.7	22.2
32.9	265.1	6.8	5.06	0.10	18.0	15.4	11.2	23.7
31.5	260.5	8.3	5.04	0.10	17.9	15.2	9.2	23.0
30.0	251.1	10.0	4.67	0.09	21.4	14.0	8.1	21.3
28.6	241.9	12.1	3.99	0.07	23.2	14.3	9.3	21.7
27.3	235.9	14.7	3.31	0.08	21.2	14.3	12.7	21.0
25.9	231.2	17.8	2.95	0.07	18.1	13.9	14.8	21.4
24.6	226.0	21.5	2.83	0.06	16.7	14.2	14.2	21.2
23.4	220.1	26.1	2.58	0.05	15.4	14.1	11.5	20.6

Alt (km)	Temp (K)	Press (mb)	$^{48}O_3$ vmr	$^{48}O_3$ err	$^{668}O_3$ enr	$^{668}O_3$ enr err	$^{686}O_3$ enr	$^{686}O_3$ enr err
at3 sr27		*Latitude:-68.0*		*Longitude:215.3*			*Filter:12*	
41.4	264.6	2.6	3.80	0.11	16.8	22.5	9.7	22.2
39.9	260.9	3.2	3.84	0.10	16.6	17.6	3.8	19.4
38.4	257.2	3.8	4.00	0.09	15.2	17.4	1.6	19.1
37.0	255.4	4.6	4.31	0.10	13.7	15.7	4.9	19.3
35.5	255.6	5.6	4.67	0.10	14.0	14.5	9.4	19.8
34.1	255.6	6.8	4.97	0.10	17.4	13.6	13.7	19.9
32.6	254.0	8.3	5.19	0.10	21.0	12.3	16.5	19.6
31.2	252.5	10.0	5.49	0.10	21.1	12.2	15.7	19.3
29.8	251.2	12.1	5.83	0.10	18.9	12.4	12.6	20.8
at3 sr28		*Latitude:-68.2*		*Longitude:169.3*			*Filter: 9*	
41.7	254.7	2.6	4.99	0.20	27.4	37.9	30.0	31.2
40.2	251.3	3.2	5.02	0.20	-1.7	27.7	34.5	30.4
38.8	248.1	3.8	5.22	0.19	-3.7	27.7	20.3	27.3
37.4	246.6	4.6	5.43	0.18	10.2	24.0	-0.8	27.3
36.0	246.3	5.6	5.52	0.18	21.8	26.0	-9.5	25.0
34.6	245.2	6.8	5.54	0.18	24.5	18.4	-4.4	19.5
33.2	243.4	8.3	5.54	0.17	20.2	16.9	4.4	20.6
31.8	241.9	10.0	5.58	0.14	14.6	14.9	9.1	20.5
30.5	241.3	12.1	5.70	0.13	12.0	13.9	12.8	20.5
29.1	240.7	14.7	5.92	0.13	14.1	13.5	18.6	20.5
27.7	239.9	17.8	6.07	0.12	17.4	12.8	23.1	19.7
26.4	239.3	21.5	6.02	0.12	18.2	13.0	21.5	19.8
25.0	239.4	26.1	5.82	0.17	12.6	14.9	11.4	22.6

Table B.2 continued. (See notes on page 135.)

Alt (km)	Temp (K)	Press (mb)	$^{48}O_3$ vmr	$^{48}O_3$ err	$^{668}O_3$ enr	$^{668}O_3$ enr err	$^{686}O_3$ enr	$^{686}O_3$ enr err
at3 sr30		*Latitude:-68.3*		*Longitude:123.6*			*Filter:12*	
41.4	252.7	2.6	5.49	0.16	32.2	17.6	6.0	16.6
40.0	248.7	3.2	5.53	0.14	25.2	16.1	9.9	17.0
38.6	246.7	3.8	5.55	0.13	16.8	14.8	13.5	17.6
37.2	245.1	4.6	5.61	0.13	14.1	14.6	14.1	17.5
35.8	244.0	5.6	5.69	0.13	15.0	14.3	13.1	16.8
34.4	242.9	6.8	5.83	0.12	17.2	14.3	13.4	16.7
33.0	242.0	8.3	6.03	0.12	19.5	13.6	15.8	18.0
31.6	241.0	10.0	6.12	0.11	20.3	12.7	17.2	19.1
30.3	238.9	12.1	5.98	0.11	17.7	12.3	15.1	18.9
28.9	235.8	14.7	5.79	0.11	14.3	11.5	11.7	18.3
27.6	233.0	17.8	5.75	0.11	14.2	11.4	11.0	18.1
26.3	232.4	21.5	5.78	0.11	16.1	12.2	12.3	19.2
25.0	232.3	26.1	5.63	0.11	14.0	12.0	10.6	18.9
at3 sr33		*Latitude:-68.6*		*Longitude: 54.7*			*Filter:12*	
41.4	259.3	2.6	5.30	0.15	8.4	17.5	10.1	19.6
39.9	256.1	3.2	5.82	0.15	12.6	15.1	7.1	18.2
38.4	253.8	3.8	6.24	0.16	20.0	13.9	5.3	17.2
37.0	251.7	4.6	6.60	0.16	20.7	13.7	7.8	17.5
35.6	249.2	5.6	6.92	0.15	18.1	13.0	12.9	19.3
34.2	246.5	6.8	7.06	0.14	17.0	12.8	15.3	19.7
32.8	243.7	8.3	7.01	0.13	17.8	11.9	13.3	19.0
31.4	240.8	10.0	6.92	0.12	17.9	11.6	9.8	18.4
30.1	238.6	12.1	6.89	0.12	15.9	11.3	8.3	18.2
28.7	237.8	14.7	6.86	0.13	14.4	11.0	9.1	18.1
27.4	237.5	17.8	6.72	0.12	15.9	11.2	11.8	18.6
26.0	236.8	21.5	6.38	0.10	17.4	12.2	13.3	19.9
24.7	235.9	26.1	5.86	0.09	13.4	11.9	10.5	19.6
at3 sr34		*Latitude:-68.5*		*Longitude: 32.1*			*Filter: 9*	
41.4	264.7	2.6	5.80	0.23	37.4	31.2	11.2	29.1
39.9	262.2	3.2	6.36	0.25	35.5	30.8	22.3	31.0
38.5	259.6	3.8	6.59	0.24	22.2	27.6	12.6	28.1
37.0	255.2	4.6	6.51	0.22	10.7	20.2	0.5	23.4
35.6	250.2	5.6	6.36	0.20	13.0	20.5	4.7	24.6
34.1	247.2	6.8	6.48	0.19	19.0	18.1	17.4	23.3
32.7	246.1	8.3	7.09	0.19	8.6	16.5	16.1	22.7
31.4	245.6	10.0	7.83	0.22	-8.2	11.0	4.9	20.2
30.0	246.2	12.1	7.91	0.22	-8.8	11.0	-0.2	19.3
28.6	246.7	14.7	7.35	0.15	7.7	11.5	3.4	19.7
27.2	246.7	17.8	6.79	0.13	23.6	12.8	10.1	20.6
25.8	246.1	21.5	6.48	0.17	24.2	14.5	13.1	21.9
24.4	243.6	26.1	6.03	0.18	14.1	14.1	10.4	21.7
at3 sr36		*Latitude:-69.3*		*Longitude:139.6*			*Filter:12*	
41.7	251.7	2.6	5.05	0.14	11.0	18.2	3.5	18.7
40.3	248.0	3.2	5.31	0.14	14.5	17.7	7.7	19.0
38.9	245.9	3.8	5.38	0.14	16.5	15.0	9.7	18.6
37.5	243.8	4.6	5.41	0.14	20.7	15.4	11.9	19.0
36.1	242.6	5.6	5.55	0.12	24.8	14.0	14.0	18.7
34.7	241.7	6.8	5.75	0.12	25.4	13.9	15.4	18.7
33.3	240.7	8.3	5.90	0.12	23.0	13.1	16.1	19.1
32.0	239.6	10.0	5.87	0.12	20.2	12.8	16.0	19.1
30.6	238.7	12.1	5.72	0.10	18.1	12.5	15.1	19.4
29.3	237.9	14.7	5.63	0.10	16.5	12.3	13.5	19.3
27.9	237.3	17.8	5.72	0.09	14.8	12.6	11.9	20.0
26.6	236.8	21.5	5.87	0.10	13.7	12.8	10.7	20.4
25.2	236.2	26.1	5.78	0.10	13.6	12.6	10.2	19.5

Table B.2 continued. (See notes on page 135.)

Alt (km)	Temp (K)	Press (mb)	$^{48}O_3$ vmr	$^{48}O_3$ err	$^{668}O_3$ enr	$^{668}O_3$ enr err	$^{686}O_3$ enr	$^{686}O_3$ enr err
at3 sr39	*Latitude:-69.4*	*Longitude: 71.1*	*Filter:12*					
41.4	259.1	2.6	4.95	0.13	10.3	19.6	19.4	21.3
39.9	254.1	3.2	5.36	0.14	23.6	15.7	15.2	18.8
38.5	249.0	3.8	5.62	0.15	26.2	16.0	14.8	18.8
37.1	246.8	4.6	5.86	0.13	19.9	13.3	16.7	18.9
35.7	246.4	5.6	6.19	0.13	16.9	13.0	15.5	18.5
34.3	245.5	6.8	6.52	0.13	18.2	12.4	11.6	18.9
32.9	244.1	8.3	6.64	0.12	18.8	12.3	9.5	18.6
31.5	242.2	10.0	6.51	0.12	17.6	11.9	10.6	18.8
30.1	240.0	12.1	6.39	0.11	16.5	11.8	12.7	19.1
28.8	237.8	14.7	6.42	0.11	16.6	12.0	13.5	19.5
27.4	235.6	17.8	6.51	0.11	17.3	12.1	12.7	19.3
26.1	234.4	21.5	6.42	0.10	16.2	11.7	10.2	18.2
24.8	234.1	26.1	6.04	0.09	11.6	11.3	5.9	17.5
at3 sr40	*Latitude:-69.6*	*Longitude: 47.9*	*Filter: 9*					
41.5	264.8	2.6	5.30	0.21	15.2	43.1	0.6	37.7
40.0	262.2	3.2	5.87	0.23	44.9	42.8	2.1	33.4
38.5	258.5	3.8	6.34	0.24	57.5	36.4	1.2	29.8
37.1	255.2	4.6	6.79	0.23	43.6	24.8	6.3	28.2
35.6	252.6	5.6	7.13	0.23	25.7	21.7	12.5	24.7
34.2	250.0	6.8	7.18	0.22	16.3	19.8	17.1	25.2
32.8	247.0	8.3	7.02	0.21	12.5	17.8	17.6	25.1
31.4	244.3	10.0	6.83	0.19	10.4	17.1	11.2	23.9
30.0	242.4	12.1	6.80	0.20	10.8	13.9	4.0	21.9
28.7	241.3	14.7	7.02	0.20	14.4	14.2	4.9	22.0
27.3	241.4	17.8	7.23	0.21	18.5	15.6	10.8	24.3
25.9	241.3	21.5	7.05	0.16	18.7	15.1	11.8	23.6
24.6	240.1	26.1	6.48	0.12	13.3	14.2	7.9	22.4
at3 sr45	*Latitude:-69.9*	*Longitude:293.1*	*Filter:12*					
25.9	235.5	17.8	3.32	0.07	17.1	15.5	10.6	24.5
24.6	226.0	21.5	2.85	0.06	16.1	15.6	10.0	24.7
23.3	222.7	26.1	2.61	0.06	16.2	20.0	10.4	30.7
at3 sr46	*Latitude:-70.0*	*Longitude:269.8*	*Filter: 9*					
40.9	280.3	2.6	3.91	0.17	0.4	63.7	-15.0	42.4
26.1	236.0	17.8	3.14	0.11	18.9	20.9	10.4	30.1
24.7	232.0	21.5	2.87	0.09	22.3	20.3	1.4	25.1
23.4	226.9	26.1	2.66	0.08	16.9	19.1	-1.3	23.8
at3 sr48	*Latitude:-70.0*	*Longitude:224.4*	*Filter:12*					
41.0	266.6	2.6	3.78	0.11	31.5	25.2	14.2	24.1
39.5	263.6	3.2	3.92	0.11	29.3	24.4	20.7	25.0
at3 sr51	*Latitude:-70.3*	*Longitude:109.4*	*Filter:12*					
41.8	256.1	2.6	4.98	0.14	30.4	20.6	5.3	20.1
40.3	252.4	3.2	5.27	0.13	13.6	17.9	8.0	19.4
38.9	249.2	3.8	5.55	0.14	11.1	15.8	10.1	19.6
37.5	246.4	4.6	5.86	0.15	17.0	15.3	10.1	19.4
36.1	245.2	5.6	6.26	0.14	21.0	15.6	7.7	19.9
34.7	244.8	6.8	6.60	0.14	19.8	15.4	6.6	21.0
33.3	244.3	8.3	6.74	0.13	16.1	12.8	8.7	19.2
31.9	244.1	10.0	6.62	0.12	17.1	12.9	11.6	19.7

Table B.2 continued. (See notes on page 135.)

Alt (km)	Temp (K)	Press (mb)	$^{48}O_3$ vmr	$^{48}O_3$ err	$^{668}O_3$ enr	$^{668}O_3$ enr err	$^{686}O_3$ enr	$^{686}O_3$ enr err
at3 sr54		*Latitude:-70.6*		*Longitude: 39.8*			*Filter:12*	
41.4	263.7	2.6	4.40	0.12	2.8	21.5	17.9	24.5
39.9	261.7	3.2	4.91	0.12	9.5	19.4	16.9	23.6
38.4	260.4	3.8	5.55	0.13	18.0	18.8	13.8	22.6
36.9	257.7	4.6	6.19	0.14	21.4	17.7	12.5	23.2
35.5	254.2	5.6	6.53	0.14	23.8	17.1	12.2	23.7
34.0	252.4	6.8	6.62	0.13	25.3	13.8	11.9	21.0
32.6	251.1	8.3	6.86	0.13	21.8	13.4	11.7	20.8
31.2	250.0	10.0	7.18	0.14	15.6	14.4	11.4	23.9
29.8	248.5	12.1	7.25	0.13	12.6	12.3	10.8	21.5
28.4	246.5	14.7	7.21	0.13	13.4	11.7	10.3	20.6
at3 sr57		*Latitude:-70.7*		*Longitude:331.4*			*Filter:12*	
40.9	269.2	2.6	3.73	0.10	44.6	26.9	7.5	26.3
39.4	267.2	3.2	4.04	0.10	29.1	25.3	7.4	25.5
37.9	265.9	3.8	4.51	0.11	12.9	22.3	9.8	25.8
36.3	266.0	4.6	5.02	0.12	9.0	20.2	14.7	27.7
34.8	264.6	5.6	5.36	0.12	13.6	16.9	17.4	25.8
33.3	261.2	6.8	5.53	0.11	18.9	15.6	16.3	24.2
31.9	258.2	8.3	5.58	0.11	21.3	16.5	13.4	26.3
30.4	255.2	10.0	5.35	0.11	22.2	16.8	11.7	27.0
29.0	248.9	12.1	4.83	0.10	22.2	14.8	12.5	24.2
27.6	242.7	14.7	4.33	0.09	20.3	14.7	14.9	24.8
26.2	238.6	17.8	3.87	0.09	18.5	18.8	16.8	31.6
24.9	234.2	21.5	3.40	0.08	18.1	18.7	15.3	31.1
23.6	229.2	26.1	2.96	0.07	16.2	18.3	9.1	29.3

Alt (km)	Temp (K)	Press (mb)	$^{48}O_3$ vmr	$^{48}O_3$ err	$^{668}O_3$ enr	$^{668}O_3$ enr err	$^{686}O_3$ enr	$^{686}O_3$ enr err
at3 sr58		*Latitude:-70.8*		*Longitude:308.2*			*Filter: 9*	
41.0	280.2	2.6	4.17	0.17	37.2	39.3	-14.2	41.8
39.4	277.1	3.2	4.35	0.18	26.7	37.0	8.9	34.1
37.9	272.0	3.8	4.81	0.18	10.3	32.4	17.2	36.4
36.3	269.8	4.6	5.49	0.19	1.4	35.6	11.3	36.5
34.8	268.0	5.6	5.91	0.20	14.8	25.0	10.4	30.4
33.3	264.9	6.8	5.91	0.19	33.0	22.3	12.1	28.4
31.8	261.1	8.3	5.68	0.16	35.3	23.0	10.1	30.4
30.3	256.5	10.0	5.35	0.15	24.2	21.1	11.6	30.9
28.9	250.9	12.1	4.88	0.17	12.5	18.9	18.6	28.2
27.5	244.7	14.7	4.25	0.15	5.7	18.1	21.9	29.1
26.1	239.5	17.8	3.61	0.09	7.8	23.0	16.2	32.2
24.8	235.9	21.5	3.15	0.09	14.7	21.8	6.7	29.0
23.4	233.3	26.1	2.74	0.08	20.1	21.7	-0.8	27.1
at3 sr63		*Latitude:-71.1*		*Longitude:169.9*			*Filter:12*	
41.6	259.0	2.6	4.61	0.13	6.0	24.7	14.0	24.9
40.1	255.4	3.2	4.97	0.13	14.6	22.1	15.9	26.3
38.7	251.2	3.8	5.10	0.13	25.2	18.2	12.9	22.1
37.3	246.9	4.6	5.19	0.13	26.7	17.1	9.6	20.8
35.9	244.4	5.6	5.36	0.12	22.2	17.7	11.4	22.8
34.5	243.0	6.8	5.38	0.11	20.1	18.0	15.1	24.3
33.1	240.8	8.3	5.32	0.10	20.7	14.6	15.0	20.8
31.8	238.9	10.0	5.48	0.10	18.5	13.0	11.9	19.2
30.4	237.7	12.1	5.79	0.10	15.1	12.1	10.4	18.7
29.1	236.6	14.7	5.92	0.10	14.1	12.9	11.5	20.2
27.7	235.5	17.8	5.91	0.11	14.2	13.9	12.1	22.0
26.4	234.9	21.5	5.83	0.10	14.1	14.1	10.8	22.0
25.1	234.6	26.1	5.62	0.09	14.1	14.8	9.4	22.5

Table B.2 continued. (See notes on page 135.)

Alt (km)	Temp (K)	Press (mb)	$^{48}O_3$ vmr	$^{48}O_3$ err	$^{668}O_3$ enr	$^{668}O_3$ enr err	$^{686}O_3$ enr	$^{686}O_3$ enr err
at3 sr64		*Latitude:-71.1*		*Longitude:147.1*			*Filter: 9*	
41.8	260.1	2.6	5.44	0.23	23.6	47.9	-57.0	18.9
40.4	254.0	3.2	5.50	0.23	10.0	39.1	-49.2	22.1
38.9	249.4	3.8	5.41	0.20	4.1	23.4	-2.2	29.6
37.5	246.4	4.6	5.55	0.19	16.3	25.7	37.1	33.3
36.1	244.2	5.6	5.80	0.22	24.0	23.6	32.5	29.3
34.7	242.4	6.8	5.91	0.21	9.1	18.4	13.8	22.6
33.4	240.9	8.3	6.05	0.20	-5.3	15.3	0.9	19.6
32.0	239.9	10.0	6.31	0.18	6.4	15.6	-1.5	20.5
30.6	239.7	12.1	6.36	0.16	26.2	16.9	3.4	22.6
29.3	238.9	14.7	6.22	0.20	33.4	15.4	10.9	20.6
27.9	238.0	17.8	6.20	0.16	28.7	15.2	12.7	21.4
26.6	237.4	21.5	6.15	0.13	21.6	14.7	7.6	20.8
25.2	236.7	26.1	5.72	0.13	13.3	15.4	1.6	20.8
at3 sr66		*Latitude:-71.6*		*Longitude:299.3*			*Filter:12*	
23.6	230.8	26.1	3.01	0.06	16.5	18.3	7.4	29.3
at3 sr69		*Latitude:-71.7*		*Longitude:229.9*			*Filter:12*	
41.1	267.7	2.6	3.71	0.10	31.8	32.4	9.5	31.4
39.6	266.1	3.2	4.12	0.11	36.1	27.2	8.4	28.0
38.1	262.3	3.8	4.36	0.11	25.6	23.4	7.1	26.7
36.6	260.6	4.6	4.40	0.10	20.4	20.0	11.1	24.8
35.1	259.6	5.6	4.52	0.10	23.8	19.3	15.4	25.0
33.7	256.8	6.8	4.82	0.10	23.5	17.6	15.7	24.3

Alt (km)	Temp (K)	Press (mb)	$^{48}O_3$ vmr	$^{48}O_3$ err	$^{668}O_3$ enr	$^{668}O_3$ enr err	$^{686}O_3$ enr	$^{686}O_3$ enr err
at3 sr70		*Latitude:-71.8*		*Longitude:206.9*			*Filter: 9*	
41.4	270.0	2.6	4.83	0.24	-48.6	43.5	-35.6	32.6
39.9	264.3	3.2	5.03	0.22	10.1	50.3	-32.3	26.0
38.4	256.5	3.8	4.86	0.19	33.6	39.4	6.4	32.0
37.0	252.4	4.6	4.78	0.17	25.3	28.8	35.3	33.8
35.5	251.3	5.6	4.96	0.16	28.3	24.8	30.5	30.8
34.1	248.7	6.8	5.27	0.16	24.0	23.1	19.3	27.7
32.7	245.0	8.3	5.52	0.15	6.4	18.7	17.8	26.6
31.3	242.3	10.0	5.78	0.14	3.0	14.7	13.6	24.8
30.0	241.4	12.1	6.16	0.16	16.5	15.0	6.8	22.4
28.6	240.3	14.7	6.48	0.17	26.0	14.8	7.2	21.7
27.2	239.2	17.8	6.60	0.21	23.4	15.6	11.7	22.3
25.9	237.8	21.5	6.52	0.19	16.2	16.7	9.9	25.3
24.6	235.5	26.1	6.05	0.16	9.9	14.7	3.3	22.2
at3 sr72		*Latitude:-71.8*		*Longitude:161.3*			*Filter:12*	
41.6	258.0	2.6	4.66	0.13	15.2	24.9	18.2	24.7
40.1	253.2	3.2	4.79	0.12	22.6	20.4	20.2	23.1
38.7	249.8	3.8	5.08	0.13	20.4	19.2	15.3	22.6
37.3	249.0	4.6	5.37	0.13	14.8	17.6	11.8	21.8
35.9	244.8	5.6	5.35	0.12	15.3	16.1	12.1	21.4
34.5	241.5	6.8	5.32	0.11	19.5	14.6	11.8	20.7
33.1	241.0	8.3	5.64	0.11	21.2	14.7	9.7	20.6
31.7	240.5	10.0	5.99	0.11	20.5	14.5	10.1	21.1
30.4	238.8	12.1	6.09	0.11	18.6	13.9	12.3	21.2
29.0	236.7	14.7	6.12	0.11	16.1	14.1	12.2	22.1
27.7	235.3	17.8	6.17	0.11	13.8	14.4	10.0	22.6
26.4	234.6	21.5	6.03	0.11	13.0	16.5	8.8	25.5
25.0	234.4	26.1	5.57	0.09	14.4	13.9	10.5	21.3

Table B.2 continued. (See notes on page 135.)

Alt (km)	Temp (K)	Press (mb)	$^{48}O_3$ vmr	$^{48}O_3$ err	$^{668}O_3$ enr	$^{668}O_3$ enr err	$^{686}O_3$ enr	$^{686}O_3$ enr err
at3 sr78	*Latitude:-72.0*		*Longitude: 22.8*			*Filter:12*		
41.4	267.3	2.6	4.20	0.12	18.9	23.2	6.6	24.8
39.9	264.4	3.2	4.67	0.12	19.2	26.6	13.7	29.9
38.4	262.5	3.8	5.20	0.15	20.2	18.1	17.8	24.1
36.9	260.3	4.6	5.49	0.14	21.9	17.5	14.8	23.5
35.4	258.8	5.6	5.71	0.13	23.0	17.0	13.2	23.1
34.0	257.5	6.8	5.90	0.12	22.0	16.3	14.5	24.4
32.5	255.1	8.3	5.86	0.12	19.9	15.7	13.4	25.1
31.1	251.5	10.0	5.55	0.11	18.1	15.5	12.2	25.3
29.7	247.3	12.1	5.27	0.10	17.3	15.4	13.1	26.1
28.3	244.7	14.7	5.20	0.09	16.9	15.8	13.7	26.7
26.9	243.1	17.8	5.29	0.10	16.4	16.4	14.0	27.8
25.5	242.4	21.5	5.27	0.10	16.9	16.8	14.9	28.8
at3 sr81	*Latitude:-72.1*		*Longitude:313.1*			*Filter:12*		
41.2	270.2	2.6	4.11	0.12			17.4	34.5
39.7	268.9	3.2	4.43	0.12			8.3	33.1
38.2	267.0	3.8	4.75	0.12			6.5	31.9
36.7	263.5	4.6	5.16	0.13			11.0	31.7
35.2	260.0	5.6	5.88	0.14			14.7	30.3
33.7	258.0	6.8	6.54	0.14			14.3	24.6
32.3	257.9	8.3	6.84	0.16			14.1	26.9
30.8	255.9	10.0	6.91	0.14			15.3	28.9
29.4	253.5	12.1	6.95	0.13			14.4	29.8
27.9	251.2	14.7	6.73	0.13			11.7	29.4
at3 sr82	*Latitude:-72.2*		*Longitude:288.4*			*Filter: 9*		
41.3	275.9	2.6	4.04	0.17	-21.4	75.6	16.4	54.2
39.7	273.8	3.2	4.53	0.20	-21.5	64.4	-35.3	30.3
38.2	270.2	3.8	5.03	0.20	8.3	40.9	-34.8	24.0
36.7	266.8	4.6	5.40	0.21	30.8	40.5	-9.2	34.3
35.2	265.6	5.6	5.91	0.20	23.7	24.5	4.1	28.1
33.6	267.8	6.8	6.56	0.22	10.6	21.1	9.4	29.6
32.1	267.2	8.3	6.83	0.22	13.8	21.2	13.8	31.4
30.6	266.8	10.0	6.44	0.20	22.5	22.2	13.3	32.3
29.1	260.5	12.1	5.70	0.16	24.6	23.8	9.5	37.1
27.7	255.5	14.7	4.93	0.12	22.7	18.3	6.9	30.3
26.2	249.1	17.8	4.08	0.12	21.0	24.8	6.6	38.0
24.8	239.6	21.5	3.39	0.10	17.6	28.0	6.9	44.0
23.5	231.7	26.1	2.95	0.07	16.3	24.3	7.3	36.5
at3 sr84	*Latitude:-72.2*		*Longitude:243.0*			*Filter:12*		
26.3	240.5	17.8	3.50	0.07	18.5	19.9	14.8	32.6
25.0	235.1	21.5	3.04	0.07	17.4	23.4	12.0	37.8
23.7	229.5	26.1	2.68	0.06	17.6	22.3	10.5	35.3

Table B.2 continued. (See notes on page 135.)

Alt (km)	Temp (K)	Press (mb)	$^{48}O_3$ vmr	$^{48}O_3$ err	$^{668}O_3$ enr	$^{668}O_3$ enr err	$^{686}O_3$ enr	$^{686}O_3$ enr err
at3 sr87		*Latitude:-72.3*		*Longitude:173.7*			*Filter:12*	
41.4	259.4	2.6	4.16	0.12	7.2	26.0	11.5	25.5
40.0	258.1	3.2	4.79	0.13	15.4	25.8	10.7	28.9
38.5	256.2	3.8	5.15	0.13	27.2	22.4	10.0	25.3
37.1	251.1	4.6	5.18	0.14	28.2	22.5	14.2	26.8
35.6	248.3	5.6	5.38	0.13	21.0	23.1	16.6	29.9
34.2	246.9	6.8	5.70	0.12	15.9	16.3	16.1	23.5
32.8	244.8	8.3	5.93	0.12	16.9	17.0	16.4	25.5
31.5	243.2	10.0	6.16	0.12	19.3	17.8	15.1	26.5
30.1	239.8	12.1	6.40	0.14	18.0	18.7	10.6	29.0
28.7	236.0	14.7	6.49	0.13	15.3	14.3	7.2	22.7
27.4	235.4	17.8	6.35	0.12	13.3	18.2	8.0	28.7
26.1	234.6	21.5	5.93	0.10	12.4	15.1	11.2	24.4
24.8	232.3	26.1	5.36	0.10	13.0	19.3	12.5	30.7
at3 sr88		*Latitude:-72.3*		*Longitude:150.0*			*Filter: 9*	
41.7	262.7	2.6	5.37	0.23	22.2	68.6	-16.8	40.7
40.3	253.8	3.2	5.47	0.22	33.8	64.6	-4.6	44.6
38.8	250.9	3.8	5.32	0.21	23.0	42.2	-0.5	33.6
37.4	250.2	4.6	5.08	0.18	11.8	31.6	8.6	30.4
36.0	247.7	5.6	5.25	0.18	17.1	25.7	15.4	29.1
34.6	244.6	6.8	5.71	0.20	20.1	30.0	9.5	31.4
33.2	242.8	8.3	5.94	0.20	23.6	29.3	10.4	32.2
31.8	242.6	10.0	5.97	0.16	35.0	21.8	18.3	30.6
30.5	241.8	12.1	6.16	0.15	35.5	19.3	12.4	27.4
29.1	239.9	14.7	6.47	0.18	17.9	19.7	0.3	26.2
27.7	239.0	17.8	6.52	0.17	5.8	17.7	3.0	24.3
26.4	238.3	21.5	6.19	0.20	7.5	20.6	12.7	31.2
25.0	237.6	26.1	5.66	0.12	15.8	18.8	11.5	27.8
at3 sr94		*Latitude:-72.4*		*Longitude:347.0*			*Filter: 9*	
41.7	269.3	2.6	4.80	0.20	29.2	65.6	-12.9	33.6
40.2	266.0	3.2	5.14	0.23	11.2	52.6	20.4	41.0
38.7	260.8	3.8	5.47	0.22	4.2	33.1	8.7	34.1
37.2	256.6	4.6	5.90	0.21	16.1	29.6	-13.1	31.9
35.8	255.0	5.6	6.28	0.26	24.5	33.7	0.4	39.3
34.4	252.8	6.8	6.53	0.25	31.5	24.8	14.3	32.1
32.9	251.6	8.3	6.77	0.25	28.0	29.9	4.6	36.2
31.5	251.4	10.0	7.02	0.27	16.6	23.0	-1.8	30.9
30.1	252.5	12.1	7.32	0.19	13.0	16.9	6.6	26.7
28.6	253.1	14.7	7.59	0.20	14.1	22.2	11.8	36.4
27.2	253.2	17.8	7.74	0.18	14.4	18.1	7.0	31.4
25.8	253.3	21.5	7.79	0.22	14.7	17.1	5.5	27.7
24.3	253.4	26.1	7.17	0.21	13.6	19.5	14.7	34.0
at3 ss02		*Latitude: 49.0*		*Longitude:211.0*			*Filter:12*	
40.2	229.7	2.6	7.28	0.20	14.0	13.4	9.0	13.3
38.9	226.6	3.2	7.37	0.19	11.3	13.0	10.8	13.3
37.6	224.2	3.8	7.05	0.17	12.5	11.3	13.8	13.4
36.4	222.7	4.6	6.77	0.16	14.2	11.1	16.1	13.6
35.1	221.3	5.6	6.88	0.15	14.3	11.1	15.1	13.5
33.9	220.7	6.8	7.19	0.15	14.1	10.1	12.4	13.3
32.6	221.0	8.3	7.40	0.15	14.5	9.6	10.4	13.1
31.3	221.3	10.0	7.30	0.14	14.5	9.5	10.0	13.0
30.1	221.2	12.1	6.97	0.12	13.6	9.6	10.5	13.4
28.8	220.8	14.7	6.52	0.11	12.9	9.8	11.4	14.1
27.6	220.4	17.8	6.04	0.10	13.9	9.9	12.6	14.3
26.3	219.5	21.5	5.49	0.09	16.5	10.6	13.4	14.9
25.1	218.0	26.1	4.83	0.08	17.0	13.7	11.6	18.3

Table B.2 continued. (See notes on page 135.)

Alt (km)	Temp (K)	Press (mb)	$^{48}O_3$ vmr	$^{48}O_3$ err	$^{668}O_3$ enr	$^{668}O_3$ enr err	$^{686}O_3$ enr	$^{686}O_3$ enr err
at3 ss03		*Latitude: 48.9*		*Longitude:188.4*		*Filter: 9*		
40.4	231.7	2.6	7.12	0.29	41.3	22.4	4.1	19.6
39.1	229.8	3.2	7.00	0.27	37.2	21.4	2.5	19.4
37.8	228.4	3.8	6.77	0.24	26.1	20.5	0.1	18.0
36.5	227.9	4.6	6.48	0.21	17.3	19.5	-0.2	17.6
35.2	227.5	5.6	6.30	0.20	13.1	19.1	3.5	18.2
33.9	226.8	6.8	6.18	0.20	11.1	15.1	10.2	17.9
32.6	225.4	8.3	6.08	0.20	11.2	12.4	17.2	17.9
31.4	223.9	10.0	6.08	0.19	15.2	12.6	19.8	18.1
30.1	222.6	12.1	6.19	0.16	21.2	12.7	16.9	16.8
28.8	221.9	14.7	6.26	0.13	23.4	12.2	11.8	14.9
27.6	221.4	17.8	6.13	0.12	19.4	11.5	8.2	14.2
26.3	221.1	21.5	5.68	0.15	12.6	12.3	8.4	14.8
25.1	220.8	26.1	4.99	0.13	7.7	11.9	9.2	15.1
at3 ss07		*Latitude: 48.6*		*Longitude:120.6*		*Filter:12*		
40.3	237.8	2.6	6.17	0.17	17.9	13.4	16.0	14.1
39.0	232.9	3.2	6.42	0.16	15.7	13.0	13.7	13.7
37.6	232.0	3.8	6.50	0.16	15.4	12.2	14.4	15.5
36.3	232.4	4.6	6.53	0.16	16.9	12.3	16.3	16.1
35.0	232.4	5.6	6.50	0.15	19.2	12.5	18.1	16.4
33.7	231.4	6.8	6.43	0.13	21.6	11.4	19.7	16.5
32.4	229.9	8.3	6.62	0.12	20.9	11.0	18.3	16.2
31.1	228.4	10.0	7.17	0.14	15.7	10.0	12.7	15.0
29.8	227.0	12.1	7.64	0.16	11.0	9.1	7.9	13.7
28.5	225.6	14.7	7.56	0.16	11.1	9.0	8.5	13.6
27.2	224.2	17.8	6.79	0.13	16.9	10.0	15.5	15.0
26.0	222.4	21.5	5.85	0.10	20.7	12.3	20.6	17.5
24.7	220.4	26.1	5.04	0.09	14.8	11.7	15.1	16.7

Alt (km)	Temp (K)	Press (mb)	$^{48}O_3$ vmr	$^{48}O_3$ err	$^{668}O_3$ enr	$^{668}O_3$ enr err	$^{686}O_3$ enr	$^{686}O_3$ enr err
at3 ss10		*Latitude: 48.2*		*Longitude: 30.1*		*Filter:12*		
39.7	238.4	2.6	6.25	0.17	12.4	14.7	19.3	15.9
38.3	235.0	3.2	6.75	0.17	8.7	14.0	20.8	16.2
37.0	231.7	3.8	6.74	0.16	12.8	12.6	19.1	15.3
35.7	228.2	4.6	6.50	0.15	18.3	11.4	14.9	14.2
34.4	224.6	5.6	6.22	0.13	19.3	11.5	11.2	13.9
33.1	221.4	6.8	5.89	0.12	15.8	10.9	10.6	13.7
31.9	219.0	8.3	5.52	0.10	12.5	10.1	12.3	13.4
30.6	216.7	10.0	5.24	0.09	13.7	10.1	14.8	13.7
29.4	214.5	12.1	5.12	0.09	19.4	10.5	16.7	13.8
28.2	213.0	14.7	5.12	0.09	22.5	10.8	14.8	13.7
27.0	211.7	17.8	5.09	0.09	17.4	10.3	8.1	12.9
25.8	210.6	21.5	4.92	0.08	7.1	9.8	-0.1	11.7
24.6	210.4	26.1	4.54	0.07	0.0	9.4	-3.6	11.3
at3 ss11		*Latitude: 48.2*		*Longitude: 7.5*		*Filter: 9*		
39.7	236.0	2.6	7.36	0.32	11.3	23.0	29.0	27.0
38.3	230.8	3.2	7.14	0.29	20.8	23.0	22.8	24.8
37.0	226.8	3.8	6.59	0.25	27.6	16.2	16.2	20.2
35.8	224.3	4.6	6.23	0.23	28.9	16.3	9.3	19.1
34.5	221.8	5.6	6.06	0.22	24.9	16.0	2.6	18.4
33.2	219.8	6.8	5.74	0.19	19.6	15.1	-4.1	17.5
32.0	218.7	8.3	5.27	0.14	16.6	13.9	-8.9	16.7
30.8	217.7	10.0	4.94	0.12	17.0	13.9	-7.0	16.9
29.5	216.6	12.1	4.90	0.12	19.7	14.1	3.4	18.8
28.3	215.6	14.7	5.06	0.17	19.5	12.9	14.1	15.2
27.1	214.5	17.8	5.15	0.17	13.7	12.1	17.1	15.4
25.9	213.6	21.5	5.01	0.11	5.2	11.1	13.8	14.1
24.7	213.1	26.1	4.58	0.08	0.9	10.8	12.0	13.5

Table B.2 continued. (See notes on page 135.)

Alt (km)	Temp (K)	Press (mb)	$^{48}O_3$ vmr	$^{48}O_3$ err	$^{668}O_3$ enr	$^{668}O_3$ enr err	$^{686}O_3$ enr	$^{686}O_3$ enr err
at3 ss13		*Latitude: 46.9*		*Longitude:141.6*			*Filter:12*	
40.3	234.1	2.6	5.71	0.18	15.5	13.5	20.6	17.1
39.0	231.7	3.2	5.93	0.17	15.3	13.4	16.7	16.5
37.7	230.4	3.8	6.00	0.17	14.5	13.2	16.8	16.4
36.4	231.2	4.6	6.00	0.16	13.4	11.8	19.1	16.8
35.0	232.1	5.6	5.98	0.15	12.8	11.7	20.0	16.9
33.7	231.4	6.8	5.91	0.15	13.7	11.9	19.0	16.9
32.4	229.2	8.3	5.83	0.13	16.1	10.8	17.5	16.6
31.1	226.8	10.0	6.01	0.13	16.9	10.8	15.8	16.3
29.9	224.6	12.1	6.43	0.13	15.7	9.8	14.4	14.9
28.6	222.5	14.7	6.73	0.13	14.7	9.3	14.1	14.2
27.3	220.5	17.8	6.50	0.12	16.1	9.4	15.5	14.3
26.1	219.2	21.5	5.82	0.10	18.6	10.9	17.2	16.0
24.8	218.7	26.1	5.01	0.08	18.1	12.9	15.6	18.3
at3 ss16		*Latitude: 46.5*		*Longitude: 73.8*			*Filter:12*	
40.0	245.0	2.6	6.01	0.16	15.3	15.0	14.4	15.8
38.6	240.8	3.2	6.24	0.16	13.1	14.6	14.3	15.7
37.2	236.7	3.8	6.28	0.16	16.2	12.1	17.2	16.1
35.9	232.7	4.6	6.35	0.15	18.2	12.2	18.1	16.1
34.6	229.6	5.6	6.47	0.15	17.9	12.1	15.7	15.8
33.3	228.7	6.8	6.47	0.13	16.9	11.9	12.7	16.8
32.0	228.3	8.3	6.20	0.12	15.9	11.8	11.2	16.6
30.7	226.3	10.0	5.75	0.11	14.5	10.6	11.3	14.9
29.4	222.4	12.1	5.32	0.09	13.7	10.3	12.3	14.6
28.2	218.4	14.7	5.07	0.09	14.9	10.4	13.8	14.8
27.0	215.9	17.8	4.90	0.08	16.7	11.4	14.8	15.8
25.7	214.8	21.5	4.67	0.07	15.8	12.0	12.8	16.2
24.5	213.6	26.1	4.29	0.06	9.5	11.4	6.3	15.4
at3 ss17		*Latitude: 46.5*		*Longitude: 51.2*			*Filter: 9*	
40.3	244.3	2.6	7.13	0.29	38.5	26.2	12.1	18.9
38.9	242.3	3.2	7.44	0.29	12.7	21.6	21.3	20.0
37.5	240.2	3.8	7.18	0.25	13.1	14.6	21.4	17.6
36.2	234.8	4.6	6.61	0.22	25.6	16.0	21.2	17.6
34.8	229.1	5.6	6.16	0.20	30.8	16.6	22.9	18.1
33.5	223.6	6.8	5.85	0.18	23.8	15.8	22.9	18.2
32.3	223.2	8.3	5.60	0.16	11.7	16.2	19.3	20.3
31.0	223.0	10.0	5.42	0.14	5.8	15.2	13.9	19.3
29.8	221.7	12.1	5.33	0.16	8.6	12.1	8.9	15.9
28.5	218.4	14.7	5.25	0.16	14.8	11.6	6.2	14.7
27.3	215.1	17.8	5.07	0.15	18.6	11.8	7.0	14.7
26.1	213.4	21.5	4.76	0.11	19.0	13.1	9.3	15.8
24.9	213.3	26.1	4.34	0.08	16.0	14.7	9.7	17.1
at3 ss19		*Latitude: 46.1*		*Longitude: 6.1*			*Filter:12*	
39.8	242.0	2.6	5.50	0.15	24.2	18.6	16.2	16.8
38.4	237.1	3.2	5.73	0.18	23.5	14.3	23.5	16.5
37.1	232.1	3.8	5.99	0.18	23.3	14.2	26.2	16.8
35.8	228.5	4.6	6.36	0.19	20.6	13.8	20.2	15.8
34.5	226.8	5.6	6.68	0.14	16.6	12.7	10.4	16.4
33.2	225.0	6.8	6.50	0.13	14.4	12.5	4.8	15.6
32.0	222.0	8.3	5.83	0.11	15.2	11.4	5.5	14.5
30.7	219.4	10.0	5.44	0.09	10.6	9.9	3.5	13.1
29.5	217.4	12.1	5.30	0.09	8.2	9.6	3.4	13.0
28.3	215.5	14.7	5.16	0.08	13.8	10.3	9.7	13.9
27.1	213.5	17.8	5.02	0.08	17.1	11.3	13.3	14.7
25.9	211.6	21.5	4.88	0.07	9.7	10.6	6.6	13.8
24.7	210.8	26.1	4.32	0.07	1.4	11.2	-0.9	13.9

Table B.2 continued. (See notes on page 135.)

Alt (km)	Temp (K)	Press (mb)	$^{48}O_3$ vmr	$^{48}O_3$ err	$^{668}O_3$ enr	$^{668}O_3$ enr err	$^{686}O_3$ enr	$^{686}O_3$ enr err
at3 ss22		*Latitude: 45.6*		*Longitude:298.4*			*Filter:12*	
39.6	231.0	2.6	6.76	0.18	13.2	13.2	13.6	15.2
38.3	228.7	3.2	7.21	0.18	11.5	11.6	8.4	13.6
37.0	227.2	3.8	7.26	0.17	14.6	11.8	8.4	13.7
35.7	224.9	4.6	7.06	0.15	19.5	10.5	13.5	13.3
34.4	221.6	5.6	6.90	0.14	22.3	10.2	17.8	13.5
33.2	218.3	6.8	6.93	0.13	20.0	10.0	16.1	13.3
32.0	216.2	8.3	7.00	0.13	15.9	9.8	11.7	13.2
30.7	214.8	10.0	6.99	0.12	13.9	9.6	9.1	13.2
29.5	213.7	12.1	6.87	0.12	15.6	9.6	10.5	13.2
28.3	212.8	14.7	6.59	0.12	17.6	10.5	12.6	13.5
27.1	212.1	17.8	6.13	0.11	14.6	10.2	10.5	13.1
25.9	211.8	21.5	5.47	0.09	6.9	10.4	4.4	13.0
24.7	212.3	26.1	4.67	0.07	1.0	10.7	-0.1	13.1
at3 ss23		*Latitude: 45.5*		*Longitude:275.7*			*Filter: 9*	
39.7	236.2	2.6	7.27	0.30	25.4	24.6	20.0	28.2
38.4	231.3	3.2	7.02	0.28	24.5	24.4	9.7	26.2
37.1	226.9	3.8	6.75	0.26	19.4	20.8	-4.2	23.4
35.8	223.6	4.6	6.41	0.24	13.9	17.0	-15.4	20.9
34.5	220.4	5.6	6.02	0.22	10.1	16.5	-18.1	20.5
33.3	217.7	6.8	5.70	0.17	8.8	12.0	-12.0	15.9
32.0	215.8	8.3	5.56	0.15	9.6	12.0	-4.8	17.0
30.8	213.8	10.0	5.58	0.13	11.8	12.1	-0.1	17.7
29.6	213.0	12.1	5.65	0.13	14.8	12.4	2.9	14.2
28.4	213.1	14.7	5.56	0.12	17.9	12.6	6.7	14.1
27.2	213.1	17.8	5.23	0.12	20.8	12.9	11.9	14.6
26.0	212.9	21.5	4.71	0.14	21.1	13.5	14.6	15.3
24.8	212.7	26.1	4.09	0.12	15.5	13.0	9.1	14.7

Alt (km)	Temp (K)	Press (mb)	$^{48}O_3$ vmr	$^{48}O_3$ err	$^{668}O_3$ enr	$^{668}O_3$ enr err	$^{686}O_3$ enr	$^{686}O_3$ enr err
at3 ss25		*Latitude: 45.2*		*Longitude:230.6*			*Filter:12*	
40.0	227.7	2.6	6.02	0.17	27.5	15.3	16.7	16.3
38.7	226.1	3.2	6.78	0.17	29.6	13.9	10.5	14.8
37.4	224.5	3.8	7.03	0.17	28.3	13.5	11.7	14.7
36.2	222.3	4.6	6.92	0.15	23.2	11.4	16.0	13.7
34.9	220.2	5.6	6.82	0.14	17.2	10.9	17.6	13.9
33.6	218.8	6.8	6.78	0.13	13.2	10.6	15.7	13.6
32.4	218.8	8.3	6.72	0.13	11.9	10.5	12.9	15.1
31.2	218.9	10.0	6.64	0.13	11.5	10.4	10.4	14.8
29.9	218.3	12.1	6.54	0.13	11.0	10.1	8.3	14.0
28.7	217.2	14.7	6.35	0.13	11.6	9.9	8.0	13.5
27.5	216.0	17.8	5.94	0.11	15.3	10.1	11.5	13.7
26.2	215.5	21.5	5.31	0.08	19.1	12.0	15.9	15.6
25.0	215.4	26.1	4.59	0.07	15.8	11.7	13.0	15.3
at3 ss28		*Latitude: 44.7*		*Longitude:162.9*			*Filter:12*	
40.3	232.9	2.6	5.90	0.17	17.2	14.5	5.1	17.3
38.9	231.7	3.2	6.08	0.16	17.1	14.5	4.3	17.2
37.6	230.5	3.8	6.22	0.16	20.3	12.4	12.7	15.8
36.3	229.4	4.6	6.37	0.15	21.9	12.1	19.8	16.3
35.0	228.5	5.6	6.50	0.15	20.7	11.9	19.9	16.1
33.7	228.0	6.8	6.54	0.13	19.2	11.8	16.8	16.7
32.4	227.4	8.3	6.45	0.12	18.2	11.7	14.5	16.8
31.1	226.0	10.0	6.28	0.12	16.8	11.3	13.6	16.3
29.9	223.7	12.1	6.09	0.12	15.7	10.5	14.0	15.4
28.6	221.5	14.7	5.85	0.12	16.5	10.5	16.2	15.4
27.4	219.8	17.8	5.54	0.09	17.5	11.2	17.7	16.3
26.1	218.6	21.5	5.12	0.09	13.3	10.8	12.7	15.7
24.9	217.5	26.1	4.59	0.07	3.6	11.1	1.0	15.1

Table B.2 continued. (See notes on page 135.)

Alt (km)	Temp (K)	Press (mb)	$^{48}O_3$ vmr	$^{48}O_3$ err	$^{668}O_3$ enr	$^{668}O_3$ enr err	$^{686}O_3$ enr	$^{686}O_3$ enr err
at3 ss29		*Latitude: 44.6*		*Longitude:140.3*			*Filter: 9*	
40.9	240.8	2.6	7.38	0.30	13.2	28.6	-19.9	26.5
39.5	240.4	3.2	7.17	0.30	13.7	18.2	-25.5	17.8
38.2	240.1	3.8	6.79	0.26	18.3	18.4	-22.2	18.0
36.8	239.8	4.6	6.57	0.24	26.4	19.4	-2.2	21.8
35.5	238.9	5.6	6.49	0.20	34.6	18.8	26.9	22.3
34.1	237.4	6.8	6.51	0.19	32.5	18.5	37.3	24.0
32.8	235.4	8.3	6.57	0.22	21.0	13.8	24.7	19.4
31.4	232.1	10.0	6.61	0.22	10.5	11.6	6.9	16.0
30.1	228.6	12.1	6.61	0.22	10.8	11.6	1.3	15.4
28.8	225.9	14.7	6.54	0.16	16.9	12.3	4.0	15.8
27.6	224.5	17.8	6.32	0.12	20.6	12.6	7.5	16.2
26.3	223.1	21.5	5.81	0.11	16.8	12.7	8.2	16.5
25.0	221.5	26.1	5.02	0.11	8.5	14.6	5.7	18.2
at3 ss31		*Latitude: 44.2*		*Longitude: 95.2*			*Filter:12*	
40.4	245.5	2.6	5.61	0.15	11.8	17.6	13.7	17.2
39.0	244.3	3.2	6.43	0.16	17.5	14.5	4.7	16.7
37.6	243.2	3.8	6.66	0.16	21.7	14.8	6.0	17.0
36.2	239.2	4.6	6.40	0.16	22.5	12.1	14.1	16.1
34.9	234.7	5.6	6.32	0.16	19.9	11.9	19.2	16.8
33.6	231.0	6.8	6.58	0.16	16.2	11.6	18.7	16.6
32.3	228.8	8.3	7.00	0.14	14.3	10.8	16.2	16.8
31.0	226.7	10.0	7.32	0.14	14.5	10.7	14.0	16.5
29.7	225.2	12.1	7.43	0.13	15.8	10.4	12.0	16.1
28.4	223.9	14.7	7.21	0.12	17.0	10.4	11.3	15.9
27.1	222.6	17.8	6.59	0.11	17.5	11.1	12.1	16.4
25.9	221.3	21.5	5.78	0.09	15.1	12.3	11.4	17.6
24.6	220.0	26.1	4.92	0.08	7.5	11.7	5.1	16.8

Alt (km)	Temp (K)	Press (mb)	$^{48}O_3$ vmr	$^{48}O_3$ err	$^{668}O_3$ enr	$^{668}O_3$ enr err	$^{686}O_3$ enr	$^{686}O_3$ enr err
at3 ss34		*Latitude: 43.6*		*Longitude: 4.9*			*Filter:12*	
40.0	242.6	2.6	6.46	0.18	20.7	14.8	9.2	16.5
38.6	240.5	3.2	6.81	0.17	20.9	14.6	7.8	16.3
37.3	235.8	3.8	6.71	0.18	18.5	11.8	13.1	14.9
35.9	229.8	4.6	6.55	0.17	15.2	11.5	16.4	15.3
34.7	224.9	5.6	6.43	0.16	12.8	11.3	15.2	15.1
33.4	223.3	6.8	6.32	0.14	12.5	11.1	12.6	15.8
32.1	222.2	8.3	6.26	0.14	13.2	11.1	11.4	15.7
30.9	220.4	10.0	6.29	0.12	14.0	10.6	11.4	15.0
29.6	218.1	12.1	6.27	0.11	14.6	10.3	11.6	14.6
28.4	215.9	14.7	6.06	0.10	15.4	10.3	11.2	14.4
27.2	214.3	17.8	5.64	0.09	14.5	11.1	9.4	14.6
26.0	213.0	21.5	5.09	0.08	9.8	10.7	5.1	14.2
24.8	212.0	26.1	4.46	0.07	2.1	11.4	-0.3	14.4
at3 ss35		*Latitude: 43.4*		*Longitude:342.4*			*Filter: 9*	
40.2	238.6	2.6	7.59	0.30	4.6	19.9	-0.6	21.1
38.8	237.0	3.2	7.74	0.30	-5.9	18.1	-6.9	20.0
37.5	235.4	3.8	7.65	0.28	-5.0	18.6	0.7	21.0
36.2	232.1	4.6	7.39	0.24	4.4	14.6	12.0	21.0
34.9	228.0	5.6	7.06	0.22	16.3	15.9	11.1	21.0
33.6	224.5	6.8	6.72	0.21	27.6	14.3	-2.6	17.9
32.3	223.3	8.3	6.44	0.19	31.4	14.4	-13.7	16.3
31.0	222.2	10.0	6.21	0.17	22.5	13.4	-9.5	17.2
29.8	220.9	12.1	5.96	0.15	5.9	13.5	5.0	17.5
28.5	219.3	14.7	5.60	0.14	-5.4	12.8	17.5	18.3
27.3	217.9	17.8	5.15	0.13	0.6	13.1	18.1	18.4
26.1	216.7	21.5	4.69	0.14	14.9	12.8	10.5	18.2
24.9	215.5	26.1	4.30	0.12	21.4	13.5	3.0	17.1

Table B.2 continued. (See notes on page 135.)

Alt (km)	Temp (K)	Press (mb)	$^{48}O_3$ vmr	$^{48}O_3$ err	$^{668}O_3$ enr	$^{668}O_3$ enr err	$^{686}O_3$ enr	$^{686}O_3$ enr err
at3 ss42	*Latitude: 40.5*		*Longitude: 26.7*		*Filter: 9*			
40.5	249.2	2.6	6.20	0.25	-5.2	24.3	23.6	27.8
39.1	245.6	3.2	6.66	0.26	1.1	25.4	24.1	27.5
37.7	242.3	3.8	7.32	0.26	13.6	20.6	16.2	26.1
36.3	239.4	4.6	7.41	0.25	18.1	19.7	10.9	25.1
35.0	235.9	5.6	6.72	0.24	9.4	16.7	10.9	23.1
33.7	231.3	6.8	6.03	0.23	-0.2	13.7	13.2	21.4
32.4	226.7	8.3	5.98	0.21	7.3	14.1	14.5	20.9
31.1	223.3	10.0	6.25	0.18	22.6	12.3	13.1	17.1
29.8	221.0	12.1	6.24	0.18	29.4	12.7	9.2	16.6
28.6	219.5	14.7	5.87	0.19	25.7	13.2	4.3	16.1
27.3	219.6	17.8	5.43	0.17	17.7	12.4	3.6	15.9
26.1	219.2	21.5	5.08	0.14	13.1	12.6	8.9	17.2
24.9	216.7	26.1	4.66	0.10	11.9	13.5	13.1	18.6
at3 ss44	*Latitude: 40.0*		*Longitude:341.7*		*Filter:12*			
40.2	245.6	2.6	5.22	0.16	41.5	17.8	42.9	20.9
38.8	240.9	3.2	6.47	0.18	25.6	15.6	26.3	18.3
37.5	236.7	3.8	7.54	0.18	9.8	11.2	11.1	15.2
36.1	232.8	4.6	7.93	0.17	5.1	10.7	5.3	14.4
34.8	229.5	5.6	7.80	0.16	8.9	10.6	6.5	14.7
33.5	227.3	6.8	7.44	0.15	14.7	10.8	9.9	15.1
32.3	225.5	8.3	7.06	0.13	15.4	10.7	10.9	15.1
31.0	223.4	10.0	6.65	0.12	13.0	10.2	10.1	15.1
29.7	221.3	12.1	6.15	0.10	11.6	10.1	9.4	15.1
28.5	219.7	14.7	5.61	0.09	13.0	11.0	10.0	16.0
27.2	218.4	17.8	5.15	0.08	16.6	11.4	12.4	16.3
26.0	216.8	21.5	4.79	0.09	18.1	12.8	13.3	17.4
24.8	214.8	26.1	4.43	0.09	12.6	13.5	7.7	17.6

Alt (km)	Temp (K)	Press (mb)	$^{48}O_3$ vmr	$^{48}O_3$ err	$^{668}O_3$ enr	$^{668}O_3$ enr err	$^{686}O_3$ enr	$^{686}O_3$ enr err
at3 ss47	*Latitude: 39.4*		*Longitude:274.0*		*Filter:12*			
39.7	241.8	2.6	6.45	0.18	22.6	17.7	15.3	16.7
38.4	238.8	3.2	6.68	0.17	22.3	14.3	19.3	17.3
37.0	235.7	3.8	6.80	0.17	21.1	14.1	17.7	17.1
35.7	231.8	4.6	6.97	0.16	18.6	13.0	10.7	16.2
34.4	227.0	5.6	7.04	0.15	15.5	12.4	5.7	15.5
33.1	222.1	6.8	6.86	0.14	13.1	11.9	7.6	15.4
31.9	217.9	8.3	6.51	0.12	12.0	11.5	12.1	15.5
30.6	213.9	10.0	6.10	0.11	12.2	11.5	14.0	15.8
29.4	211.5	12.1	5.75	0.10	13.4	11.0	12.0	15.1
28.2	209.5	14.7	5.54	0.09	14.3	11.0	9.1	14.7
27.1	208.7	17.8	5.36	0.09	14.4	11.7	8.0	15.1
25.9	209.5	21.5	5.03	0.10	13.9	12.5	8.7	15.8
24.7	210.0	26.1	4.43	0.07	13.4	13.4	10.4	16.2
at3 ss48	*Latitude: 39.1*		*Longitude:251.5*		*Filter: 9*			
39.9	242.4	2.6	6.31	0.26	3.0	36.4	13.6	34.4
38.5	237.7	3.2	6.63	0.27	5.8	30.7	1.9	32.3
37.2	233.6	3.8	6.59	0.26	18.5	29.9	-6.9	27.4
35.9	230.0	4.6	6.35	0.27	28.9	22.7	-10.0	20.9
34.6	226.4	5.6	6.07	0.25	26.0	22.1	-4.5	22.2
33.3	222.7	6.8	5.85	0.21	12.1	19.9	6.6	19.4
32.1	219.1	8.3	5.74	0.19	2.5	18.3	13.3	20.5
30.8	216.7	10.0	5.77	0.15	3.6	14.4	14.4	18.7
29.6	214.9	12.1	5.91	0.14	10.8	13.5	15.1	17.9
28.4	214.2	14.7	5.99	0.14	16.6	11.3	16.8	15.6
27.2	214.8	17.8	5.77	0.12	17.9	11.3	14.6	15.1
25.9	214.9	21.5	5.21	0.11	16.2	12.8	6.5	16.3
24.7	213.9	26.1	4.44	0.10	13.7	14.1	-2.9	17.0

Table B.2 continued. (See notes on page 135.)

Alt (km)	Temp (K)	Press (mb)	$^{48}O_3$ vmr	$^{48}O_3$ err	$^{668}O_3$ enr	$^{668}O_3$ enr err	$^{686}O_3$ enr	$^{686}O_3$ enr err
at3 ss50		*Latitude: 38.7*		*Longitude:206.4*		*Filter:12*		
39.9	237.8	2.6	5.53	0.15	31.4	17.1	22.3	17.4
38.6	233.7	3.2	6.47	0.19	15.2	14.3	13.0	15.8
37.3	230.0	3.8	6.87	0.18	10.3	13.1	13.1	15.6
36.0	226.7	4.6	6.77	0.15	13.7	12.2	18.2	15.8
34.7	224.2	5.6	6.65	0.14	16.4	12.4	18.9	15.9
33.4	223.5	6.8	6.71	0.13	14.8	11.6	13.2	16.0
32.1	223.1	8.3	6.74	0.13	13.1	11.4	9.0	15.5
30.9	221.8	10.0	6.64	0.13	13.5	11.3	9.3	15.6
29.6	219.9	12.1	6.50	0.12	14.1	11.2	11.2	15.9
28.4	218.5	14.7	6.33	0.12	14.2	10.2	12.1	14.5
27.2	217.7	17.8	5.98	0.11	16.0	10.3	13.5	14.5
25.9	216.1	21.5	5.39	0.09	17.5	12.5	14.2	16.8
24.7	213.4	26.1	4.62	0.07	12.6	13.5	8.6	17.6
at3 ss53		*Latitude: 37.9*		*Longitude:138.9*		*Filter:12*		
40.3	236.1	2.6	6.28	0.17	16.0	13.9	7.8	14.0
39.0	234.0	3.2	5.91	0.16	18.5	14.3	13.0	15.8
37.7	234.1	3.8	5.82	0.16	22.1	14.5	19.4	17.6
36.3	235.1	4.6	6.01	0.15	23.7	14.3	19.1	17.5
35.0	235.6	5.6	6.36	0.13	21.2	13.0	13.9	17.3
33.7	235.9	6.8	6.64	0.13	16.0	12.4	10.5	16.8
32.3	232.9	8.3	6.71	0.14	11.4	11.4	11.2	16.5
31.0	228.6	10.0	6.62	0.13	10.5	11.3	13.8	16.9
29.7	224.8	12.1	6.47	0.12	12.1	11.5	15.0	17.6
28.5	221.4	14.7	6.25	0.11	13.0	11.6	12.4	17.4
27.2	219.4	17.8	5.90	0.09	13.1	10.8	8.5	15.4
26.0	219.1	21.5	5.36	0.08	15.3	11.0	8.1	15.3
24.8	217.0	26.1	4.63	0.08	17.8	14.5	10.3	19.2

Alt (km)	Temp (K)	Press (mb)	$^{48}O_3$ vmr	$^{48}O_3$ err	$^{668}O_3$ enr	$^{668}O_3$ enr err	$^{686}O_3$ enr	$^{686}O_3$ enr err
at3 ss54		*Latitude: 37.5*		*Longitude:116.4*		*Filter: 9*		
40.8	245.7	2.6	7.05	0.30	15.3	33.3	-20.4	22.2
39.4	244.7	3.2	6.74	0.27	8.3	24.7	-1.1	22.1
38.0	244.1	3.8	6.46	0.24	7.2	24.6	11.8	24.8
36.6	243.0	4.6	6.48	0.25	11.9	17.6	10.4	21.9
35.3	240.9	5.6	6.82	0.25	18.3	17.3	5.6	20.7
33.9	238.0	6.8	7.26	0.25	22.6	17.2	7.1	19.5
32.6	233.4	8.3	7.54	0.23	23.3	17.0	11.5	19.2
31.2	229.2	10.0	7.52	0.21	19.3	16.1	13.2	19.8
30.0	227.0	12.1	7.35	0.20	13.5	14.6	10.5	20.8
28.7	224.9	14.7	7.09	0.26	10.1	12.9	5.6	17.9
27.4	223.3	17.8	6.58	0.25	12.7	12.9	3.9	17.2
26.1	221.1	21.5	5.74	0.20	18.6	14.7	6.8	19.0
24.9	217.7	26.1	4.80	0.14	17.8	17.0	8.5	22.1
at3 ss56		*Latitude: 37.0*		*Longitude: 71.3*		*Filter:12*		
40.5	245.4	2.6	5.93	0.16	7.1	14.5	12.7	18.5
39.2	243.1	3.2	6.21	0.16	24.2	16.2	9.3	17.9
37.8	241.4	3.8	6.29	0.16	28.4	15.4	7.9	17.6
36.4	240.1	4.6	6.34	0.16	24.4	14.5	8.9	17.7
35.1	238.0	5.6	6.52	0.15	18.9	13.4	11.8	17.9
33.7	234.9	6.8	6.75	0.15	15.4	12.4	14.7	18.0
32.4	231.7	8.3	6.94	0.15	14.6	12.2	16.7	18.3
31.1	228.6	10.0	7.08	0.16	15.5	11.5	17.6	18.1
29.8	226.1	12.1	7.20	0.16	15.9	11.5	17.0	18.0
28.5	224.9	14.7	7.13	0.13	15.8	13.0	14.8	20.8
27.2	223.4	17.8	6.55	0.11	15.6	12.9	11.8	19.8
26.0	218.9	21.5	5.64	0.09	15.1	13.0	9.9	18.2
24.8	214.8	26.1	4.69	0.07	13.6	13.8	10.7	18.8

Table B.2 continued. (See notes on page 135.)

Alt (km)	Temp (K)	Press (mb)	$^{48}O_3$ vmr	$^{48}O_3$ err	$^{668}O_3$ enr	$^{668}O_3$ enr err	$^{686}O_3$ enr	$^{686}O_3$ enr err
at3 ss59		*Latitude: 36.1*		*Longitude: 3.8*			*Filter:12*	
40.5	250.9	2.6	5.62	0.15	7.9	18.7	9.4	20.1
39.1	246.3	3.2	5.82	0.15	14.0	14.6	17.5	18.5
37.7	242.3	3.8	6.31	0.15	22.3	15.5	22.3	19.1
36.3	240.4	4.6	6.93	0.16	26.5	15.3	22.1	20.9
35.0	237.7	5.6	7.13	0.15	25.7	13.7	19.1	19.1
33.6	231.9	6.8	7.03	0.14	21.7	12.1	15.2	17.5
32.3	226.9	8.3	6.96	0.13	17.1	11.9	12.7	17.7
31.0	225.2	10.0	6.78	0.13	14.5	13.0	12.7	19.9
29.8	222.8	12.1	6.34	0.11	14.3	11.9	14.1	18.3
28.5	218.7	14.7	5.85	0.10	15.7	11.6	14.5	17.6
27.3	215.9	17.8	5.54	0.09	16.7	11.4	12.6	16.4
26.1	214.7	21.5	5.22	0.08	16.0	11.4	10.7	16.2
24.9	214.2	26.1	4.70	0.08	13.4	15.1	9.7	20.7
at3 ss60		*Latitude: 35.8*		*Longitude:341.3*			*Filter: 9*	
40.6	254.9	2.6	5.72	0.24	37.9	47.5	42.8	37.1
39.1	248.7	3.2	6.99	0.28	23.3	28.3	10.6	28.5
37.7	241.8	3.8	7.49	0.28	3.5	24.1	-2.7	25.5
36.4	236.7	4.6	7.28	0.30	-7.5	17.1	4.2	22.2
35.1	233.6	5.6	7.29	0.29	0.4	18.4	16.1	24.3
33.7	230.7	6.8	7.78	0.25	17.4	18.0	19.4	24.4
32.4	227.9	8.3	8.24	0.23	25.5	17.8	14.8	23.0
31.1	225.9	10.0	8.20	0.33	19.9	14.1	9.9	19.7
29.9	224.3	12.1	7.81	0.31	11.7	12.9	9.6	19.6
28.6	222.1	14.7	7.27	0.19	7.8	12.1	11.5	24.0
27.4	220.0	17.8	6.63	0.16	8.5	12.7	7.9	23.8
26.1	219.6	21.5	5.81	0.18	11.2	16.5	-1.0	23.0
24.9	219.6	26.1	4.85	0.12	13.7	18.1	-7.7	22.3

Alt (km)	Temp (K)	Press (mb)	$^{48}O_3$ vmr	$^{48}O_3$ err	$^{668}O_3$ enr	$^{668}O_3$ enr err	$^{686}O_3$ enr	$^{686}O_3$ enr err
at3 ss65		*Latitude: 34.2*		*Longitude:228.7*			*Filter:12*	
40.0	238.5	2.6	5.90	0.16	16.1	17.3	17.0	17.6
38.7	236.2	3.2	6.69	0.17	19.3	16.1	18.6	17.6
37.3	233.1	3.8	6.96	0.18	15.0	12.5	18.9	15.8
36.0	229.2	4.6	6.90	0.17	12.5	12.2	18.1	15.7
34.7	225.5	5.6	6.87	0.16	16.1	12.1	16.9	16.6
33.5	222.3	6.8	7.04	0.16	19.7	12.3	15.0	16.7
32.2	220.9	8.3	7.32	0.15	17.4	12.2	12.8	16.8
31.0	220.6	10.0	7.43	0.14	13.5	12.3	11.8	17.8
29.7	219.7	12.1	7.19	0.14	11.9	11.0	12.2	16.2
28.5	218.4	14.7	6.62	0.12	13.2	10.9	13.2	16.0
27.2	217.2	17.8	5.89	0.11	15.2	12.1	12.8	17.3
26.0	216.1	21.5	5.15	0.09	16.1	15.1	11.1	21.2
24.8	214.8	26.1	4.43	0.08	14.9	16.5	8.8	21.8
at3 ss66		*Latitude: 34.0*		*Longitude:206.2*			*Filter: 9*	
40.1	246.2	2.6	6.91	0.29	31.7	30.4	28.2	30.7
38.8	241.7	3.2	7.11	0.29	9.8	26.0	33.8	29.3
37.4	236.9	3.8	7.04	0.27	-6.7	22.5	28.5	27.6
36.1	232.3	4.6	6.97	0.25	6.3	21.0	15.9	26.3
34.8	228.2	5.6	7.04	0.26	23.6	18.3	2.1	24.5
33.5	225.7	6.8	7.15	0.24	24.5	16.7	-5.9	17.9
32.2	224.8	8.3	7.05	0.22	16.0	15.6	-3.6	18.2
30.9	223.7	10.0	6.72	0.19	13.4	15.3	5.3	18.8
29.6	222.1	12.1	6.33	0.17	18.2	16.0	15.0	19.7
28.4	220.2	14.7	6.05	0.16	22.8	14.2	19.5	18.6
27.2	218.2	17.8	5.77	0.13	21.3	13.8	18.8	18.5
25.9	216.4	21.5	5.30	0.10	17.6	13.3	16.4	18.2
24.7	214.5	26.1	4.58	0.08	15.6	13.2	12.3	17.7

Table B.2 continued. (See notes on page 135.)

Alt (km)	Temp (K)	Press (mb)	$^{48}O_3$ vmr	$^{48}O_3$ err	$^{668}O_3$ enr	$^{668}O_3$ enr err	$^{686}O_3$ enr	$^{686}O_3$ enr err
at3 ss68		*Latitude: 33.3*		*Longitude:161.2*			*Filter:12*	
40.0	241.2	2.6	6.84	0.19	3.1	14.8	7.1	15.7
38.7	237.8	3.2	6.97	0.20	10.5	13.4	9.5	15.8
37.3	233.7	3.8	6.96	0.19	20.9	14.1	15.7	16.5
36.0	230.1	4.6	7.02	0.18	24.0	14.1	19.4	17.5
34.7	227.4	5.6	7.19	0.17	21.0	13.4	18.6	17.8
33.4	225.5	6.8	7.39	0.15	16.8	11.1	15.2	16.2
32.1	224.7	8.3	7.35	0.14	14.1	10.8	13.0	15.8
30.9	223.7	10.0	7.01	0.13	13.0	11.7	12.7	17.3
29.6	222.6	12.1	6.53	0.12	13.0	12.2	12.5	18.1
28.4	220.5	14.7	6.09	0.13	13.8	11.5	11.7	16.7
27.1	217.8	17.8	5.66	0.12	14.8	11.6	12.0	16.8
25.9	215.7	21.5	5.14	0.10	15.5	14.0	13.9	19.8
24.7	213.7	26.1	4.45	0.08	15.4	15.6	15.1	21.9
at3 ss71		*Latitude: 31.8*		*Longitude: 71.3*			*Filter:12*	
40.6	245.3	2.6	5.15	0.14	45.1	21.8	22.5	19.7
39.2	243.8	3.2	6.00	0.16	26.9	19.5	10.5	20.4
37.9	242.3	3.8	6.39	0.18	16.9	16.1	7.0	18.4
36.5	240.4	4.6	6.39	0.19	15.8	14.9	12.2	18.4
35.1	238.7	5.6	6.58	0.17	16.6	14.7	16.5	19.8
33.8	237.0	6.8	7.28	0.16	15.7	14.2	15.5	20.7
32.4	235.2	8.3	8.05	0.16	14.4	12.4	12.8	19.2
31.1	232.6	10.0	8.09	0.16	13.6	11.7	12.1	18.3
29.8	227.2	12.1	7.53	0.15	14.1	10.8	13.1	17.4
28.5	222.3	14.7	6.93	0.13	15.6	11.0	13.7	17.6
27.3	220.5	17.8	6.42	0.11	16.4	14.4	12.2	22.1
26.0	218.6	21.5	5.76	0.10	15.6	15.1	10.6	22.3
24.8	216.4	26.1	4.88	0.09	14.1	16.0	10.6	22.9

Alt (km)	Temp (K)	Press (mb)	$^{48}O_3$ vmr	$^{48}O_3$ err	$^{668}O_3$ enr	$^{668}O_3$ enr err	$^{686}O_3$ enr	$^{686}O_3$ enr err
at3 ss72		*Latitude: 31.5*		*Longitude: 48.8*			*Filter: 9*	
40.8	252.1	2.6	6.41	0.27	6.4	31.8	11.1	30.3
39.4	244.2	3.2	6.82	0.28	-13.4	24.9	14.6	28.6
38.0	239.2	3.8	7.10	0.26	1.4	20.3	12.4	24.9
36.7	238.2	4.6	7.09	0.24	20.4	23.6	9.1	24.2
35.3	236.9	5.6	7.08	0.23	28.1	19.9	10.2	22.7
34.0	235.2	6.8	7.56	0.23	23.2	17.1	14.4	22.7
32.7	232.8	8.3	8.23	0.22	15.1	14.2	12.7	21.5
31.4	230.4	10.0	8.54	0.26	10.7	12.1	4.6	17.9
30.1	229.0	12.1	8.34	0.24	11.6	12.2	-0.2	17.1
28.8	227.4	14.7	7.79	0.23	13.7	14.4	3.4	19.6
27.5	225.6	17.8	6.92	0.20	12.3	14.9	11.8	21.8
26.2	222.0	21.5	5.86	0.15	9.4	15.0	14.2	22.2
25.0	217.9	26.1	4.85	0.11	10.5	16.2	6.2	22.9
at3 ss74		*Latitude: 31.3*		*Longitude: 3.6*			*Filter:12*	
40.6	255.6	2.6	5.01	0.14	11.6	19.8	13.8	22.4
39.2	251.1	3.2	5.67	0.15	22.4	18.6	17.1	21.2
37.8	243.9	3.8	6.00	0.17	25.0	15.2	24.8	19.5
36.4	238.5	4.6	6.16	0.16	22.6	14.9	29.1	20.2
35.0	236.0	5.6	6.85	0.17	17.4	13.7	23.0	20.3
33.7	234.1	6.8	7.88	0.17	13.4	12.6	14.5	19.5
32.4	231.9	8.3	8.14	0.16	12.6	12.0	12.4	18.8
31.1	226.7	10.0	7.46	0.17	14.3	10.6	15.8	17.1
29.8	222.2	12.1	6.95	0.16	15.7	10.7	16.2	17.2
28.6	220.1	14.7	6.91	0.13	15.4	13.7	11.1	21.6
27.3	218.7	17.8	6.62	0.12	14.4	14.0	7.0	21.2
26.1	217.3	21.5	5.79	0.10	13.5	14.9	7.3	21.6
24.9	215.8	26.1	4.75	0.08	11.9	16.9	9.3	23.8

Table B.2 continued. (See notes on page 135.)

Alt (km)	Temp (K)	Press (mb)	$^{48}O_3$ vmr	$^{48}O_3$ err	$^{668}O_3$ enr	$^{668}O_3$ enr err	$^{686}O_3$ enr	$^{686}O_3$ enr err
at3 ss78		*Latitude: 26.4*		*Longitude:139.0*		*Filter: 9*		
40.4	245.9	2.6	7.23	0.30	42.8	48.1	7.7	34.3
39.0	243.1	3.2	7.75	0.33	19.9	34.0	31.8	33.9
37.7	240.2	3.8	7.54	0.29	-3.5	29.0	32.5	32.1
36.3	235.7	4.6	6.97	0.26	2.6	28.8	13.0	28.0
35.0	233.2	5.6	6.52	0.32	22.8	24.0	-5.1	27.5
33.7	231.6	6.8	6.45	0.25	21.4	20.6	-17.6	20.2
32.3	230.7	8.3	7.00	0.24	7.4	17.1	-12.6	19.7
31.0	229.9	10.0	7.76	0.22	9.6	14.1	4.4	19.1
29.7	228.5	12.1	8.00	0.26	20.9	15.5	14.2	20.8
28.4	226.1	14.7	7.47	0.24	27.9	16.4	14.1	20.9
27.2	221.6	17.8	6.47	0.17	24.4	17.7	12.7	22.7
25.9	218.1	21.5	5.43	0.18	15.4	15.2	12.9	20.5
24.7	215.9	26.1	4.44	0.10	6.5	18.0	8.6	25.7
at3 ss80		*Latitude: 25.5*		*Longitude: 94.1*		*Filter:12*		
40.7	252.3	2.6	5.60	0.16	21.9	20.5	13.4	21.3
39.3	250.9	3.2	6.00	0.16	20.7	18.7	17.0	21.5
37.8	248.4	3.8	6.36	0.17	17.1	16.8	18.0	21.1
36.4	245.7	4.6	6.57	0.15	16.2	14.8	15.6	20.7
35.0	242.5	5.6	6.76	0.15	17.4	14.3	13.2	19.9
33.7	238.1	6.8	7.08	0.14	16.3	13.3	12.1	19.3
32.3	233.6	8.3	7.43	0.16	13.4	12.7	11.0	19.8
31.0	229.4	10.0	7.53	0.15	13.2	12.4	9.6	19.4
29.7	225.6	12.1	7.35	0.14	15.5	12.5	9.2	19.2
28.5	222.7	14.7	7.04	0.13	16.8	13.7	10.2	21.0
27.2	220.7	17.8	6.59	0.12	15.7	13.2	11.5	20.0
26.0	218.9	21.5	5.90	0.10	14.2	12.1	11.5	17.1
24.7	217.1	26.1	4.92	0.08	12.3	11.9	9.0	16.8

Alt (km)	Temp (K)	Press (mb)	$^{48}O_3$ vmr	$^{48}O_3$ err	$^{668}O_3$ enr	$^{668}O_3$ enr err	$^{686}O_3$ enr	$^{686}O_3$ enr err
at3 ss83		*Latitude: 24.2*		*Longitude: 26.7*		*Filter:12*		
40.7	252.4	2.6	6.03	0.17	21.4	20.6	14.8	22.9
39.3	248.2	3.2	6.16	0.16	14.4	18.1	3.9	20.6
37.9	246.7	3.8	6.18	0.18	13.2	16.1	6.0	19.5
36.5	245.0	4.6	6.58	0.16	18.3	16.8	12.2	20.7
35.1	241.4	5.6	7.40	0.16	19.9	17.3	13.7	23.8
33.7	237.4	6.8	8.10	0.16	16.9	13.1	13.4	19.4
32.4	233.4	8.3	8.36	0.20	13.9	12.9	13.2	19.9
31.1	229.5	10.0	8.28	0.18	13.3	12.7	13.1	20.1
29.8	226.2	12.1	8.10	0.15	14.1	12.6	13.2	20.4
28.5	223.7	14.7	7.80	0.16	14.4	14.2	13.0	23.1
27.3	222.2	17.8	7.12	0.14	13.0	15.4	11.2	24.4
26.0	220.0	21.5	6.03	0.12	11.2	18.2	8.9	27.2
24.8	215.7	26.1	4.76	0.09	9.6	16.7	6.1	24.0
at3 ss84		*Latitude: 24.0*		*Longitude: 4.1*		*Filter: 9*		
40.8	257.1	2.6	5.84	0.24	52.7	53.3	7.1	36.6
39.4	253.2	3.2	6.24	0.26	49.9	46.6	14.8	34.6
37.9	247.6	3.8	6.64	0.26	32.9	35.1	10.9	31.3
36.5	242.7	4.6	6.81	0.24	12.5	25.8	0.7	27.1
35.2	239.2	5.6	6.97	0.23	-9.1	19.3	8.4	23.5
33.8	236.7	6.8	7.33	0.24	-8.9	15.2	16.9	24.1
32.5	234.4	8.3	7.84	0.23	10.7	16.1	15.8	23.2
31.2	230.4	10.0	8.21	0.21	22.1	14.9	14.4	21.9
29.9	226.0	12.1	8.26	0.26	17.3	14.1	14.9	21.3
28.6	223.5	14.7	7.99	0.28	8.2	12.9	11.6	20.3
27.3	222.2	17.8	7.25	0.18	9.6	13.6	5.4	21.2
26.1	220.9	21.5	6.00	0.16	19.5	16.5	4.5	22.6
24.8	218.7	26.1	4.59	0.14	22.5	19.4	11.0	26.3

Table B.2 continued. (See notes on page 135.)

Alt (km)	Temp (K)	Press (mb)	$^{48}O_3$ vmr	$^{48}O_3$ err	$^{668}O_3$ enr	$^{668}O_3$ enr err	$^{686}O_3$ enr	$^{686}O_3$ enr err
at3 ss86	*Latitude: 22.8*	*Longitude:319.3*	*Filter:12*					
40.8	257.8	2.6	4.94	0.14	42.7	28.6	21.4	27.5
39.4	254.1	3.2	5.29	0.14	36.6	23.4	27.3	25.5
37.9	249.2	3.8	5.62	0.15	23.3	16.2	25.3	21.6
36.5	244.8	4.6	5.99	0.16	21.5	12.4	18.6	18.1
35.1	241.7	5.6	6.47	0.17	21.0	12.2	15.8	17.5
33.8	238.9	6.8	7.20	0.18	17.8	14.0	15.1	21.9
32.4	236.5	8.3	8.16	0.20	14.8	14.5	11.9	23.0
31.1	233.6	10.0	8.81	0.17	13.2	13.9	8.9	22.4
29.8	229.2	12.1	8.68	0.15	13.6	11.4	8.7	18.5
28.5	225.4	14.7	7.93	0.14	15.3	12.7	9.8	20.1
27.2	222.1	17.8	6.96	0.13	15.6	13.7	10.5	21.3
26.0	218.7	21.5	5.92	0.11	13.8	15.8	11.0	23.1
24.7	217.0	26.1	4.77	0.08	11.6	14.9	11.0	21.2
at3 ss89	*Latitude: 20.9*	*Longitude:252.0*	*Filter:12*					
40.6	254.3	2.6	5.20	0.15	15.3	26.1	4.2	24.6
39.2	251.7	3.2	5.47	0.14	15.3	20.8	7.0	22.7
37.8	247.4	3.8	6.00	0.18	19.3	19.4	14.0	23.6
36.4	243.7	4.6	6.94	0.21	19.1	18.5	18.3	24.4
35.0	241.2	5.6	7.87	0.18	16.5	15.5	16.5	22.9
33.6	237.1	6.8	8.39	0.18	15.9	13.1	13.4	19.9
32.3	234.3	8.3	8.65	0.17	16.4	13.6	10.9	21.3
31.0	232.5	10.0	8.82	0.18	15.4	15.0	9.0	23.7
29.7	229.7	12.1	8.62	0.17	14.2	12.8	8.6	20.3
28.4	225.6	14.7	7.87	0.15	14.3	12.4	10.7	19.9
27.1	221.0	17.8	6.85	0.13	14.0	15.3	13.3	24.2
25.9	217.9	21.5	5.77	0.12	12.8	20.2	13.1	31.2
24.7	214.5	26.1	4.63	0.09	12.5	20.9	10.2	30.3

Alt (km)	Temp (K)	Press (mb)	$^{48}O_3$ vmr	$^{48}O_3$ err	$^{668}O_3$ enr	$^{668}O_3$ enr err	$^{686}O_3$ enr	$^{686}O_3$ enr err
at3 ss90	*Latitude: 20.0*	*Longitude:229.7*	*Filter: 9*					
40.8	257.0	2.6	6.07	0.26	43.9	37.2	27.0	37.8
39.4	254.8	3.2	6.21	0.25	59.2	31.0	-1.5	37.8
37.9	250.4	3.8	7.04	0.26	32.7	25.8	-42.0	27.3
36.5	243.5	4.6	7.95	0.41	2.2	39.1	-52.1	26.3
35.1	238.6	5.6	8.05	0.30	-0.1	18.3	-23.4	22.9
33.8	235.6	6.8	7.86	0.26	14.6	19.2	12.7	26.7
32.5	233.2	8.3	7.89	0.23	23.1	19.8	25.7	27.1
31.2	231.4	10.0	8.18	0.28	17.3	17.5	15.2	24.3
29.8	229.2	12.1	8.40	0.25	13.1	14.4	7.9	20.4
28.6	226.5	14.7	8.18	0.28	15.6	16.5	6.4	24.4
27.3	223.5	17.8	7.25	0.16	20.9	18.8	3.9	21.0
26.0	219.8	21.5	5.84	0.16	22.2	24.3	2.3	23.2
24.8	215.1	26.1	4.38	0.12	16.8	21.8	8.3	25.7
at3 ss92	*Latitude: 19.5*	*Longitude:184.6*	*Filter:12*					
40.5	252.9	2.6	6.01	0.17	20.3	22.3	7.5	22.4
39.0	248.3	3.2	6.50	0.18	24.3	19.5	14.5	21.5
37.6	243.4	3.8	7.00	0.18	21.1	16.9	16.9	21.5
36.3	238.5	4.6	7.52	0.18	15.2	15.7	14.8	21.2
34.9	235.4	5.6	7.90	0.17	13.3	15.1	13.9	21.2
33.6	234.1	6.8	8.06	0.17	14.5	14.1	14.2	21.6
32.3	233.9	8.3	8.28	0.16	16.6	14.5	13.6	22.2
30.9	232.7	10.0	8.61	0.16	16.6	13.4	12.2	21.0
29.6	229.0	12.1	8.60	0.15	14.6	11.8	11.3	18.9
28.3	224.1	14.7	7.88	0.14	12.9	13.3	11.3	21.1
27.1	219.2	17.8	6.77	0.12	11.9	14.5	10.4	22.6
25.9	215.7	21.5	5.65	0.10	11.0	15.5	8.0	22.6
24.6	214.0	26.1	4.57	0.08	11.7	14.9	5.8	20.8

Table B.2 continued. (See notes on page 135.)

Alt (km)	Temp (K)	Press (mb)	$^{48}O_3$ vmr	$^{48}O_3$ err	$^{668}O_3$ enr	$^{668}O_3$ enr err	$^{686}O_3$ enr	$^{686}O_3$ enr err
at3 ss95		*Latitude: 17.0*		*Longitude:117.5*			*Filter:12*	
40.4	248.8	2.6	6.07	0.18	11.3	26.1	9.1	28.0
39.0	246.4	3.2	6.71	0.17	23.3	17.9	15.3	20.7
37.6	242.7	3.8	6.91	0.18	24.3	18.5	19.9	22.9
36.3	238.9	4.6	6.95	0.17	19.1	17.9	18.1	23.4
34.9	236.6	5.6	7.08	0.16	17.2	18.4	13.5	24.8
33.6	234.4	6.8	7.48	0.17	16.6	17.9	12.2	26.0
32.3	231.5	8.3	8.11	0.21	15.5	13.9	12.2	21.4
31.0	229.1	10.0	8.38	0.20	16.0	15.5	12.1	24.3
29.7	226.8	12.1	8.11	0.18	17.0	14.0	13.8	22.4
28.4	225.2	14.7	7.71	0.17	15.7	13.9	15.1	22.7
27.1	223.9	17.8	7.24	0.15	12.9	18.5	12.9	29.6
25.9	219.9	21.5	6.30	0.12	11.6	17.1	9.9	25.7
24.6	214.1	26.1	4.91	0.09	12.2	16.7	8.6	23.5
at3 ss96		*Latitude: 16.2*		*Longitude: 95.1*			*Filter: 9*	
40.7	253.3	2.6	5.86	0.26	4.9	49.8	8.6	36.0
39.3	252.0	3.2	6.45	0.28	38.1	52.5	31.5	39.5
37.9	247.8	3.8	7.23	0.28	36.6	28.5	8.4	32.3
36.5	244.1	4.6	7.76	0.27	36.6	23.5	-4.2	28.1
35.1	241.4	5.6	7.94	0.30	42.9	24.5	-3.6	26.2
33.8	237.6	6.8	8.04	0.35	32.5	26.4	-1.6	31.5
32.4	233.5	8.3	8.10	0.23	15.6	16.3	5.6	21.4
31.1	230.5	10.0	8.21	0.29	10.2	17.6	12.6	25.8
29.8	228.0	12.1	8.19	0.28	12.8	17.0	13.5	25.3
28.5	228.0	14.7	7.77	0.21	16.7	15.6	10.8	22.4
27.2	224.6	17.8	6.98	0.32	17.1	22.3	6.0	32.4
26.0	221.1	21.5	5.99	0.15	12.4	18.9	1.7	26.4
24.7	217.9	26.1	4.79	0.10	5.7	16.9	0.9	22.9
at3 ss98		*Latitude: 15.0*		*Longitude: 50.2*			*Filter:12*	
40.6	252.9	2.6	6.11	0.18	25.1	31.9	6.2	21.9
39.1	250.4	3.2	6.54	0.18	24.2	20.9	7.8	23.1
37.7	247.6	3.8	6.55	0.17	24.2	20.6	11.6	25.2
36.3	244.8	4.6	6.55	0.16	24.0	20.5	15.8	26.7
34.9	241.1	5.6	7.08	0.16	20.6	17.0	17.6	23.9
33.6	233.8	6.8	7.93	0.17	15.8	14.2	14.7	21.2
32.3	231.9	8.3	8.40	0.18	14.3	16.3	11.0	25.7
31.0	228.7	10.0	8.35	0.16	15.7	13.3	10.5	21.4
29.7	227.2	12.1	8.12	0.17	17.0	17.0	12.8	27.0
28.4	225.9	14.7	7.87	0.15	16.6	14.3	15.0	22.8
27.1	224.1	17.8	7.38	0.13	15.0	13.1	13.8	20.8
25.8	222.1	21.5	6.41	0.13	13.1	18.8	10.8	28.6
24.6	215.0	26.1	5.00	0.10	11.9	19.9	9.5	29.2
at3 ss102		*Latitude: 11.6*		*Longitude:298.1*			*Filter: 9*	
40.8	258.5	2.6	6.32	0.28	16.8	38.4	-6.1	39.0
39.3	255.0	3.2	7.18	0.31	30.0	52.1	-18.9	35.7
37.9	248.6	3.8	7.88	0.30	2.4	28.5	-18.0	28.0
36.5	242.6	4.6	8.22	0.28	-9.2	18.8	-5.0	26.2
35.1	240.1	5.6	8.47	0.30	9.8	24.0	5.0	27.6
33.8	238.3	6.8	8.63	0.34	22.6	19.6	10.8	23.0
32.4	236.8	8.3	8.58	0.32	22.5	16.7	14.0	23.0
31.1	233.9	10.0	8.49	0.26	18.7	18.7	9.7	27.8
29.8	230.5	12.1	8.38	0.23	14.3	14.7	6.0	22.7
28.5	226.8	14.7	8.10	0.23	11.1	18.3	9.8	28.4
27.2	224.2	17.8	7.38	0.24	11.3	15.8	13.3	24.1
25.9	221.6	21.5	6.23	0.19	11.8	21.9	9.8	31.6
24.7	217.2	26.1	4.96	0.13	11.3	24.2	3.0	33.9

Table B.2 continued. (See notes on page 135.)

Alt (km)	Temp (K)	Press (mb)	$^{48}O_3$ vmr	$^{48}O_3$ err	$^{668}O_3$ enr	$^{668}O_3$ enr err	$^{686}O_3$ enr	$^{686}O_3$ enr err
at3 ss104		*Latitude: 10.0*		*Longitude:253.3*			*Filter:12*	
40.6	249.6	2.6	5.29	0.16	14.5	24.4	16.5	25.4
39.2	247.7	3.2	6.04	0.18	17.9	25.1	16.4	27.0
37.8	246.5	3.8	7.05	0.22	18.7	22.6	14.9	27.8
36.4	243.4	4.6	7.71	0.22	19.2	15.9	13.9	21.9
35.1	238.5	5.6	8.08	0.21	19.9	16.4	14.8	23.4
33.7	235.6	6.8	8.68	0.20	19.1	14.4	15.1	21.9
32.4	234.4	8.3	9.37	0.21	16.8	14.0	13.7	22.0
31.1	233.3	10.0	9.53	0.21	15.0	16.3	11.7	26.7
29.7	229.8	12.1	9.16	0.17	14.1	12.8	10.1	21.3
28.4	227.2	14.7	8.51	0.15	13.3	12.6	10.0	21.1
27.2	225.1	17.8	7.58	0.17	12.4	17.0	12.3	27.8
25.9	220.1	21.5	6.39	0.16	12.4	15.7	14.9	25.2
24.7	216.2	26.1	5.08	0.13	13.1	26.6	15.2	41.7

Alt (km)	Temp (K)	Press (mb)	$^{48}O_3$ vmr	$^{48}O_3$ err	$^{668}O_3$ enr	$^{668}O_3$ enr err	$^{686}O_3$ enr	$^{686}O_3$ enr err
at3 ss107		*Latitude: 3.4*		*Longitude:187.4*			*Filter:12*	
40.6	253.0	2.6	6.20	0.18	18.9	29.1	13.0	28.8
39.2	248.8	3.2	6.54	0.17	13.6	19.5	17.2	22.2
37.8	244.0	3.8	6.67	0.17	13.6	18.5	17.5	23.2
36.4	240.7	4.6	7.12	0.17	14.5	18.8	16.3	24.5
35.0	238.1	5.6	7.71	0.22	15.7	20.2	16.4	29.5
33.7	234.6	6.8	8.26	0.20	17.1	15.7	15.6	23.6
32.4	233.5	8.3	8.76	0.21	16.9	22.5	13.8	35.4
31.1	231.7	10.0	8.88	0.18	15.6	15.7	13.9	25.4
29.7	227.9	12.1	8.68	0.16	14.2	13.2	14.3	22.1
28.5	227.1	14.7	8.43	0.18	12.9	19.7	12.8	33.0
27.2	224.9	17.8	7.75	0.15	13.0	16.7	11.5	26.8
25.9	218.6	21.5	6.56	0.12	14.0	15.6	11.3	24.0
24.7	215.7	26.1	5.23	0.09	14.8	15.8	10.4	23.7